

Lignocellulose deconstruction using glyceline and a chelator-mediated Fenton system

Lourdes M. Orejuela

Dissertation submitted to the faculty of the Virginia Polytechnic Institute and State University in partial fulfillment of the requirements for the degree of

Doctor of Philosophy

In

Macromolecular Science and Engineering

Scott Renneckar, Chair

Barry Goodell, Co-Chair

Charles F. Frazier

Kevin J. Edgar

Richard Helm

December 05, 2017

Blacksburg, VA

Keywords: deep eutectic solvent (DES), chelator-mediated Fenton system (CMF), pretreatment, biomass saccharification, structural analysis

Lignocellulose deconstruction using glyceline and a chelator-mediated Fenton system

Lourdes M. Orejuela

Abstract

Non-edible plant biomass (lignocellulose) is a valuable precursor for liquid biofuels, through the processes of pretreatment and saccharification followed by fermentation into products such as ethanol or butanol. However, it is difficult to gain access to the fermentable sugars in lignocellulose, and this problem is principally associated with limited enzyme accessibility. Hence, biomass pretreatments that destroy native cell wall structure and allows enzyme access are required for effective biomass conversion techniques. This research studied two novel pretreatment methods on two wood species: 1) a deep eutectic solvent (DES) that, under heat, swells lignocellulose and partially solubilizes cell wall materials by causing breakage of lignin-carbohydrate linkages and depolymerization of the biomass components, and 2) a chelator-mediated Fenton reaction (CMF) that chemically modifies the nanostructure of the cell wall through a non-enzymatic cell wall deconstruction. After pretreatment, utilizing analytical techniques such as nuclear magnetic spectroscopy, wide angle x-ray scattering, and gel permeation chromatography, samples were analyzed for chemical and structural changes in the solubilized and residual materials.

After single stage DES (choline-chloride-glycerol) and two stage, CMF followed by DES pretreatments, lignin/carbohydrate fractions were recovered, leaving a cellulose-rich fraction

with reduced lignin and hemicellulose content as determined by compositional analysis. Lignin and heteropolysaccharide removal by DES was quantified and the aromatic-rich solubilized biopolymer fragments were analyzed as water insoluble high molecular weight fractions and water-ethanol soluble low molecular weight compounds. After pretreatment for the hardwood sample, enzyme digestibility reached a saccharification yield of 78% (a 13-fold increase) for the two stage (DES/CMF) pretreated biomass even with the presence of some lignin and xylan remained on the pretreated fiber; only a 9-fold increase was observed after the other sequence of CMF followed by DES treatment. Single stage CMF treatment or single stage DES pretreatment improved 5-fold glucose yield compared to the untreated sample for the hardwood sample. The enhancement of enzymatic saccharification for softwood was less than that of hardwoods with only 4-fold increase for the sequence CMF followed by DES treatment. The other sequence of treatments reached up to 2.5-fold improvement. A similar result was determined for the single stage CMF treatment while the single stage DES treatment reached only 1.4-fold increase compared to the untreated softwood. Hence, all these pretreatments presented different degrees of biopolymer removal from the cell wall and subsequent digestibility levels; synergistic effects were observed for hardwood particularly in the sequence DES followed by CMF treatment while softwoods remained relatively recalcitrant. Overall, these studies revealed insight into two novel methods to enhance lignocellulosic digestibility of biomass adding to the methodology to deconstruct cell walls for fermentable sugars.

General Audience Abstract

Wood is a valuable material that can be used to produce liquid biofuels. Wood main components are biopolymers cellulose, hemicellulose and lignin that form a complex structure. Nature has locked up cellulose in a protective assembly that needs to be destroyed to gain access to cellulose, convert it to glucose and then ferment it to bioalcohol. This process is principally associated with limited enzyme accessibility. Therefore, biomass pretreatments that deconstruct native cell wall structure and allow enzyme access are required for effective biomass conversion techniques. This research studied two novel pretreatment methods on two wood species: 1) a deep eutectic solvent called glyceline that, under heat, swells wood and partially solubilizes cell wall materials by causing breakage of bonds and converting it into smaller molecules (monomers and oligomers), and 2) a chelator-mediated Fenton system (CMF) that chemically modifies the structure of the cell wall. Pretreatments were tested individually and in sequence in sweetgum and southern yellow pine. After pretreatments, utilizing analytical techniques, fractions were investigated for chemical and structural changes in the solubilized and residual materials. Treated wood samples were exposed to enzymatic conversion. A maximum 78% of glucose yield was obtained for the glyceline followed by CMF pretreated wood. For yellow pine only a 24% of glucose yield was obtained for the CMF followed by glyceline treatment. All these pretreatments presented different degrees of biopolymer removal from the cell wall and subsequent enzyme conversion levels. Overall, these studies revealed insight into two novel methods to enhance wood conversion adding to the methodology to deconstruct cell walls for fermentable sugars.

Acknowledgements

I would like to take the opportunity to express my appreciation of the support, understanding, and guidance of those who have accompanied me on this wonderful journey of pursuing a doctoral degree. First and foremost, I would like to sincerely thank my advisor and committee chair, Dr. Scott Renneckar, for his invaluable guidance, patience and mentorship throughout the years of my doctoral studies at Virginia Tech. Dr. Renneckar's constant support and open advice have been extremely important on both academic and personal levels, for which I am very grateful. At the same time, I would also like to thank my Ph.D. committee members, Dr. Barry Goodell and Dr. Charles E. Frazier for taking the time to serve as advisors in my research work. Their relevant and wise advice has allowed me to complete my research. It has been an honor for me to work under such wonderful people and great advisors.

Furthermore, I would like to acknowledge my committee members Dr. Kevin Edgar, and Dr. Richard F. Helm for their valuable recommendations and suggestions in improving my research at Virginia Tech. Also, I would like to thank Dr. David Contreras, Dr. Carolina Parra, Dra. Marcela Norambuena and Karen Bustamante, from the Centro de Biotecnología of Universidad de Concepcion, for their great cooperation with my research in Chile.

In addition, I would like to thank the following schools and departments for sponsoring this research and my graduate studies: Virginia Tech Graduate School, Macromolecular and Innovation Institute, Macromolecular Science and Engineering Program at Virginia Tech, Blacksburg VA, particularly to Dr. Judy Riffle, Instituto de Fomento al Talento Humano,

Secretaria Nacional de Ciencia y Tecnologia and Universidad San Francisco de Quito, from Quito, Ecuador. I would like to thank all the wonderful people in the Department of Sustainable Biomaterials who have helped me with every need that arose during my student life, especially, Dr. Robert Smith, head of the Department and true friend, Dr. Ann Norris, Angela Riegel and Debbie Garnand. My appreciation goes also to my fellow colleagues in our department whose friendship made my time pleasant and accomplishing. Special thanks to Dr. Yuichiro Otsuka, Dr. Noppadon Sathitsuksanoh, Dr. Katia Rodriguez and Dr. Wei Zhang, Yun Qiang, Shreya Roy Choudhury, Liampeng Zhuang, Yuan Zhu, Justin Serin, Atanur Satir, Christa Stable, Mohammad Tasooji, Guigui Wan and Niloofar Yousefi-Shivyari.

I also feel very thankful for Ms. Barbara Smith, Linda and Ruthie Taylor my dear friends who have given me great support and joyful moments during my tough times. I would also like to thank all my friends and family members for their love and support.

I would like to express my gratitude and admiration to my parents Dr. Luis Orejuela and Ms. Hilda Escobar for teaching me to strive for my dreams and goals and defining a great philosophy of life for me.

I also thank my children Edgar Javier, Christina and Diego for their love, happiness and support without which I could not have completed this work. Last but not least, I am faithfully indebted to my husband, Jorge Fernando. He has made my dreams his and has walked with me along life paths with love, patience and care. No words can express my gratefulness to him.

Table of Contents

Abstract.....	
General Audience Abstract.....	
Acknowledgements.....	v
Table of Contents.....	vii
List of Tables.....	xiv
Chapter 1 Introduction and background.....	1
1.1 Introduction and Background.....	1
1.2 References.....	7
Chapter 2 Literature review.....	9
2.1 Introduction to lignocellulose cell wall deconstruction.....	9
2.2 Lignocellulose Biomass Recalcitrance.....	9
2.3 Lignocellulose Biomass Conversion.....	11
2.3.1 Lignocellulose Biodegradation/Bioconversion.....	11
2.3.2 Lignocellulosic Biomass Conversion.....	18
2.4 Deconstruction of cell wall for biorefinery purposes.....	21
2.4.1 Pretreatments to reduce biomass recalcitrance and enhance cellulose accessibility	22
2.4.2 Enzymatic Hydrolysis.....	24
2.4.3 Dissolution of Biomass.....	26
2.5 Deep Eutectic Solvents.....	35
2.5.1 Concept.....	35
2.5.2 Classification of DESs.....	36
2.6 Type III DES: Choline chloride-glycerol - a mixture of choline chloride (HBA) and glycerol (HBD).....	36
2.6.1 Hydroxyethyltrimethylammonium (Choline) Chloride.....	37
2.6.2 Glycerol – 1,2,3-Trihydroxpropane or glycerin.....	39
2.6.3 Glyceline, a choline chloride-glycerol DES mixture (1:2 molar ratio).....	40
2.7 Interactions between choline chloride and glycerol.....	42
2.7.1 The hole theory: relationship between viscosity and conductivity.....	42
2.7.2 Intermolecular Interactions between HBD and HBA of a DES.....	44

2.8	Biomass solubility in deep eutectic solvents.....	53
2.8.1	Degradation Products from Lignocellulosic Biomass in the Biorefinery.....	55
2.9	References	57
Chapter 3 Lignocellulose Cell Wall Deconstruction with a Deep Eutectic Solvent and a Chelator-mediated Fenton System.....		77
3.1	Abstract	77
3.2	Keyword.....	78
3.3	Introduction	78
3.4	Experimental	80
3.4.1	Materials and Methods.....	80
3.4.2	Preparation of Biomass Samples	80
3.4.3	Deep eutectic solvent pretreatments	80
3.4.4	Compositional Analysis.....	84
3.4.5	Processing of DES filtrates and supernatants	85
3.5	Results and Discussion.....	85
3.5.1	Reaction pretreatments in SG and YP extractive-free biomass	86
3.5.2	Compositional analysis	86
3.5.3	Mass loss.....	86
3.5.4	Mass balances	89
3.5.5	Effect of the pretreatments in lignocellulosic biomass	91
3.5.6	Biopolymer removal in SG and YP biomass during the pretreatments	92
3.6	Conclusions	105
Chapter 4 Enzymatic saccharification of pretreated lignocellulosic biomass with glyceline and a chelator-mediated Fenton System.....		112
4.1	Abstract	112
4.2	Key words	112
4.3	Introduction	113
4.4	Experimental	119
4.4.1	Materials	119
4.4.2	Glyceline deep eutectic solvent and chelator-mediated Fenton pretreatments	119
4.4.3	Biomass Structural Carbohydrate Analysis	120

4.4.4	Enzymatic hydrolysis.....	120
4.4.5	Determination of released glucose	121
4.4.6	X-ray diffraction (XRD) of untreated and pretreated SG and YP biomass	121
4.5	Results and discussion.....	122
4.5.1	Enhanced enzymatic hydrolysis of biomass through lignin and hemicellulose removal during the single and double stage pretreatments with a deep eutectic solvent DES and a CMF system	123
4.5.2	XRD crystallinity of untreated and single and double stage DES and CMF pretreated biomass and cellulose	127
4.5.3	Effect of delignification on single and double stage pretreated SG and YP with a Glyceline DES and a CMF system, on the crystallinity and on the enzyme digestibility...	131
4.5.4	Effect of hemicellulose removal on single and double stage pretreated SG and YP with glyceline and a CMF system, on the crystallinity and on the enzyme digestibility	132
4.6	Conclusions	134
4.7	Acknowledgements	134
Chapter 5 Structural analysis of recovered lignin fractions isolated from biomass after glyceline and chelator-mediated Fenton pretreatments		141
5.1	Abstract	141
5.2	Keywords	142
5.3	Introduction	142
5.4	Materials and Methods	145
5.4.1	Materials	145
5.4.2	Single and double stage DES and chelator-mediated Fenton pretreatments	145
5.4.3	Liquid-liquid extraction lignin recovery.....	146
5.4.4	Elemental analysis of GLY SG, GLY YP, CMF followed by GLY SG and CMF followed by DES YP lignin fractions	147
5.4.5	DES SG, DES YP, CMF followed by DES SG and CMF followed by DES YP lignin fractions acetylation.....	147
5.4.6	Quantitative ¹ H NMR analysis	148
5.4.7	Quantitative ³¹ P-NMR analysis of recovered DES SG, DES YP, CMF+DES SG and CMF+DES YP lignin fractions	148
5.4.8	Two dimensional ¹³ C- ¹ H heteronuclear single quantum coherence (HSQC) NMR spectroscopy of recovered DES SG, DES YP, CMF+DES SG and CMF+DES YP lignin fractions	149

5.4.9 Gel permeation chromatography of recovered GLY SG, GLY YP, CMF followed by GLY SG and CMF followed by GLY YP lignin fractions.....	151
5.5 Results and Discussion.....	152
5.5.1 Single stage GLY and CMF and double stage GLY+CMF and CMF+GLY lignin yields through liquid-liquid extraction	152
5.5.2 Quantitative ³¹ P-NMR of recovered single stage GLY and CMF and double stage GLY followed by CMF and CMF followed by GLY lignin fractions.....	152
5.5.3 Two Dimensional HSQC Nuclear Magnetic Resonance of single stage GLY and CMF and double stage GLY followed by CMF and CMF followed by GLY lignin fractions	159
5.5.4 Molecular weight of single stage GLY and CMF and double stage GLY followed by CMF and CMF followed by GLY lignin fractions.....	166
5.6 Conclusions	169
5.7 Acknowledgements	170
5.8 References	171
Chapter 6 Summary and Conclusions.....	177
Appendix A Physical and chemical effects of choline chloride-glycerol deep eutectic solvent in lignocellulose biomass	184
A1.1 Abstract	184
A1.2 Key words	185
A1.3 Introduction	185
A1.4 Materials and Methods	186
A1.4.1 Materials	186
A1.4.2 Methods.....	187
A1.5 Results and Discussion.....	188
A1.5.1 Glyceline DES preparation	188
A1.5.2 Qualitative solubility of isolated biopolymers with ChCl, glycerol and GLY	189
A1.5.3 Qualitative Observations of SG and YP biomass pretreatments with glycerol and glyceline.....	190
A1.5.4 Swelling of sweetgum and yellow pine biomass	191
A1.6 Conclusions	196

List of Figures

Figure 2-1 Mechanism for generation of Fe ²⁺ and H ₂ O ₂ (in situ) and disruption of cell wall by brown-rot fungi through the production of hydroxyl radicals in a chelator-mediated Fenton system.	17
Figure 2-2 Scheme of a biorefinery to obtain biofuels and biomaterials.....	22
Figure 2-3 Lignocellulosic Biomass Conversion: pretreatments and value-added products.....	24
Figure 2-4 Scheme of the reaction of biomass with an IL and DMSO. Taken from reference [210]. Under fair use.	27
Figure 2-5 Mechanism of cellulose dissolution in ILs. Taken from [27]. Use under fair use.....	31
Figure 2-6 Swelling of cellulose fiber in IL (similar to swelling in NMMO-water (20%).Taken from [32]. Use under fair use.....	32
Figure 2-7 Molecular model of the β form of choline chloride. Taken from reference [25]. Use under fair use.....	38
Figure 2-8 Structure of glycerol.....	39
Figure 2-9 Schematic synthesis of glyceline. Adapted from [15, 38]	40
Figure 2-10 Schematic representation of a hydrogen bond	44
Figure 2-11 Schematic representation of the interaction between choline chloride (HBA) and glycerol (HBD). Adapted from [43]. Use under fair use.	45
Figure 2-12 Molar conductivity versus fluidity of three DESs at 20oC. Taken from reference [45], Use under fair use.....	47
Figure 2-13 Temperature dependence of the transient confinement radius. Taken from reference [48]. Under fair use.	48

Figure 2-14 Simulation result showing that the hydrogen bonds formed between glycerol molecules and Cl ⁻ dominate over those established between the Ch ⁺ cation and Cl ⁻ anion energy-minimized structure, taken from [343]). Under fair use.	49
Figure 2-15 Vibrational modes of the IR peaks of glyceline. Taken from reference [316]. Under fair use.....	52
Figure 2-16 Charge densities of glycerol, ChCl and glyceline. Taken from [344]. Under fair use.	52
Figure 2-17 Mechanism of the β-O-4 linkage cleavage during the reaction between an acidic DES and lignin. Taken from reference [52], use under fair use.	55
Figure 3-1 Cell wall deconstruction with GLY and a CMF system treatments.....	77
Figure 3-2 Flow Chart of Biomass pretreatment with glyceline.....	82
Figure 3-3 Flow Chart of Biomass pretreatment with chelator-mediated Fenton system	83
Figure 3-4 Diagram of GLY, CMF, and in sequence biomass pretreatments in this study.....	84
Figure 3-5 Sweetgum and Yellow Pine Mass Loss (%) during the pretreatments. CMF+GLY = CMF followed by DES and DES+CMF = CMF followed by GLY	88
Figure 3-6 Pretreatment Mass Loss: Species Comparison	88
Figure 3-7 Total mass balance closure for cellulose, hemicellulose and lignin in SG and YP biomasses with GLY and CMF pretreatments (single and double stage).....	91
Figure 3-8 Biopolymer removal from SG and YP biomass samples in single stage treatments ..	94
Figure 3-9 Biopolymer removal from SG and YP - double stage pretreatments.....	100
Figure 3-10 Cumulative biopolymer removal from SG and YP biomass samples during the single and double stage pretreatments.	103
Figure 4-1 Cellulose representation and hydrogen bond network (dotted lines).....	116

Figure 4-2 Enzymatic Glucan Digestibility Profiles of Untreated and pretreated SG with a DES and a CMF system.	127
Figure 4-3 Enzymatic Glucan Digestibility Profiles of Untreated and pretreated YP with a DES and a CMF system.	127
Figure 5-1 ³¹ P NMR functional group analysis: aliphatic OH, phenolic OH and carboxylic OH groups of recovered lignin fractions from sweetgum (A) and yellow pine (B).	155
Figure A1-1 GLY after heating at 80oC for 30 min (A), after 2h of cooling (B), after 24 h of stabilization (C) and after 2 h of heating (simulating the pretreatment) (D).	188
Figure A1-2 ¹ H-NMR of GLY mixture at molar ratio (1:2).....	189
Figure A1-3 Swelling of SG and YP in water and GLY at ambient temperature	191
Figure A1-4 Swelling of SG and YP in glycerol and GLY at 150oC.....	192
Figure A1-5 Schematic of the quadrupole moment of benzene, viewed edge-on, showing regions of positive and negative partial charges, taken from reference [38]. Use under fair use.....	195
Figure A1-6 Schematic of the quadrupole moment of benzene, viewed edge-on, showing regions of positive and negative partial charges, taken from reference [38]. Use under fair use.....	195

List of Tables

Table 2-1 Molecular structure of biomass cell wall.....	11
Table 2-2 Parameters for an effective lignocellulosic biomass conversion.....	21
Table 2-3 Properties of glyceline.....	41
Table 3-1 AIL and ASL removal in the single and double stage CMF/GLY pretreatments	98
Table 3-2 Mass loss for GLY and CMF pretreatments applied to SG and YP biomasses	103
Table 3-3 Efficiency factor for the pretreatments in sequence for SG and YP biomasses.....	104
Table 4-1 Chemical composition (relative) of untreated and pretreated ground SG and YP biomass samples.....	123
Table 4-2 Effects of biomass composition in crystallinity and glucan digestibility.....	131
Table 5-1 Chemical composition of isolated GLY SG, GLY YP, CMF+GLY SG and CMF+GLY YP lignin fractions	153
Table 5-2 Aromatic region - Assignments of the ^{13}C - ^1H correlation signals for the lignin structures observed in the 2D HSQC NMR spectra of recovered lignin fractions	161
Table 5-3 Assignments of the ^{13}C - ^1H correlation signals for the lignin structures observed in the 2D HSQC NMR spectra.....	165
Table 5-4 Molar abundance (per 100C ₉) of side chain linkages in lignin	166
Table 5-5 Molar Masses of recovered GLY SG, CMF+GLY SG, GLY YP and CMF+GLY YP lignin fractions.	169
Table A1-1 Dissolution of Isolated biopolymers in glyceline at 150°C	190
Table A1-2 Kraft lignin treated in ChCl, glycerol and glyceline at 150°C for 2h.....	190

Chapter 1 Introduction and background

1.1 Introduction and Background

Lignocellulosic biomass is an abundant natural resource for sustainable energy via direct combustion as well as for production of renewable biofuel precursors, valuable chemicals and advanced biomaterials. Lignocellulose has been used since the dawn of the mankind as a feedstock for energy and integrated into human life for materials that range from housing to extracts. Recently, the trend to replace fossil fuels for transportation with biofuels is growing after US policy in Renewable Fuels Standards 2, and 1st generation bioethanol is by far the liquid biofuel mostly used globally [1]. Bioethanol can be produced from different raw materials such as agricultural crops that contain sugars, such as sugar beets and sugar cane to grains such as starch and structural polymers such as cellulose within plant cell walls [2]. Sugars and starch, feedstocks for first generation biofuel production, are edible and compete with human nutritional needs and require various cultivation inputs, limiting the sustainability of the system. Cellulosic bioethanol, a second generation biofuel, is produced from available, usually, inexpensive plant biomass, therefore it is seen as a possible, affordable solution to liquid biofuel production. However, several technical drawbacks in bioethanol production technologies still need to be overcome to develop their potential utilization worldwide [3].

Major lignocellulose components are cellulose, hemicellulose and lignin [4] and have been used to create high value materials for society. Wood pulp and paper industries started in the late 1800's and were prevalent in the past century, concomitantly cellulose and cellulose derivatives industry was developed and a variety of products such as textiles [5, 6], coatings for films and

packing [7], drug delivery systems [8, 9], photographic films [10], and thermoplastics [11] have been in the commercial market. More recent cellulose derivatives with potential applications are biodegradable polymers [12], dialysis membranes [13], nanocellulose and nanomaterials [14, 15] which are some of the more niche high value materials. Heteropolysaccharides, most commonly known as hemicelluloses, have also found applications as biodegradable films for the food industry and biomedical uses in drug delivery system, especially 4-O-methylglucuronoxylan the most common hardwood hemicellulose [16], the main softwood hemicellulose, galactoglucomannan also has been studied for colon targeted drug delivery systems [17]. Likewise, lignin isolated from plants have been used as source of phenolic compounds with potential applications as phenolic resins [18], polyurethanes [19], antioxidants [20] and dispersants [21]. Much research has been performed for advanced material applications of plant polymers, however only cellulose derivatives and lignosulfonates are commercially available due to the unique applications they can fill in the market. New methods of lignocellulose biomass processing and biopolymers isolation are crucial to produce bio-based chemicals and bioplastics that also provide alternative sources of plant-based chemicals that can serve society. The interest in lignocellulosic biofuels provides a platform to develop novel materials based on renewable carbon materials, as a mix of high volume fuels and high value bioproducts to make an economically compelling case for a biorefinery. However, current pretreatment methods such as steam-explosion and dilute acid pretreatment do not provide interesting materials for a biorefinery, as significant hemicellulose depolymerization happens and uncontrolled repolymerization of lignin creates heterogeneous lignin.

Novel solvents such as deep eutectic solvents (DESs) that increase enzymatic accessibility show promise for biomass pretreatment. DES is typically a binary mixture of two solvents that consist

of a hydrogen bond donor and acceptor, which create a lower melting point mixture compared to each individual component [22]. DESs are a new kind of ionic liquids, as their use in biomass processing is growing in the academic community due to the fact that some DESs come from natural sources, are inexpensive, easy to prepare and handle, biodegradable and biocompatible [23]. Thus they can overcome the disadvantages of the ILs but share their properties as good solvent systems such as being liquids at room temperature and having low vapor pressure. In this regard, DES also overcome the drawbacks of most of the organic solvents used in biomass organosolv pretreatments.

Among the variety of DES used in biomass pretreatments, choline chloride-glycerol DES (GLY) is attractive because their components are available on the market at the MT scale. A closer look to the GLY chemical structure shows that is a complex mixture composed by cholinium [Ch^+] cations and chlorine [Cl^-] anions. Cl^- serves as a hydrogen bond acceptor (HBA) and glycerol as the hydrogen bond donor (HBD). This eutectic mixture has interesting physico-chemical properties that give rise specific interactions between its components. GLY is viscous at room temperature but its fluidity increases with temperature and with the free volume, hence charge transport is affected by small changes in chemical structure [24, 25]. Moreover, main interactions in GLY are hydrogen bonds between Cl^- anion and two OH groups at the ends of glycerol and, the third OH group in glycerol molecule is involved in intermolecular hydrogen bonding between glycerol molecules [26].

Studies conducted by several research groups worldwide have determined GLY physico-chemical properties (high viscosity, slight basic pH, dipolarity due to the presence of OH groups with an unequal sharing of electrons, conductivity, and surface tension) [27-34]. It has been also

described that between the ChCl and glycerol are present non-specific interactions and solvophobic interactions. Among the non-specific forces, instantaneous-dipole/induce dipole force (dispersion London force), dipole/induced dipole forces (induction or Derby forces), and dipole/dipole forces (Coulomb forces) can be included [35]. Moreover, GLY is an asymmetric bulky moiety with low lattice energy and macro and nanoscale mobility of components within GLY are determined by H-bonds and ionic interactions. More complex interactions may ionize to some extent and lead to multiple ions within the DES. Therefore, GLY complexity can be visualized through the behavior of each of its components. Glycerol is a neutral strong HBD due to its three OH groups and has a faster long-range diffusion compare to that of Ch^+ cation, due to its relative larger size. In the anhydrous state, GLY shows a non-Newtonian behavior and becomes Newtonian when water content is above 2.5 wt%. GLY molar conductivity is a function of its fluidity, thus its viscosity controls charge transport, charge carriers being Ch^+ and Cl^- . Through diffusion dynamics, it has been found that on the nanometer length scale mobility of Ch^+ cation was larger than glycerol mobility. The hole theory developed by Abbott has suggested that glycerol forms multiple tighter and stronger H-bonds between its neighboring OH groups and Cl^- anion so that a close ring type structure is formed surpassing the lone OH group from Ch^+ cation. Thus, the distance between Cl^- anion and Ch^+ cation is increased to a larger extent for GLY indicating reduced interactions within the eutectic mixture. Therefore, physical-chemical properties GLY make this DES a unique novel solvent that can be used widely as a lignocellulose solvent agent in biomass pretreatments.

Interactions between GLY and lignocellulose biomass are governed by heating. At temperatures greater than 100°C , lignin softens and thermal expansion occurs, Ch^+ DES cation may interact with π systems of lignin [36] creating a DES-lignin association thus lignin carbohydrate bonds

cleave leading to a partial removal of lignin and hemicellulose. This chemistry makes GLY an exceptional pretreatment agent for lignocellulose biomass processing in biorefinery settings.

On the other hand, mimicking the action of brown rot fungi on lignocellulose to modify the cell wall nanostructure via chelator-mediated Fenton system without the use of enzymes, generating a non selective depolymerization of biopolymers and a concomitant lignin recondensation producing fermentable sugars would be an interesting approach to utilize nature's path to deconstruct wood cell walls.

In this study, a novel biomass pretreatment method has been attempted combining the technology of deep eutectic solvents with the chemistry of a chelator-mediated Fenton system and determine if any synergism exist between these treatments.

In this work it is hypothesized that having a more open cell wall with CMF treatment would allow more access, more porosity due to breakage of linkages in the lignocellulose matrix, and subsequent DES treatment would remove biopolymer fragments leaving a substrate more digestible to enzyme saccharification. If DES is first applied and then CMF treatment, at temperatures that this solvent is used, it would break more linkages in the cell wall that CMF treatment would remove leaving a cellulose rich fraction more amenable for enzymatic hydrolysis producing better yields of glucose.

The specific objectives of this research are:

- Evaluate how these treatments impact fractionation of lignocellulose, individually and in sequence;
- Discern the interactions between the deep eutectic solvent and the biomass substrate;

- Determine conversion of cellulose from pretreated samples into fermentable sugar by addition of enzymes and understand differences in accessibilities;
- Evaluate the effect of the pretreatments on isolated lignin biopolymer functionality and structure. Determine the MW and evaluate lignin structure of isolated lignin extracts.

To achieve these objectives, the dissertation is composed of 8 chapters. Chapter 1 provides the introduction and background of this entire research. Chapter 2 focuses in the literature review on lignocellulosic biomass, types and characteristics, biomass pretreatments, special emphasis has been made in organosolv pretreatment and fungal lignocellulose biodegradation, to emphasize the brown-rot mechanism, and finally new technologies for biopolymer structural analysis.

Additional information on novel deep eutectic solvents and their characteristics that make them special solvents for advanced separation techniques are included in the literature review. Chapter 3 illustrates a novel approach for biomass pretreatment of sweetgum and yellow pine particles applying choline chloride-glycerol deep eutectic solvent and chelator-mediated Fenton system separately (single stage) or in sequence (double stage). A detailed mass balance of biomass components after pretreatments and biopolymer separation processes is described. Chapter 4 details the pretreated biomass saccharification processes to evaluate the pretreatment efficiency and explore the influence of pretreatment and residual lignin and xylan in cellulose digestibility. Chapter 5 describes lignin fractionation during the pretreatments and its structural analysis. Chapter 6 provides a summary and conclusions of this dissertation.

1.2 References

1. Balat, M., *Production of bioethanol from lignocellulosic materials via the biochemical pathway: a review*. Energy conversion and management, 2011. **52**(2): p. 858-875.
2. Chakraborty, S. and A. Gaikwad, *Production of Cellulosic Fuels*. Proceedings of the National Academy of Sciences India Section a-Physical Sciences, 2012. **82**(1): p. 59-69.
3. Gomez, L.D., C.G. Steele-King, and S.J. McQueen-Mason, *Sustainable liquid biofuels from biomass: the writing's on the walls*. New Phytologist, 2008. **178**(3): p. 473-485.
4. Fengel, D. and G. Wegener, *Wood: chemistry, ultrastructure, reactions*. 1983: Walter de Gruyter.
5. Christian, B., *Method of waterproofing cellulose textiles*. 1950.
6. Christian, G., *Process for flame-proofing of cellulose-containing textiles*. 1969.
7. Lowey, H., *Ethylcellulose coatings* 1958.
8. Donbrow, M. and Y. Samuelov, *Zero order drug delivery from double-layered porous films: release rate profiles from ethyl cellulose, hydroxypropyl cellulose and polyethylene glycol mixtures*. Journal of Pharmacy and Pharmacology, 1980. **32**(1): p. 463-470.
9. Edgar, K.J., *Cellulose esters in drug delivery*. Cellulose, 2007. **14**(1): p. 49-64.
10. Adelstein PZ, M.J., *Permanence of processed ester polyester base photographic films*. Photographic Science and Engineering, 1965. **9**(5): p. 305-313
11. Huang, M.-R. and X.-G. Li, *Thermal degradation of cellulose and cellulose esters*. Journal of Applied Polymer Science, 1998. **68**(2): p. 293-304.
12. Demirbas, A., *Biodegradable Plastics from Renewable Resources*. Energy Sources, Part A: Recovery, Utilization, and Environmental Effects, 2007. **29**(5): p. 419-424.
13. Xiao, Y. and T.-S. Chung, *Functionalization of cellulose dialysis membranes for chiral separation using beta-cyclodextrin immobilization*. Journal of Membrane Science, 2007. **290**(1): p. 78-85.
14. Morán, J.I., et al., *Extraction of cellulose and preparation of nanocellulose from sisal fibers*. Cellulose, 2008. **15**(1): p. 149-159.
15. Habibi, Y., L.A. Lucia, and O.J. Rojas, *Cellulose nanocrystals: chemistry, self-assembly, and applications*. Chemical reviews, 2010. **110**(6): p. 3479-3500.
16. Ebringerová, A. and T. Heinze, *Xylan and xylan derivatives - biopolymers with valuable properties, I. Naturally occurring xylans structures, isolation procedures and properties*. Macromolecular Rapid Communications, 2000. **21**(9): p. 542-556.
17. Leopold, C.S., *A Practical Approach in the Design of Colon-specific Drug Delivery Systems, in Drug Targeting: Organ-Specific Strategies, in Drug Targeting: Organ-Specific Strategies*, G.M.a.D.K.F. Meijer, Editor. 2001, Wiley-VCH Verlag GmbH: Weinheim, FRG.
18. Effendi, A., H. Gerhauser, and A.V. Bridgwater, *Production of renewable phenolic resins by thermochemical conversion of biomass: A review*. Renewable and Sustainable Energy Reviews, 2008. **12**(8): p. 2092-2116.
19. Saraf, V.P. and W.G. Glasser, *Engineering plastics from lignin. III. Structure property relationships in solution cast polyurethane films*. Journal of Applied Polymer Science, 1984. **29**(5): p. 1831-1841.
20. Dizhbite, T., et al., *Characterization of the radical scavenging activity of lignins—natural antioxidants*. Bioresource Technology, 2004. **95**(3): p. 309-317.

21. Zhou, M., et al., *Properties of Different Molecular Weight Sodium Lignosulfonate Fractions as Dispersant of Coal-Water Slurry*. Journal of Dispersion Science and Technology, 2006. **27**(6): p. 851-856.
22. Abbott, A.P., et al., *Deep eutectic solvents formed between choline chloride and carboxylic acids: Versatile alternatives to ionic liquids*. Journal of the American Chemical Society, 2004. **126**(29): p. 9142-9147.
23. Domínguez de María, P. and Z. Maugeri, *Ionic liquids in biotransformations: from proof-of-concept to emerging deep-eutectic-solvents*. Current Opinion in Chemical Biology, 2011. **15**(2): p. 220-225.
24. Smith, E.L., A.P. Abbott, and K.S. Ryder, *Deep eutectic solvents (DESs) and their applications*. Chemical reviews, 2014. **114**(21): p. 11060-11082.
25. Tang, B. and K.H. Row, *Recent developments in deep eutectic solvents in chemical sciences*. Monatshefte für Chemie - Chemical Monthly, 2013. **144**(10): p. 1427-1454.
26. Wagle, D.V., G.A. Baker, and E. Mamontov, *Differential Microscopic Mobility of Components within a Deep Eutectic Solvent*. Journal of Physical Chemistry Letters, 2015. **6**(15): p. 2924-2928.
27. Abbott, A.P., R.C. Harris, and K.S. Ryder, *Application of hole theory to define ionic liquids by their transport properties*. The Journal of Physical Chemistry B, 2007. **111**(18): p. 4910-4913.
28. Shahbaz, K., et al., *Prediction of the surface tension of deep eutectic solvents*. Fluid phase equilibria, 2012. **319**: p. 48-54.
29. Mjalli, F.S. and O.U. Ahmed, *Characteristics and intermolecular interaction of eutectic binary mixtures: Reline and Glyceline*. Korean Journal of Chemical Engineering, 2016. **33**(1): p. 337-343.
30. D'Agostino, C., et al., *Molecular motion and ion diffusion in choline chloride based deep eutectic solvents studied by H-1 pulsed field gradient NMR spectroscopy*. Physical Chemistry Chemical Physics, 2011. **13**(48): p. 21383-21391.
31. Leron, R.B. and M.-H. Li, *Molar heat capacities of choline chloride-based deep eutectic solvents and their binary mixtures with water*. Thermochimica Acta, 2012. **530**: p. 52-57.
32. Wu, S.H., et al., *Vapor pressure of aqueous choline chloride-based deep eutectic solvents (ethaline, glyceline, maline and reline) at 30-70 degrees C*. Thermochimica Acta, 2012. **544**: p. 1-5.
33. Lin, C.-M., et al., *Henry's constant of carbon dioxide-aqueous deep eutectic solvent (choline chloride/ethylene glycol, choline chloride/glycerol, choline chloride/malonic acid) systems*. The Journal of Chemical Thermodynamics, 2014. **68**: p. 216-220.
34. Leron, R.B., A.N. Soriano, and M.-H. Li, *Densities and refractive indices of the deep eutectic solvents (choline chloride+ ethylene glycol or glycerol) and their aqueous mixtures at the temperature ranging from 298.15 to 333.15 K*. Journal of the Taiwan Institute of Chemical Engineers, 2012. **43**(4): p. 551-557.
35. Reichardt, C., *Polarity of ionic liquids determined empirically by means of solvatochromic pyridinium N-phenolate betaine dyes*. Green Chemistry, 2005. **7**(5): p. 339-351.
36. Pillai, K.V. and S. Rennecker, *Cation- π Interactions as a Mechanism in Technical Lignin Adsorption to Cationic Surfaces*. Biomacromolecules, 2009. **10**(4): p. 798-804.

Chapter 2 Literature review

2.1 Introduction to lignocellulose cell wall deconstruction

Lignocellulosic biomass is an abundant renewable material. Approximately 200 billion tons/year of vegetable matter grows, but only 4-5% is utilized, while the rest is stored or recycled via natural routes [1]. Plant dry matter is one of the main sources energy and bioproducts considered environmentally friendly due to the carbon cycle [2]. Biofuels are the most important renewable energy resource with almost 10% of the annual global primary energy demand. Plant biomass conversion has received much attention in the last decade, it is important to attain efficient processes for an effective biomass conversion with sustainable yields of desired biofuels and value-added chemicals to develop a bio-based economy [3].

2.2 Lignocellulose Biomass Recalcitrance

The architecture and chemical composition of the cell wall contribute to lignocellulosic biomass recalcitrance [4]. McCann and Carpita [5] have defined **biomass recalcitrance** as the resistance of lignocellulosic biomass to be converted into other products due to the presence of some features that increase energy consumption and therefore the cost, making the biorefinery operations very complex. The reasons why enzymes or other chemicals are prevented to cellulose access in the cell wall and its conversion to sugars are: cellulose microstructure, solubility and crystallinity limit access to cellulose chains, the degree of polymerization and branching of hemicellulose polymer surrounding cellulose, linked to lignin forming the lignin-carbohydrate complex; and the presence of lignin, its concentration and its cross-linking pattern.

Thus, an improved understanding of the interfaces between treatment agents (solvents, catalyst, and chemicals) and cell-wall substrates is crucial [6-8] [9-13].

The structural framework (ultrastructure) of the plant is provided by the cell wall network [14]. The secondary wall composition varies within and among plant species [15]. Cell wall types and their size confers different properties to the biomass. Each cell wall accommodates particular clusters of biopolymers depending upon the stage of development [5]. The main features of cell walls of angiosperms (hardwoods) such as sweet gum are summarized in Table 2-1 and reveal the differences between monocots and dicots for angiosperms.

At the nanoscale level, cellulose crystallinity is a barrier for catalysts, chemicals or enzymes needed for its depolymerization [16]. Also, microfibrils can coalesce forming aggregates and reducing the effective surface area [15]. Fernandes et al. have conducted solid state NMR experiments and found that cellulose microfibrils had a diameter of 2.3 – 3.0 nm which is equivalent to 18-24 chains [17]; these data were confirmed with data in SANS performed by Thomas et al. [18] (2.3 – 2.8 nm). Microfibril size changed with species ranging from < 2 nm to < 6 nm, which was confirmed by wide angle X-ray scanning techniques WAXS (3.3 – 3.6 nm) suggesting that adherent amorphous chains contributed to larger diameter. Using electron microscope Donaldson et al. [19] found that wood microfibrils diameter varied from 4-13 nm .

Table 2-1 Molecular structure of biomass cell wall

Angiosperms (Higher Plants)	
Monocots	Dicots
Type II wall	Type I wall
a) GAXs/primary cell wall rich in phenyl propanoid units [20] b) GAXs/primary cell wall rich in phenyl propanoid units - sites of network polymerization of lignin [20]	Xyloglucan-cellulose matrix surrounded by pectin network [21].
Secondary cell wall	
Cellulose microfibrils are as crystalline assemblies of 24 to 36 (1→4)-β-D-glucan chains ([21, 22]. Amorphous and ordered cellulose chains enclose a crystalline core or amorphous sections are extended through the whole length of a microfibril [23]	
Primary cell wall	
Cellulose microfibrils serves as a frame where xyloglucan and cellulose bind through (1-4)-β-D glucopyranose bonds. Cellulose chain extension varies among species [21]	

2.3 Lignocellulose Biomass Conversion

2.3.1 Lignocellulose Biodegradation/Bioconversion

Lignocellulosic biomass is colonized by fungi and bacteria in aerobic conditions. Dependent upon the organism, these can be classified as different kinds of decay as described by Kirk [24] white rot, brown rot, soft rot, bacteria-tunneling and erosion conversion. Most microorganisms utilize cellulose and hemicelluloses as energy and carbon source playing a fundamental function in carbon cycle. Basidiomycetes: white rot and brown rot fungi have evolved with the capability

to break down lignin to CO₂, as well as cellulose and hemicellulose. Brown rot decomposition is associated with gymnosperms (softwood or conifers), and the white rot decomposition with angiosperms (hardwoods) [24, 25].

2.3.1.1 Brown-rot fungi

They represent around 10% of the taxonomic diversity of lignocellulosic degrading basidiomycetes [26-28]. They are the prevailing wood decay fungi in coniferous forests in the north hemisphere [29]. Recent comparative and functional genomic studies of wood rot fungi point out that brown-rot fungi have evolved from white-rot fungi and have missed critical enzymes to disrupt lignocellulosic matrix, mainly for cellulose and lignin polymers [30, 31]. Latest genome analysis of cellulose and hemicellulose-degrading enzymes in several white and brown rot fungi have indicated that white-rot fungi possess a greater enzymatic variety for lignocellulose attack than brown-rot fungi [32].

Since brown-rot fungi produce extracellular enzymes, they are still able to degrade polysaccharides and modify lignin due to a lower energy mechanism developed to initiate attack of wood and improve the lignocellulosic biomass efficiency [30, 31, 33]. Some of the lignin modified compounds mediate the production of ·OH radicals and increase brown-rot fungi access to holocellulose [34, 35]. Hence, metabolites of non-enzymatic processes are produced only at initial steps of decay.

Brown-rot decay initiates via accumulation of spores or mycelial parts that are transported by the water, wind, or by insects or animals to wood or other lignocellulosic surfaces. Mycelial growth in wood may also occur in direct soil contact. For this to happen, suitable conditions of temperature and moisture should be met (moisture content above the fiber saturation point, not

saturated lumen and temperature between 10°C and 45°C). A single fungus can generate millions to billions of spores. However, in fact only a few survive to initiate decay in LC biomass [25]. In wood cells, the hyphae start growing in the lumens initiating decay, the colonization spreads through ray cells and axial parenchyma where carbohydrates are deposited as energy supply for the fungus. Fungal mycelia penetrate the cell wall via pit membranes or bore holes whose mechanism is not yet well understood [26, 36]. The hyphae proliferate in the lumen [26, 28, 37] and release a glucan film that covers the cell wall (hyphal sheath) that binds to the S₃ layer [37]; the S₂ layer is intensively degraded and is not next to the hyphae, so that the degradation compounds diffuse through the S₃ into the S₂ layer which has less lignin content than S₁ or S₂ [38]. This helps to explain the preferential degradation of cellulose in S₂ in the cell wall [25].

2.3.1.1.1 Biodegradation Mechanism of Brown-rot Fungi

Brown-rot fungi infect lignocellulosic biomass in a two-step process: 1) oxidative radical-based reactions, and 2) enzymatic hydrolysis of the polysaccharides occurs, producing sugars for fungal metabolism [39]. In 1965, Halliwell [40] studied cellulose and demonstrated that it was degraded by free radicals as in Fenton reaction chemistry so he suggested that Fenton mechanism was involved in lignocellulosic biodegradation. Koenigs [41-43] showed that cellulose of softwood was oxidatively degraded supporting Halliwell's findings. These studies provided insight that iron was present in lignocellulosic biomass in enough quantities to be oxidized by the hydrogen peroxide produced by brown-rot fungi extracellularly, developing the oxidative hypothesis.

Arantes and Milagres [44] found recent evidence that supported earlier work and additionally showed that degrading plant enzymes' size does not permit them to diffuse into the lignocellulosic biomass cell wall. The hypothesis that low molecular weight compounds initiate Fenton reactions was supported by the work done by Blanchette et al. [45], Flournoy et al. [46] and other scientists. The production of hydroxyl radicals in liquid culture medium have been demonstrated by Illman and Highley [37], and Dutton et al. [47]. Additionally, recent research of brown-rot fungi genome, transcriptome, and secretome has supported the influence of Fenton chemistry in lignocellulosic biodegradation [30, 33].

Non-Enzymatic Pathways

Brown-rot fungi have developed a mechanism to decay lignocellulosic biomass. First, the fungi aim to solubilize iron III from iron oxy(hydr)oxides contained in wood cell wall; secondly, they assist the reduction of iron to iron II; and thirdly, they produce H₂O₂ [25].

1. Location and solubilization of iron: Insoluble iron oxides complexes are found in the lumen or in the cell wall [35, 48]. To take part in Fenton reactions, these iron complexes need to be dissolved and then reduced to ferrous iron.

Recent studies on oxalate biosynthesis conducted by Zhuang et al. [49] tested the influence on oxalate production by two enzymes in *G. trabeum*, peroxisomal glyoxylate dehydrogenase and cytosolic oxaloacetate acetylhydrolase. He worked with ¹³C NMR and metabolic pathway analyses and found that the oxalate pathway depends on the C/N ratio. When high levels of N are present (low C/N ratio) the cytosolic oxaloacetate acetylhydrolases pathway is favorable. In the opposite case. When the ratio C/N was high (low levels of N), peroxisomal glyoxylate dehydrogenases contribute to oxalate biosynthesis.

Brown-rot fungi secrete oxalic acid extracellularly [47, 50] and bind and solubilize iron from iron complexes in the lumen [48]. The dissolution of iron is strongly influenced by pH conditions, at physiological environments in the vicinity of fungal hyphae in the lumen of decomposed biomass, high oxalate/Fe ratios are present (oxalate pKa = 1.27 and 4.27) so that the pH is around 2. At this pH, oxalic acid binds iron and forms oxalate/Fe complexes that are soluble [48, 51-53]. Under these acidic conditions, OH groups are protonated so that they weaken the Fe-O bond in an adsorption process (not reductive dissolution) in which Fe³⁺ ions can be detached from the iron/oxalate complexes by an iron ligand [51]. Oxalate-iron complexes move to the cell wall, decreasing the concentration of the oxalic acid and increasing therefore the pH [53, 54]. However, the lignocellulose matrix has a high buffering capacity and maintains the pH of the wood cell wall [55]. A hyphae length away, where the pH is about 3.6, there is a low concentrations of oxalate/Fe molar ratio so that the affinity of oxalate for iron decreases and consequently a temporary relocation of Fe³⁺ from oxalate-iron complexes to the cellulose of cell wall occurs [52]. At pH = 3.6 or higher, withdrawal of iron from Fe-oxalate complexes or from cellulose occurs by Fe³⁺ chelating-reducing agents, having a higher affinity for Fe³⁺, as it has been shown by using fungal biomimetic reductants [48, 52].

More recently, Zhu et al. [56] have found that when H₂O₂ is present, iron sequestered by oxalate was reduced by 2,3-DHBA producing ·OH radicals. The amount of iron reduction by the chelator was a function of the concentration of oxalate. Iron withdrawal from oxidized iron was influenced by both pH and oxalate concentration. It was suggested that when brown rot fungi secreted oxalate, the chelator-mediated Fenton reactions (CMF) were enhanced, at the beginning of the decay, revealing hints for the hypothesis of oxalate regulation by brown-rot fungi [57-59].

2. Hydrogen peroxide: The presence of H_2O_2 in brown-rot decay is attributed to two different sources, molecular oxygen reduction and methanol oxidation. A variety of pathways have been proposed by Kerem et al. [60], Hyde and Wood [53], Hirano et al. [61] and, Daniel et al. [62]. At the initial stage of fungal attack, demethylation of lignin occurs and therefore methanol is generated [35, 63] which is metabolized by alcohol oxidase enzymes generated by brown rot fungi [33, 62, 64]. Methanol is not a source of fungal nutrition, however the enzyme and methanol may aid as source of H_2O_2 during decay [62]. Methanol role in biomass decomposition is still under debate, alcohol oxidase is not stable at pH conditions suitable for biomass decomposition by these fungi and the enzyme access to the S_2 layer is not yet well understood [46].

3. Iron-reducing chelators: Several mechanisms have been suggested to describe the reduction from iron III to iron II during the brown-fungal decomposition. The more widely supported mechanism for iron reduction involves extracellular low molecular weight fungal aromatic compounds as Fe^{3+} reductants for in situ generation of Fe^{2+} and H_2O_2 , and cell wall degradation by hydroxyl free radicals (Figure 2-1).

Lignin degradation products may play the same role as fungal aromatic compounds resulting from fungal attack, but this is not well understood yet. These aromatic molecules accept nucleophilic substituents such as $-OH$ or $-OCH_3$, which self-oxidize in the presence of Fe^{3+} and therefore generate Fe^{2+} . It has been demonstrated that these low molecular weight Fe^{3+} -mediating and Fe^{3+} reductants (phenolate or hydroquinone) can play the role of assisting the Fenton reaction by reducing Fe^{3+} to Fe^{2+} [34, 48, 65-67]. Fungal Fe^{3+} reductants being molecules small enough to easily diffuse into the biomass cell wall [48]. Several researchers have

demonstrated that their presence in brown fungal degradation is very critical [65-70].

Compounds such as 2,5-dihydroquinone reduce Fe^{3+} to Fe^{2+} with concurrent generation of semiquinone radical, capable of producing H_2O_2 [71, 72]. This mechanism of Fe^{3+} reduction and formation of H_2O_2 is called **chelator mediated Fenton reaction** [48, 54, 73]. Fe^{3+} reductants can reduce more than one mole of Fe^{3+} [48, 74, 75]. This supports the hypothesis that there is a connection between lignin demethylation and holocellulose loss, both processes take place concurrently [39].

Lately, it has been found evidence indicating that brown rot fungi possess two different mechanisms for holocellulose disruption: 1) radical-based (oxidative); and 2) enzymatic. In cellulose oxidation by hydroxyl radicals, hydrogen abstraction from the glucose monomers of cellulose or hemicelluloses may occur [76] creating carbon centers radicals, which react with oxygen to give peroxy radicals [72]. The polysaccharide undergoes several oxidoreduction reactions and cleavage of the molecule chain may occurs [77, 78].

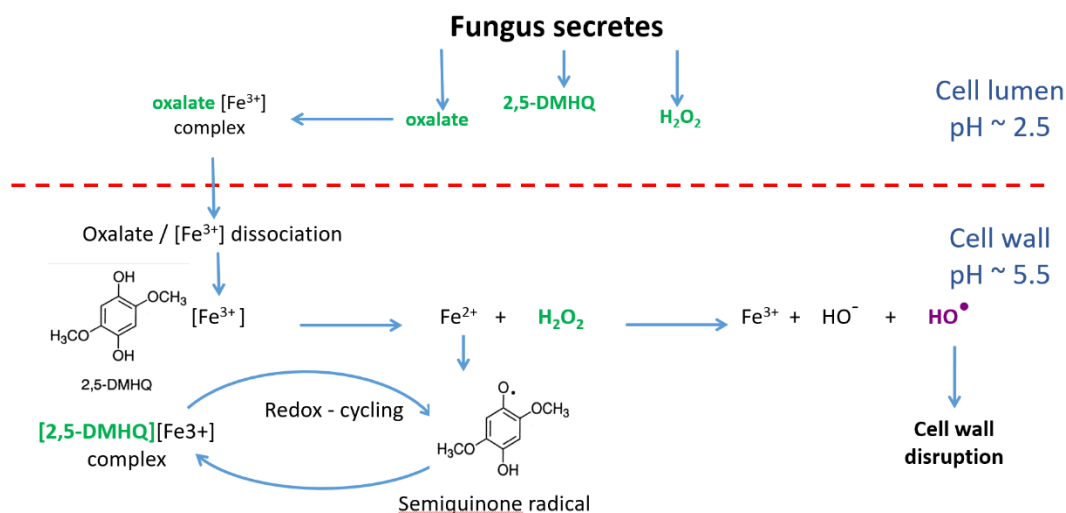


Figure 2-1 Mechanism for generation of Fe^{2+} and H_2O_2 (in situ) and disruption of cell wall by brown-rot fungi through the production of hydroxyl radicals in a chelator-mediated Fenton system.

Thanks to the new analytical techniques it has been found that lignin from decayed biomass also undergoes oxidative demethylation [39] [79, 80]; chain oxidation [80-82], depolymerization [83] and repolymerization [35, 84-86], among other modifications; however, lignin remains as a polymeric molecule [83, 87]. It is believed that lignin disruption of aryl-ether bonds is the initial step in the attack of brown rot fungi [35, 80-82, 88, 89] generating phenolic groups or demethylation. Hydroxyl radical generated through biomimetic brown rot Fenton reactions can also lead to lignin demethylation in softwoods [77, 84, 90]. These lignin modifications may therefore facilitate diffusion of enzymes to the inaccessible polysaccharides in the lignocellulose matrix.

2.3.2 Lignocellulosic Biomass Conversion

Forests, agricultural lands and agro-industry wastes are the three largest potential biomass sources to produce alternative energy through chemical/biological conversion into fuels imparting energy for industry, commerce and housing [91], as well as value-added bioproducts.

Cellulose, mainly in the secondary cell wall, needs to be separated from the complex lignocellulosic matrix, for industrial uses. In this regard, several processes have been invented since 19th century to obtain pulp for paper industries, textiles and cellulose derivatives. All of these processes have the objective to free cellulose for further applications in value-added products. Yet, lignin, hemicellulose and by-products are burned for energy or discarded as waste [92-95]. Most of these conversion processes are water and energy intense, use harsh chemicals, high temperatures and in some cases high pressures and contaminate air and water [92, 96-100].

A different approach to cellulose conversion to sugars is a chemical – catalytic process. Hu et al. [101] have published a review of cellulose applying acid catalysts such as acid resins, metal

oxides, H-form zeolites, heteropoly acids, functionalized silicas, immobilized ionic liquids, carbonaceous acids and magnetic acids. They have pointed out the relevant role of 1) reaction media (water or other solvents), 2) auxiliary methods (e.g. pretreatment techniques and advanced heating methods with microwave or ultrasound radiations), and 3) novel techniques (mechanocatalytic and oxidation-hydrolysis approaches). Other studies have also been published regarding polysaccharide catalytic hydrolysis [102-108], as the entry point into biorefinery schemes for energetically efficient biomass processes to transform cellulose into biofuels and biochemicals.

The ionosolv process is another method to deconstruct biomass cell walls. Dissolution of biomass with ionic liquids (ILs) has been extensively investigated as shown in recent reviews [109, 110]. ILs are salts that are liquid at room temperature. Nevertheless, there are still several disadvantages on the application of this technology. Since Abbott's publication on deep eutectic solvents (DESs) in 2004 [111] defining DESs as mixtures of hydrogen bond donor and hydrogen bond acceptor, that have a melting point lower than the melting points of the DES components, several research groups have studied DES, natural DES and low transition temperature mixtures (LTTMs) as green media for lignocellulose conversion and as alternative options to implement sustainability in biorefineries [112-124]. In this regard, comprehensive reviews have been published by Duran et al. [125] and Vigier et al [126]. These novel technologies may provide beneficial routes for biomass conversion into carbohydrates in a simpler, more efficient and less costly manner.

Recently, Cheng et al. [127] have indicated that factors that need to be taken into account in the pretreatments to overcome biomass recalcitrance towards an efficient lignocellulose conversion,

are: 1) structure of cellulose chains (from crystalline microfibrils to macrofibrils and fibers), 2) lignin content that obstructs the access to polysaccharides and can react with chemicals/enzymes; 3) inhibitory/toxic compounds for enzymes and yeast than can be produced during the pretreatments. Moreover, Maurya et al. [128] have indicated that the key parameters for an effective pretreatment for biological conversion of lignocellulosic biomass are crystallinity (cellulose degree of crystallinity), accessibility (surface area), lignin concentration, hemicellulose content and hemicellulose acetylation. Table 2-2 summarizes the effect of these parameters in lignocellulosic biomass.

The discovery and extraction of natural gas on shale formations promise an inexpensive source of energy in the USA [129, 130]. This fact might diminish projects for biomass conversion for energy purposes in USA. Nevertheless, some industrial cellulosic bioethanol plants have been established for a capacity of 115 KMgy (gallons per year) as it has been listed in the Ethanol Producer Magazine (January 2016) [131], namely Dupont Cellulosic Ethanol LLC-Nevada, IA (30 MMgy); Poet-DSM Advanced Biofuels-Project Liberty (25 MMgy); Abengoa Bioenergy Biomass of Kansas LLC (25 MMgy). Other minor plants are American Process Inc Thomston Biorefinery, GA; BP Biofuel Demonstration Plant, Jennings Facility, LA; Dupont Cellulosic Ethanol LLC-Vonore, TN [131]. In any case, new technologies for lignocellulosic matrix deconstruction to access its components and their commercial applications still need to be developed worldwide. The expectations in Europe and other countries such as Canada [132], China and Malaysia are different for the near future. In Europe, forest and paper industries pursue integration of biorefineries with the pulp and paper mills or establishment of new biorefinery plants [132-136].

Table 2-2 Parameters for an effective lignocellulosic biomass conversion

Cellulose Crystallinity	Surface Area	Lignin Content	Hemicellulose Content and Degree of Acetylation
2/3 of cellulose is in crystalline state [137]. The decrease of crystallinity can eventually increase the lignocellulose digestion [138].	Biomass has two types of surface areas: <u>External</u> - dependent upon particle size and shape. <u>Internal</u> – dependent upon the capillarity of cellulose. Lignin removal will increase internal surface area [6].	Lignin gives structural rigidity to lignocellulosic biomass. It impedes swelling of the lignocellulose matrix. Lignin obstructs and sometimes can bind the contact of enzymes with polysaccharides therefore reducing hydrolysis efficiency [138].	It is a physical barrier which covers cellulose fibers. Its removal increases the substrate pore size enhancing accessibility and cellulose hydrolysis [6, 139, 140]. Acetyl residues are attached to the hemicellulose backbone and may hold back chain disruption, decreasing their concentration will benefit cellulose hydrolysis [137].

2.4 Deconstruction of cell wall for biorefinery purposes

Conversion of biomass into bioenergy and valuable chemicals is escalating global demand due to its low carbon emissions. The market trend pushes to renewable and sustainable products that may replace the petroleum based fuels and commodities. Thus, governments of industrialized countries are establishing policies to replace gradually fossil fuels by biofuels. Bioethanol is the most utilized liquid biofuel for transportation [141].

Liquid biofuels are obtained in a process that has several steps, specifically pretreatment, biomass fractionation, polysaccharides hydrolysis, and monosaccharides fermentation to bioethanol or other liquid fuels, or microbial fermentation of the monosaccharides to the target products [142]. Figure 2-2 provides a general scheme of the steps in biomass processing for bioethanol production. Thus the first step of lignocellulosic biomass conversion is pretreatment to unlock the plant cell wall network and make the polysaccharides accessible to biological processing (enzymatic hydrolysis and fermentation) [137, 143-146].

A more efficient conversion of biomass in chemicals and biofuels would need to overcome its recalcitrant nature and would take into account the following: 1) cost-effective pretreatments, 2) effective process integration - value-added products and lower cost of production, and 3) development of biocatalysts that could ferment C₅ and C₆ sugars efficiently (in high yields) [147].

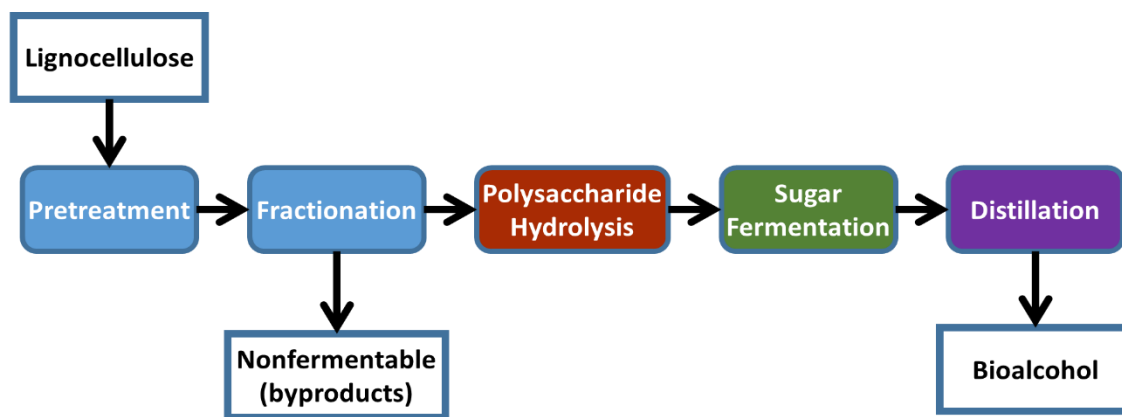


Figure 2-2 Scheme of a biorefinery to obtain biofuels and biomaterials.

2.4.1 Pretreatments to reduce biomass recalcitrance and enhance cellulose accessibility

A pretreatment is a method needed to overcome chemical and physical impediments that exist in the lignin-carbohydrate composite and deliver the majority of cell wall constituents available for conversion into valuable products [7, 93, 95, 148, 149]. The effect of pretreatment has been recognized for a long time [8, 92, 150-152] and it is a crucial step for a biorefinery.

Pretreatments known for pulping processes such as soda pulping and organosolv pulping have been applied in diverse biomass substrates (e.g. hardwood, wheat straw, oil palm waste, sugarcane bagasse, corn residues, and rice husks) to recover glucose, xylose and lignin. Figure 2-3 summarizes the different techniques classified into 5 general methods (physical, thermal,

thermochemical, chemical, and biotechnological pretreatment methods). Depending upon the biomass type and the scope of the treatment also combinatorial ones can be applied.

Several pretreatment methods have been investigated for bioconversion. Their characteristics, energy consumption and the effect of the pretreatment in the three lignocellulose biopolymers have been studied. Some of these processes are also energy intensive, for instance physical methods such as freeze drying [153], wet disk or ball milling [154, 155] or refining [156], however they do not employ harmful and expensive reagents. For thermal pretreatments, liquid hot water (LHW) [157-159] and extrusion [160, 161] are used. For thermochemical pretreatments steam explosion [162, 163], supercritical CO₂ explosion [164] and ammonia fiber steam explosion AFEX [165, 166] have been developed. However AFEX has better performance in terms of biomass accessibility for enzyme saccharification of corn stover. Among the chemical pretreatment methods of biomass processing, diluted acid pretreatment [167] has had a relative success, wet oxidative pretreatment [168] and organosolv [169-171] also have been applied to yield sugars that can be fermented to produce biofuels. Novel pretreatments with the so called green solvents ILs and DES have been developed in the last decade. Several studies have been published in the last 5 years in biomass pretreatments using ionic liquids and the details of their application have been pointed out in several reviews [109, 110, 113, 125, 172, 173]. Regarding the biotechnological pretreatments, comparative studies of brown and white-rot fungi [174-176] have been carried out as well. More recently, the action of the oxidative enzymes lytic polysaccharide mono-oxygenases (LPMOs) has been revealed as a key factor for biomass enzymatic hydrolysis enhancement [177].

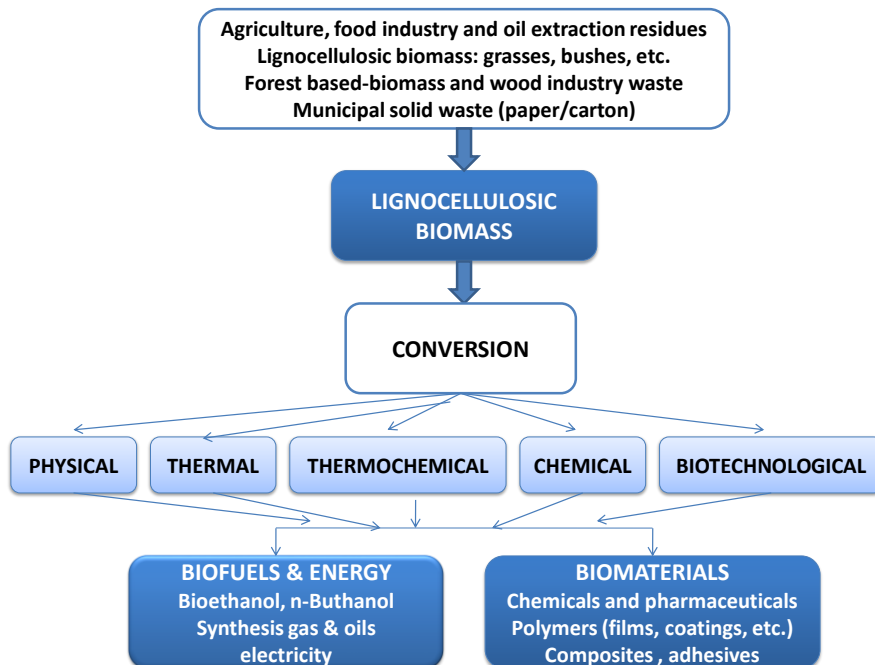


Figure 2-3 Lignocellulosic Biomass Conversion: pretreatments and value-added products.

2.4.2 *Enzymatic Hydrolysis*

Carbohydrate digestibility shows the amount of polysaccharide in the biomass that is released during enzymatic saccharification. Enzymatic hydrolysis is catalyzed by cellulases applied as cocktails; endoglucanases which catalyze cellulose breakdown and release cellulose oligomers; exoglucanases (cellobiohydrolases) which catalyze the liberation of cellobiose from cellulose chain ends; and β -glycosidases which catalyze the hydrolysis of oligomers to glucose [185]. Oxidative enzymes (lytic polysaccharide mono-oxygenases LPMOs) assist to the total hydrolysis of cellulose [186, 187]. Cellulose/xylanase synergy improved overall enzymatic conversion reducing costs for cellulosic ethanol or other biofuel conversion [188]. Hemicellulose hydrolysis is also important in LC biomass conversion, since this polysaccharide shields the cellulose, therefore an additional group of enzymes is needed, the so called hemicellulases (e.g. xylanases,

mannanases, esterases, and α -glucuronoxidases) which work together for an effective hydrolysis of polysaccharides [189].

For cost and environmental concerns – less formation of undesirable by-products, less acid waste and no need for corrosion resistant equipment, enzymatic hydrolysis has advantages over to acid hydrolysis. The solvent/enzyme/catalyst system access to cellulose chains regulates how fast and how far the hydrolysis reaction can be conducted and it is of relevant interest in order to achieve sustainable energy production [138, 177, 190-192]. Typically, the yield of the enzymatic hydrolysis is low in biomass without pretreatment (around 20% of available glucan) [128].

Among the various methods of lignocellulose saccharification, the most common are the separated hydrolysis saccharification (SHS) in which hydrolysis and fermentation are two steps and the simultaneous saccharification and fermentation (SSF) [185, 193]. Enzymes from extremophilic organisms are also being investigated to prepare novel enzymatic cocktails for the biomass conversion [194-198]. Although their characterization for this application is still in its infancy, they are considered potential candidates for biorefinery applications [197, 199, 200]. Biomass crystallinity is very important in the saccharification process. In general, it is increased after most thermal/chemical pretreatments (except AFEX and some ILs treatments) and this is contrary to Fan's conclusion that low crystallinity is preferred for biomass enzymatic hydrolysis [201]. Even though the impact of pretreatments vary, most of them remove or redistribute amorphous components including lignin, hemicellulose and extractives [202]. Hence, biomass crystallinity is affected by its other components and the crystalline structure of untreated and pretreated biomass cannot be compared so that it is difficult to built a relationship between biomass crystallinity and enzymatic hydrolysis [203]. Xu et al. [203] has suggested to calculate

cellulose crystallinity (a percentage of crystalline component of cellulose), balancing mass crystallinity (a percentage of crystalline cellulose in whole biomass) with cellulose content.

2.4.3 Dissolution of Biomass

2.4.3.1 Dissolution of cellulose

The solubility of lignocellulosic biomass in organic solvents has been studied to obtain some information of the mechanisms that are involved in wood dissolution. Solubility of cellulose has been investigated to functionalize it for industrial applications. As early as 1940, Reid et al. used solvents such as monoethanolamine for wood pulping dissolution. McCormick et al. in 1985 [204] published the dissolution of cellulose in LiCl and N, N dimethylacetamide (DMAc) up to 15%. Additionally, Vasilakos et al. [205] worked with hydrogen donor solvents such as tetralin for the liquefaction of α -cellulose at around 400°C and pressure up to 500 psi for 30 min achieving 100% of depolymerization.

Later, a 20% of cellulose dissolution was obtained by mixing a cellulose slurry in aqueous NMMO (N-methylmorpholine oxide) [206]. Another solvent studied for cellulose dissolution is Tetrabutylammonium fluoride hydrate (TBAF) mixed with DMSO [207]. A process of cellulose dissolution in solution of NaOH/H₂O was described by Qi et al. [208]; the first step was to form a complex of cellulose-NaOH and then this complex is dissolved in an aqueous urea solution.

Recently, a homogenous reaction has been developed to yield cellulose carbanilates (Figure 2-4), lignocellulosic biomass is mixed with ILs and DMSO or DMF (60%) for 24 h until complete dissolution of cellulose resulting a very viscous solution which is diluted to 20%. These solvents can be recycled and reused [209].

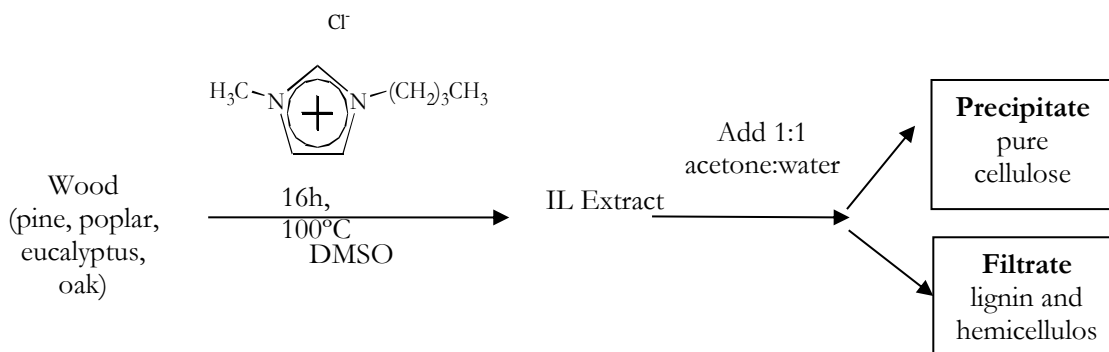


Figure 2-4 Scheme of the reaction of biomass with an IL and DMSO. Taken from reference [210]. USE Under fair use.

To choose the most suitable solvent one must balance solvent capacity and solvent selectivity.

Cellulose is not dissolved by common solvents that work at room temperature [210].

2.4.3.2 Dissolution of Hemicellulose

To study acetylation patterns of xylan as well as to perform structural characterization, xylan has been isolated from delignified corn stover and aspen by extraction with DMSO [211]. Xylan was also removed by alkaline-peroxide extraction, this extraction deacetylated the hemicellulose to a high degree, xylose was the major product and small amounts of arabinose, glucose and galactose were obtained that were studied by FTIR, NMR and GPC techniques [212].

2.4.3.3 Dissolution of Lignin

Native lignins being aromatic polyphenolic polymers are insoluble, but isolated lignin fragments show solubility in common solvents such as dioxane, ethylene glycol, acetone, tetrahydrofuran, dimethylsulfoxide, and dimethylformamide [213]. Solvents with greater ability to swell and dissolve lignin include methanol, ethanol, and phenol. Recently, some ILs have been used to dissolve alkaline lignin [214].

2.4.3.4 Dissolution of Lignocellulose Matrix

Wood solubility in commercial solvents is not yet well understood and theoretical formulations or basic generalized rules need to be developed. Most of the publications have taken into account only the solvent boiling point [213]. A better understanding of the impact of the pretreatments on biomass fractionation will allow us a more effective biomass use. Lagan et al. [215] have demonstrated that two processes take place and cause morphological changes: 1) cellulose dehydration and 2) hemicellulose-lignin phase separation during steam explosion pretreatment with dilute acid or ammonia fiber expansion. A balance between the entropy and enthalpy of hydration is responsible to overcome kinetic obstacles. These findings suggest that new pretreatments favor hemicellulose/lignin phase separation and also the increase of the cell wall matrix porosity. Other considerations may include biomass molecular size, surface area, polarity, polarizability and strength of H-bonding. Additionally, solvent parameters such as refractive index, dielectric constant, molar volume and Hildebrand parameter may have also effect in biomass.

2.4.3.4.1 Lignocellulosic Biomass dissolution in Ionic Liquids

Ionic liquids (ILs) are salts of cations and anions that are liquid at ambient temperature; possess very low vapor pressure, low melting point (less than 100°C), good thermal stability and are inflammable [109, 216, 217]. The first report of cellulose dissolution in an ionic liquid (IL) was in 1934 (patent 1943176 USA). Later, Moens and Khan investigated the reactivity of the lignocellulosic derivatives and biomass in ILs in 2001 [218, 219]. Nevertheless, the significance of ILs in cellulose dissolution was not discovered until 2002 when Swatloski et al. [220] found

that 1-*n*-butyl-3-methylimidazolium chloride [C₄mim][Cl⁻] could dissolve cellulose up to 25 wt% by microwave heating, regenerating cellulose by adding water.

Recently, ionic liquids have been used to deconstruct biomass to its components. This can be done by two different ways 1) isolating hemicelluloses and lignin from cellulose and 2) dissolving cellulose in an IL followed by precipitation by adding anti-solvents [102, 109, 110, 113, 128, 146, 151, 152, 221-229]. The majority of cations in ILs are bulky organic residues such as imidazolium, pyridinium, pyrrolydinium, ammonium, phosphonium, piperidinium, thiazolium and sulfonium; anions can be halides, organic or inorganic anions [230]. ILs characteristics are high thermal stability, low flammability, high conductivity and a wide electrochemical potential window (-4 to 4 V) [231], thus due to these properties, ILs may have applications in both industrial [230] and laboratory settings [232, 233]. ILs can be considered as “designer solvents” [234, 235], their properties can be attuned to meet the needs of a specific method or desired product.

ILs have been employed in dissolution of both softwoods and hardwoods [236-241], grasses and agricultural wastes [152, 242-244], and in enzymatic saccharification of corn stover [245], straw [246], and macadamia nut shells [247]; as well as in the study of physical properties of bamboo [248]. Kilpelainen et al. [249] reported that both softwoods and hardwoods are soluble in some ILs based in imidazolium under mild environments, for instance, in chloride- and acetate-based ILs [250] and in 1-*n*-butyl-3-methylimidazolium chloride [C₄mim]Cl [251]. Rinaldi and Schuth [252, 253] have performed ¹³C and ^{35/37}Cl NMR measurements on models showing that cellulose dissolution in this IL involved H-bonding between the hydroxyl residues of the carbohydrates and the chloride ions of the IL solvent in a stoichiometrical relationship of 1:1.

Vanoye and his group [254] studied the kinetics of cellobiose acid hydrolysis in 1-ethyl-3-methylimidazolium chloride, ([C2mim]Cl) IL showing the presence of two competing reactions, hydrolysis of oligosaccharides and decomposition of sugar. The rates of these reactions were sensitive to acid pK_a below zero, for acids with pK_a the decomposition of glucose is slower than the hydrolysis, and therefore the hydrolysis could be conducted with high selectivity for glucose. Experimentally cellulose, hemicellulose (xylan), and *Miscanthus* grass biomass, showed similar hydrolysis rates and a random chain bond cleavage, contrary to end-group chain degradation detected with dilute acids.

It has been demonstrated that cellulose dissolution and regeneration using ILs is accompanied only with a physical change and chemical reactions occur depending on IL, and there is always some DP loss. A lower crystallinity with 1,3-dimethyl-imidazolium methyl phosphonate DMIMMPh IL was observed. FTIR spectra of the precipitated cellulose showed a C-O-C stretching $-(1\rightarrow4)$ -glycosyl bonds, indicating the regeneration of the amorphous cellulose. In XRD analyses, regenerated cellulose displayed an amorphous diffraction peak near 2θ of 21° , confirming its lower crystallinity [255]. Liu et al., 2014 [256] studied the dissolution of corn stover after regeneration, pine wood, poplar wood, wheat and rice straw in DMSO/AmimCl using a microwave and found that cellulose morphology changed from I to II. Pine wood showed the highest dissolving ability.

Lignocellulose dissolution with ILs was studied by Fort et al. in 2007 [242] by treating hardwoods and softwood with [C4mim][Cl] IL at 100°C from 2 to 24 h, this research group found that softwoods presented better dissolution than hardwoods. Then, a study conducted by Zavrel et al. [257] found that [C2mim] [CH₃COO] IL totally dissolved spruce, beech, and

chestnut chips and partially dissolved silver fir chips, hypothesizing that π - π interactions with the aromatic compounds of lignin have contributed to the biomass dissolution ability of this IL. It has been well established that cellulose dissolution in ILs is due to hydrogen bonding formation between anions of the IL and hydroxyl groups of cellulose [258, 259] at a 1:1 stoichiometric ratio [251]. During this process, the original inter- and intramolecular H-bonding of cellulose is destroyed allowing a complete cellulose dissolution [260]. Oxygen and hydrogen atoms of cellulose are involved in the formation of electron-donor electron-acceptor complexes that interact with the IL; IL ions are in a free state in solution and can interact with cellulose resulting in the formation of cation-cellulose-anion complexes (Figure 2-5) [172, 261]. In these interactions cellulose atoms act as electron donor and hydrogen atoms act as electron acceptors whereas the cation in IL serves as the electron acceptor and the anion as electron donor [261]. The oxygen and hydrogen atoms separates during the interactions causing distortions in the lattice of cellulose, the H-bond opens and finally cellulose dissolves [172]. This process is temperature dependent, the reaction between biomass and ILs starts around 80-90°C, cellulose swells and dissolves without much changes in its polydispersity, but significant changes in its crystallinity.

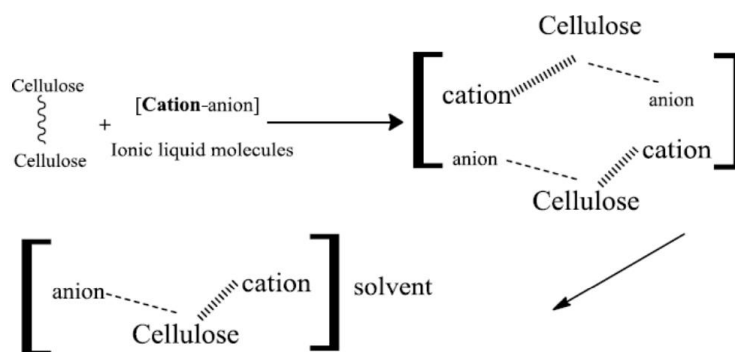


Figure 2-5 Mechanism of cellulose dissolution in ILs. Taken from [27]. Use under fair use.

Navard and Cuissinat [262, 263] have studied cellulose dissolution as a tool to reveal fiber structure. They found that different solvents have different pathways to dissolve cellulose and observed that cellulose dissolved in a “complete dissolution mode” described as a large swelling by ballooning and complete dissolution. These authors explained that primary and S1 layer of the biomass cell wall confine the IL in the balloons until a maximal swelling ratio is reached due to the osmotic pressure, then the balloons burst and the IL goes out rapidly (Figure 2-6). The elasticity and semi permeability of primary and S1 layer of the cell wall contribute to the balloon formation so that the cellulose dissolution process is due to the morphological structure of native cellulose and no delignification or hemicellulose removal occurs at temperatures 80-90°C. At temperatures higher than 100°C, lignin is soften (T_g of lignin between 100 and 170°C, [264]) and partial removal of lignin and hemicellulose occurs, indicating partial disruption of covalent linkages between cellulose and lignin of the LCC [265].

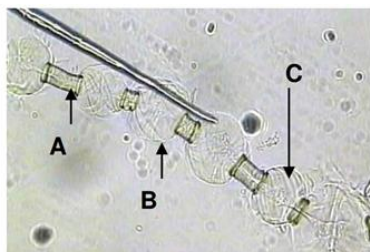
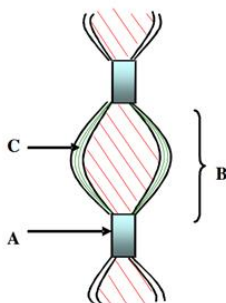


Figure 2-6: Wood fiber (Buckeye VFC) in NMMO – water (20%)



Schematic drawing of a swollen fiber of native cellulose

Figure 2-6 Swelling of cellulose fiber in IL (similar to swelling in NMMO-water (20%)). Taken from [32]. Use under fair use.

Different factors can affect the degree of delignification of biomass substrates during the pretreatment, temperature is one of the most important parameters to be taken into account, as well as the extent of the reaction. The higher the temperature and the longer the reaction time; the greater the amount of lignin and hemicellulose removal is observed. The most effective IL for cellulose and for lignocellulose biomass so far has been proven to be 1-ethyl-3-methylimidazolium acetate [C₂C₁Im][OAc] [109, 250, 257, 266-268]. Maki-Arvela et al. [269] has pointed out the relationship between IL's Hildebrand solubility parameters and hydrogen bond basicity. They found out that small polarizable anions aim at dissolution of cellulose. In this regard, [C₂C₁Im][OAc] IL has a small cation [C₂C₁Im]⁺ and a small anion [OAc]⁻ and both of them have been found to be powerful at cellulose and lignocellulose dissolution [250, 270]. Moreover, the chain length of the alkyl group impacts parameters such as melting point and viscosity [271, 272], the longer the length of the alkyl chain the higher the temperature for cellulose dissolution would be needed due to the higher viscosity; however elevated temperatures allow different lignin contents in the IL stream and favor formation of degradation products or undesired cellulose derivatization [110, 257, 273]. Through swelling of the cellulose fiber and an efficient mass transport, cellulose crystallinity is reduced and a partial removal of lignin and hemicellulose is achieved so the total surface area is increased [274, 275] and therefore enzyme hydrolysis is enhanced achieving better saccharification yields.

More recently, van Osch et al. [276] have published a comprehensive review of the ILs and DES in lignocellulose fractionation highlighting the tunability of the physicochemical properties of both solvent types by changing the nature and the ratio of their components. Regarding lignin dissolution with ILs, it has been observed that some aprotic and protic ILs can partially dissolve lignin and both anion and cation play important roles in dissolving lignin [276]. Janesko et al.

[277] found that cations or anions with electron rich aromatic π -systems improved lignin dissolution. For instance, imidazolium cations interact with lignin phenyl rings through aromatic rings. On the other hand, halide anions with hydrogen bonding capacity such as chloride or bromine have shown lignin solubility up to 10-15% wt% [278, 279]. A recent study has reported that good lignin ILs may combine $[\text{Cl}^-]$ anions and *p*-conjugated [1-*amyl*-3-methylimidazolium]⁺ cations [257]. In fact, ILs capability of lignin dissolution can be predicted through their polarities, comparing their Hildebrand solubility parameters to those of lignin. Maximum solubility has been observed when these values are the same, when the intermolecular forces are alike [273]. Moreover, Kamlet-Taft β parameter for hydrogen bond basicity helps to see if a solvent has good lignin dissolution properties, as moderate to high basic ILs are better lignin solvents [280]. Unfortunately, most of these studies have been conducted in commercial or model lignins which differ from the native lignin within the cell wall and does not represent the solubility of native lignin, their solubility does not necessarily represents all the interactions undergoing between native lignin and ILs within the cell wall.

Ionic liquids (PIL) that have a proton available for hydrogen bonding can also withdraw lignin from biomass [281]. Lignin extraction with PIL[pyrr][Ac] showed a great extent of fiber penetration. Partial dissolution of xylan, disrupted the biomass fibers enough to attain an increased unmodified lignin isolation. Tan and MacFarlane in 2009 [282] reviewed ILs in biomass conversion highlighting that they can be used for cellulose modification / functionalization, thermochemical depolymerization (pyrolysis), enzymatic depolymerization, fractionation, extraction/separation of biomass components and in biomass pretreatment. Some studies have shown that the presence of halogen can cause contamination of water [283]. For this reason, some halogen free ILs have been prepared using renewable compounds such as

bioalcohols and carboxylic acids as anions and/or alkylation agents, therefore halogen anions can be avoided [284]. Other issues such as cost and time consuming factor, difficult purification of ILs have limited their use in industrial settings [285]. The initial perception of ILs as green solvents has dramatically changed lately as green chemistry techniques such as environmental factor (E-factor), atom economy and greenness of some lab-scale preparative methods have been applied to several ILs [286-289]. Some studies have been published regarding the environmental potential risks linked to ILs preparation, environmental impacts in ILs application and their environmental fate [286].

2.5. Deep Eutectic Solvents

2.5.1 Concept

A deep eutectic solvent has been defined by Abbot et al. [290] as a mixture containing large nonsymmetric ions that have low lattice energy and low melting points. A DES is a mixture of a hydrogen bond donor (HBD) and a hydrogen bond acceptor (HBA) which forms a eutectic (melting temperature is lowered relative to the two individual components) when the two components are added together in a correct ratio [111].

The physicochemical properties of a DES depend upon its components and its exact molar ratio in the DES mixture, making them suitable for specific laboratory and industrial applications. Thus, these new media present some benefits such as immiscibility with many organic solvents, tolerance to water, tunable acidity, stabilization of intermediates, disruption of hydrogen bond networks, and dissolution of polyols [291].

2.5.2 Classification of DESs

In 2007, Abbott [292] has classified DES in four categories: Type I – mixture of a quaternary salt of a heteroatom with a metal halide, Type II which is a mixture of quaternary salt of a heteroatom with a hydrated metal halide, Type III which is a mixture of a quaternary salt of a heteroatom (HBA) with a hydrogen bond donor (HBD), type IV DES such a mixture of a metal halide with a hydrogen bond donor (HBD).

2.5.2.1 Type I DES, for instance $ZnCl_2$, $SnCl_2$, $FeCl_3$ with some quaternary ammonium salts can form DES, the properties depend upon the strength of the interactions between the DES components. Each system behave differently and is tailored for different applications [293, 294].

2.5.2.2 Type II DES, hydrates such as $CrCl_3 \cdot 6H_2O$ mixed with an organic salt such as choline chloride due to its low cost, biodegradability and low toxicity of the latter [293].

2.5.2.3 Type III DES, choline chloride based eutectic solvents have found an important role in applied chemistry. Choline chloride has been extensively used as HBA to produce DES mixtures with cheap and safe HBD such as polycarboxylic acids, polyamides and polyalcohol (most common used are urea, glycerol and ethylene glycol) [111, 295-297].

2.5.2.4 Type IV DES, mixtures of metal chlorides such as $ZnCl_2$ with a HBD such as urea, ethylene glycol, acetamide or hexanediol [293].

2.6 Type III DES: Choline chloride-glycerol - a mixture of choline chloride (HBA) and glycerol (HBD)

Choline-based DESs are the most common DESs used for different applications due to its relative low viscosity, low toxicity, biodegradability and low price [118, 293, 296]. Glyceline is a mixture of choline chloride with glycerol in a molar ratio of 1:2. Abbot et al. in 2011 [298]

reported a study of glycerol eutectics as solvent systems as well as their physico-chemical properties (viscosity, conductivity, density, free volume, self-diffusion coefficient and surface tension). The type III DESs possess similar physico-chemical properties to imidazolium-based ILs so that they can be replaced by the choline chloride based DESs in many applications. Zhang et al. [297] have highlighted fields of application such as lubrication, functional material preparation, electrochemistry, polishing and plating of metals, organic synthesis, catalytic conversion, and biomass conversion. The applicability of choline based eutectics in biocatalysis have been studied due to their compatibility with enzymes [293, 299, 300]. Dominguez de Maria [113] has also published the trend to use bio-based and low cost DESs in biomass processing as pretreatments, as cellulose dissolution agents or neoteric switchable solvents to fractionate biomass in biorefineries and in biomass conversion. Other research groups have also investigated the application of choline based solvents in natural products extraction [301-303].

2.6.1 Hydroxyethyltrimethylammonium (Choline) Chloride

Choline chloride (ChCl) is an organic salt that can be extracted from biomass or synthesized by the Davy process technology from ethylene oxide, hydrochloride acid, and trimethylamine [304], a high atom economy process [291]. In 1978, Petrouleas [305] studied the X-ray diffraction of ChCl and found two different types of crystalline forms Choline chloride could exist in two different forms, α and β form (Figure 2-7). The alpha form was sensitive for ionizing radiation and is present at room temperature. The polymorph β formed appeared at 78°C and it was non-sensitive to ionizing radiation [306, 307].

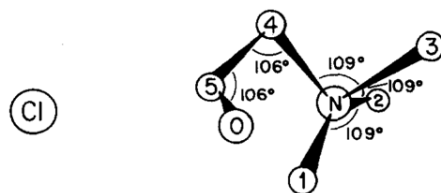


Figure 2-7 Molecular model of the β form of choline chloride. Taken from reference [25]. Use under fair use.

Choline chloride is used as a food additive for chickens and pets as well as additive in fluids (hydraulic fracturing). It is an important part of cell membrane phospholipids and as a neurotransmitter (acetylcholine). It is associated with the mobility of B vitamin in the body, due to its similarity. It is soluble in polar solvents and it does not accumulate in the body [308]. It is available in the market in the order of tons at US\$ 600-800/metric ton [309] or US\$ 320 for 5 kg [310].

Choline chloride is one of the most common quaternary ammonium salts used in the synthesis of DES [294, 295, 311, 312], when this compound is mixed with metal halides or HBD, the physico-chemical properties are usually enhanced. The melting point of the mixture at a particular ratio is significantly depressed, creating a eutectic and making it a liquid at ambient temperature [111]. For instance, choline chloride:urea has a melting point of 12°C, even though choline chloride and urea have a melting point of 302°C and 133°C, respectively [293]. These mixtures also have a lower viscosity and a higher conductivity than their pure components. This behavior is thought to be due to the fact that choline chloride has an asymmetric structure with a polar functional group (Figure 2-7) [293].

2.6.2 Glycerol – 1,2,3-Trihydroxpropane or glycerin

Glycerol is a polyol, an organic molecule found in nature forming esters in triglycerides and fats. It is a clear, viscous, colorless, odorless and sweet-tasting liquid [313]. It has been isolated since the 2800 BC by the reaction with ash to produce soap. It is a cheap and nonhazardous organic compound. Since 1940, glycerol has been produced from epichlorohydrine obtained from propylene, from fossil oil industry. Nowadays, glycerol is a by-product of the biodiesel fuel industry [314]. Traditionally, it has been used as viscosity modifier and a freezing point suppressant because its high viscosity and high boiling point. It has a strong hydrogen bond network cohesion and a high boiling point (290°C) [315]. These two properties also make glycerol not suitable as organic solvent for separation processes such as filtration or distillation [298]. It is a suitable feedstock for the production of several value-added chemicals (solvents, green reaction media, antifreeze agents, and detergents), fine chemicals (drugs, drug delivery systems, catalytic conversion, etc.), materials (polymers and biomaterials) and fuels and fuel additives [314-318]. The chemical structure of glycerol is shown in Figure 2-8.

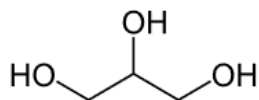


Figure 2-8 Structure of glycerol

Gu et al. [319] have reported that glycerol, due to its tolerance to the presence of hydrophobic reagents, can catalyze organic reactions such as Michael additions of amines, anilines and indols, ring opening of styrene oxide and acid-catalyzed dimerizations of tertiary alcohols. Also, He et al. have reported the use of glycerol as medium for electrophilic activation of aldehydes with indoles and 1,3-cyclohexandione, in the absence of a catalyst, to produce di(indolyl)methane derivatives. The authors hypothesized that it was a hydrogen bonding network between the

carbonyl group of the aldehyde and the OH group of the glycerol solvent. Glycerol has a high viscosity (1200 cP at room temperature), low toxicity and it is used as media to accelerate the reaction rates in hydrophobic substrates in organic synthesis [315]. Therefore, glycerol has properties similar to water such as hydrophilicity, non toxicity, biodegradability and poor miscibility with most organic substances.

2.6.3 *Glyceline, a choline chloride-glycerol DES mixture (1:2 molar ratio)*

In 2011, Abbott et al. studied the properties of glycerol after the addition of ChCl, in different ratios. The addition of 33 mol% of ChCl to glycerol had a tremendous effect in its fluidity, its viscosity decreased by a factor of 3 as the salt concentration increased. The viscosity-temperature profile of glyceline followed the Arrhenius like behavior. ChCl disrupted the structure of glycerol and enabled reactions on the OH groups that were no longer hydrogen bonded intermolecularly. The freezing point decreased from 17.8°C to – 40°C but the surface tension increased as the concentration of ChCl increased [298]. Figure 2-9 shows an scheme of glyceline, the mixture of a mole of choline chloride with two moles of glycerol components are mixed together under heat (80°C, for around 30 min) [116, 298].

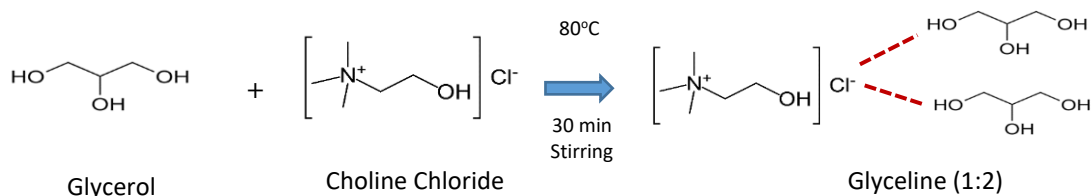


Figure 2-9 Schematic synthesis of glyceline. Adapted from [15, 38]

2.6.3.1 Physico-chemical properties of glyceline

When two different compounds are mixed together the new binary system will exhibit changes in at inter and intra-molecular levels, the new mixture present different properties. Table 2-3 summarizes the most common physico-chemical properties of glyceline.

Table 2-3 Properties of glyceline

Property	Glyceline	References
Molecular Weight (gmol ⁻¹)	107.94	Abbott et al., 2007 [320] Shahbaz et. al., 2012 [321] Mjalli et al, 2012 [322]
Density exp (gcm ⁻³)	1.19 1.1920 1.3558 1.192	Abbott et al., 2011 Shahbaz et al., 2012 [321] Leron & Li, 2012 [323]
Viscosity (cP)	376	Mjalli & Ahmed, 2016 [322]
Freezing Point (°C)	-36 -36.15 -40	Abbott et al. 2011 [298] Shahbaz et al., 2012 [321] AlOmar et al., 2012 [324]
Melting Point (°C)	No apparent	Harris, 2009 [325]
Surface Tension exp (mNm ⁻¹)	57.24 55.4	Shahbaz et al., 2012 [326] Abbott et al., 2014 [327]
Conductivity (μScm ⁻¹) at 20°C	2.03x10 ⁻³ 1.05 x10 ⁻³	Mjalli & Ahmed, 2016 [322] Abbott e al 2011 [298]
Molar Volume (cm ³ mol ⁻¹)	90.44 (at 20°C)	Mjalli & Ahmed, 2016 [322]
Molar Heat Capacity (303,15 K) (Jmol ⁻¹ K ⁻¹)	237.7	Leron & Li, 2012 [328]
Refractive Index	1.4864	Mjalli & Ahmed, 2016 [322]

2.6.3.2 Toxicity, cytotoxicity and biodegradability of glyceline

Hayyan et al. [329] have studied the toxicity of ChCl and its ChCl-glycyl DES, reline and ethaline DESs by using two gram positive bacteria *Bacillus subtilis* and *Staphylococcus aureus*, and also two gram negative bacteria *Escherichia coli* and *Pseudomonas aeruginosa*. Their cytotoxicity was investigated by using *Artemia salina* Linch. In general, all these DESs were not toxic and presented a higher cytotoxicity than the corresponding components, these results indicated that their toxicological effects were different depending upon the chemical structure of the DESs components. Other toxicological and biodegradable assessments of cholinium based DESs, reline, ethaline and metal containing salts) were carried out by Juneidi et al. [330]. Toxicity was evaluated by *Aspergillus niger* for pure and aqueous DESs, results showed that the minimum inhibitory concentration (MIC) ranged from 1 – 650 mgmL⁻¹. Acute toxicity was evaluated by lethal concentration at 50% of the concentration (LC₅₀) of the same DESs on *Cyprinius carpio* fish. The LC₅₀ varied from harmless to high toxic depending upon the chemical structure of the components, highly toxic for metal salts. However, DESs showed higher toxicity than their corresponding individual components and the dependence of the toxicity upon the DESs concentration was observed. Concerning biodegradability (closed bottle test), all DESs were readily biodegradable. More research needs to be conducted regarding toxicity and biodegradability before these DESs be applicable at large scale.

2.7 Interactions between choline chloride and glycerol

2.7.1 The hole theory: relationship between viscosity and conductivity

Abbott and his co-workers have developed the so-called “hole theory” to explain the similarity of physical and solvent properties of DESs mixtures with ILs [336]. These authors have highlighted that the use of ILs and DESs as solvents is due to their higher viscosity compared to molecular solvents and its effect upon the conductivity. The relative high viscosity in ambient temperature ILs is because ions have relative large radii (3-4 Å) compared to the radii of the voids (2 Å) [337, 338].

In another study for ILs conducted by Abbott et al., the authors shown that the viscosity of a fluid is related to the free volume and the probability to find voids of appropriate dimensions for the solvent molecules/ions to move into; this phenomenon was associated to the temperature of the system [339]. The depression of freezing point at the eutectic composition was connected to the mole fraction of the HBD in the eutectic mixture and the fluidity and charge transport were affected by small changes in chemical structure. Studying the probabilities of finding a hole of a particular radius r in a liquid, they showed that a decrease in the surface tension of the DES caused an increase in the free volume whereas a decrease in ions/molecules caused an increased in the conductivity. In each fluid the mobility of the ions/molecules was dependent upon the size of the voids, the size of migrating species and the radii of the cations and complexed anions. In the case of a DES, it was assumed that the anions move with the HBD as Abbot et al. have demonstrated for less viscous DES such as EtNH₃Cl⁻-acetamide and other more viscous DESs. These findings suggested that the Cl⁻ anion moved independently of the HBD and the mechanism of mass transport could change close to the freezing temperature. This research group also studied the dependence of conductivity on viscosity applying the equation (1) and confirmed that the protons EtNH₃⁺ were associated and not labile.

$$\kappa = \frac{z^2 F e}{6\pi\eta} \left(\frac{1}{R_+} + \frac{1}{R_-} \right) \frac{\rho}{M_w} \quad (1)$$

Where ρ is the density, M_w is the molar mass of fluid, z is the charge on the ion, F is the Faraday constant and e is the electronic charge. The results have showed that there are good correlations between the observed and calculated conductivities assuming that the anion is complexed with the HBD [339].

2.7.2 Intermolecular Interactions between HBD and HBA of a DES

2.7.2.1 Hydrogen bonding interactions

The main interactions in type III DES are hydrogen-bonds. A hydrogen-bond is formed when hydrogen atoms are bound by small and highly electronegative atoms such as O, N or F. A representation of an H-bond is shown in Figure 2-10 indicating a hydrogen bond donor (D) and hydrogen bond acceptor (A) [340].

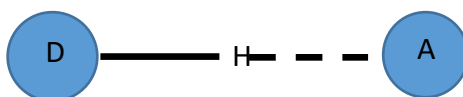


Figure 2-10 Schematic representation of a hydrogen bond

The reduction of lattice energy of the system occurs through the HBD that complexes to the anion (HBA) withdrawing the electron density of the anion from the cation (Figure 2-10), weakening the anion/cation interaction and also lowering the melting temperatures [325]. A hydrogen bond donor is a species which electronegativity relative to hydrogen in a covalent bond is such that the withdrawal of electrons leaves the proton partially unshielded and the bond becomes capable of donating the proton (Figure 2-11). To interact with this donor bond, the

acceptor species must have either a lone pair of electrons or polarizable π electrons. These hydrogen bonds are directional and the strength is 20 kJ mol^{-1} [325].

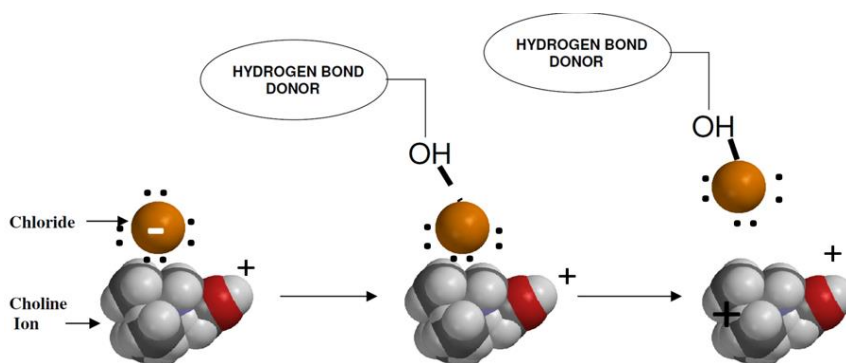


Figure 2-11 Schematic representation of the interaction between choline chloride (HBA) and glycerol (HBD). Adapted from [43]. Use under fair use.

ChCl has formed other eutectic mixtures with urea or ethylene glycol as well. In the case of ChCl:urea, at molar ratio 1:2 made a mixture with good solubility properties that dissolved inorganic salts, aromatic acids, aminoacids, and metal oxides (e.g. CuO) due to the high Cl^- anion concentration. These DESs formed strong hydrogen bonds and had also a high conductivity (cca. 1 mS cm^{-1} at 30°C) as the cation species was dissociated in the eutectic solvent and could move independently (Figure 2-11) [295]. Other DESs were made by mixing ChCl with dicarboxylic acids as HBD [111]. In this case, the molar ratio was 1:1, indicating that it was needed 1 mole of choline chloride and 1 mole of the dicarboxylic acid (two $-\text{COOH}$ functionalities) was needed to attain a eutectic, therefore confirming that each Cl^- anion interacted with two hydrogen bonds. These DESs had the rheology of a gel due to the fact that had many hydrogen bond donating groups in the system that caused bridging of the acids between neighboring Cl^- anions.

Hydrogen bonds and ionic interactions play a key role in determining macroscopic behavior in GLY. It is known that the HBD forms a complex with the Cl^- of the salt resulting in an asymmetric bulky moiety which decreases the lattice energy and therefore decrease the freezing point of the system [111]. More complex interactions can also be present if the HBD may ionize to some extent, leading to multiple ions within the DES.

A better understanding of the individual components can be achieved through a microscopic study. In this regard, pulsed field gradient NMR (PFG NMR), a technique to determine self-diffusion coefficients was used by Abbott research group to provide information on both molecular dynamics and molecular/ionic interactions between the species within the GLY mixture. D'Agostino et al. [341] investigated GLY using this technique and found that neutral HBD such as glycerol had faster long-range diffusion compare to that of the Ch^+ cation, due to its relative larger size. It was also found that in the anhydrous state GLY showed some non-Newtonian behavior but became Newtonian when the water content rose above 2.5 wt%. At higher water content, GLY had a high viscosity suggesting that glycerol was a strong HBD due to the fact that it had three hydroxyl groups [342]. In the plot of molar conductivity versus fluidity shown in Figure 2-12, a linear dependence was observed suggesting that viscosity controlled charge transport in this system, charge carriers being Ch^+ cation and Cl^- anion.

Wagle et al. [343] have studied the diffusion dynamics on the nanometer length scale of GLY and found that the mobility of Ch^+ cation was larger than glycerol mobility. This research group used quasielastic neutron scattering (QENS) as a tool to study the interparticle distances corresponding to pico — to nanosecond time scale. They studied GLY mixtures containing deuterated glycerol or deuterated ChCl to probe the diffusion dynamics of the HBD or Ch^+ cation within GLY. This experiment allowed them to make the following observations: 1) GLY

was a glass-forming liquid (no crystallization signs were detected upon heating from the glassy state at the baseline temperature), 2) the dynamics of GLY constituents exhibited vibrational degrees of freedom at microscopic levels; and 3) Ch^+ cation showed less elastic scattering than glycerol molecules. Therefore these observations allowed them to conclude that it was an enhancement in local diffusive displacements of Ch^+ cation compared to glycerol within glyceline.

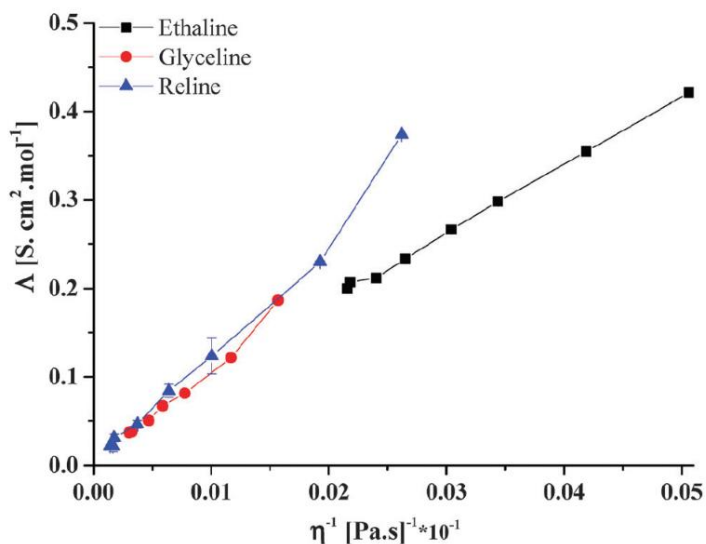


Figure 2-12 Molar conductivity versus fluidity of three DESs at 20°C. Taken from reference [45], Use under fair use.

Wagle and co-workers also observed that the GLY formed a complex of three components and possibly the Cl^- anion could participate in hydrogen bonding attracting enough proton density from both Ch^+ cation and glycerol, yielding an appreciable signal associated with its fast diffusional dynamics regardless of which GLY component was deuterated. The long-range diffusion of a DES has been analyzed by using the hole theory, as discussed above, suggesting that Ch^+ has the larger hydrodynamic radius (hard sphere radius of $\text{Ch}^+ = 3.39 \text{ \AA}$) compared to the glycerol hydrodynamic radius (hard sphere radius of glycerol = 3.00 \AA). A plot of transient

confinement versus temperature (Figure 2-13), shows that Ch^+ cation exhibited larger localized displacements.

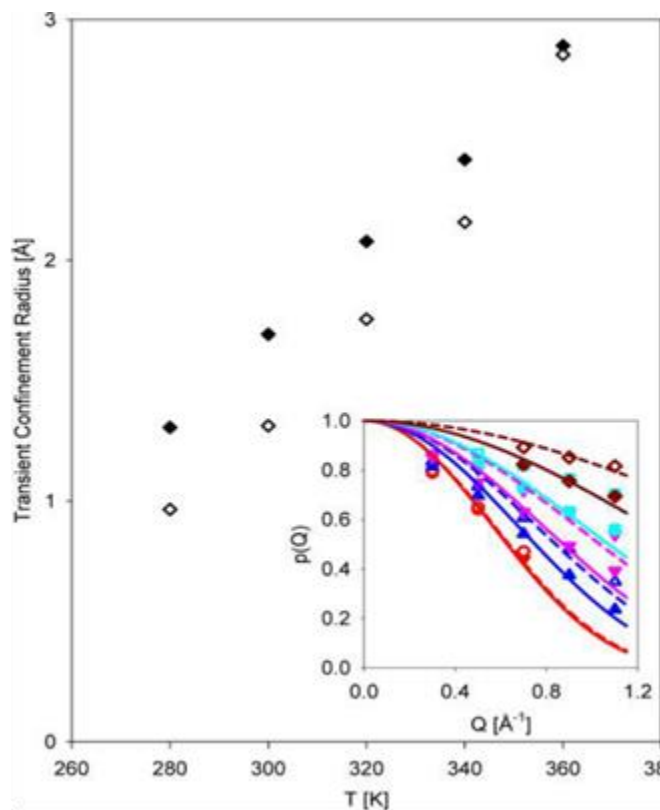


Figure 2-13 Temperature dependence of the transient confinement radius. Taken from reference [48]. Use under fair use.

2.7.2.2 Macro and nanoscale mobility of components within glyceline

The molecular orientations and the interactions between Ch^+ and Cl^- were crucial for understanding the mobility of the components within GLY. The question arisen in Wagle's study was if Ch^+ cation was larger in size how it could be less spatially restricted (Figure 2-14). Wagle et al. solved this question turning to simulations which revealed that the Cl^- anion played a key role in the formation of hydrogen bonded network. A competitive hydrogen bonding interaction was observed between glycerol and Ch^+ cation for binding with Cl^- anion.

Glycerol formed multiple tighter and stronger hydrogen bonds between its neighboring OH groups and Cl^- anion so that a closed ring type structure was formed (Figure 2-14), surpassing the lone hydroxyl group from Ch^+ cation. The distance between Cl^- anion and Ch^+ cation had increased to a large extent for GLY, indicating a reduced interaction within the eutectic mixture. These results explained the more restricted local mobility of glycerol, despite its smaller size compared to Ch^+ cation, therefore Ch^+ species experienced less restrictive local transient confinement than glycerol. Hence, at the nanometer scale, the long-range translational diffusion was strongly suppressed and the diffusive dynamics were dominated by the localized motions that were not affected by the confinement of the solvent [343].

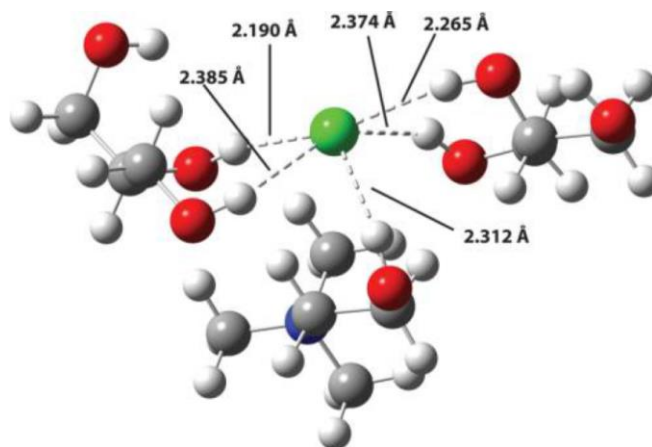


Figure 2-14 Simulation result showing that the hydrogen bonds formed between glycerol molecules and Cl^- dominate over those established between the Ch^+ cation and Cl^- anion energy-minimized structure, taken from [343]). Use under fair use.

2.7.2.3 Effect of temperature and water in glyceline

The properties of a DES are dependent of its components and external means as changes in temperature or addition of a cosolvent may considerably modify the main properties of a DES

and the interactions within the system. Most common DES are hygroscopic and GLY is, in fact GLY is miscible with water so that it is of a relevant importance to gain a better understanding of aqueous DES mixtures. Pandey A. and Pandey S. et al. [344] studied the effect of temperature and water by using solvatochromic probes dissolved in ChCl-gly and other ChCl-based DESs, to reveal insights on physicochemical properties and on solute-solvent interactions by using different absorbance probes to evaluate empirical solvent parameters and fluorescence probes to achieve information on DESs polarity. This research group assessed the effect of temperature on the response of betaine dye 33. Experimentally, they calculated the values for $E_T(30)_{\text{WATER}}$ and $E_T(30)_{\text{TMS}}$ as being 63.1 Kcal.mol⁻¹ and 30.7 Kcal.mol⁻¹, respectively. E_N^T was dimensionless and varied between 0 for TMS (non polar) and 1 for water (polar). The results showed that E_N^T decreased linearly as temperature increased within the three investigated DESs. This implied that dipolarity/polarizability or HBD acidity also decreased due to the average thermal reorientation of the dipoles [345]. Dipolarity/polarizability and HBA did not change with temperature. FTIR and Raman spectroscopy applied to these systems showed that the H-bonding interactions between DESs and added water were relevant for ethaline and ChCl-gly DES. As Pandey et al. [346] concluded in their work polarity of a solvent is difficult to define and assess quantitatively. At the molecular level, there were numerous solute-solvent interactions that the polarity of these complex mixtures could not be described by a single physical constant.

Nevertheless, the solubility of solvatochromic probes in DESs and in particular in ChCl-gly, have helped to evaluate the DES polarity in terms of the optical spectroscopic responses of UV-vis absorbance probes. The charge transfer of these probes is affected by the H-bonding ability and also by other solute-solvent interactions. Results obtained by Abbot and Pandey research groups have demonstrated that GLY is a dipolar solvent due to the presence of the OH groups

where an unequal sharing of electrons is present. Therefore this DES has a higher H-bonding capability reflected in the charge-transfer absorbance and fluorescence transitions of the solvatochromic probes.

2.7.2.4 Overall solvation capabilities of glyceline

In 2005, Reickardt reported an empirically polarity of ILs taking into account specific a non-specific interactions forces between HBDs and HBAs. A comparison of DESs to ILs allows us to describe these type of interactions for DESs as well. Among the specific interactions forces can be included HDB and HBA interactions, and solvophobic interactions. For the non-specific interaction forces, instantaneous-dipole / induced dipole forces (dispersion London force), dipole / induced dipole forces (induction or Debye forces), dipole / dipole forces (Coulomb forces). Therefore, the complexity of the DESs, herein of glyceline is due to the several interactions identified for these solvent systems.

Zhu et al. [347] simulated the vibrational modes of IR peaks of GLY to obtain more insights of the interactions between ChCl and glycerol in the DES mixture and made three important observations: 1) two gas-phase stable configurations (Figure 2-15), 2) OH groups from glycerol were the H bond donors and glycerol acted as HBD as well as HBA; and 3) weak electrostatic interactions between Cl⁻ and glycerol.

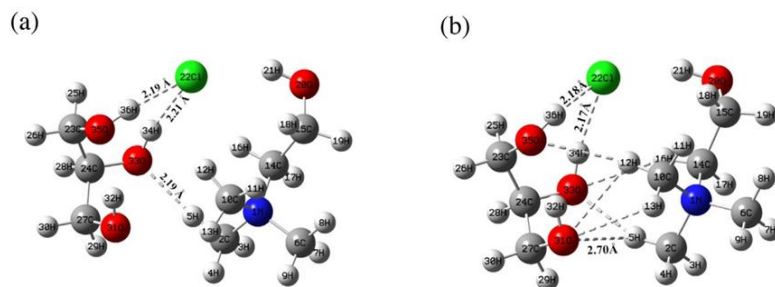


Figure 2-15 Vibrational modes of the IR peaks of glycylglycine. Taken from reference [316]. Use under fair use.

More recently, other computational studies conducted by Aissaoui et al. [348] confirmed that intermolecular interactions between Cl^- anion of ChCl and H atom of OH groups of glycerol were the main interactions in GLY, as previously reported. According to these authors, sigma profile interpretations of ChCl, glycerol and GLY showed three distinct regions: an electropositive region (HBD), a non polar region, and an electronegative region (HBA) (Figure 2-16). Hence, H atoms of OH of glycerol presented regions of high electropositivity (HBD) and had orientation towards the Cl^- anion of ChCl, H atoms in ChCl were not induced to build H bonds with an O atom in the glycerol molecule, Cl^- anion, highly negatively charged (HBA), attracted H-atoms of the glycerol molecule generating H-bonds. N atoms in the ammonium salt occurred in the non-polar region of the sigma profile as well as CH_2 and CH_3 moieties.

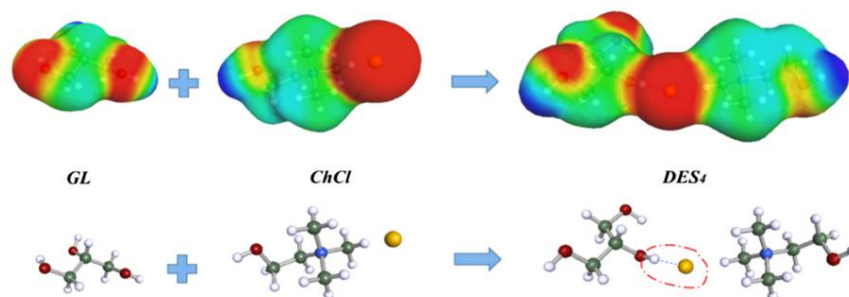


Figure 2-16 Charge densities of glycerol, ChCl and glycylglycine. Taken from [344]. Use under fair use.

2.8 Biomass solubility in deep eutectic solvents

In 2004, Abbot and co-workers [111] initiated the study of deep eutectic mixtures as novel solvents using quaternary ammonium salt blends such as choline chloride acting as hydrogen-bond acceptor and carboxylic acids or amides as hydrogen-bond donors. The eutectic mixtures were obtained by stirring the two components at around 100°C until a homogenous colorless liquid was produced. More recently, Francisco et al. [116] reported low transition temperature mixtures (LTTMs) as innovative solvents for biomass dissolution. Some natural amino acids with suitable functional groups as choline chloride and nicotinic acid, as well as different natural acids from fruits and vegetables were combined to obtain clear liquids. These mixtures were called LTTMs because they presented only glass transition temperatures in differential scanning calorimetry analysis. Some mixtures were screened as solvents for lignin, cellulose and starch. Their solubility was determined with the cloud point method (progressive addition of biopolymer to the LTTM in a range of 60-100°C). High selectivity for the separation of lignin was found with the mixture choline chloride-lactic acid whereas cellulose was found to be insoluble in these mixtures. Solubility tests of wheat straw biomass were carried out in histidine:lactic acid (1:2), under constant stirring for 24 h. LTTM solutions were colored, indicating some solubility of lignin. The remaining biomass was filtered and recovered with ethanol. Similarly, using the same lignocellulose biomass and the same reaction conditions but changing to ChCl-oxalic acid DES, Jablonky et al. [120] achieved a delignification of 57.9%.

More recently, Alvarez-Vasco et al. [331] has shown that treating poplar with ChCl-lactic acid at 145°C for 6 h, a lignin extraction yield of 78% can be reached and the lignin can be recovered from the DES liquor by adding a mixture of water-ethanol as antisolvent. These authors found that

some amount of DES was precipitated with lignin, suggesting strong interactions between DES with ChCl , these findings confirm Guo et al. work in which ChCl -based DESs were prepared with phenols [332]. Jablonsky et al. called this lignin DESL and ^{13}C -NMR studies showed that acidic DES favored β -O-4 cleavage without affecting C-C bond breakage in lignin. Moreover, Alvarez-Vasco et al. [331] have proposed a mechanism for this selective cleavage studying a lignin dimeric model compound guaiacylglycerol- β -guaiacyl ether (GBG) treated in ChCl -lactic acid DES at 145°C , finding that the reaction followed a mechanism similar to lignin acidolysis catalyzed by HCl (Figure 2-17). Interestingly, only small amounts of by-products were detected as opposed to lignin acidolysis. Furthermore, no recondensation products were found so biomass treated with DES can overcome one of the major disadvantages of kraft pulping processing. However, a mechanism of the interactions between a DES and native lignin has not yet been elucidated and deeper studies are required to gain a better understanding of lignin solubility and extraction from the lignocellulose to ensure the use of DESs in biomass conversion.

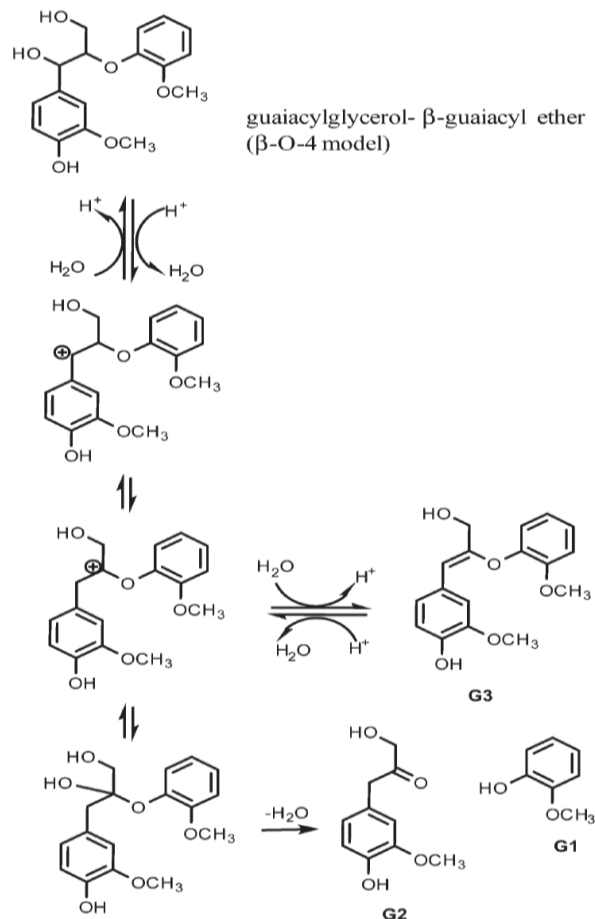


Figure 2-17 Mechanism of the β -O-4 linkage cleavage during the reaction between an acidic DES and lignin. Taken from reference [52]. Use under fair use.

2.8.1 Degradation Products from Lignocellulosic Biomass in the Biorefinery

Several degradation products can be formed during dilute acid and organosolv pretreatments of lignocellulosic biomass to obtain bioethanol or other biorefinery products. Compounds such as furans, organic acids, phenolics, pentoses (monomers and oligomers) and hexoses, depending heavily upon the reaction conditions have been detected [349]. Additionally, at high temperatures, biomass monosaccharides can produce pseudo-lignin [350, 351], humins [352, 353] and other compounds, in organosolv pretreatments including DESs, which can be inhibitors for biomass processing enzymes and microorganisms on the one hand, but in the other hand may be value-

added chemicals. The influence of the reaction conditions on the resulting products is crucial and needs to be taken into account in the designing of better biomass processing methods.

Efficient methods to enhanced deconstruction and dissolution of lignocellulosic biomass with recoveries of the three main biomass components are still under extensive research throughout the scientific community worldwide.

2.9 References

1. Nelson, P., E. Hood, and R. Powell, *The Bioeconomy: A New Era of Products Derived from Renewable Plant-Based Feedstock*. Chapter-1, Plant Biomass Conversion, 2010.
2. Cherubini, F., *The biorefinery concept: using biomass instead of oil for producing energy and chemicals*. Energy Conversion and Management, 2010. **51**(7): p. 1412-1421.
3. Chaturvedi, V. and P. Verma, *An overview of key pretreatment processes employed for bioconversion of lignocellulosic biomass into biofuels and value added products*. 3 Biotech, 2013. **3**(5): p. 415-431.
4. DeMartini, J.D., et al., *Investigating plant cell wall components that affect biomass recalcitrance in poplar and switchgrass*. Energy & Environmental Science, 2013. **6**(3): p. 898-909.
5. McCann, M.C. and N.C. Carpita, *Biomass recalcitrance: a multi-scale, multi-factor, and conversion-specific property*. Journal of Experimental Botany, 2015. **66**(14): p. 4109-4118.
6. Chandra, R.P., et al., *Substrate pretreatment: The key to effective enzymatic hydrolysis of lignocellulosics?*, in *Biofuels*. 2007, Springer. p. 67-93.
7. Zheng, Y., Z. Pan, and R.H. Zhang, *Overview of biomass pretreatment for cellulosic ethanol production*. International journal of agricultural and biological engineering, 2009. **2**(3): p. 51-68.
8. Mosier, N., et al., *Features of promising technologies for pretreatment of lignocellulosic biomass*. Bioresource technology, 2005. **96**(6): p. 673-686.
9. York, W.S. and M.A. O'Neill, *Biochemical control of xylan biosynthesis—which end is up?* Current opinion in plant biology, 2008. **11**(3): p. 258-265.
10. Bonawitz, N.D., et al., *Disruption of Mediator rescues the stunted growth of a lignin-deficient Arabidopsis mutant*. Nature, 2014. **509**(7500): p. 376-380.
11. Ciesielski, P.N., et al., *Engineering plant cell walls: tuning lignin monomer composition for deconstructable biofuel feedstocks or resilient biomaterials*. Green Chemistry, 2014. **16**(5): p. 2627-2635.
12. Van Acker, R., et al., *Improved saccharification and ethanol yield from field-grown transgenic poplar deficient in cinnamoyl-CoA reductase*. Proceedings of the National Academy of Sciences, 2014. **111**(2): p. 845-850.
13. Yuan, Y., et al., *The Arabidopsis DUF231 domain-containing protein ESK1 mediates 2-O-and 3-O-acetylation of xylosyl residues in xylan*. Plant and cell physiology, 2013: p. pct070.
14. Sjostrom, E., *Wood chemistry: fundamentals and applications*. 2013: Elsevier.
15. Ding, S.-Y., et al., *How does plant cell wall nanoscale architecture correlate with enzymatic digestibility?* Science, 2012. **338**(6110): p. 1055-1060.
16. Himmel, M.E., et al., *Biomass recalcitrance: engineering plants and enzymes for biofuels production*. science, 2007. **315**(5813): p. 804-807.
17. Fernandes, A.N., et al., *Nanostructure of cellulose microfibrils in spruce wood*. Proceedings of the National Academy of Sciences, 2011. **108**(47): p. E1195-E1203.
18. Thomas, L.H., et al., *Structure of cellulose microfibrils in primary cell walls from collenchyma*. Plant physiology, 2013. **161**(1): p. 465-476.
19. Donaldson, L., *Cellulose microfibril aggregates and their size variation with cell wall type*. Wood science and technology, 2007. **41**(5): p. 443-460.

20. Carpita, N.C., *Structure and biogenesis of the cell walls of grasses*. Annual review of plant biology, 1996. **47**(1): p. 445-476.
21. Carpita, N.C. and D.M. Gibeaut, *Structural models of primary cell walls in flowering plants: consistency of molecular structure with the physical properties of the walls during growth*. The Plant Journal, 1993. **3**(1): p. 1-30.
22. McCann, M. and K. Roberts, *Architecture of the primary cell wall*. The cytoskeletal basis of plant growth and form, 1991: p. 109-129.
23. Viëtor, R.J., et al., *Conformational features of crystal-surface cellulose from higher plants*. The Plant Journal, 2002. **30**(6): p. 721-731.
24. Kirk, T.K., *Degradation and conversion of lignocelluloses*. The filamentous fungi, 1983. **4**: p. 266-295.
25. Arantes, V. and B. Goodell, *Current Understanding of Brown-Rot Fungal Biodegradation Mechanisms: A Review*, in *Deterioration and Protection of Sustainable Biomaterials*, T.P. Schultz, B. Goodell, and D.D. Nicholas, Editors. 2014. p. 3-21.
26. Liese, W., *Ultrastructural aspects of woody tissue disintegration*. Annual Review of Phytopathology, 1970. **8**(1): p. 231-258.
27. Gilbertson, R.L., *Wood-rotting fungi of North America*. Mycologia, 1980. **72**(1): p. 1-49.
28. Wilcox, W.W., N. Parameswaran, and W. Liese, *Ultrastructure of brown rot in wood treated with pentachlorophenol*. Holzforschung-International Journal of the Biology, Chemistry, Physics and Technology of Wood, 1974. **28**(6): p. 211-217.
29. McFee, W. and E. Stone, *The persistence of decaying wood in the humus layers of northern forests*. Soil Science Society of America Journal, 1966. **30**(4): p. 513-516.
30. Eastwood, D.C., et al., *The plant cell wall—decomposing machinery underlies the functional diversity of forest fungi*. Science, 2011. **333**(6043): p. 762-765.
31. Hibbett, D.S. and M.J. Donoghue, *Analysis of character correlations among wood decay mechanisms, mating systems, and substrate ranges in homobasidiomycetes*. Systematic biology, 2001. **50**(2): p. 215-242.
32. Hori, C., et al., *Genomewide analysis of polysaccharides degrading enzymes in 11 white- and brown-rot Polyporales provides insight into mechanisms of wood decay*. Mycologia, 2013. **105**(6): p. 1412-1427.
33. Martinez, D., et al., *Genome, transcriptome, and secretome analysis of wood decay fungus Postia placenta supports unique mechanisms of lignocellulose conversion*. Proceedings of the National Academy of Sciences, 2009. **106**(6): p. 1954-1959.
34. Filley, T., et al., *Lignin demethylation and polysaccharide decomposition in spruce sapwood degraded by brown rot fungi*. Organic Geochemistry, 2002. **33**(2): p. 111-124.
35. Xu, G. and B. Goodell, *Mechanisms of wood degradation by brown-rot fungi: chelator-mediated cellulose degradation and binding of iron by cellulose*. Journal of Biotechnology, 2001. **87**(1): p. 43-57.
36. Daniel, G., *Use of electron microscopy for aiding our understanding of wood biodegradation*. FEMS microbiology reviews, 1994. **13**(2): p. 199-233.
37. Illman, B.L., D.C. Meinholtz, and T.L. Highley, *Oxygen free radical detection in wood colonized by the brown-rot fungus, Postia placenta*, in *Biodeterioration Research 2*. 1989, Springer. p. 497-509.
38. Sachs, I.B., I.T. Clark, and J.C. Pew. *Investigation of lignin distribution in the cell wall of certain woods*. in *Journal of Polymer Science Part C: Polymer Symposia*. 1963. Wiley Online Library.

39. Arantes, V., J. Jellison, and B. Goodell, *Peculiarities of brown-rot fungi and biochemical Fenton reaction with regard to their potential as a model for bioprocessing biomass*. Applied Microbiology and Biotechnology, 2012. **94**(2): p. 323-338.
40. Halliwell, G., *Catalytic decomposition of cellulose under biological conditions*. Biochem. j, 1965. **95**: p. 35-40.
41. Koenigs, J., *Effects of hydrogen peroxide on cellulose and on its susceptibility to cellulase*. Material und Organismen=, 1972.
42. Koenigs, J.W., *Production of hydrogen peroxide by wood-rotting fungi in wood and its correlation with weight loss, depolymerization, and pH changes*. Archives of Microbiology, 1974. **99**(1): p. 129-145.
43. Koenigs, J.W., *Hydrogen peroxide and iron: a microbial cellulolytic system?* Cellulose as a Chemical and Energy Resource, 1975.
44. Arantes, V. and A.M. Milagres, *Relevance of low molecular weight compounds produced by fungi and involved in wood biodegradation*. Química Nova, 2009. **32**(6): p. 1586-1595.
45. Blanchette, R.A., et al., *Cell wall alterations in loblolly pine wood decayed by the white-rot fungus, Ceriporiopsis subvermispora*. Journal of Biotechnology, 1997. **53**(2): p. 203-213.
46. Flournoy, D.S., T.K. Kirk, and T. Highley, *Wood decay by brown-rot fungi: changes in pore structure and cell wall volume*. Holzforschung-International Journal of the Biology, Chemistry, Physics and Technology of Wood, 1991. **45**(5): p. 383-388.
47. Dutton, M.V., et al., *Oxalate production by basidiomycetes, including the white-rot species Coriolus versicolor and Phanerochaete chrysosporium*. Applied Microbiology and Biotechnology, 1993. **39**(1): p. 5-10.
48. Goodell, B., et al., *Low molecular weight chelators and phenolic compounds isolated from wood decay fungi and their role in the fungal biodegradation of wood*. Journal of Biotechnology, 1997. **53**(2): p. 133-162.
49. Zhuang, L., et al., *Investigating oxalate biosynthesis in the wood-decaying fungus Gloeophyllum trabeum using 13 C metabolic flux analysis*. RSC Advances, 2015. **5**(126): p. 104043-104047.
50. Takao, S., *Organic acid production by basidiomycetes I. Screening of acid-producing strains*. Applied microbiology, 1965. **13**(5): p. 732-737.
51. Lee, S.O., et al., *Study on the kinetics of iron oxide leaching by oxalic acid*. International Journal of Mineral Processing, 2006. **80**(2): p. 144-152.
52. Arantes, V., et al., *Effect of pH and oxalic acid on the reduction of Fe 3+ by a biomimetic chelator and on Fe 3+ desorption/adsorption onto wood: Implications for brown-rot decay*. International Biodeterioration & Biodegradation, 2009. **63**(4): p. 478-483.
53. Hyde, S.M. and P.M. Wood, *A mechanism for production of hydroxyl radicals by the brown-rot fungus Coniophora puteana: Fe (III) reduction by cellobiose dehydrogenase and Fe (II) oxidation at a distance from the hyphae*. Microbiology, 1997. **143**(1): p. 259-266.
54. Goodell, B., D. Nicholas, and T. Schultz. *Brown-rot fungal degradation of wood: our evolving view*. in *Current knowledge of wood deterioration mechanisms and its impact on biotechnology and wood preservation. Symposium at the 221st National Meeting of the American Chemical Society, San Diego, California, USA, 1-5 April 2001*. 2003. American Chemical Society.

55. Goodell, B., Q. YUHUI, and J. Jellison. *Fungal decay of wood: Soft rot-brown rot-white rot*. in *ACS symposium series*. 2008. Oxford University Press.
56. Zhu, Y.L., et al., *Iron sequestration in brown-rot fungi by oxalate and the production of reactive oxygen species (ROS)*. *International Biodeterioration & Biodegradation*, 2016. **109**: p. 185-190.
57. Evans, C., *Enzymes and small molecular mass agents with lignocellulose degradation*. *FEMS Microbiology Reviews*, 1994. **13**: p. 235-240.
58. Schilling, J.S. and J. Jellison, *Oxalate regulation by two brown rot fungi decaying oxalate-amended and non-amended wood*. *Holzforschung*, 2005. **59**(6): p. 681-688.
59. Schilling, J.S., *Oxalate production and cation translocation during wood biodegradation by fungi*. 2006, USDA Forest Service.
60. Kerem, Z., K.A. Jensen, and K.E. Hammel, *Biodegradative mechanism of the brown rot basidiomycete *Gloeophyllum trabeum*: evidence for an extracellular hydroquinone-driven Fenton reaction*. *FEBS letters*, 1999. **446**(1): p. 49-54.
61. Hirano, T., H. Tanaka, and A. Enoki, *Extracellular substance from the brown-rot basidiomycete *Tyromyces palustris* that reduces molecular oxygen to hydroxyl radicals and ferric iron to ferrous iron*. *Journal of the Japan Wood Research Society (Japan)*, 1995.
62. Daniel, G., et al., *Characteristics of *Gloeophyllum trabeum* alcohol oxidase, an extracellular source of H₂O₂ in brown rot decay of wood*. *Applied and environmental microbiology*, 2007. **73**(19): p. 6241-6253.
63. Niemenmaa, O., A. Uusi-Rauva, and A. Hatakka, *Demethoxylation of [O¹⁴CH₃]-labelled lignin model compounds by the brown-rot fungi *Gloeophyllum trabeum* and *Poria (Postia) placenta**. *Biodegradation*, 2008. **19**(4): p. 555-565.
64. Wymelenberg, A.V., et al., *Comparative transcriptome and secretome analysis of wood decay fungi *Postia placenta* and *Phanerochaete chrysosporium**. *Applied and environmental microbiology*, 2010. **76**(11): p. 3599-3610.
65. Paszczynski, A., et al., *De Novo Synthesis of 4, 5-Dimethoxycatechol and 2, 5-Dimethoxyhydroquinone by the Brown Rot Fungus *Gloeophyllum trabeum**. *Applied and Environmental Microbiology*, 1999. **65**(2): p. 674-679.
66. Shimokawa, T., et al., *Production of 2, 5-dimethoxyhydroquinone by the brown-rot fungus *Serpula lacrymans* to drive extracellular Fenton reaction*. *Holzforschung*, 2004. **58**(3): p. 305-310.
67. Suzuki, M.R., et al., *Fungal hydroquinones contribute to brown rot of wood*. *Environmental microbiology*, 2006. **8**(12): p. 2214-2223.
68. Jellison, J., Y. Chen, and F. Fekete, *Regulation of hyphal sheath formation and bio-chelator production by the brown-rot fungi *Gloeophyllum trabeum* and *Postia placenta**. *Holzforschung*, 1997. **51**: p. 503-510.
69. Newcombe, D., et al., *Production of small molecular weight catalysts and the mechanism of trinitrotoluene degradation by several *Gloeophyllum* species*. *Enzyme and Microbial Technology*, 2002. **30**(4): p. 506-517.
70. Wei, D., et al., *Laccase and its role in production of extracellular reactive oxygen species during wood decay by the brown rot basidiomycete *Postia placenta**. *Applied and environmental microbiology*, 2010. **76**(7): p. 2091-2097.

71. Buettner, G.R., *The pecking order of free radicals and antioxidants: lipid peroxidation, α -tocopherol, and ascorbate*. Archives of biochemistry and biophysics, 1993. **300**(2): p. 535-543.
72. Halliwell, B. and J.M. Gutteridge, *Free radicals in biology and medicine*. Vol. 3. 1999: Oxford university press Oxford.
73. Goodell, B., et al., *Iron-reducing capacity of low-molecular-weight compounds produced in wood by fungi*. Holzforschung, 2006. **60**(6): p. 630-636.
74. Arantes, V. and A.M. Milagres, *Evaluation of different carbon sources for production of iron-reducing compounds by Wolfiporia cocos and Perenniporia medulla-panis*. Process Biochemistry, 2006. **41**(4): p. 887-891.
75. Cragg, S.M., et al., *Lignocellulose degradation mechanisms across the Tree of Life*. Current Opinion in Chemical Biology, 2015. **29**: p. 108-119.
76. Ek, M., et al., *Study on the selectivity of bleaching with oxygen-containing species*. Holzforschung-International Journal of the Biology, Chemistry, Physics and Technology of Wood, 1989. **43**(6): p. 391-396.
77. Hammel, K.E., et al., *Reactive oxygen species as agents of wood decay by fungi*. Enzyme and microbial technology, 2002. **30**(4): p. 445-453.
78. Kirk, T.K., et al., *Characteristics of cotton cellulose depolymerized by a brown-rot fungus, by acid, or by chemical oxidants*. Holzforschung-International Journal of the Biology, Chemistry, Physics and Technology of Wood, 1991. **45**(4): p. 239-244.
79. Kirk, T.K., *Effects of a brown-rot fungus, Lenzites trabea, on lignin in spruce wood*. Holzforschung-International Journal of the Biology, Chemistry, Physics and Technology of Wood, 1975. **29**(3): p. 99-107.
80. Kirk, T.K. and E. Adler, *Methoxyl-deficient structural elements in lignin of sweetgum decayed by a brown-rot fungus*. Acta Chem. Scand, 1970. **24**(3379): p. 90.
81. Koenig, A.B., et al., *NMR structural characterization of Quercus alba (white oak) degraded by the brown rot fungus, Laetiporus sulphureus*. Journal of wood chemistry and technology, 2010. **30**(1): p. 61-85.
82. Martínez, A.T., et al., *Selective lignin and polysaccharide removal in natural fungal decay of wood as evidenced by in situ structural analyses*. Environmental microbiology, 2011. **13**(1): p. 96-107.
83. Agosin, E., et al., *Solid-state fermentation of pine sawdust by selected brown-rot fungi*. Enzyme and microbial technology, 1989. **11**(8): p. 511-517.
84. Arantes, V., et al., *Lignocellulosic polysaccharides and lignin degradation by wood decay fungi: the relevance of nonenzymatic Fenton-based reactions*. Journal of industrial microbiology & biotechnology, 2011. **38**(4): p. 541-555.
85. Kleman-Leyer, K., et al., *Changes in molecular size distribution of cellulose during attack by white rot and brown rot fungi*. Applied and Environmental Microbiology, 1992. **58**(4): p. 1266-1270.
86. Highley, T.L. and W.V. Dashek, *Biotechnology in the study of brown-and white-rot decay*. Forest products biotechnology, 1998: p. 15-36.
87. Jin, L., T.P. Schultz, and D.D. Nicholas, *Structural characterization of brown-rotted lignin*. Holzforschung-International Journal of the Biology, Chemistry, Physics and Technology of Wood, 1990. **44**(2): p. 133-138.
88. Eriksson, K.-E.L., R. Blanchette, and P. Ander, *Microbial and enzymatic degradation of wood and wood components*. 2012: Springer Science & Business Media.

89. Yelle, D.J., et al., *Multidimensional NMR analysis reveals truncated lignin structures in wood decayed by the brown rot basidiomycete Postia placenta*. Environmental microbiology, 2011. **13**(4): p. 1091-1100.
90. Arantes, V., et al., *Biomimetic oxidative treatment of spruce wood studied by pyrolysis-molecular beam mass spectrometry coupled with multivariate analysis and C-13-labeled tetramethylammonium hydroxide thermochemolysis: implications for fungal degradation of wood*. Journal of Biological Inorganic Chemistry, 2009. **14**(8): p. 1253-1263.
91. Limayem, A. and S.C. Ricke, *Lignocellulosic biomass for bioethanol production: current perspectives, potential issues and future prospects*. Progress in Energy and Combustion Science, 2012. **38**(4): p. 449-467.
92. Millett, M.A., A.J. Baker, and L.D. Satter, *Pretreatments to enhance chemical, enzymatic, and microbiological attack of cellulosic materials*. 1976: US Department of Agriculture, Forest Service, Forest Products Laboratory.
93. Mood, S.H., et al., *Lignocellulosic biomass to bioethanol, a comprehensive review with a focus on pretreatment*. Renewable & Sustainable Energy Reviews, 2013. **27**: p. 77-93.
94. María, P.D.d., P.M. Grande, and W. Leitner, *Current Trends in Pretreatment and Fractionation of Lignocellulose as Reflected in Industrial Patent Activities*. Chemie Ingenieur Technik, 2015.
95. Behera, S., et al., *Importance of chemical pretreatment for bioconversion of lignocellulosic biomass*. Renewable & Sustainable Energy Reviews, 2014. **36**: p. 91-106.
96. Rydholm, S.A., *Pulping processes*. Pulping processes., 1965.
97. Garrote, G., et al., *Hydrothermal and pulp processing of Eucalyptus*. Bioresource Technology, 2003. **88**(1): p. 61-68.
98. Henriksson, M., et al., *Cellulose nanopaper structures of high toughness*. Biomacromolecules, 2008. **9**(6): p. 1579-1585.
99. Weinstock, A., et al., *A new environmentally benign technology and approach to bleaching kraft pulp. Polyoxometalates for selective delignification and waste mineralization*. New Journal of Chemistry, 1996. **20**(2): p. 269.
100. Spence, K.L., et al., *A comparative study of energy consumption and physical properties of microfibrillated cellulose produced by different processing methods*. Cellulose, 2011. **18**(4): p. 1097-1111.
101. Hu, L., et al., *Chemocatalytic hydrolysis of cellulose into glucose over solid acid catalysts*. Applied Catalysis B-Environmental, 2015. **174**: p. 225-243.
102. Yan, Y.J. and G.H. Jiang, *Recent Advances in Catalytic Conversion of Cellulose Into Variable Chemicals and Bio-Fuels*. Journal of Biobased Materials and Bioenergy, 2014. **8**(6): p. 553-569.
103. Wang, N., et al., *Effects of metal ions on the hydrolysis of bamboo biomass in 1-butyl-3-methylimidazolium chloride with dilute acid as catalyst*. Bioresource Technology, 2014. **173**: p. 399-405.
104. Wang, L., et al., *Selective Catalytic Production of 5-Hydroxymethylfurfural from Glucose by Adjusting Catalyst Wettability*. Chemsuschem, 2014. **7**(2): p. 402-406.
105. Xie, X.N., et al., *Selective conversion of microcrystalline cellulose into hexitols over a Ru/ Bmim (3)PW12O40 catalyst under mild conditions*. Catalysis Today, 2014. **233**: p. 70-76.

106. Xu, A., J. Wang, and H. Wang, *Effects of anionic structure and lithium salts addition on the dissolution of cellulose in 1-butyl-3-methylimidazolium-based ionic liquid solvent systems*. *Green chemistry*, 2010. **12**(2): p. 268-275.
107. Zhang, X., et al., *Phenolics production through catalytic depolymerization of alkali lignin with metal chlorides*. *BioResources*, 2014. **9**(2): p. 3347-3360.
108. Sun, R.Y., et al., *Versatile Nickel-Lanthanum(III) Catalyst for Direct Conversion of Cellulose to Glycols*. *Acs Catalysis*, 2015. **5**(2): p. 874-883.
109. Brandt, A., et al., *Deconstruction of lignocellulosic biomass with ionic liquids*. *Green Chemistry*, 2013. **15**(3): p. 550-583.
110. Badgujar, K.C. and B.M. Bhanage, *Factors governing dissolution process of lignocellulosic biomass in ionic liquid: Current status, overview and challenges*. *Bioresource technology*, 2015. **178**: p. 2-18.
111. Abbott, A.P., et al., *Deep eutectic solvents formed between choline chloride and carboxylic acids: Versatile alternatives to ionic liquids*. *Journal of the American Chemical Society*, 2004. **126**(29): p. 9142-9147.
112. Dai, Y., et al., *Natural deep eutectic solvents as new potential media for green technology*. *Anal Chim Acta*, 2013. **766**: p. 61-8.
113. de Maria, P.D., *Recent trends in (ligno)cellulose dissolution using neoteric solvents: switchable, distillable and bio-based ionic liquids*. *Journal of Chemical Technology and Biotechnology*, 2014. **89**(1): p. 11-18.
114. Gunny, A.A.N., et al., *Synergistic action of deep eutectic solvents and cellulases for lignocellulosic biomass hydrolysis*. *Materials Research Innovations*, 2014. **18**: p. 65-67.
115. Xu, C.P., et al., *Lignin depolymerisation strategies: towards valuable chemicals and fuels*. *Chemical Society Reviews*, 2014. **43**(22): p. 7485-7500.
116. Francisco, M., A. van den Bruinhorst, and M.C. Kroon, *New natural and renewable low transition temperature mixtures (LTTMs): screening as solvents for lignocellulosic biomass processing*. *Green Chemistry*, 2012. **14**(8): p. 2153-2157.
117. Cvjetko Bubalo, M., et al., *Green solvents for green technologies*. *Journal of Chemical Technology and Biotechnology*, 2015.
118. De Oliveira Vigier, K., G. Chatel, and F. Jerome, *Contribution of Deep Eutectic Solvents for Biomass Processing: Opportunities, Challenges, and Limitations*. *ChemInform*, 2015. **46**(26).
119. Gunny, A.A.N., et al., *Applicability evaluation of Deep Eutectic Solvents-Cellulase system for lignocellulose hydrolysis*. *Bioresource Technology*, 2015. **181**: p. 297-302.
120. Jablonský, M., et al., *Deep Eutectic Solvents: Fractionation of Wheat Straw*. *BioResources*, 2015. **10**(4): p. 8039-8047.
121. Procentese, A., et al., *Deep eutectic solvent pretreatment and subsequent saccharification of corncob*. *Bioresource Technology*, 2015. **192**: p. 31-36.
122. Kumar, A.K., B.S. Parikh, and M. Pravakar, *Natural deep eutectic solvent mediated pretreatment of rice straw: bioanalytical characterization of lignin extract and enzymatic hydrolysis of pretreated biomass residue*. *Environmental Science and Pollution Research*, 2015: p. 1-11.
123. Xu, G.-C., et al., *Enhancing cellulose accessibility of corn stover by deep eutectic solvent pretreatment for butanol fermentation*. *Bioresource Technology*, 2015.

124. Yiin, C., et al., *Screening of hydrogen bond acceptor for the synthesis of low transition temperature mixtures with malic acid*. Energy and Sustainability V: Special Contributions, 2015. **206**: p. 229.
125. Durand, E., J. Lecomte, and P. Villeneuve, *From green chemistry to nature: The versatile role of low transition temperature mixtures*. Biochimie, 2015.
126. Vigier, K.D., G. Chatel, and F. Jerome, *Contribution of Deep Eutectic Solvents for Biomass Processing: Opportunities, Challenges, and Limitations*. Chemcatchem, 2015. **7**(8): p. 1250-1260.
127. Cheng, G., et al., *Theory, practice and prospects of X- ray and neutron scattering for lignocellulosic biomass characterization: towards understanding biomass pretreatment*. Energy & Environmental Science, 2015. **8**(2): p. 436-455.
128. Maurya, D.P., A. Singla, and S. Negi, *An overview of key pretreatment processes for biological conversion of lignocellulosic biomass to bioethanol*. 3 Biotech, 2015. **5**(5): p. 597-609.
129. Hovland, M., *Are there commercial deposits of methane hydrates in ocean sediments?* Energy, Exploration & Exploitation, 2000. **18**(4): p. 339-347.
130. Bolonkin, A., et al., *Innovative unconventional oil extraction technologies*. Fuel Processing Technology, 2014. **124**: p. 228-242.
131. International, B., *U.S. ethanol plants*. 2016, Ethanol Producer Magazine.
132. Mabee, W.E., et al., *Canadian biomass reserves for biorefining*. Applied biochemistry and biotechnology, 2006. **129**(1-3): p. 22-40.
133. Menrad, K., A. Klein, and S. Kurka, *Interest of industrial actors in biorefinery concepts in Europe*. Biofuels, Bioproducts and Biorefining, 2009. **3**(3): p. 384-394.
134. Mandl, M.G., *Status of green biorefining in Europe*. Biofuels, Bioproducts and Biorefining, 2010. **4**(3): p. 268-274.
135. Hayes, D.J., *An examination of biorefining processes, catalysts and challenges*. Catalysis Today, 2009. **145**(1-2): p. 138-151.
136. Charlton, A., et al., *The biorefining opportunities in Wales: Understanding the scope for building a sustainable, biorenewable economy using plant biomass*. Chemical Engineering Research and Design, 2009. **87**(9): p. 1147-1161.
137. Chang, V.S. and M.T. Holtzapple. *Fundamental factors affecting biomass enzymatic reactivity*. in *Twenty-First Symposium on Biotechnology for Fuels and Chemicals*. 2000. Springer.
138. Kumar, R. and C.E. Wyman, *Does change in accessibility with conversion depend on both the substrate and pretreatment technology?* Bioresource technology, 2009. **100**(18): p. 4193-4202.
139. Jeoh, T., et al. *Measuring cellulase accessibility of dilute-acid pretreated corn stover*. in *Prepr Symp Am Chem Soc Div Fuel Chem*. 2005.
140. Ishizawa, C.I., et al., *Porosity and its effect on the digestibility of dilute sulfuric acid pretreated corn stover*. Journal of agricultural and food chemistry, 2007. **55**(7): p. 2575-2581.
141. Balat, M., *Production of bioethanol from lignocellulosic materials via the biochemical pathway: a review*. Energy conversion and management, 2011. **52**(2): p. 858-875.
142. Guo, M.X., W.P. Song, and J. Buhain, *Bioenergy and biofuels: History, status, and perspective*. Renewable & Sustainable Energy Reviews, 2015. **42**: p. 712-725.

143. Chundawat, S.P.S., et al., *Thermochemical pretreatment of lignocellulosic biomass*. Bioalcohol Production: Biochemical Conversion of Lignocellulosic Biomass, 2010(3): p. 24-72.
144. FitzPatrick, M., et al., *A biorefinery processing perspective: Treatment of lignocellulosic materials for the production of value-added products*. Bioresource Technology, 2010. **101**(23): p. 8915-8922.
145. Resch, M.G., et al., *Fungal cellulases and complexed cellulosomal enzymes exhibit synergistic mechanisms in cellulose deconstruction*. Energy & Environmental Science, 2013. **6**(6): p. 1858-1867.
146. Wahlstrom, R.M. and A. Suurnakki, *Enzymatic hydrolysis of lignocellulosic polysaccharides in the presence of ionic liquids*. Green Chemistry, 2015. **17**(2): p. 694-714.
147. Khanal, S.K., et al., *Bioenergy and biofuel from biowastes and biomass*. 2010: American Society of Civil Engineers (ASCE).
148. Silveira, M.H.L., et al., *Current Pretreatment Technologies for the Development of Cellulosic Ethanol and Biorefineries*. Chemsuschem, 2015. **8**(20): p. 3366-3390.
149. Yang, B. and C.E. Wyman, *Pretreatment: the key to unlocking low-cost cellulosic ethanol*. Biofuels, Bioproducts and Biorefining, 2008. **2**(1): p. 26-40.
150. Hendriks, A. and G. Zeeman, *Pretreatments to enhance the digestibility of lignocellulosic biomass*. Bioresource technology, 2009. **100**(1): p. 10-18.
151. Blanch, H.W., *Bioprocessing for biofuels*. Current Opinion in Biotechnology, 2012. **23**(3): p. 390-395.
152. Blanch, H.W., B.A. Simmons, and D. Klein-Marcuschamer, *Biomass deconstruction to sugars*. Biotechnology Journal, 2011. **6**(9): p. 1086-1102.
153. Chang, K.-L., et al., *Enhanced enzymatic conversion with freeze pretreatment of rice straw*. Biomass and Bioenergy, 2011. **35**(1): p. 90-95.
154. Hiden, A., et al., *Wet disk milling pretreatment without sulfuric acid for enzymatic hydrolysis of rice straw*. Bioresource Technology, 2009. **100**(10): p. 2706-2711.
155. Binod, P., et al., *Short duration microwave assisted pretreatment enhances the enzymatic saccharification and fermentable sugar yield from sugarcane bagasse*. Renewable Energy, 2012. **37**(1): p. 109-116.
156. Park, J., et al., *Use of mechanical refining to improve the production of low-cost sugars from lignocellulosic biomass*. Bioresource Technology, 2016. **199**: p. 59-67.
157. Mosier, N., et al., *Optimization of pH controlled liquid hot water pretreatment of corn stover*. Bioresource technology, 2005. **96**(18): p. 1986-1993.
158. Pérez, J., et al., *Optimizing liquid hot water pretreatment conditions to enhance sugar recovery from wheat straw for fuel-ethanol production*. Fuel, 2008. **87**(17): p. 3640-3647.
159. Kim, Y., N.S. Mosier, and M.R. Ladisch, *Enzymatic digestion of liquid hot water pretreated hybrid poplar*. Biotechnology Progress, 2009. **25**(2): p. 340-348.
160. Karunanithy, C. and K. Muthukumarappan, *Influence of extruder temperature and screw speed on pretreatment of corn stover while varying enzymes and their ratios*. Applied biochemistry and biotechnology, 2010. **162**(1): p. 264-279.
161. Karunanithy, C. and K. Muthukumarappan, *Optimization of alkali soaking and extrusion pretreatment of prairie cord grass for maximum sugar recovery by enzymatic hydrolysis*. Biochemical Engineering Journal, 2011. **54**(2): p. 71-82.

162. Öhgren, K., et al., *Effect of hemicellulose and lignin removal on enzymatic hydrolysis of steam pretreated corn stover*. *Bioresource technology*, 2007. **98**(13): p. 2503-2510.
163. Ballesteros, I., et al. *Ethanol production from steam-explosion pretreated wheat straw*. in *Twenty-Seventh Symposium on Biotechnology for Fuels and Chemicals*. 2006. Springer.
164. Gu, T.Y., M.A. Held, and A. Faik, *Supercritical CO₂ and ionic liquids for the pretreatment of lignocellulosic biomass in bioethanol production*. *Environmental Technology*, 2013. **34**(13-14): p. 1735-1749.
165. Teymour, F., et al., *Optimization of the ammonia fiber explosion (AFEX) treatment parameters for enzymatic hydrolysis of corn stover*. *Bioresource technology*, 2005. **96**(18): p. 2014-2018.
166. Lau, M.W. and B.E. Dale, *Cellulosic ethanol production from AFEX-treated corn stover using *Saccharomyces cerevisiae* 424A (LNH-ST)*. *Proceedings of the National Academy of Sciences*, 2009. **106**(5): p. 1368-1373.
167. Esteghlalian, A., et al., *Modeling and optimization of the dilute-sulfuric-acid pretreatment of corn stover, poplar and switchgrass*. *Bioresource Technology*, 1997. **59**(2): p. 129-136.
168. Varga, E., et al., *Pretreatment of corn stover using wet oxidation to enhance enzymatic digestibility*. *Applied biochemistry and biotechnology*, 2003. **104**(1): p. 37-50.
169. Jimenez, L., et al., *Organosolv pulping of olive tree trimmings by use of ethylene glycol/soda/water mixtures*. *Holzforchung*, 2004. **58**(2): p. 122-128.
170. Pan, X., et al., *The bioconversion of mountain pine beetle-killed lodgepole pine to fuel ethanol using the organosolv process*. *Biotechnology and bioengineering*, 2008. **101**(1): p. 39-48.
171. Zhu, Z., et al., *Comparative study of corn stover pretreated by dilute acid and cellulose solvent-based lignocellulose fractionation: Enzymatic hydrolysis, supramolecular structure, and substrate accessibility*. *Biotechnology and bioengineering*, 2009. **103**(4): p. 715-724.
172. Feng, L. and Z.-l. Chen, *Research progress on dissolution and functional modification of cellulose in ionic liquids*. *Journal of Molecular Liquids*, 2008. **142**(1): p. 1-5.
173. Dai, Y., et al., *Ionic liquids and deep eutectic solvents in natural products research: mixtures of solids as extraction solvents*. *Journal of natural products*, 2013. **76**(11): p. 2162-2173.
174. Yang, X., et al., *Effect of biopretreatment on thermogravimetric and chemical characteristics of corn stover by different white-rot fungi*. *Bioresource technology*, 2010. **101**(14): p. 5475-5479.
175. Wan, C. and Y. Li, *Microbial pretreatment of corn stover with *Ceriporiopsis subvermispora* for enzymatic hydrolysis and ethanol production*. *Bioresource Technology*, 2010. **101**(16): p. 6398-6403.
176. Zeng, Y., et al., *Comparative studies on thermochemical characterization of corn stover pretreated by white-rot and brown-rot fungi*. *Journal of agricultural and food chemistry*, 2011. **59**(18): p. 9965-9971.
177. Jung, S., et al., *Enhanced lignocellulosic biomass hydrolysis by oxidative lytic polysaccharide monooxygenases (LPMOs) GH61 from *Gloeophyllum trabeum**. *Enzyme and Microbial Technology*, 2015. **77**: p. 38-45.
178. Agbor, V.B., et al., *Biomass pretreatment: Fundamentals toward application*. *Biotechnology Advances*, 2011. **29**(6): p. 675-685.

179. Demirbas, M.F., *Biorefineries for biofuel upgrading: a critical review*. Applied Energy, 2009. **86**: p. S151-S161.
180. Kumar, P., et al., *Methods for pretreatment of lignocellulosic biomass for efficient hydrolysis and biofuel production*. Industrial & Engineering Chemistry Research, 2009. **48**(8): p. 3713-3729.
181. Singh, S., B.A. Simmons, and K.P. Vogel, *Visualization of Biomass Solubilization and Cellulose Regeneration During Ionic Liquid Pretreatment of Switchgrass*. Biotechnology and Bioengineering, 2009. **104**(1): p. 68-75.
182. Sathitsuksanoh, N., et al., *Solvent fractionation of lignocellulosic biomass*. Bioalcohol Production: Biochemical Conversion of Lignocellulosic Biomass, 2010(3): p. 122-140.
183. Barakat, A., et al., *Eco-friendly dry chemo-mechanical pretreatments of lignocellulosic biomass: Impact on energy and yield of the enzymatic hydrolysis*. Applied Energy, 2014. **113**: p. 97-105.
184. Huang, H.J., et al., *A review of separation technologies in current and future biorefineries*. Separation and Purification Technology, 2008. **62**(1): p. 1-21.
185. Paulova, L., et al., *Lignocellulosic ethanol: Technology design and its impact on process efficiency*. Biotechnology Advances, 2015. **33**(6): p. 1091-1107.
186. Beeson, W.T., et al., *Cellulose Degradation by Polysaccharide Monoxygenases*, in *Annual Review of Biochemistry, Vol 84*, R.D. Kornberg, Editor. 2015. p. 923-946.
187. Dimarogona, M., E. Topakas, and P. Christakopoulos, *Recalcitrant polysaccharide degradation by novel oxidative biocatalysts*. Applied Microbiology and Biotechnology, 2013. **97**(19): p. 8455-8465.
188. Harris, P.V., et al., *New enzyme insights drive advances in commercial ethanol production*. Current Opinion in Chemical Biology, 2014. **19**: p. 162-170.
189. Bhattacharya, A.S., A. Bhattacharya, and B.I. Pletschke, *Synergism of fungal and bacterial cellulases and hemicellulases: a novel perspective for enhanced bio-ethanol production*. Biotechnology Letters, 2015. **37**(6): p. 1117-1129.
190. Sun, Y. and J. Cheng, *Hydrolysis of lignocellulosic materials for ethanol production: a review*. Bioresource technology, 2002. **83**(1): p. 1-11.
191. Khare, S.K., A. Pandey, and C. Larroche, *Current perspectives in enzymatic saccharification of lignocellulosic biomass*. Biochemical Engineering Journal, 2015. **102**: p. 38-44.
192. Siqueira, G., et al., *Enhancement of cellulose hydrolysis in sugarcane bagasse by the selective removal of lignin with sodium chlorite*. Applied Energy, 2013. **102**: p. 399-402.
193. Hasunuma, T. and A. Kondo, *Consolidated bioprocessing and simultaneous saccharification and fermentation of lignocellulose to ethanol with thermotolerant yeast strains*. Process Biochemistry, 2012. **47**(9): p. 1287-1294.
194. Klose, H., et al., *Hyperthermophilic endoglucanase for in planta lignocellulose conversion*. Biotechnology for Biofuels, 2012. **5**.
195. McClendon, S.D., et al., *Thermoascus aurantiacus is a promising source of enzymes for biomass deconstruction under thermophilic conditions*. Biotechnology for Biofuels, 2012. **5**.
196. Gladden, J.M., et al., *Discovery and characterization of ionic liquid-tolerant thermophilic cellulases from a switchgrass-adapted microbial community*. Biotechnology for Biofuels, 2014. **7**.

197. Cobucci-Ponzano, B., et al., *Novel thermophilic hemicellulases for the conversion of lignocellulose for second generation biorefineries*. *Enzyme and Microbial Technology*, 2015. **78**: p. 63-73.
198. Limadinata, P.A., A.T. Li, and Z. Li, *Temperature-responsive nanobiocatalysts with an upper critical solution temperature for high performance biotransformation and easy catalyst recycling: efficient hydrolysis of cellulose to glucose*. *Green Chemistry*, 2015. **17**(2): p. 1194-1203.
199. Turner, P., G. Mamo, and E.N. Karlsson, *Potential and utilization of thermophiles and thermostable enzymes in biorefining*. *Microb Cell Fact*, 2007. **6**(9): p. 1-23.
200. Datta, S., et al., *Ionic liquid tolerant hyperthermophilic cellulases for biomass pretreatment and hydrolysis*. *Green Chemistry*, 2010. **12**(2): p. 338-345.
201. Fan, L., Y.H. Lee, and D.H. Beardmore, *Mechanism of the enzymatic hydrolysis of cellulose: effects of major structural features of cellulose on enzymatic hydrolysis*. *Biotechnology and Bioengineering*, 1980. **22**(1): p. 177-199.
202. Zeng, M., et al., *Microscopic examination of changes of plant cell structure in corn stover due to hot water pretreatment and enzymatic hydrolysis*. *Biotechnology and bioengineering*, 2007. **97**(2): p. 265-278.
203. Xu, F., Y.-C. Shi, and D. Wang, *X-ray scattering studies of lignocellulosic biomass: a review*. *Carbohydrate polymers*, 2013. **94**(2): p. 904-917.
204. McCormick, C.L., P.A. Callais, and B.H. Hutchinson Jr, *Solution studies of cellulose in lithium chloride and N, N-dimethylacetamide*. *Macromolecules*, 1985. **18**(12): p. 2394-2401.
205. Vasilakos, N.P. and D.M. Austgen, *Hydrogen-donor solvents in biomass liquefaction*. *Industrial & Engineering Chemistry Process Design and Development*, 1985. **24**(2): p. 304-311.
206. Cuissinat, C. and P. Navard. *Swelling and Dissolution of Cellulose Part 1: Free Floating Cotton and Wood Fibres in N-Methylmorpholine-N-oxide–Water Mixtures*. in *Macromolecular Symposia*. 2006. Wiley Online Library.
207. Ass, B.A., E. Frollini, and T. Heinze, *Studies on the homogeneous acetylation of cellulose in the novel solvent dimethyl sulfoxide/tetrabutylammonium fluoride trihydrate*. *Macromolecular bioscience*, 2004. **4**(11): p. 1008-1013.
208. Qi, H., et al., *The dissolution of cellulose in NaOH-based aqueous system by two-step process*. *Cellulose*, 2011. **18**(2): p. 237-245.
209. Barthel, S. and T. Heinze, *Acylation and carbanilation of cellulose in ionic liquids*. *Green Chemistry*, 2006. **8**(3): p. 301-306.
210. de Wild, P.J. and W.J.J. Huijgen, *Solvent-Based Biorefinery of Lignocellulosic Biomass*. *Biomass Power for the World*, 2015: p. 289.
211. Naran, R., et al., *Extraction and characterization of native heteroxylans from delignified corn stover and aspen*. *Cellulose*, 2009. **16**(4): p. 661-675.
212. Sun, R., et al., *Physico-chemical and structural characterization of hemicelluloses from wheat straw by alkaline peroxide extraction*. *Polymer*, 2000. **41**(7): p. 2647-2656.
213. Horvath, A.L., *Solubility of structurally complicated materials: I. Wood*. *Journal of physical and chemical reference data*, 2006. **35**(1): p. 77-92.
214. Akiba, T., A. Tsurumaki, and H. Ohno, *Induction of lignin solubility for a series of polar ionic liquids by the addition of a small amount of water*. *Green Chemistry*, 2017. **19**(9): p. 2260-2265.

215. Langan, P., et al., *Common processes drive the thermochemical pretreatment of lignocellulosic biomass*. *Green Chemistry*, 2014. **16**(1): p. 63-68.
216. Rogers, R.D. and K.R. Seddon, *Ionic liquids--solvents of the future?* *Science*, 2003. **302**(5646): p. 792-793.
217. Rogers, R.D. and G.A. Voth, *Ionic liquids*. *Accounts of chemical research*, 2007. **40**(11): p. 1077-1078.
218. Moens, L. and N. Khan, *Reactivity of lignocellulosic biomass derivatives in ionic liquids*. *Abstracts of Papers of the American Chemical Society*, 2001. **221**: p. U620-U621.
219. Moens, L. and N. Khan, *Application of room-temperature ionic liquids to the chemical processing of biomass-derived feedstocks*. *Green Industrial Applications of Ionic Liquids*, ed. R.D. Rogers, K.R. Seddon, and S. Volkov. Vol. 92. 2003. 157-171.
220. Swatloski, R.P., et al., *Ionic liquids: New solvents for non-derivitized cellulose dissolution*. *Abstracts of Papers of the American Chemical Society*, 2002. **224**: p. U622-U622.
221. Miyafuji, H., *Application of ionic liquids for effective use of woody biomass*. *Journal of Wood Science*, 2015. **61**(4): p. 343-350.
222. Zhang, S.J., et al., *Ionic liquid-based green processes for energy production*. *Chemical Society Reviews*, 2014. **43**(22): p. 7838-7869.
223. Sathitsuksanoh, N., A. George, and Y.H.P. Zhang, *New lignocellulose pretreatments using cellulose solvents: a review*. *Journal of Chemical Technology and Biotechnology*, 2013. **88**(2): p. 169-180.
224. Vancov, T., et al., *Use of ionic liquids in converting lignocellulosic material to biofuels*. *Renewable Energy*, 2012. **45**: p. 1-6.
225. Patel, D.D. and J.M. Lee, *Applications of ionic liquids*. *Chemical Record*, 2012. **12**(3): p. 329-355.
226. Chakraborty, S. and A. Gaikwad, *Production of Cellulosic Fuels*. *Proceedings of the National Academy of Sciences India Section a-Physical Sciences*, 2012. **82**(1): p. 59-69.
227. Hossain, M.M. and L. Aldous, *Ionic Liquids for Lignin Processing: Dissolution, Isolation, and Conversion*. *Australian Journal of Chemistry*, 2012. **65**(11): p. 1465-1477.
228. Mora-Pale, M., et al., *Room Temperature Ionic Liquids as Emerging Solvents for the Pretreatment of Lignocellulosic Biomass*. *Biotechnology and Bioengineering*, 2011. **108**(6): p. 1229-1245.
229. Tadesse, H. and R. Luque, *Advances on biomass pretreatment using ionic liquids: An overview*. *Energy & Environmental Science*, 2011. **4**(10): p. 3913-3929.
230. Plechkova, N.V. and K.R. Seddon, *Applications of ionic liquids in the chemical industry*. *Chemical Society Reviews*, 2008. **37**(1): p. 123-150.
231. Freudenmann, D., et al., *Ionic Liquids: New Perspectives for Inorganic Synthesis?* *Angewandte Chemie-International Edition*, 2011. **50**(47): p. 11050-11060.
232. Olivier-Bourbigou, H., L. Magna, and D. Morvan, *Ionic liquids and catalysis: Recent progress from knowledge to applications*. *Applied Catalysis a-General*, 2010. **373**(1-2): p. 1-56.
233. Zhong, T., et al., *Progress in the Application of Basic Ionic Liquids to Organic Synthesis*. *Chinese Journal of Organic Chemistry*, 2010. **30**(7): p. 981-987.
234. Guo, F., et al., *Synthesis and Applications of Ionic Liquids in Clean Energy and Environment: A Review*. *Current Organic Chemistry*, 2015. **19**(5): p. 455-468.

235. Siankevich, S., et al., *Enhanced Conversion of Carbohydrates to the Platform Chemical 5-Hydroxymethylfurfural Using Designer Ionic Liquids*. *Chemsuschem*, 2014. **7**(6): p. 1647-1654.
236. Kline, L.M., et al., *SIMPLIFIED DETERMINATION OF LIGNIN CONTENT IN HARD AND SOFT WOODS VIA UV-SPECTROPHOTOMETRIC ANALYSIS OF BIOMASS DISSOLVED IN IONIC LIQUIDS*. *Bioresources*, 2010. **5**(3): p. 1366-1383.
237. Xu, J.K., Y.C. Sun, and R.C. Sun, *Synergistic effects of ionic liquid plus alkaline pretreatments on eucalyptus: Lignin structure and cellulose hydrolysis*. *Process Biochemistry*, 2015. **50**(6): p. 955-965.
238. Qu, C., et al., *Dissolution and acetylation of ball-milled birch (*Betula platyphylla*) and bamboo (*Phyllostachys nigra*) in the ionic liquid Bmim Cl for HSQC NMR analysis*. *Holzforschung*, 2012. **66**(5): p. 607-614.
239. Wen, J.L., et al., *Structural elucidation of whole lignin from Eucalyptus based on preswelling and enzymatic hydrolysis*. *Green Chemistry*, 2015. **17**(3): p. 1589-1596.
240. Cox, B.J. and J.G. Ekerdt, *Pretreatment of yellow pine in an acidic ionic liquid: Extraction of hemicellulose and lignin to facilitate enzymatic digestion*. *Bioresource Technology*, 2013. **134**: p. 59-65.
241. Socha, A.M., et al., *Comparison of sugar content for ionic liquid pretreated Douglas-fir woodchips and forestry residues*. *Biotechnology for Biofuels*, 2013. **6**.
242. Fort, D.A., et al., *Can ionic liquids dissolve wood? Processing and analysis of lignocellulosic materials with 1-n-butyl-3-methylimidazolium chloride*. *Green Chemistry*, 2007. **9**(1): p. 63-69.
243. Brandt, A., et al., *The effect of the ionic liquid anion in the pretreatment of pine wood chips*. *Green Chemistry*, 2010. **12**(4): p. 672-679.
244. Brandt, A., et al., *Ionic liquid pretreatment of lignocellulosic biomass with ionic liquid-water mixtures*. *Green Chemistry*, 2011. **13**(9): p. 2489-2499.
245. He, Y.C., et al., *Enhancement of enzymatic saccharification of corn stover with sequential Fenton pretreatment and dilute NaOH extraction*. *Bioresource Technology*, 2015. **193**: p. 324-330.
246. Fu, D.B., G. Mazza, and Y. Tamaki, *Lignin Extraction from Straw by Ionic Liquids and Enzymatic Hydrolysis of the Cellulosic Residues*. *Journal of Agricultural and Food Chemistry*, 2010. **58**(5): p. 2915-2922.
247. Teh, W.X., et al., *Pretreatment of Macadamia Nut Shells with Ionic Liquids Facilitates Both Mechanical Cracking and Enzymatic Hydrolysis*. *ACS Sustainable Chemistry & Engineering*, 2015. **3**(5): p. 992-999.
248. Muhammad, N., et al., *Effect of ionic liquid on thermo-physical properties of bamboo biomass*. *Wood Science and Technology*, 2015. **49**(5): p. 897-913.
249. Kilpelainen, I., et al., *Dissolution of wood in ionic liquids*. *Journal of Agricultural and Food Chemistry*, 2007. **55**(22): p. 9142-9148.
250. Zhao, H., et al., *Regenerating cellulose from ionic liquids for an accelerated enzymatic hydrolysis*. *Journal of Biotechnology*, 2009. **139**(1): p. 47-54.
251. Remsing, R.C., et al., *Mechanism of cellulose dissolution in the ionic liquid 1-n-butyl-3-methylimidazolium chloride: a ¹³C and ^{35/37}Cl NMR relaxation study on model systems*. *Chemical Communications*, 2006(12): p. 1271-1273.
252. Rinaldi, R. and F. Schuth, *Design of solid catalysts for the conversion of biomass*. *Energy & Environmental Science*, 2009. **2**(6): p. 610-626.

253. Rinaldi, R. and F. Schuth, *Acid Hydrolysis of Cellulose as the Entry Point into Biorefinery Schemes*. Chemsuschem, 2009. **2**(12): p. 1096-1107.
254. Vanoye, L., et al., *Kinetic model for the hydrolysis of lignocellulosic biomass in the ionic liquid, 1-ethyl-3-methyl-imidazolium chloride*. Green Chemistry, 2009. **11**(3): p. 390-396.
255. Hassan, E., F. Mutelet, and M. Bouroukba, *Experimental and theoretical study of carbohydrate-ionic liquid interactions*. Carbohydrate Polymers, 2015. **127**: p. 316-324.
256. Liu, J.F., et al., *Enhanced saccharification of lignocellulosic biomass with 1-allyl-3-methylimidazolium chloride (AmimCl) pretreatment*. Chinese Chemical Letters, 2014. **25**(11): p. 1485-1488.
257. Zavrel, M., et al., *High-throughput screening for ionic liquids dissolving (ligno-)cellulose*. Bioresource Technology, 2009. **100**(9): p. 2580-2587.
258. Swatloski, R.P., et al., *Dissolution of cellose with ionic liquids*. Journal of the American Chemical Society, 2002. **124**(18): p. 4974-4975.
259. Moulthrop, J.S., et al., *High-resolution ¹³C NMR studies of cellulose and cellulose oligomers in ionic liquid solutions*. Chemical Communications, 2005(12): p. 1557-1559.
260. Zhang, H., et al., *1-Allyl-3-methylimidazolium chloride room temperature ionic liquid: a new and powerful nonderivatizing solvent for cellulose*. Macromolecules, 2005. **38**(20): p. 8272-8277.
261. Hina, S., Y. Zhang, and H. Wang, *ROLE OF IONIC LIQUIDS IN DISSOLUTION AND REGENERATION OF CELLULOSE*. Rev. Adv. Mater. Sci, 2015. **40**: p. 215-226.
262. Navard, P. and I. ebrary, *The European polysaccharide network of excellence (EPNOE): research initiatives and results*. 1. Aufl.;1; ed. 2012, New York: Springer.
263. Cuissinat, C., P. Navard, and T. Heinze, *Swelling and dissolution of cellulose, Part V: cellulose derivatives fibres in aqueous systems and ionic liquids*. Cellulose, 2008. **15**(1): p. 75-80.
264. Irvine, G.M., *THE GLASS TRANSITIONS OF LIGNIN AND HEMICELLULOSE AND THEIR MEASUREMENT BY DIFFERENTIAL THERMAL-ANALYSIS*. Tappi Journal, 1984. **67**(5): p. 118-121.
265. Jin, Z., et al., *Covalent linkages between cellulose and lignin in cell walls of coniferous and nonconiferous woods*. Biopolymers, 2006. **83**(2): p. 103-110.
266. Froschauer, C., et al., *Separation of hemicellulose and cellulose from wood pulp by means of ionic liquid/cosolvent systems*. Biomacromolecules, 2013. **14**(6): p. 1741-1750.
267. Groff, D., et al., *Acid enhanced ionic liquid pretreatment of biomass*. Green Chemistry, 2013. **15**(5): p. 1264-1267.
268. Sun, N., et al., *Complete dissolution and partial delignification of wood in the ionic liquid 1-ethyl-3-methylimidazolium acetate*. Green Chemistry, 2009. **11**(5): p. 646-655.
269. Maki-Arvela, P., et al., *Dissolution of lignocellulosic materials and its constituents using ionic liquids-A review*. Industrial Crops and Products, 2010. **32**(3): p. 175-201.
270. Kosan, B., C. Michels, and F. Meister, *Dissolution and forming of cellulose with ionic liquids*. Cellulose, 2008. **15**(1): p. 59-66.
271. Kuhlmann, E., et al., *Imidazolium dialkylphosphates—a class of versatile, halogen-free and hydrolytically stable ionic liquids*. Green Chemistry, 2007. **9**(3): p. 233-242.
272. Sathitsuksanoh, N., et al., *How Alkyl Chain Length of Alcohols Affects Lignin Fractionation and Ionic Liquid Recycle During Lignocellulose Pretreatment*. BioEnergy Research, 2015. **8**(3): p. 973-981.

273. Wang, X., et al., *Cellulose extraction from wood chip in an ionic liquid 1-allyl-3-methylimidazolium chloride (AmimCl)*. *Bioresource technology*, 2011. **102**(17): p. 7959-7965.
274. Arora, R., et al., *Monitoring and analyzing process streams towards understanding ionic liquid pretreatment of switchgrass (Panicum virgatum L.)*. *BioEnergy Research*, 2010. **3**(2): p. 134-145.
275. Li, W.Y., et al., *Rapid dissolution of lignocellulosic biomass in ionic liquids using temperatures above the glass transition of lignin*. *Green Chemistry*, 2011. **13**(8): p. 2038-2047.
276. van Osch, D., et al., *Ionic liquids and deep eutectic solvents for lignocellulosic biomass fractionation*. *Physical Chemistry Chemical Physics*, 2017. **19**(4): p. 2636-2665.
277. Janesko, B.G., *Modeling interactions between lignocellulose and ionic liquids using DFT-D*. *Physical Chemistry Chemical Physics*, 2011. **13**(23): p. 11393-11401.
278. Pu, Y., N. Jiang, and A.J. Ragauskas, *Ionic liquid as a green solvent for lignin*. *Journal of Wood Chemistry and Technology*, 2007. **27**(1): p. 23-33.
279. Lee, S.H., et al., *Ionic Liquid-Mediated Selective Extraction of Lignin From Wood Leading to Enhanced Enzymatic Cellulose Hydrolysis*. *Biotechnology and Bioengineering*, 2009. **102**(5): p. 1368-1376.
280. Lee, J.-M., S. Ruckes, and J.M. Prausnitz, *Solvent polarities and kamlet-taft parameters for ionic liquids containing a pyridinium cation*. *The Journal of Physical Chemistry B*, 2008. **112**(5): p. 1473-1476.
281. Achinivu, E.C., et al., *Lignin extraction from biomass with protic ionic liquids*. *Green Chemistry*, 2014. **16**(3): p. 1114-1119.
282. Tan, S.S.Y. and D.R. MacFarlane, *Ionic Liquids in Biomass Processing*, in *Ionic Liquids*, B. Kirchner, Editor. 2009. p. 311-339.
283. Mikkola, S.K., et al., *Impact of Amphiphilic Biomass-Dissolving Ionic Liquids on Biological Cells and Liposomes*. *Environmental Science & Technology*, 2015. **49**(3): p. 1870-1878.
284. Wasserscheid, P., A. Bösmann, and R. Van Hal, *Halogen-free ionic liquids*. 2011, Google Patents.
285. Jouzani, G.S. and M.J. Taherzadeh, *Advances in consolidated bioprocessing systems for bioethanol and butanol production from biomass: a comprehensive review*. *Biofuel Research Journal-Brj*, 2015. **2**(1): p. 152-195.
286. Bubalo, M.C., et al., *A brief overview of the potential environmental hazards of ionic liquids*. *Ecotoxicology and environmental safety*, 2014. **99**: p. 1-12.
287. Cvjetko, M., J. Vorkapić-Furač, and P. Žnidaršič-Plazl, *Isoamyl acetate synthesis in imidazolium-based ionic liquids using packed bed enzyme microreactor*. *Process Biochemistry*, 2012. **47**(9): p. 1344-1350.
288. Deetlefs, M. and K.R. Seddon, *The green synthesis of ionic liquids*. *Handbook of Green Chemistry*, 2010.
289. Sheldon, R.A., *The E factor: fifteen years on*. *Green Chemistry*, 2007. **9**(12): p. 1273-1283.
290. Smith, E.L., A.P. Abbott, and K.S. Ryder, *Deep eutectic solvents (DESs) and their applications*. *Chemical reviews*, 2014. **114**(21): p. 11060-11082.

291. Vigier, K.D.O. and F. Jérôme, *Choline Chloride-Derived ILs for Activation and Conversion of Biomass*, in *Production of Biofuels and Chemicals with Ionic Liquids*. 2014, Springer. p. 61-87.
292. Abbott, A.P., et al., *Eutectic-Based Ionic Liquids with Metal-Containing Anions and Cations*. *Chemistry—A European Journal*, 2007. **13**(22): p. 6495-6501.
293. Zhang, Q., et al., *Deep eutectic solvents: syntheses, properties and applications*. *Chemical Society Reviews*, 2012. **41**(21): p. 7108-7146.
294. Abbott, A.P., et al., *Quaternary ammonium zinc-or tin-containing ionic liquids: water insensitive, recyclable catalysts for Diels–Alder reactions*. *Green Chemistry*, 2002. **4**(1): p. 24-26.
295. Abbott, A.P., et al., *Novel solvent properties of choline chloride/urea mixtures*. *Chemical Communications*, 2003(1): p. 70-71.
296. Yingying, Z., et al., *Properties and applications of choline-based deep eutectic solvents*. *Progress in Chemistry*, 2013. **6**: p. 003.
297. Zhang, Y.Y., et al., *Properties and Applications of Choline-Based Deep Eutectic Solvents*. *Progress in Chemistry*, 2013. **25**(6): p. 881-892.
298. Abbott, A.P., et al., *Glycerol eutectics as sustainable solvent systems*. *Green Chemistry*, 2011. **13**(1): p. 82-90.
299. Lindberg, D., M. de la Fuente Revenga, and M. Widersten, *Deep eutectic solvents (DESs) are viable cosolvents for enzyme-catalyzed epoxide hydrolysis*. *Journal of biotechnology*, 2010. **147**(3): p. 169-171.
300. Huang, Z.L., et al., *Deep eutectic solvents can be viable enzyme activators and stabilizers*. *Journal of Chemical Technology and Biotechnology*, 2014. **89**(12): p. 1975-1981.
301. Zhao, B.Y., et al., *Biocompatible Deep Eutectic Solvents Based on Choline Chloride: Characterization and Application to the Extraction of Rutin from Sophora japonica*. *ACS Sustainable Chemistry & Engineering*, 2015. **3**(11): p. 2746-2755.
302. Cvjetko Bubalo, M., et al., *Green extraction of grape skin phenolics by using deep eutectic solvents*. *Food Chemistry*, 2016. **200**: p. 159-166.
303. Dai, Y., et al., *Application of natural deep eutectic solvents to the extraction of anthocyanins from Catharanthus roseus with high extractability and stability replacing conventional organic solvents*. *Journal of Chromatography A*, 2016. **1434**: p. 50-56.
304. Wikipedia, *Choline Chloride*, in *Wikipedia*. 2015, Wikimedia Foundation: n.p.
305. Petrouleas, V., R.M. Lemmon, and A. Christensen, *X-RAY-DIFFRACTION STUDY OF CHOLINE CHLORIDES BETA-FORM*. *Journal of Chemical Physics*, 1978. **68**(5): p. 2243-2246.
306. Senko, M.E. and D.H. Templeton, *UNIT CELLS OF CHOLINE HALIDES AND STRUCTURE OF CHOLINE CHLORIDE*. *Acta Crystallographica*, 1960. **13**(4): p. 281-285.
307. Hjortas, J. and H. Sorum, *RE-INVESTIGATION OF CRYSTAL STRUCTURE OF CHOLINE CHLORIDE*. *Acta Crystallographica Section B-Structural Crystallography and Crystal Chemistry*, 1971. **B 27**(JUL15): p. 1320-&.
308. Aldrich, G. *Dealing with choline chloride - Petfood Industry*. 2008 [cited 2016 7/12/2016].
309. Group, A. *Chemicals*. 2016 [cited 2016 7/12/2016].
310. SIGMA-ALDRICH. *Products*. 2016 [cited 2016 7/12/2016].

311. Rengstl, D., *Choline as a cation for the design of low-toxic and biocompatible ionic liquids, surfactants, and deep eutectic solvents*. 2014.
312. Abbas, Q. and L. Binder, *Synthesis and characterization of choline chloride based binary mixtures*. ECS Transactions, 2010. **33**(7): p. 49-59.
313. Gu, Y. and F. Jérôme, *Glycerol as a sustainable solvent for green chemistry*. Green Chemistry, 2010. **12**(7): p. 1127-1138.
314. Pagliaro, M., et al., *From glycerol to value-added products*. Angewandte Chemie International Edition, 2007. **46**(24): p. 4434-4440.
315. Wolfson, A., et al., *Glycerol derivatives as green reaction mediums*. Green Chemistry Letters and Reviews, 2012. **5**(1): p. 7-12.
316. Behr, A., et al., *Improved utilisation of renewable resources: new important derivatives of glycerol*. Green Chemistry, 2008. **10**(1): p. 13-30.
317. Mota, C.J., et al., *Glycerin derivatives as fuel additives: the addition of glycerol/acetone ketal (solketal) in gasolines*. Energy & Fuels, 2010. **24**(4): p. 2733-2736.
318. García, J.I., et al., *Green solvents from glycerol. Synthesis and physico-chemical properties of alkyl glycerol ethers*. Green Chemistry, 2010. **12**(3): p. 426-434.
319. Gu, Y., J. Barrault, and F. Jerome, *Glycerol as an efficient promoting medium for organic reactions*. Advanced Synthesis & Catalysis, 2008. **350**(13): p. 2007-2012.
320. Abbott, A.P., et al., *Extraction of glycerol from biodiesel into a eutectic based ionic liquid*. Green Chemistry, 2007. **9**(8): p. 868-872.
321. Shahbaz, K., et al., *Prediction of the surface tension of deep eutectic solvents*. Fluid phase equilibria, 2012. **319**: p. 48-54.
322. Mjalli, F.S. and O.U. Ahmed, *Characteristics and intermolecular interaction of eutectic binary mixtures: Reline and Glyceline*. Korean Journal of Chemical Engineering, 2016. **33**(1): p. 337-343.
323. Leron, R.B., A.N. Soriano, and M.-H. Li, *Densities and refractive indices of the deep eutectic solvents (choline chloride+ ethylene glycol or glycerol) and their aqueous mixtures at the temperature ranging from 298.15 to 333.15 K*. Journal of the Taiwan Institute of Chemical Engineers, 2012. **43**(4): p. 551-557.
324. AlOmar, M.K., et al., *Glycerol-based deep eutectic solvents: Physical properties*. Journal of Molecular Liquids, 2016. **215**: p. 98-103.
325. Harris, R.C., *Physical Properties of Alcohol Based Deep Eutectic Solvents*. 2009, University of Leicester.
326. Shahbaz, K., et al., *Eutectic solvents for the removal of residual palm oil-based biodiesel catalyst*. Separation and Purification Technology, 2011. **81**(2): p. 216-222.
327. Abbott, A.P., et al., *Evaluating water miscible deep eutectic solvents (DESs) and ionic liquids as potential lubricants*. Green Chemistry, 2014. **16**(9): p. 4156-4161.
328. Leron, R.B. and M.-H. Li, *Molar heat capacities of choline chloride-based deep eutectic solvents and their binary mixtures with water*. Thermochimica Acta, 2012. **530**: p. 52-57.
329. Hayyan, M., et al., *Are deep eutectic solvents benign or toxic?* Chemosphere, 2013. **90**(7): p. 2193-2195.
330. Juneidi, I., M. Hayyan, and M.A. Hashim, *Evaluation of toxicity and biodegradability for cholinium-based deep eutectic solvents*. Rsc Advances, 2015. **5**(102): p. 83636-83647.
331. Alvarez-Vasco, C., et al., *Unique low-molecular-weight lignin with high purity extracted from wood by deep eutectic solvents (DES): a source of lignin for valorization*. Green Chemistry, 2016. **18**(19): p. 5133-5141.

332. Guo, W., et al., *Formation of deep eutectic solvents by phenols and choline chloride and their physical properties*. Journal of Chemical & Engineering Data, 2013. **58**(4): p. 866-872.
333. Sharma, M., et al., *Dissolution of α -chitin in deep eutectic solvents*. RSC Advances, 2013. **3**(39): p. 18149.
334. Abougor, H., *Utilization of deep eutectic solvent as a pretreatment option for lignocellulosic biomass*. 2014, Tennessee Technological University.
335. Mukesh, C., et al., *Choline chloride-thiourea, a deep eutectic solvent for the production of chitin nanofibers*. Carbohydrate polymers, 2014. **103**: p. 466.
336. Abbott, A.P., G. Capper, and S. Gray, *Design of improved deep eutectic solvents using hole theory*. ChemPhysChem, 2006. **7**(4): p. 803-806.
337. Abbott, A.P., et al., *Selective extraction of metals from mixed oxide matrixes using choline-based ionic liquids*. Inorganic chemistry, 2005. **44**(19): p. 6497-6499.
338. Abbott, A., et al., *Electropolishing of stainless steel in an ionic liquid*. Transactions of the IMF, 2005. **83**(1): p. 51-53.
339. Abbott, A.P., *Application of hole theory to the viscosity of ionic and molecular liquids*. ChemPhysChem, 2004. **5**(8): p. 1242-1246.
340. Jeffrey, G.A. and G.A. Jeffrey, *An introduction to hydrogen bonding*. Vol. 12. 1997: Oxford university press New York.
341. D'Agostino, C., et al., *Molecular motion and ion diffusion in choline chloride based deep eutectic solvents studied by H-1 pulsed field gradient NMR spectroscopy*. Physical Chemistry Chemical Physics, 2011. **13**(48): p. 21383-21391.
342. D'Agostino, C., et al., *Molecular and ionic diffusion in aqueous - deep eutectic solvent mixtures: probing inter-molecular interactions using PFG NMR*. Physical Chemistry Chemical Physics, 2015. **17**(23): p. 15297-15304.
343. Wagle, D.V., G.A. Baker, and E. Mamontov, *Differential Microscopic Mobility of Components within a Deep Eutectic Solvent*. Journal of Physical Chemistry Letters, 2015. **6**(15): p. 2924-2928.
344. Pandey, A. and S. Pandey, *Solvatochromic Probe Behavior within Choline Chloride-Based Deep Eutectic Solvents: Effect of Temperature and Water*. Journal of Physical Chemistry B, 2014. **118**(50): p. 14652-14661.
345. Hertz, H., *Y. Marcus: Introduction to Liquid State Chemistry*. John Wiley & Sons, London, New York, Sidney, Toronto 1977. 357 Seiten, Preis: \$12, 50, \$24, 00. Berichte der Bunsengesellschaft für physikalische Chemie, 1978. **82**(6): p. 665-665.
346. Pandey, A., et al., *How polar are choline chloride-based deep eutectic solvents?* Physical Chemistry Chemical Physics, 2014. **16**(4): p. 1559-1568.
347. Zhu, S., et al., *Vibrational analysis and formation mechanism of typical deep eutectic solvents: An experimental and theoretical study*. Journal of Molecular Graphics and Modelling, 2016. **68**: p. 158-175.
348. Aissaoui, T., et al., *Computational investigation of the microstructural characteristics and physical properties of glycerol-based deep eutectic solvents*. Journal of Molecular Modeling, 2017. **23**(10): p. 1-11.
349. Rasmussen, H., H.R. Sørensen, and A.S. Meyer, *Formation of degradation compounds from lignocellulosic biomass in the biorefinery: sugar reaction mechanisms*. Carbohydrate research, 2014. **385**: p. 45-57.

350. Hu, F., S. Jung, and A. Ragauskas, *Pseudo-lignin formation and its impact on enzymatic hydrolysis*. *Bioresource Technology*, 2012. **117**: p. 7-12.
351. Sannigrahi, P., et al., *Pseudo-lignin and pretreatment chemistry*. *Energy & Environmental Science*, 2011. **4**(4): p. 1306-1310.
352. Dee, S.J. and A.T. Bell, *A Study of the Acid-Catalyzed Hydrolysis of Cellulose Dissolved in Ionic Liquids and the Factors Influencing the Dehydration of Glucose and the Formation of Humins*. *ChemSusChem*, 2011. **4**(8): p. 1166-1173.
353. Patil, S.K. and C.R. Lund, *Formation and growth of humins via aldol addition and condensation during acid-catalyzed conversion of 5-hydroxymethylfurfural*. *Energy & Fuels*, 2011. **25**(10): p. 4745-4755.

Chapter 3 Lignocellulose Cell Wall Deconstruction with a Deep Eutectic Solvent and a Chelator-mediated Fenton System

3.1 Abstract

A deep eutectic solvent (DES) and a chelator-mediated Fenton (CMF) system were applied individually and in sequence to deconstruct the cell wall of hardwood sweet gum (SG) and softwood yellow pine (YP). Lignocellulosic biomass samples were treated with choline chloride:glycerol DES (GLY) at 150°C for 2h, as well as with CMF reagents at room temperature in a 3-step process, that includes ferric chloride biomass impregnation, chelation with 2,3 dihydroxybenzoic acid (DHBA) and a subsequent redox reaction with a hydrogen peroxide H_2O_2 solution. The pretreatment performance was monitored by mass loss, compositional analysis of native/pretreated biomasses, and recovery of the material removed in the processes, for mass balance determination. Each treatment generated a significant removal of polysaccharides and lignin from the biomass cell wall, demonstrating that the lignocellulose matrix was disrupted. These pretreatments can potentially be utilized in biorefinery settings to fractionate cell wall biomass which can then be enzymatic hydrolyzed to fermentable sugars and recover non fermentable compounds.

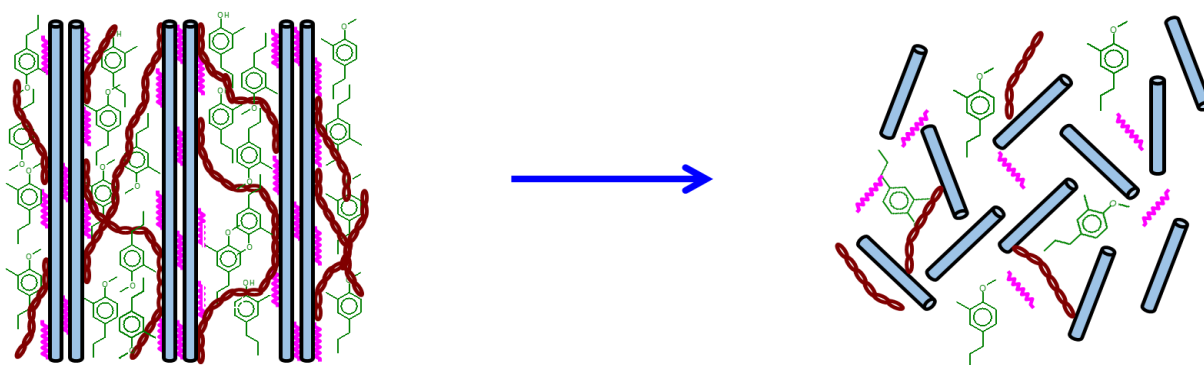


Figure 3-1 Cell wall deconstruction with GLY and a CMF system treatments

3.2 Keyword

Lignocellulose, biofuels, pretreatment, deep eutectic solvent (DES), glyceline (GLY) chelator-mediated Fenton system (CMF), polysaccharides, mass balance.

3.3 Introduction

Lignocellulosic biomass is considered the fourth largest energy source in the world after coal, oil and natural gas, and it has been used since the dawn of humankind on earth [1]. Our society has depended on fossil fuels and chemicals derived from fossil fuels since the fossil fuel industry emerged and developed [2] about 200 years ago. Since then, global greenhouse gas (GHG) emissions (of CO₂, CH₄, N₂O, hydrofluorocarbons-HFCs, perfluorinated compounds-PFCs and SF₆ increased by 70% between 1970 and 2004 causing environmental and political concern [3]. Biomass is an environmentally friendly resource due to its abundance and renewability [4, 5]. It supplies liquid fuel for transportation and has become the most important renewable energy resource accounting for up to 10% of the annual global energy demand in some parts of the world [6, 7]. Utilization of biofuels has increased over the last 15 years and it is projected that bioenergy will provide around 30% of the world's energy by 2050 [8]. Environmental issues such as the greenhouse effect, environmental pollution and shortage of fossil fuels call for developing renewable energies [9-11]. However, the challenge is to develop new technologies which convert vast amounts of biomass and biomass waste in a low-cost and efficient way [12]. A biorefinery is a system of sustainable, environmentally and resource friendly technologies for the production of materials and energy derived from plant biomass [13]. Biorefineries have the potential to replace fossil based petrochemical industry by the conversion of carbohydrates from lignocellulosic feedstocks into fermentable sugars to produce liquid biofuels and bioproducts [14-16].

The secondary cell walls of lignified plant biomass are composed primarily of cellulose, hemicellulose and lignin that form a complex network which is recalcitrant to physical, chemical and biological deconstruction [17]. To access biomass polymers in current biorefineries a “pretreatment” process is needed to disrupt cell wall (Figure 3-1), to allow fractionation, subsequent enzymatic conversion of the biomass components to bioethanol and other useful products [18, 19]. Pretreatments are needed because enzymes are too large to penetrate the intact structure of the wood cell wall, and are relatively slow when attacking just the substrate surfaces [20-22]. Various pretreatment technologies have been developed, of which some are in the demonstrative or pilot stage; however, most are water and energy intensive [23-26]. Conversion of biomass to biofuels and biochemicals requires plant cell wall deconstruction technology that has yet to be improved [27-30].

Recently, researchers have developed more environmentally-friendly methods to disassemble biomass, such as deep eutectic solvents (DES) and the chelator-mediated Fenton (CMF) system. DES are thermally stable, biodegradable, inexpensive and easy to prepare [31-35]. These new solvents overcome weaknesses of traditional methods by selectively separating biopolymers of lignocellulosic materials and minimizing the use of water and energy and the formation of by-products [31, 36-44]. The CMF system, based on the mechanism employed by brown rot fungi [45-55], is currently being explored for application in biorefineries [56, 57].

CMF reagents are used in small quantities and DES are inexpensive and benign. Therefore, this study attempts to develop a more environmentally friendly method for cell wall deconstruction that combines the chemistry of CMF system with the technology of DESs.

3.4 Experimental

3.4.1 *Materials and Methods*

Chemicals used in this research were purchased from Sigma-Aldrich. Ethanol, toluene, FeCl₃, 2,5-di-hydroxybenzoic acid, acetic acid, sodium acetate, ethanol, and hydrogen peroxide were purchased from Acros and used as received. Deionized water (DI-water) was produced by Millipore Direct Q3UV with a resistivity of 18.2 mΩ.

3.4.2 *Preparation of Biomass Samples*

A mature sweet gum (SG) (*Liquidambar styraciflua*) hardwood tree from Blacksburg, VA was debarked, machined to cubes, and stored in a freezer before use. Prior to pretreatments, the biomass was knife milled using a Wiley mill and sorted to a particle size between 40 to 60 mesh on a metal screen (250–420 μm). Then, the SG particles were Soxhlet extracted using toluene/ethanol (427 mL/1000 mL) followed by ethanol and water according to the ASTM D1105-96 standard protocol [58] to produce extractive-free wood. The resulting extractive-free SG particles were air-dried at ambient temperature for 48 h and then in a vacuum oven at 40°C for 24 h. YP (*Pinus* spp.) sapwood was obtained from the Brooks Center at Virginia Tech and the extractive-free biomass was prepared following the NREL 24268 standard protocol [59].

3.4.3 *Deep eutectic solvent pretreatments*

3.4.3.1 *Choline chloride-glycerol DES (glyceline – GLY) preparation*

Choline chloride, a hydrogen bond acceptor (HBA), and glycerol, a hydrogen bond donor (HBD) were purchased from Sigma-Aldrich (>98%), and were used as received. Raw materials were mixed at a 1:2 molar ratio of HBA and HBD. The system was heated with stirring in an oil bath

at 80°C until the mixture became a transparent homogeneous liquid (~ 30 min). (Adapted from [31]).

3.4.3.2 Glyceline pretreatment

SG and YP ground biomass (8 g each) with defined moisture content [59] were prepared according to ASTM and NREL standard protocols (extractive-free biomass [58], and were treated with 80 g of DES (1:2) in an oil bath at 150°C, for 2 h with constant stirring (adapted from [31, 60]) (Figure 3-2). Samples and controls (RT) were tested in triplicate. After the reaction, samples and controls were vacuum filtered with hot water, and the GLY filtrate was weighed for mass balance, and the reaction yield was determined. The pretreated biomass was washed with antisolvent hot deionized water (DI), resulting in a water insoluble (WI) precipitate that included lignin and other degradation compounds. WI precipitates were separated by centrifugation and freeze dried for further analysis. The pretreated biomass was washed with ethanol and the filtrate was collected for air drying, weighing for mass balance, and further analyses. GLY pretreatment was processed as overviewed in Figure 3-2 and was performed in triplicate.

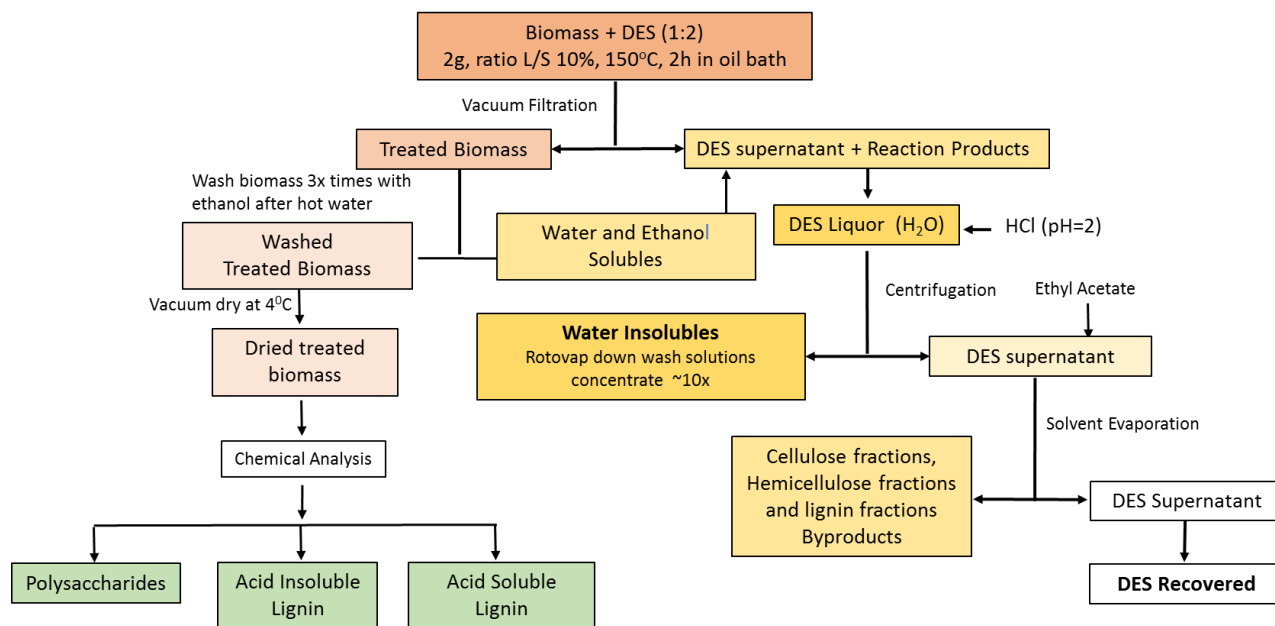


Figure 3-2 Flow Chart of Biomass pretreatment with glyceline

3.4.3.3 CMF pretreatment

Ground SG and YP wood (4 g each), prepared following standard protocol (extractive-free, dried and predetermined moisture content (MC)) were treated according to the protocol described in Figure 5-4, with 25 mL of 50 mM iron (III) chloride hexahydrate ($\text{FeCl}_3 \cdot 6\text{H}_2\text{O}$) in a 1 M acetate buffer solution (pH = 4). Samples were well mixed for 10 min and then oven dried at 30°C overnight. The next day, 25 mL of 50 mM 2,3-dihydroxybenzoic acid (DHBA) solution were added to each sample and incubated in a water bath shaker for 30 min at room temperature and 175 rpm. H_2O_2 solution (25 mL, 2 M) was added to each sample, mixed for 5 min by hand and then placed in a water bath shaker at 30°C and 175 rpm overnight. The next day, samples were filtered and the filtrates were kept frozen for further analysis. Fresh 1 M H_2O_2 solution (50 mL) was added to each sample for 30°C and 175 rpm incubation overnight. The next day, the samples were filtered and the filtrates were kept frozen for further analysis. The CMF pretreated biomass

was washed thoroughly with DI water, then air dried for 36 h, and weighed. All samples were then placed in cold storage (4°C) until further analysis (Figure 3-3). Samples and controls (in buffer solution) were conducted in triplicate.

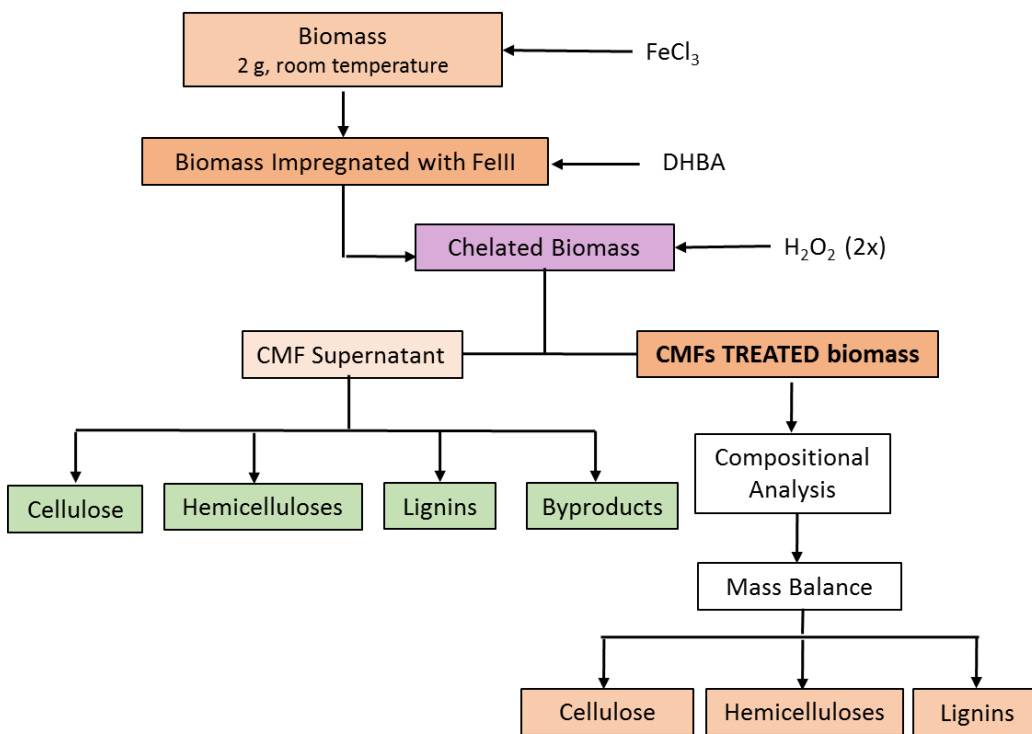


Figure 3-3 Flow Chart of Biomass pretreatment with chelator-mediated Fenton system

3.4.3.4 Pretreatments in sequence (double stage)

A GLY and a CMF system treatments were evaluated separately or in sequence with either GLY or CMF treatment conducted first to allow comparison of the sequence effectiveness on extractive-free biomass in releasing cellulose/hemicellulose and lignin as overviewed in (Figure 3-4).

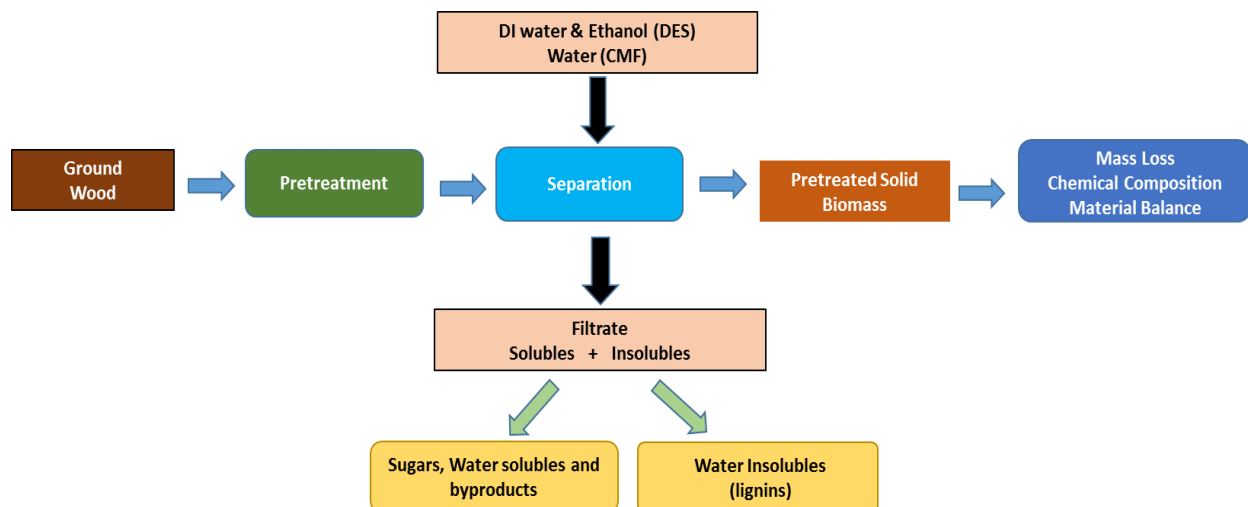


Figure 3-4 Diagram of GLY, CMF, and in sequence biomass pretreatments in this study

3.4.4 Compositional Analysis

Lignin and carbohydrate contents of native, GLY, CMF, CMF followed by GLY, and GLY followed by CMF pretreated SG and YP biomasses were analyzed according to the NREL laboratory analytical procedure (LAP) to determine and quantify the structural carbohydrates and lignin in the biomass [61]. Acid insoluble lignin (AIL - Klason lignin) was analyzed gravimetrically through the mass difference before and after heating the acid-hydrolyzed residue at 575°C. The carbohydrates in the filtrate were analyzed in triplicate using a Metrohm Ion Chromatography (IC) installed with a pulsed amperometric detector (PAD), Metrohm Inc., USA. Monosaccharides in the filtrate were separated by a Hamilton RCX-30 (250 × 4.6 mm) column with DI water as the eluent. The eluent flow rate was 1 mL/min, and the column temperature was 32°C. NaOH (350 mmol/L) and a flow rate of 0.43 mL/min was introduced after column separation to aid the PAD signal generation at 32 °C. Five sugars, L-(+)-arabinose, D-(+)-galactose, D-(+)-glucose, D-(+)-xylose, and D-(+)-mannose, were quantified using Mag IC Net software. Linear calibration curves ($R^2 > 0.9999$ and relative standard error $< 5\%$) were run prior

to every batch test. The monosaccharide concentrations were converted to the relative percentage of their anhydro-form in the biomass according to the NREL standard.

3.4.5 Processing of DES filtrates and supernatants

Filtrates comprised of DES, DI water and material that precipitated in the hot water wash of the solid pretreated residue, were processed as indicated in Figure 3-4. To separate water insolubles from the soluble components, DES filtrates were centrifuged in a Beckman J6-HC centrifuge at 5000 rpm, 4°C for 30 min. In some cases, it was necessary to conduct a second centrifugation due to the presence of very fine particles suspended in the supernatant even after the first 30 minute centrifugation. The supernatants were collected and stored at 4°C for further analysis and the pellets were washed with 50 mL of DI water (3x) and dried overnight under vacuum at 40°C. This material was labeled as WI and stored at 4°C for further analysis. Solvent was removed from the ethanol phase of each sample using a rotary evaporator. The residuals were dried overnight under vacuum at 40°C, weighed and stored at 4°C for further analysis.

DES supernatants were acidified to a final pH of 2 and then extracted with ethyl acetate (EtOAc, 3x, 100 mL each). The combined organic layers were dried over calcium chloride (CaCl₂). Finally, the solvent was removed using a rotary evaporator. The residuals were dried overnight under vacuum at 40°C, weighed and stored at RT for later quantification and compound identification.

3.5 Results and Discussion

The yield from the pretreatments was monitored by mass loss during the processes.

Compositional analyses of SG and YP biomasses were conducted before and after the

pretreatments to examine the changes in chemical compositions. Filtrates were processed and the water insoluble (WI) fractions and ethanol soluble fractions were recovered to determine the mass balance of the reactions (Figure 3-4).

3.5.1 Reaction pretreatments in SG and YP extractive-free biomass

GLY was prepared as described in a molar ratio of (1:2) and pretreatments were conducted in triplicate on extractive-free ground SG and YP biomass. The control reactions were performed in duplicate at ambient temperature.

3.5.2 Compositional analysis

Chemical composition of both native and pretreated SG and YP biomasses were conducted to evaluate the cell wall biomass deconstruction efficiency, and also for understanding the suitability of the conditions applied in the treatments.

3.5.3 Mass loss

Mass loss represents the matter that has been dissolved/removed from both native SG and native YP biomass samples during the pretreatments. Compositional analyses of the solid pretreated biomass residues indicated that these pretreatments removed significant amounts of wood components (Figure 5-6). Intensive washing with DI hot water and ethanol 90% was conducted after the filtrations to assure the removal of GLY and any other material from the pretreated biomass. Mass losses were 24% when GLY was applied to SG, this is in agreement with the recently published data for treatment of corn cob with GLY mixed with 0.1 M NaOH which presented a 28.8% [62]. For CMF treatments, the mass loss for SG was 16%, this finding is similar to the percentage reported by Zhang et al. for SG biomass fractionation by glycerol

thermal processing (GTP) who found a percentage of 11% residual lignin and almost the same percentage for xylan loss, accounting for a 22% of mass loss [63]. For YP biomass, GLY pretreatment removed a 28% of biomass components, this is in agreement with the mass loss of 29.1% for YP biomass treated with [C₂mim][OAc] ionic liquid at 160°C for 90 min [64]; whereas for CMF treatment it was found a mass loss of 10% for YP biomass. The pretreatments in sequence, CMF followed by GLY and GLY followed by CMF resulted in a substantial increment of material removed from SG and YP samples (Figure 5-6). For the double stage CMF followed by GLY pretreatment SG biomass presented an additional mass loss of 34%, while in the double stage GLY followed by CMF, the removal was only 6.3% showing that the sequence of the pretreatments impacts in the amount of material removed from SG biomass samples, when CMF treatment is applied opens up the biomass structure and the solvent can easily access biopolymers which are depolymerized. As opposed, when GLY is applied, lignocellulose network is not open in a great extent so the CMF reagents disrupt the cell wall in a less extent. For double stage YP treatments, the mass loss was 35% and 17% for the CMF followed by GLY and GLY followed by CMF pretreatment, respectively. For hardwood, GLY applied after CMF treatment enhanced the depolymerization of biopolymers two-fold but CMF treatment removed less amount of biomass components. For softwood, GLY applied after CMF treatment removed 3.5-fold biopolymers, however, CMF applied after GLY almost biopolymer removal was almost twice as much than with only the first treatment.

The cumulative mass losses are shown in Figure 5-5, for SG treated with CMF followed by GLY was of 50% whereas for GLY followed by CMF was of 30%. In the case of YP, interestingly the cumulative mass loss for both sequences presented the same percentage of 45%, even though treatment applied separately had different biopolymer removal.

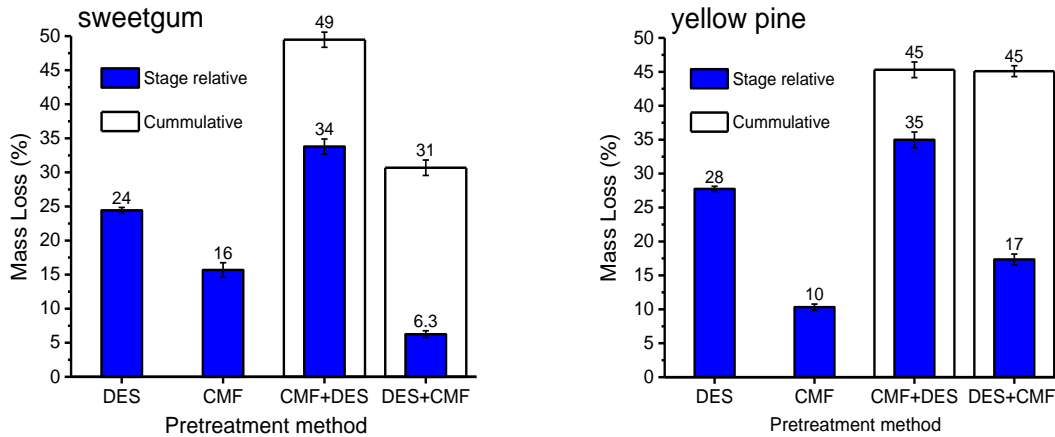


Figure 3-5 Sweetgum and Yellow Pine Mass Loss (%) during the pretreatments. CMF+GLY = CMF followed by DES and DES+CMF = CMF followed by GLY

Therefore, the sequence in which pretreatments were applied gave rise different results, cumulative mass loss for SG was greater when the sequence CMF followed by GLY was applied, whereas the cumulative mass loss for YP was 45% in both sequences, large differences were seen in single stage GLY or CMF pretreatments, especially for YP biomass, while in the case of double stage pretreatments, the order of the sequence was important particularly for SG (Figure 3-6).

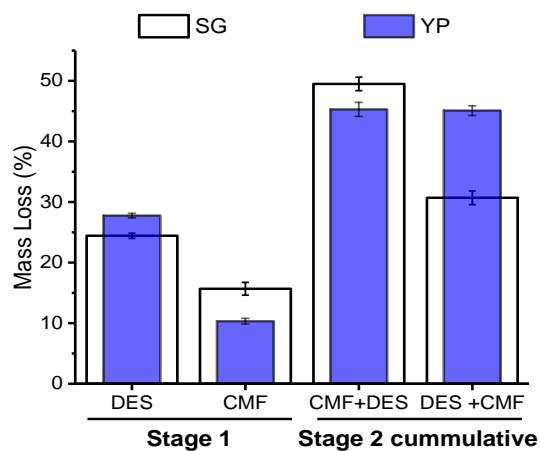


Figure 3-6 Pretreatment Mass Loss: Species Comparison

3.5.4. *Mass balances*

Mass balances were determined to estimate the total amount of removed material from pretreated biomass samples during the cell wall deconstruction. These materials were present in the filtrates or the supernatants. The pretreated solid residue was recovered, dried and kept in a cold room at 4 °C. The compositional analyses of the untreated and pretreated biomass allowed to assess the content of the three major biopolymers of lignocellulose (measured). The mass balances were used to determine the distribution of the biopolymers in the filtrates (calculated), assuming that all the material removed from biomass samples was present in the supernatant. It is worthy to mention that additional analysis of nitrogen or chloride were not conducted, to detect traces of the reagents were still present in the treated biomass.

Figure 3-7 summarizes the mass balances for 100 g of SG and YP biomasses pretreated by GLY and/or CMFs systems individually (single stage) or in sequence (double stage) and shows the cell wall biomass fractionation for both wood species after each pretreatment. The biopolymer distribution in the native and pretreated biomass revealed major shifts particularly for lignin and hemicellulose content in pretreated SG and YP biomass samples. The biopolymers removed from the lignocellulose samples during the pretreatment reactions, were present in the supernatants or filtrates and were calculated to visualize the extent of the pretreatments for both SG and YP biomass samples. As it can be seen in Figure 3-7, for SG, GLY pretreatment selectively depolymerized hemicellulose and lignin and did not impact significantly in cellulose whether it was applied individually or in sequence, during the first stage of the pretreatment when SG biomass was treated using GLY system the removal of glucan was only 0.34 g. In the second stage when SG was treated by using CMF system there was almost no glucan removal. In

this way, this pretreatment sequence GLY followed by CMF from SG selectively removed remarkable amounts of hemicellulose and lignin without a significant removal of glucan. This can greatly have a positive impact in the enzymatic saccharification of pretreated SG for bioalcohol production. In the other sequence of pretreatments - CMF followed by GLY, SG biomass have lost 6.19 g of glucan when using CMF system (single stage), however in the second stage with GLY treatment the loss of glucan was marginal. YP biomass behavior during the pretreatments was different, in the sequence GLY followed by CMF pretreatment no removal of cellulose was seen in the first stage but in the second stage a removal of 10.62 g of glucan from cellulose and/or hemicellulose was observed. When YP biomass was treated by using the other sequence (CMF followed by GLY), CMF system removed 4.54 g of cellulose whereas GLY did not removed additional amount of cellulose. Therefore, mass balance has allowed to determine the fractionation of the biopolymers and assess their content in the filtrates. It has been observed in this study that mass loss from SG and YP biomass samples has occurred mainly because of the removal of hemicelluloses and lignin from the lignocellulose matrix.

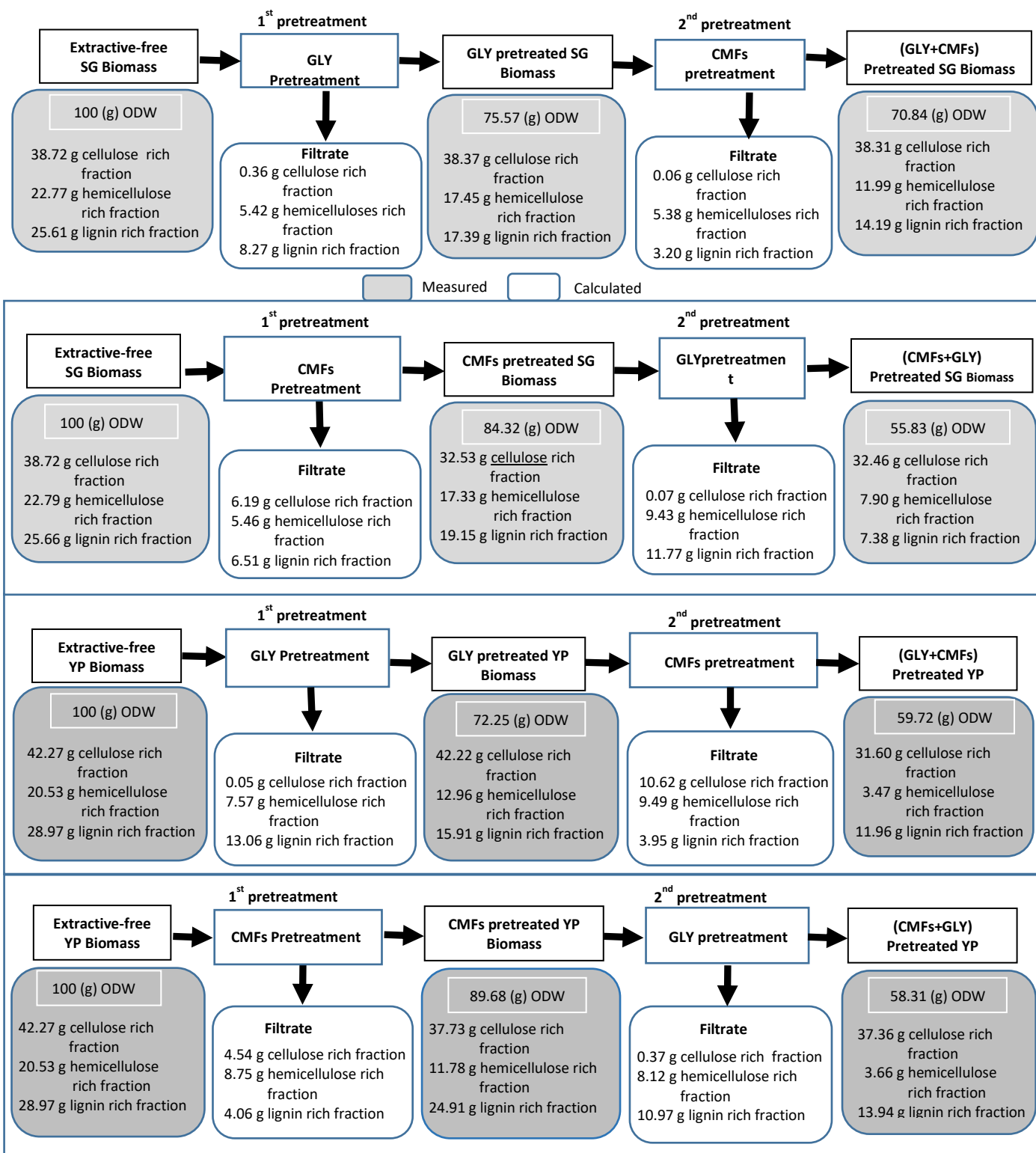


Figure 3-7 Total mass balance closure for cellulose, hemicellulose and lignin in SG and YP biomasses with GLY and CMF pretreatments (single and double stage).

3.5.5 Effect of the pretreatments in lignocellulosic biomass

The role of a pretreatment is to remove biomass features that contribute to its recalcitrance [65]. Removal of hemicelluloses and lignin have a direct impact on recalcitrance and enhancing the accessibility to glucan (cellulose) for enzymatic saccharification [66-68]. In this study, CMF system under the conditions applied during the pretreatments of SG and YP biomasses and as first stage pretreatment, disrupted the cell wall by partially removing all three components of biomass cell wall (Figure 3-8). On the other hand, GLY pretreatment was more selective, removing mostly hemicelluloses and lignins from SG and YP biomasses (Figure 3-8).

3.5.6 Biopolymer removal in SG and YP biomass during the pretreatments

Glucan Removal (cellulose fraction). The main objective of a pretreatment is to increase the enzyme accessibility to improve the digestibility of cellulose to glucose in the subsequent step towards ethanol production [69] In that context, glucan polysaccharide availability is of great importance therefore conserving the integrity of the cellulose in the pretreated biomass is relevant. Therefore, less removal or degradation of glucan is desired in an efficient lignocellulosic biomass pretreatment.

For single stage pretreatments, glucan removal by GLY treatment (single stage) was marginal for both SG and YP biomasses, (less than 1%). These data are in agreement with the results acquired by other research groups for glucan removal. Zhang et al. reported no significant change in glucan content for corn cob pretreated with choline chloride:ethylenglycol (1:2) and GLY (1:2) at 110°C for 24 h [62]. Similarly, it has been reported that glycerol did not remove significant amounts of glucan during the biomass fractionation by GTP technique [63]. Also, Kumar and his research group reported the absence of glucan in the DES liquors during the

treatment of rice straw at 60°C for 12 h with choline chloride:lactic acid (1:2) DES [70]. Besides, Xu et al. have reported that when corn stover biomass was treated with choline chloride:formic acid (1:1) at 130°C for 2 h glucan was not removed from the LC matrix [71]. Yiin and his coworkers treated oil palm biomass with maleic acid:sucrose:water (1:3:10) DES at 60°C for 12 h and reported a removal of 0.63% of cellulose [72].

CMF system (single stage) caused a glucan removal of a percentage of 16% and 11% for SG and YP, respectively. Lower results have been reported in the literature for cellulose solubilization or degradation applying other pretreatments. For instance, percentages of 8.5% for cellulose removal were obtained by Xu and his group [71] when treated corn stover with choline chloride:formic acid at 130°C for 2h, under constant stirring. Froschauner et al. [73] recovered 91,9 % of cellulose when treated birch kraft pulp with EmimOAc ionic liquid so that 8.1% of cellulose was dissolved by this IL. Sathitsuksanoh and his research group [64] also have reported 7.8% and 3.8% of cellulose removal from pine biomass treated with [C₂mim][OAc] ionic liquid at 160°C and 120°C, respectively for 90 min. This is consistent with the CMF mechanism of action in which lignin can be solubilized. Therefore, CMF reagents effectively depolymerized polysaccharides and modified lignin for both SG and YP biomasses, especially when it was applied as first pretreatment.

For double stage pretreatments, in the sequence CMF followed by GLY treatment, glucan polysaccharide was barely removed from SG and YP biomasses (0% and 1%) indicating that glyceline had very little impact in glucan polymer in the pretreated CMF biomass for both SG and YP samples. For the other sequence, GLY followed by CMF pretreatment, percentages of 0% and 25% of glucan removal were obtained for SG and YP, respectively. These results show

that glucan was not additionally fractionated by CMF system in the pretreated GLY SG, whereas a fraction of 25% of glucan was removed by CMF system from the pretreated GLY YP suggesting a non-enzymatic depolymerization of cellulose and/or glucomannan. Therefore, the order in which CMF and GLY pretreatments were applied was crucial in the removal of glucan from YP biomass.

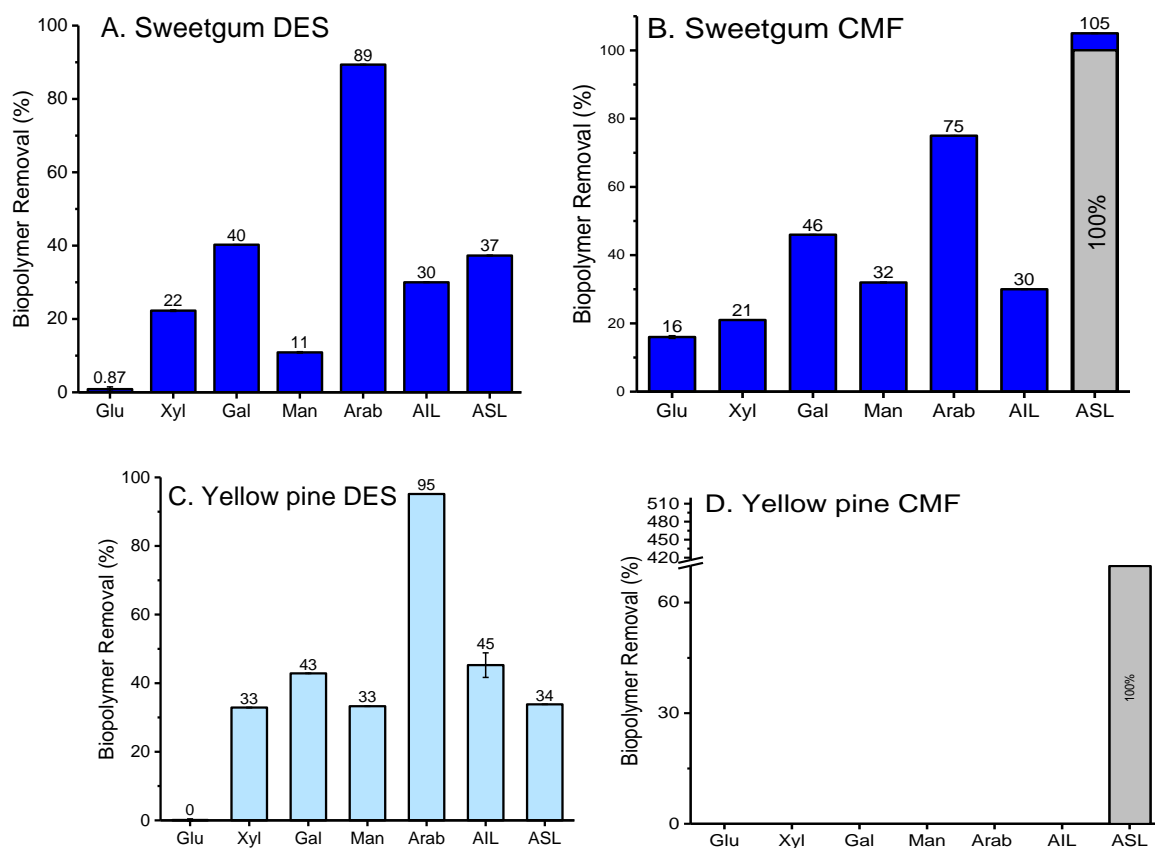


Figure 3-8 Biopolymer removal from SG and YP biomass samples in single stage treatments

Cumulative removal of glucan during the CMF and GLY pretreatments after single and double stages from SG and YP biomasses are shown in Table 1. The percentages of glucan removal from SG were 1% for the sequence GLY followed by CMF and 16% for the sequence CMF followed by GLY; whereas percentage of from yellow pine was removed in a percentage of 25%

and 12%, respectively. These data revealed that the impact of the pretreatments was species dependent when GLY treatments was applied first the removal of Glucan from SG was insignificant while from YP was relevant. On the contrary, when CMF system was the first treatment, SG exhibited a higher removal than YP. Yu et al. [74] treated *Eucaliptus grandis* with a two-step liquid hot water method and removed 6.68% of glucan in the first step at 180°C for 20 min while the removal of glucan in the second step was of 61.44% at 240°C for 20 min, observing sugar degradation at higher temperatures which was detrimental in the further step of enzymatic hydrolysis. Thus, a less percentage of glucan removal from biomass during the pretreatment is desired to assure a better yield in glucose release during the enzymatic hydrolysis step towards bioalcohol production.

Hemicellulose Fraction. Hemicelluloses have a negative impact in cellulose accessibility [66-68] as a physical barrier and also because enzymes can be adsorbed onto hemicelluloses and lower the yield of the enzymatic hydrolysis. A pretreatment has the ability to lower the hemicellulose content in the biomass subjected to the pretreatment. Figures 3-8 and 3-9 shows the removal of hemicellulose biopolymers in the biomass during the single and double stage GLY or/and CMF pretreatments.

In **the single stage** GLY treatment, the hemicellulose fractions removed from YP biomass were higher than from SG biomass ranging from 33% of both xylan and mannan removal to 95% of arabinan removal from YP biomass versus 11% of mannan removal to 89% of arabinan removal from SG biomass (Figure 3-8 A and C). The single stage CMF treatment removed fair amounts of hemicelluloses from SG and YP biomasses, higher percentages of polysaccharides removal

were observed for YP biomass, except for arabinan polymer which presented 75% of removal from SG biomass versus 49% removal from YP biomass (Figure 3-8 B and D).

In **double stage pretreatments**, during the CMF followed by GLY pretreatment sequence additional polysaccharide fractions were removed from both SG and YP biomasses. In the case of SG samples the removal ranged from 21% of mannan polysaccharide to 43% for galactan polysaccharide (Figure 3-9 A). For YP biomass, the polysaccharides removal ranged from 41% of mannan polymer to 49% of galactan polysaccharide (Figure 3-9 C). On the other hand, during the sequence DES followed by CMF pretreatment, the additional removal of polysaccharide fractions presented lower percentages ranging from 1% of arabinan polysaccharide removal to 44% of galactan polymer from SG (Figure 3-9 B). In the case of YP, the lowest percentage of extraction presented arabinan polymer (21%) versus mannan polysaccharide which had the highest percentage of 52% (Figure 3-9 D). Thus, removal of polysaccharides from both SG and YP biomasses were increased when the second pretreatment was applied.

Cumulative removal of hemicelluloses in both pretreatments sequences is shown in Figure 3-10 revealing that the hemicelluloses removal was species and pretreatment sequence dependent. Higher amounts of polysaccharides were taken out for SG biomass pretreated by using the sequence CMF followed by GLY pretreatment whereas for YP biomass both sequences extracted similar amounts of hemicelluloses. In general the removal of hemicelluloses ranged from around 46-99%.

Lignin fraction. In **single stage** pretreatment - GLY system, a proportion of total amount, 31% and 45% of acid insoluble lignin (AIL) besides a 37% and 34% of acid soluble lignin (ASL) were removed from for SG and YP, respectively (Figure 5-9, A and C). These figures are

comparable to the data already reported by Zhang and her research group [63] which are 41% of lignin removed from SG biomass fractionation after denaturing cell wall by glycerol thermal processing. Meanwhile, a percentage of 31.7% of lignin was removed from YP biomass by Sathitsuksanoh et al. [64]. Additionally, Xu and his research group [71] treated corn stover with [Bmim][Cl⁻] ionic liquid have reported a lignin removal of 23.8%, without specifying if it was AIL or ASL of the original native corn stover biomass. GLY under the conditions of the reactions in this study showed selectivity for non-cellulosic biopolymers with both SG and YP biomass samples removing portions of lignin biopolymer. In CMF pretreatment, the removal of AIL reached 30% from SG and 22% from YP. Interestingly, CMF treatment caused a removal of 105% of ASL in SG biomass and 516% for YP biomass, which can be explained as that 100% of ASL present in the original untreated biomass was removed together with an additional amount of lignin that came from the solubilization of AIL. Table 3-1 indicates the lignin acid insoluble and acid soluble fractions across the stages. YP contained relatively low amount of ASL in the original sample before pretreatment. Further, solubilized lignin was removed from biomass along with the ASL resulting in a greater amount of ASL than the initial amount. This is consistent with the CMF mechanism of action in which part of lignin is heavily modified. Thus, a percentage of 105% of ASL removed from SG represents the total removal of the original ASL in the untreated biomass along with an additional 5% of AIL removed as ASL. For YP biomass, a 516% from YP (5.16 fold of the initial amount present in the original native YP sample) was removed (Figure 3-8, B and D). Therefore, the extent of delignification of SG and YP after CMF pretreatment was significant for both SG and YP biomasses.

In **double stage** pretreatments, taking into account the sequence CMF followed by GLY pretreatment, it was observed that AIL extraction reached up to 43% from SG sample and 31%

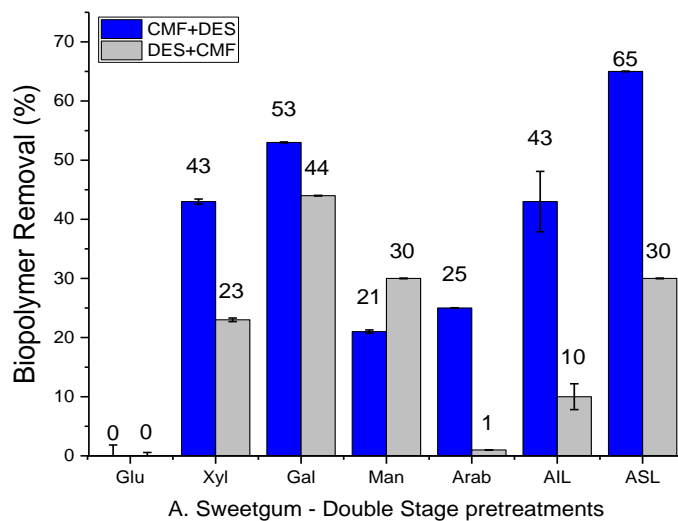
from YP biomass, and the ASL was 65% for SG samples and 85% for YP biomass (Figure 3-9, A and C). Whereas the results for the other sequence, GLY followed by CMF pretreatment were as follows 10% and 19% of AIL removal from SG and YP biomasses, respectively; and for ASL removal, a percentage of 30% was observed from SG biomass, while a percentage of 510% was detected for YP samples as a result of solubilization of portions of AIL (Figure 3-9, B and D). Hence, double stage pretreatments showed an extensive delignification for both SG and YP samples.

Table 3-1 AIL and ASL removal in the single and double stage CMF/GLY pretreatments

	Sweetgum					Yellow pine				
	untreated	DES	CMF	CMF+DES	DES+CMF	untreated	DES	CMF	CMF+DES	DES+CMF
AIL	22.09	15.16	15.41	5.96	13.01	28.47	21.57	22.34	13.56	10.28
ASL	3.56	2.23	3.74	1.41	1.18	0.5	0.46	2.56	0.38	1.68
TOTAL	25.65	15.16	19.15	7.37	14.19	28.97	22.03	24.9	13.94	11.96

Cumulative removal of lignin shown in Figure 3-10 reveals that significant amounts of lignin has been removed from both SG and YP biomasses. Regarding to lignin removal, this was species, pretreatment sequence and type of lignin dependent. Higher percentage of AIL fraction was removed from SG biomass samples (73%) during the CMF followed by GLY pretreatment sequence versus only 41% during the other pretreatment sequence. In the case of YP biomass opposite results were obtained, 52% of AIL removal during the sequence CMF followed by DES and 64% during the other pretreatment sequence. These results are in agreement with data obtained by Wang et al. [75] who achieved 60% of lignin removal from wheat straw treated by

NaOH/urea solvent at low temperature, Yu et al. [74] who treated *Eucalpitus grandis* in a two-step liquid hot water method at 180°C for 20 min and obtained a 58% of lignin removal. Related to ASL removal, YP biomass had higher percentages in both pretreatment sequences than SG biomass. A 67% percentage of ASL removal from SG was observed during the GLY followed by CMF pretreatment while a 170% (1.7 fold higher than the amount of ASL present in the original native sample). The cumulative removal of ASL from YP biomass during the both pretreatments in sequence was 6 fold and 5.44 fold from the original amount present in native YP biomass (601% and 544%, respectively). Likewise, Yuan et al. have treated poplar wood with [C₂mim][OAc] ionic liquid at 110°C for 12 h and reported some solubilization of AIL obtaining a -0.2% of ASL [76]. This can be explained by the mechanisms known for CMF in brown-rotted biomass. Hydroxyl free radicals attack the lignocellulosic matrix causing rearrangements that lead to lignin depolymerization and repolymerization [45, 53, 77-84]. Therefore, double stage pretreatments applied to SG and YP biomasses can efficiently remove lignins from the lignocellulose by depolymerizing and modifying biopolymers, particularly from SG samples.



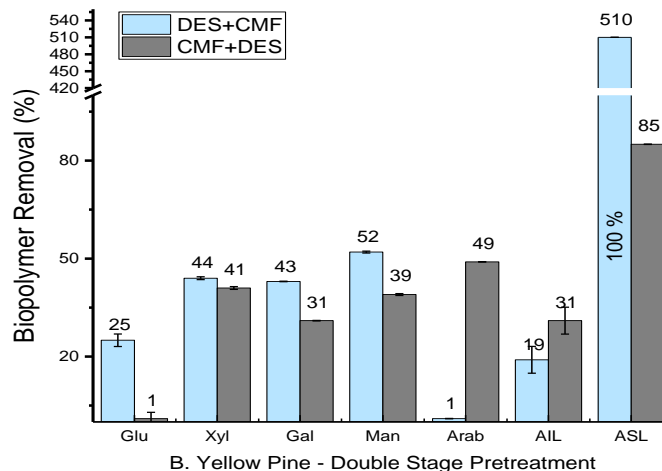


Figure 3-9 Biopolymer removal from SG and YP - double stage pretreatments

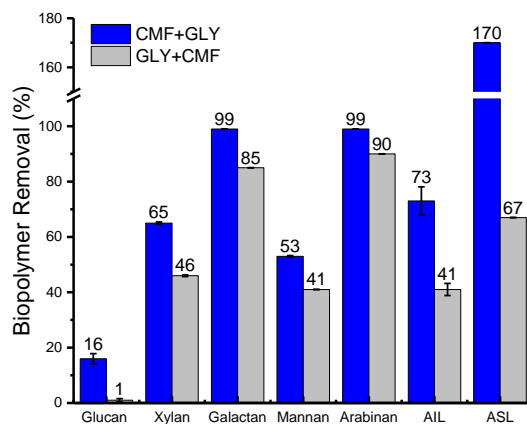
A microexamination of hemicellulose fractions removed from SG and YP biomass during the single and double stage GLY and CMF pretreatments exhibits a significant withdraw of xylan, galactan, mannan and arabinan polysaccharides (Figure 3-8 and 3-9). In the case of **single stage pretreatments**, the fractionation of polysaccharides produced after GLY treatment to SG was as follows: xylan polysaccharide removal was of a percentage of 22% and 33%, from SG and YP biomasses, respectively. The removal of galactan was similar arising up to 40% from SG and 43% from YP samples, major differences where seen in the removal of mannan polymer (11% and 33% from SG and YP samples) and arabinan polysaccharide (89% and 95% from SG and YP samples) (Figure 5-9 A and C). The fractionation of polysaccharides during CMF pretreatment resulted in different percentages of polysaccharides removal. Xylan polysaccharide presented a 21% and a 40% percentages of removal from SG and YP samples; galactan polymer presented a 46% and a 62% of displacement from SG and YP samples, respectively; Mannan polysaccharide was removed by 32% from SG samples and by 41% from YP samples; whereas arabinan polymer was removed by 75% from SG and by 49% from YP samples (Figure 3-8 C

and D). In general, removal of polysaccharides during single stage GLY or CMF pretreatments was higher for YP biomass, only in the case of arabinan polysaccharide removal from SG biomass during CMF pretreatment was higher than from YP biomass.

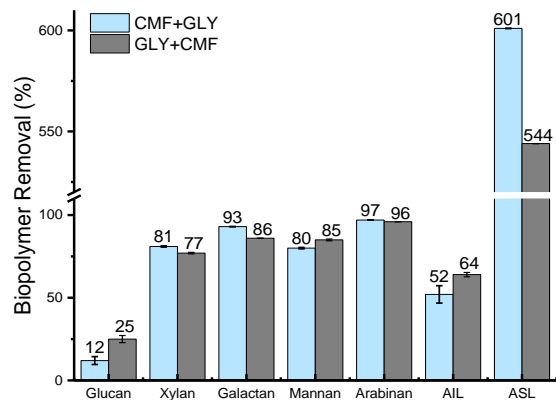
In **double stage pretreatments** (GLY followed by CMF or CMF followed by GLY), significant amounts of additional polysaccharides were removed. For the sequence CMF followed by GLY, the single stage CMF treatment applied to SG biomass removed 21% of xylan polysaccharide, the second treatment of GLY system enhanced xylan removal to 43%. Similarly, galactan and arabinan polysaccharides were removed and additional 53% and 25%, respectively, while mannan polymer was removed an additional 21%. Whereas YP biomass pretreated with double stage CMF followed by GLY reached an additional 41% of xylan removal (Fig 3-9 A y C).

Cumulative removal (Figure 3-10) of xylan biopolymer from SG after the double stage pretreatments was 65% when the sequence CMF followed by DES pretreatment was applied, and 46% when the other sequence was applied. For YP biomass the results presented higher percentages, 81% and 77% during each pretreatment sequence. These results can be compared to the fractionation of xylan in the pretreatment of *Miscanthus* with anhydrous [C₄im]:H₂SO₄ 80% IL and 20% H₂O mixtures obtained by Verdia and his coworkers at 120°C for 2 h [85] which was up to 94% of xylan removal. Also, Zhang and her group [63] subjected SG biomass to glycerol thermal processing and obtained up to 68% of xylan removal, at 240°C for 12 min. Consequently, DES and CMF double stage pretreatments efficiently removed xylan from both SG and YP biomass, particularly from YP biomass. Galactan and mannan polysaccharides were almost completely removed (99% each) from SG samples during the CMF followed by GLY pretreatment sequence whereas the results for the opposite sequence were up to 85% and 90%,

respectively. Arabinan removal was of 53% for the first sequence and 41% for the second sequence. Thus, for SG biomass deconstruction, in regard to galactan arabinan, and mannan removals the sequence CMF followed by GLY presented better results. In YP cell wall deconstruction both pretreatment sequences had similar results, Galactan polymer was removed in a percentage of 93% during the CMF+GLY pretreatment sequence and 86 % during the other pretreatment sequence. Mannan removal was 80% and 85% during the CMF followed by GLY and GLY followed by CMF pretreatment sequences, respectively. For arabinan removal, the results were 97% and 96% during these pretreatments in sequence. These data of polysaccharide fractionation are higher than those reported by Sathitsuksanoh et al. [64] for pine pretreated with [C₂mim][OAc] ionic liquid at 120°C for 90 min who reported 6.25%, 28,83%, 16.66% and 17.76% removal of xylan, galactan, arabinan and mannan polysaccharides, respectively. In general, the double stage pretreatments effectively fractionated lignocellulosic cell wall of both SG and YP biomass, however the sequence CMF followed by GLY pretreatment removed polysaccharides more efficiently for both SG and YP biomass samples.



A. Sweetgum - Cumulative removal during the pretreatments



B. Yellow pine - Cumulative removal during the pretreatments

Figure 3-10 Cumulative biopolymer removal from SG and YP biomass samples during the single and double stage pretreatments.

Efficiency factor. To calculate the efficiency and the selectivity of the pretreatments and evaluate how effective each treatment is and if the sequence in which they are applied influences the results of the cell wall deconstruction. The efficiency factor is calculated with the following ratio:

$$Ratio = \frac{\text{Mass Loss for treatment in sequence}}{\text{Mass Loss for individual treatment}}$$

The Table 3-2 summarizes the mass loss resulted in the pretreatments individually GLY and CMF, and in sequence GLY followed by CMF and CMF followed by GLY, described earlier (Figure 3-5).

Table 3-2 Mass loss for GLY and CMF pretreatments applied to SG and YP biomasses

	Mass Loss (%)			
	DES	CMF	CMF+GLY	GLY+CMF
SG	24	16	34	6
YP	28	10	35	17

The Table 3-3 shows the efficiency factors of the four pretreatments, applied individually and in sequence for SG and YP biomass samples.

Table 3-3 Efficiency factor for the pretreatments in sequence for SG and YP biomasses

Biomass Sample	Treatments	Factor
Sweetgum	CMF+GLY	1.42
	GLY+CMF	0.38
Yellow pine	CMF+GLY	1.25
	GLY+CMF	1.70

If this ratio is >1 the treatments effectively disrupt the biomass cell wall, there was synergy, whereas a ratio < 1 would indicate the inability of the pretreatments to efficiently deconstruct the cell wall (no synergy). Therefore, for SG biomass the efficiency factor for the pretreatment CMF followed by GLY is 1.42, GLY caused the major mass loss after the CMF pretreatment so that there was synergy between these two treatments. The other sequence, GLY followed by CMF presented a ratio of 0.38, majority of mass loss was caused by GLY and CMF did not impact too much biomass cell wall so there was not synergy applying the treatments in this sequence. For YP biomass, the ratio for CMF treatment followed by GLY was 1.25, GLY caused majority of mass loss after CMF treatment. There was synergy between these two pretreatments. On the other hand, in the sequence GLY followed by CMF treatment for YP biomass, the ratio was 1.70 showing that CMF treatment caused the majority of mass loss after GLY treatment so that there was synergy between these two pretreatments applied in this order of sequence. Consequently, the chemical analyses of native and pretreated solid residues SG and YP biomasses showed effects on the efficiency and selectivity of the pretreatments. The application

of the combined CMF followed by GLY treatment resulted in the highest removal of material from SG biomass (0.2%, 53% and 61% of glucan, hemicellulose and lignin fractions, respectively). Whereas for YP biomass, the highest percentage of removed material was found when GLY followed by CMF pretreatment was applied (18%, 73% and 25% of glucan, hemicellulose and lignin fractions, respectively).

3.6 Conclusions

Lignocellulosic biomass in biofuel production is governed by the cell wall deconstruction and enzyme accessibility to obtain fermentable sugars. A pretreatment for partial/complete removal of cell wall biopolymers is required to reduce the biomass recalcitrance and enhance enzyme accessibility to cellulose to convert it into monosaccharides. In this study, four pretreatments including GLY and a CMF treatment, individually (single stage) or in sequence (double stage) were applied to SG and YP biomasses. Compositional analysis was used as a tool to determine the mass balance for the processes as well as to estimate the impact of the pretreatments on the efficiency and selectivity of cell wall deconstruction (biopolymer removal). For SG biomass, in single stage pretreatments GLY selectively removed hemicelluloses (different percentages of each) and lignins (31% of AIL and 37% of ASL, respectively) was observed, without cellulose removal (< 1%). CMF system was less selective, removed all biopolymers suggesting a non-enzymatic cell wall deconstruction. In double stage treatments, the CMF followed by GLY sequence was nonselective, it showed a greater biopolymer removal than the other sequence; in contrast GLY followed by CMF sequence was more selective for hemicellulose and lignin removals. For YP biomass, single stage treatment by using GLY or CMF exhibited the same trend as in SG, a selective removal of hemicelluloses and lignins (45% of AIL and 34% of ASL)

was observed when GLY treatment was applied, however CMF system was less selective, removing less AIL than GLY treatment (22% of AIL), 516% - 5.16 fold of ASL with 11% of glucan removal. Overall, the double stage GLY+CMF treatment applied to SG biomass was less effective in removing hemicelluloses and lignins compare to YP biomass treatment, particularly for AIL and ASL removal (10% and 30% from SG biomass, 19% and 510% from YP). The double stage CMF followed by GLY treatment of SG showed a more efficient removal of lignin (43% of AIL and 65% of ASL) compared to YP lignin removal. In contrast, ASL was removed in a proportion of 544% or 5.44 fold of original amount present in native YP. Regarding the hemicellulose, its removal displayed species and type of hemicellulose dependence. These results indicated that cell wall deconstruction is possible using the chemistry of CMF and the solvent technology of GLY. These findings should be confirmed with enzymatic hydrolyses to examine the enhancement of the enzyme accessibility and the production of fermentable sugars as a basic raw material for biorefining for fermentation based processes.

3.7 References

1. Demirbas, M.F., *Biorefineries for biofuel upgrading: a critical review*. Applied Energy, 2009. **86**: p. S151-S161.
2. Nelson, P., E. Hood, and R. Powell, *The Bioeconomy: A New Era of Products Derived from Renewable Plant-Based Feedstock*. Chapter-1, Plant Biomass Conversion, 2010.
3. Metz B. Davidson R., B.P., Dave R., Meyer LA editors, *Contribution of Working Group 3 to the fourth assessment report of the intergovernmental panel on climate change 2007*, IPCC: Cambridge University Press. Cambridge, United Kingdom and New York, USA. p. 863.
4. Menon, V. and M. Rao, *Trends in bioconversion of lignocellulose: biofuels, platform chemicals & biorefinery concept*. Progress in Energy and Combustion Science, 2012. **38**(4): p. 522-550.
5. Field, C.B., et al., *Primary production of the biosphere: integrating terrestrial and oceanic components*. Science, 1998. **281**(5374): p. 237-240.
6. Agency, I.E., *World Energy Statistics*. 2015: p. 81.
7. Wang, S., et al., *Choline chloride/urea as an effective plasticizer for production of cellulose films*. Carbohydrate polymers, 2015. **117**: p. 133-139.
8. Guo, M., W. Song, and J. Buhain, *Bioenergy and biofuels: History, status, and perspective*. Renewable and Sustainable Energy Reviews, 2015. **42**: p. 712-725.
9. Langeveld, H., J. Sanders, and M. Meeusen, *The biobased economy: biofuels, materials, and chemicals in the post-oil era*. 2012: Earthscan.
10. Langeveld, J., J. Dixon, and J. Jaworski, *Development perspectives of the biobased economy: a review*. Crop Science, 2010. **50**(Supplement_1): p. S-142-S-151.
11. Elumalai, S., et al., *Chemistry and reactions of forest biomass in biorefining*. Sustainable production of fuels, chemicals, and fibers from forest biomass, 2011: p. 109-144.
12. Cherubini, F., *The biorefinery concept: using biomass instead of oil for producing energy and chemicals*. Energy Conversion and Management, 2010. **51**(7): p. 1412-1421.
13. Kamm, B., P.R. Gruber, and M. Kamm, *Biorefineries—industrial processes and products*. 2007: Wiley Online Library.
14. Jørgensen, H., J.B. Kristensen, and C. Felby, *Enzymatic conversion of lignocellulose into fermentable sugars: challenges and opportunities*. Biofuels, Bioproducts and Biorefining, 2007. **1**(2): p. 119-134.
15. Lee, J., *Biological conversion of lignocellulosic biomass to ethanol*. Journal of Biotechnology, 1997. **56**(1): p. 1-24.
16. Blanch, H.W., B.A. Simmons, and D. Klein-Marcuschamer, *Biomass deconstruction to sugars*. Biotechnology Journal, 2011. **6**(9): p. 1086-1102.
17. Keplinger, T., et al., *A zoom into the nanoscale texture of secondary cell walls*. Plant methods, 2014. **10**(1): p. 1.
18. Langan, P., et al., *Exploring new strategies for cellulosic biofuels production*. Energy & Environmental Science, 2011. **4**(10): p. 3820-3833.
19. Himmel, M.E., et al., *Biomass recalcitrance: engineering plants and enzymes for biofuels production*. science, 2007. **315**(5813): p. 804-807.

20. Arantes, V. and B. Goodell, *Current Understanding of Brown-Rot Fungal Biodegradation Mechanisms: A Review*, in *Deterioration and Protection of Sustainable Biomaterials*. 2014, American Chemical Society. p. 3-21.
21. Goodell, B., et al., *Lignocellulose oxidation by low molecular weight metal-binding compounds isolated from wood degrading fungi: A comparison of brown rot and white rot systems and the potential application of chelator-mediated Fenton reactions*. *Progress in Biotechnology* 21. *Biotechnology in the Pulp and Paper Industry.*, ed. L.V.a.R. Lantto. 2002: Elsevier Press. 37-49.
22. Goodell, B., et al., *Low Molecular Weight Chelators And Phenolic Compounds Isolated from Wood Decay Fungi and their Role in the Fungal Biodegradation of Wood*. *Journal of Biotechnology*, 1997. **53**: p. 133-162.
23. María, P.D.d., P.M. Grande, and W. Leitner, *Current Trends in Pretreatment and Fractionation of Lignocellulose as Reflected in Industrial Patent Activities*. *Chemie Ingenieur Technik*, 2015.
24. Agbor, V.B., et al., *Biomass pretreatment: Fundamentals toward application*. *Biotechnology Advances*, 2011. **29**(6): p. 675-685.
25. Mood, S.H., et al., *Lignocellulosic biomass to bioethanol, a comprehensive review with a focus on pretreatment*. *Renewable & Sustainable Energy Reviews*, 2013. **27**: p. 77-93.
26. Yang, B. and C.E. Wyman, *Pretreatment: the key to unlocking low-cost cellulosic ethanol*. *Biofuels, Bioproducts and Biorefining*, 2008. **2**(1): p. 26-40.
27. Huber, G.W., *Breaking the chemical and engineering barriers to lignocellulosic biofuels: next generation hydrocarbon biorefineries*. 2008: Citeseer.
28. Mosier, N., et al., *Features of promising technologies for pretreatment of lignocellulosic biomass*. *Bioresource technology*, 2005. **96**(6): p. 673-686.
29. Oh, Y.H., et al., *Recent advances in development of biomass pretreatment technologies used in biorefinery for the production of bio-based fuels, chemicals and polymers*. *Korean Journal of Chemical Engineering*, 2015. **32**(10): p. 1945-1959.
30. Sathitsuksanoh, N., A. George, and Y.H.P. Zhang, *New lignocellulose pretreatments using cellulose solvents: a review*. *Journal of Chemical Technology and Biotechnology*, 2013. **88**(2): p. 169-180.
31. Francisco, M., A. van den Bruinhorst, and M.C. Kroon, *New natural and renewable low transition temperature mixtures (LTTMs): screening as solvents for lignocellulosic biomass processing*. *Green Chemistry*, 2012. **14**(8): p. 2153-2157.
32. de Maria, P.D., *Recent trends in (ligno)cellulose dissolution using neoteric solvents: switchable, distillable and bio-based ionic liquids*. *Journal of Chemical Technology and Biotechnology*, 2014. **89**(1): p. 11-18.
33. de María, P.D. and Z. Maugeri, *Ionic liquids in biotransformations: from proof-of-concept to emerging deep-eutectic-solvents*. *Current opinion in chemical biology*, 2011. **15**(2): p. 220-225.
34. De Oliveira Vigier, K., G. Chatel, and F. Jerome, *Contribution of Deep Eutectic Solvents for Biomass Processing: Opportunities, Challenges, and Limitations*. *ChemInform*, 2015. **46**(26).
35. Durand, E., *Deep eutectic solvents*. 2013.
36. Abbott, A.P., et al., *Glycerol eutectics as sustainable solvent systems*. *Green Chemistry*, 2011. **13**(1): p. 82-90.

37. Choi, Y.H., et al., *Are natural deep eutectic solvents the missing link in understanding cellular metabolism and physiology?* *Plant physiology*, 2011. **156**(4): p. 1701-1705.
38. Dai, Y., et al., *Natural deep eutectic solvents as new potential media for green technology.* *Anal Chim Acta*, 2013. **766**: p. 61-8.
39. Zhang, Q.H., et al., *Green and Inexpensive Choline-Derived Solvents for Cellulose Decrystallization.* *Chemistry-a European Journal*, 2012. **18**(4): p. 1043-1046.
40. Zhang, Q., et al., *Deep eutectic solvents: syntheses, properties and applications.* *Chemical Society Reviews*, 2012. **41**(21): p. 7108-7146.
41. Abougor, H., *Utilization of deep eutectic solvent as a pretreatment option for lignocellulosic biomass.* 2014, Tennessee Technological University.
42. de María, P.D., *Deep eutectic solvents.* *Environmentally Friendly Syntheses Using Ionic Liquids*, 2014: p. 67.
43. Sheldon, R.A., *Green and sustainable manufacture of chemicals from biomass: state of the art.* *Green Chemistry*, 2014. **16**(3): p. 950-963.
44. Durand, E., J. Lecomte, and P. Villeneuve, *From green chemistry to nature: The versatile role of low transition temperature mixtures.* *Biochimie*, 2015.
45. Arantes, V. and B. Goodell, *Current Understanding of Brown-Rot Fungal Biodegradation Mechanisms: A Review*, in *Deterioration and Protection of Sustainable Biomaterials*, T.P. Schultz, B. Goodell, and D.D. Nicholas, Editors. 2014. p. 3-21.
46. Blanchette, R.A., *Degradation of the lignocellulose complex in wood.* *Canadian Journal of Botany*, 1995. **73**(S1): p. 999-1010.
47. Blanchette, R.A., et al. *Biological degradation of wood.* in *Archaeological wood: properties, chemistry, and preservation.* 1990. American Chemical Society.
48. Daniel, G., et al. *Microview of wood under degradation by bacteria and fungi.* in *Current knowledge of wood deterioration mechanisms and its impact on biotechnology and wood preservation. Symposium at the 221st National Meeting of the American Chemical Society, San Diego, California, USA, 1-5 April 2001.* 2003. American Chemical Society.
49. Daniel, G. and T. Nilsson, *Developments in the study of soft rot and bacterial decay.* *Forest products biotechnology*, 1998: p. 37-62.
50. Ferraz, A., et al., *Biodegradation of Pinus radiata softwood by white-and brown-rot fungi.* *World Journal of Microbiology and biotechnology*, 2001. **17**(1): p. 31-34.
51. Guillén, F., et al., *Biodegradation of lignocelluloses: microbial, chemical, and enzymatic aspects of the fungal attack of lignin.* *Int Microbiol*, 2005. **8**(195204): p. 187204Minami.
52. Higuchi, T., *Microbial degradation of lignin: role of lignin peroxidase, manganese peroxidase, and laccase.* *Proceedings of the Japan Academy, Series B*, 2004. **80**(5): p. 204-214.
53. Kirk, T.K., *Degradation and conversion of lignocelluloses.* *The filamentous fungi*, 1983. **4**: p. 266-295.
54. Pérez, J., et al., *Biodegradation and biological treatments of cellulose, hemicellulose and lignin: an overview.* *International Microbiology*, 2002. **5**(2): p. 53-63.
55. Sánchez, C., *Lignocellulosic residues: biodegradation and bioconversion by fungi.* *Biotechnology advances*, 2009. **27**(2): p. 185-194.
56. Norway, I.B.N.-. *BioMim receives Media attention.* 2015 [cited 2017 02/16/2017]; Available from: <http://indbiotech.no>.

57. Davis, L., *International research team seeks more efficient biomass refinement processes*. 2015.
58. ASTM, *Standard Test Method for Preparation of Extractive-Free Wood*. 1996 (Reapproved 2013).
59. Sluiter, A., et al., *Determination of extractives in biomass*. Laboratory Analytical Procedure (LAP), 2005. **1617**.
60. Procentese, A., et al., *Deep eutectic solvent pretreatment and subsequent saccharification of corncob*. *Bioresource Technology*, 2015. **192**: p. 31-36.
61. Hames, B., et al., *Preparation of samples for compositional analysis*. Laboratory Analytical Procedure (LAP). National Renewable Energy Laboratory, 2008.
62. Zhang, C.W., S.Q. Xia, and P.S. Ma, *Facile pretreatment of lignocellulosic biomass using deep eutectic solvents*. *Bioresource Technology*, 2016. **219**: p. 1-5.
63. Zhang, W., J.R. Barone, and S. Renneckar, *Biomass Fractionation after Denaturing Cell Walls by Glycerol Thermal Processing*. *ACS Sustainable Chemistry & Engineering*, 2015. **3**(3): p. 413-420.
64. Sathitsuksanoh, N., et al., *Lignin fate and characterization during ionic liquid biomass pretreatment for renewable chemicals and fuels production*. *Green Chemistry*, 2014. **16**(3): p. 1236-1247.
65. Zhu, J.Y., X.J. Pan, and R.S. Zalesny, *Pretreatment of woody biomass for biofuel production: energy efficiency, technologies, and recalcitrance*. *Applied Microbiology and Biotechnology*, 2010. **87**(3): p. 847-857.
66. Grohmann, K., et al., *The role of ester groups in resistance of plant cell wall polysaccharides to enzymatic hydrolysis*. *Applied Biochemistry and Biotechnology*, 1989. **20**(1): p. 45.
67. Zheng, Y., Z. Pan, and R.H. Zhang, *Overview of biomass pretreatment for cellulosic ethanol production*. *International journal of agricultural and biological engineering*, 2009. **2**(3): p. 51-68.
68. Zhu, L.F., et al., *Structural features affecting biomass enzymatic digestibility*. *Bioresource Technology*, 2008. **99**(9): p. 3817-3828.
69. Alvira, P., et al., *Pretreatment technologies for an efficient bioethanol production process based on enzymatic hydrolysis: a review*. *Bioresource technology*, 2010. **101**(13): p. 4851-4861.
70. Kumar, A.K., B.S. Parikh, and M. Pravakar, *Natural deep eutectic solvent mediated pretreatment of rice straw: bioanalytical characterization of lignin extract and enzymatic hydrolysis of pretreated biomass residue*. *Environmental Science and Pollution Research*, 2016. **23**(10): p. 9265-9275.
71. Xu, G.-C., et al., *Enhancing cellulose accessibility of corn stover by deep eutectic solvent pretreatment for butanol fermentation*. *Bioresource Technology*, 2015.
72. Yiin, C.L., et al., *Characterization of natural low transition temperature mixtures (LTTMs): Green solvents for biomass delignification*. *Bioresource Technology*, 2016. **199**: p. 258-264.
73. Froschauer, C., et al., *Separation of hemicellulose and cellulose from wood pulp by means of ionic liquid/cosolvent systems*. *Biomacromolecules*, 2013. **14**(6): p. 1741-1750.
74. Yu, Q., et al., *Two-step liquid hot water pretreatment of Eucalyptus grandis to enhance sugar recovery and enzymatic digestibility of cellulose*. *Bioresource Technology*, 2010. **101**(13): p. 4895-4899.

75. Wang, Q.Q., et al., *Cell wall disruption in low temperature NaOH/urea solution and its potential application in lignocellulose pretreatment*. Cellulose, 2015. **22**(6): p. 3559-3568.
76. Yuan, T.-Q., et al., *Synergistic benefits of ionic liquid and alkaline pretreatments of poplar wood. Part I: effect of integrated pretreatment on enzymatic hydrolysis*. Bioresource technology, 2013. **144**: p. 429-434.
77. Arantes, V., J. Jellison, and B. Goodell, *Peculiarities of brown-rot fungi and biochemical Fenton reaction with regard to their potential as a model for bioprocessing biomass*. Applied Microbiology and Biotechnology, 2012. **94**(2): p. 323-338.
78. Goodell, B., et al., *Low molecular weight chelators and phenolic compounds isolated from wood decay fungi and their role in the fungal biodegradation of wood*. Journal of Biotechnology, 1997. **53**(2): p. 133-162.
79. Koenig, A.B., et al., *NMR structural characterization of Quercus alba (white oak) degraded by the brown rot fungus, Laetiporus sulphureus*. Journal of wood chemistry and technology, 2010. **30**(1): p. 61-85.
80. Yelle, D.J., et al., *Evidence for cleavage of lignin by a brown rot basidiomycete*. Environmental microbiology, 2008. **10**(7): p. 1844-1849.
81. Yelle, D.J., et al., *Multidimensional NMR analysis reveals truncated lignin structures in wood decayed by the brown rot basidiomycete Postia placenta*. Environmental microbiology, 2011. **13**(4): p. 1091-1100.
82. Agosin, E., et al., *Solid-state fermentation of pine sawdust by selected brown-rot fungi*. Enzyme and microbial technology, 1989. **11**(8): p. 511-517.
83. Kirk, T.K., *Effects of a brown-rot fungus, Lenzites trabea, on lignin in spruce wood*. Holzforschung-International Journal of the Biology, Chemistry, Physics and Technology of Wood, 1975. **29**(3): p. 99-107.
84. Kirk, T.K. and E. Adler, *Methoxyl-deficient structural elements in lignin of sweetgum decayed by a brown-rot fungus*. Acta Chem. Scand, 1970. **24**(3379): p. 90.
85. Verdia, P., et al., *Fractionation of lignocellulosic biomass with the ionic liquid 1-butylimidazolium hydrogen sulfate*. Green Chemistry, 2014. **16**(3): p. 1617-1627.

Chapter 4 Enzymatic saccharification of pretreated lignocellulosic biomass with glycine and a chelator-mediated Fenton System

4.1 Abstract

Ground sweet gum (*Liquidambar styraciflua*) (SG) and southern yellow pine (*Pinus taeda spp.*) (YP) were pretreated separately (single stage) and in sequence (double stage) with choline chloride (1:2) deep eutectic solvent (DES) at 150°C for 2 h and with a chelator-mediated Fenton system (CMF) at 30°C. The saccharification efficiency of the pretreated SG and YP biomasses was studied as a function of the synergy of choline chloride-glycerol (ChCl-gly) DES technology and the chemistry of chelator-mediated Fenton system. After partially removal of hemicellulose and lignin, the cellulose enriched fibers were enzymatic hydrolyzed with enzyme cocktail of Cellic CTech3. Observing and enhancement of the cellulose hydrolysis rate, particularly for the double stage ChCl-gly DES followed by CMF pretreated SG solid residue exhibited a conversion of cellulose into glucose of 50% within 18 h and reached 78.1% of ultimate glucan digestibility after 72 h, compared to 6.1% of glucan digestibility of untreated SG biomass. This pretreated sample also presented an increased crystallinity index of 83.1% compared to the initial 67.02% of the untreated SG species, showing that the increase in crystallinity did not limit the digestibility of cellulose after the pretreatments. However, the pretreatments were not as effective on YP samples, as after 72hrs a maximum of 24% glucose was released from the softwood sample.

4.2 Key words

Biofuels, fractionation, deep eutectic solvent, chelator-mediated Fenton system, polysaccharides, delignification, crystallinity.

4.3 Introduction

Lignocellulose is a valuable renewable resource that can be converted to liquid biofuels, serving as an alternative to fossil fuels which are under scrutiny for carbon emissions [1]. Because of the issues that surround fossil resources, it is expected that a bio-based economy will grow in this century adding to energy security, environmental safety, and socioeconomic development of the rural sector [2]. Lignocellulose is a non-edible abundant material and can be found commercially from the forest products industry [3], agro-industries and urban residues [4, 5]. Further it can therefore displace first generation biofuels not only because of the variety of feedstocks but also for the additional production of value added chemicals and biomaterials in biorefinery facilities [6, 7]. The projection is that bioenergy would supply 15% of global energy demand by 2050 [8], forest lignocellulose softwood and hardwood resources are approximately 370 million tons per year [9]. Some hardwoods, such as sweetgum, can grow rapidly and have been studied as short rotation woody crops therefore could have potential applications as valuable source for bioethanol production [10-12]. Moreover, softwood species such as the group of southern yellow pines has been studied as a renewable source for bioethanol [13-15] and it is the most commercial set of softwood species within the USA. However, the production of lignocellulosic bioethanol is not cost-effective compared to cheap oil, due to technical and financial restrictions that must be overcome [16, 17]. Many advances have been made in the field of bioethanol production from lignocellulosic biomass, however more eco-friendly and more efficient saccharification technologies remain to be developed.

Lignocellulosic biomass is a complex network of three main biopolymers: cellulose, hemicellulose and lignin. These major lignocellulose components form a complex blend at the nanoscale; cellulose gives the structural strength and is surrounded by hemicellulose and lignin

that adds to rigidity of the wall. The transformation of lignocellulose to liquid fuels depend on the deconstruction of the cell wall and the conversion of the carbohydrates to sugars [18-20]. There are two approaches for lignocellulose conversion: thermal pathways and biochemical processing. Thermal conversion includes processes in which biomass is heated with or without catalysts resulting in three major streams: biochar, bio-oil and syngas. Thermal processing is considered energy self-sufficient but faces technical and economic barriers [21]. The biochemical processing of lignocellulose implies transformation to sugars, this can be attained by hydrolysis via enzymes [22] or chemicals [23]. The biochemical pathway for bioethanol production has three major steps: pretreatment, saccharification and fermentation [1, 24, 25]. Many advances have been made in the field of pretreatments, enzymes and enzymatic hydrolysis and fermentation, however still research need to be done to achieve an efficient bioethanol production.

Polysaccharide biodegradation includes aspects such as microbial and fungal enzyme systems and their interactions with the substrates, kinetics and extent of the saccharification. These aspects are influenced by some biomass structural features due to biomass recalcitrance [26]. Factors such as cellulose degree of polymerization, crystallinity, particle size, porosity, lignin and hemicellulose content play important roles in biomass conversion, as well as the biomass surface area and pore volume which are critical physical barriers for cellulose accessibility [27-29]. Some investigations have been conducted to get more insights regarding the two last factors, it has been reported that pore size is the most important factor in the cellulose enzymatic hydrolysis and CrI% had little influence [30]. Furthermore, lignin content, acetyl content and biomass crystallinity have been shown to be interrelated in the degree of conversion [31]. Chang and Holtzaple [32] reported that for low degrees of crystallinity and short hydrolysis periods,

lignin content was not important, and samples with low lignin content, crystallinity was not important. However most of the scientific publication report that a decrease in cellulose crystallinity increase the enzymatic hydrolysis rate [31, 33-35]. It is clear from the literature that enzymatic conversion is dependent upon the substrate but many parameters are inter-related.

The debate about the role of crystallinity in enzymatic hydrolysis remains, researchers have shown the relationship between the hydrogen-bond network within the cellulose crystalline regions and the enzyme performance during the hydrolysis [36]. In addition, the crystallinity index (CrI) is a three dimensional parameter that does not correlate with the two dimensional surface area associated with enzymatic cellulose hydrolysis [37, 38]. Further, CrI values published for cellulose are based in different measurement techniques [39, 40] and calculation approaches [41, 42]. On the other hand, the experimental conditions such temperature and humidity also influence the cellulose/lignocellulose crystallinity changes [43] as well as dried samples vs. the actual sample surfaces exposed to enzymes after pretreatment. Moreover, some researchers have correlated the cellulose *CrI*% to cellulose allomorphs, Chundawat et al. [36] studied molecular dynamics simulations (MD) and modified the hydrogen bond network within cellulose crystalline regions, then the enzymatic hydrolysis was performed and demonstrated that cellulase activity increased. By treating cellulose with ammonia, these authors decreased the number of intra hydrogen bonds and increasing the number of inter hydrogen bonds in the glucan chain, converting the native cellulose into cellulose III_I so that the number of exposed hydrogen bonds in cellulose was controlled. Access of endoglucanases to cellulose substrates was improved and the rate of glucan digestibility for cellulose III_I increased. This cellulose allomorph exhibited a higher *CrI*% than cellulose I_β (Figure 4-1). MD simulations showed that cellulose crystal structure influenced enzyme binding.

Recently, other pathways to access sugars linked into biomass polysaccharides to breakdown polysaccharides and lignin have been discovered, lytic polysaccharide monooxygenase enzymes [44, 45] and the AA9 group [46] can bind and disrupt crystalline cellulose chains at the surface meanwhile other cellulases attack amorphous cellulose. Therefore, the native structure of the cell wall restricts the effective access of enzymes to transform cellulose into fermentable sugars.

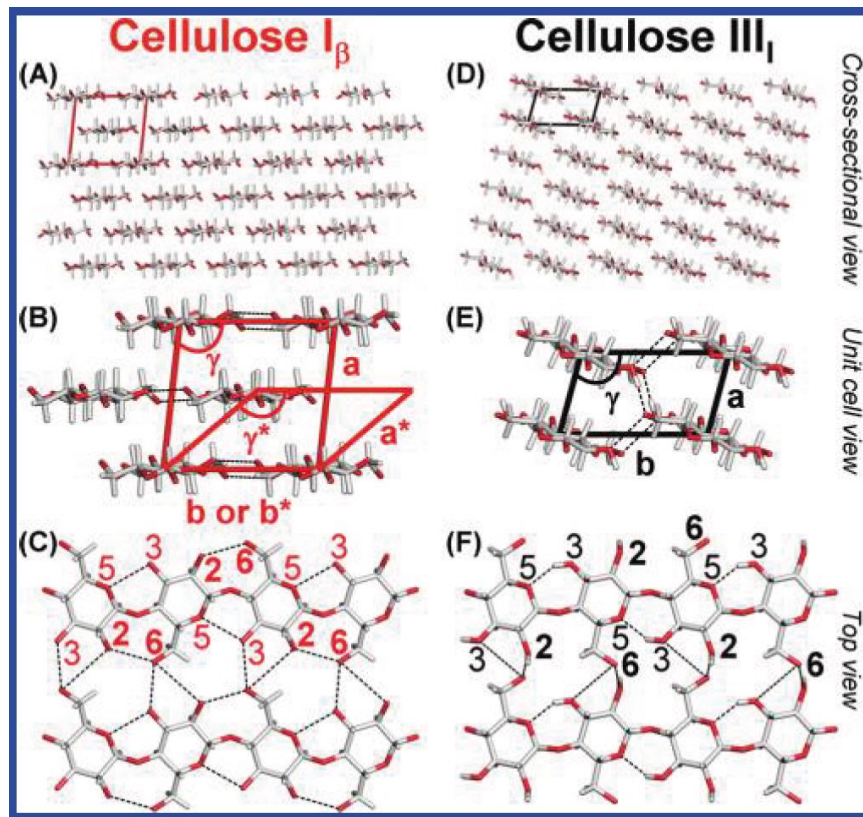


Figure 4-1 Cellulose representation and hydrogen bond network (dotted lines). Use under fair use.

Biomass pretreatment prior to enzymatic hydrolysis is a critical step for reducing the structural barriers to enzyme access to efficiently produce liquid biofuels. An extensive research has been conducted to investigate many routes to overcome lignocellulose recalcitrance for effective

enzymatic saccharification. Among the chemical methods lignocellulose to obtain biomass in a suitable manner for enzyme accessibility are dilute acid [47], alkaline pretreatment [48], steam explosion [49] and organosolv [50, 51]. These pretreatments have advantages and drawbacks and generate harmful byproducts for fermentation such as furfurals in treatments such as steam-explosion [52].

More recently, in an attempt to develop greener technologies for biomass saccharification, ionic liquids (ILs) have been used for lignocellulose biomass pretreatment because they can dissolve cellulose and lignocellulose facilitating their functionalization and catalytic conversion [53-58], however their cost and their difficult handling prevent their industrial applications. Deep eutectic solvents (DESs) are ILs substitutes [59] and have been applied to biomass processing due to their beneficial characteristics such as low vapor pressure, non-flammable, and thermal stability [60]. DESs are solvent mixtures with a freeze point lower than their components and have the ability of donating or accepting protons and electrons forming hydrogen bonds so that can increase their dissolution capability [61, 62]. DESs have been used in lignocellulosic biomass pretreatments [62-68] for their ability to depolymerize lignin into more valuable chemicals and because they are inexpensive and safe [62]. Thus, green solvent technology such as DES will continue to play an important role in lignocellulose bioprocessing.

Other technologies for pretreatment and saccharification are non-enzymatic radical based mechanisms. The chelator-mediated Fenton system has been developed as a non-enzymatic cell wall disruption system mimicking biomass brown-rot decay and has emerged as a new technology for lignocellulosic biomass deconstruction to produce sugars and other valuable products [69]. Even though researchers have indicated that CMF system should not be

considered as lignocellulose pretreatment, in this work we have used softwood and hardwood lignocellulose pretreated with CMF system and GLY as pretreatments to disrupt the cell wall. The novelty of these approach was the combination of emerging deep eutectic solvents at high temperature (150°C) with a CMF system at ambient temperature (chapter 2). These two pretreatments were applied separately (single stage) and in sequence (double stage). It has been reported that GLY (single stage) pretreatment partially removed lignin and hemicellulose whereas the CMF system (single stage) partially depolymerized cellulose, and solubilized lignin and hemicellulose; such that the degraded products of these processes remained in the pulping liquor. The biopolymers removal in the single stage GLY or CMF pretreatments was low, therefore sequential treatments were explored so that the solubilization of biopolymers during these pretreatments was enhanced and the pretreated biomass was cellulose enriched and suitable for enzymatic hydrolysis. The objective of this work is to evaluate the enhancement of glucan digestibility of GLY/CMF (single and double stage) pretreated lignocellulosic biomass and get more insights of the mechanism of how the depolymerization of lignocellulose cell wall components impacted the saccharification efficiency. Therefore, the experimental protocols supplied a route to examine the influence of the degree of cell wall disruption, along with the impact of the chemical composition on conversion efficiency, offering additional experimental insight into key factors of glucan digestibility. The following study determines the glucan digestibility of native hardwoods and softwood and the extent of the saccharification of pretreated biomass - GLY SG/YP, CMF SG/YP single stage pretreatments and CMF followed by GLY or CMF followed by GLY SG double stage pretreatment and how pretreatments affect cellulose crystallinity.

4.4 Experimental

4.4.1 Materials

All chemicals and reagents used in this study were purchased from Sigma-Aldrich, unless otherwise mentioned. A mature sweet gum (*Liquidambar styraciflua*) tree and from Blacksburg, VA was debarked, cut to cubes, and stored frozen before use. Southern yellow pine lumber (*Pinus spp.*) was purchased locally. Both biomasses were milled using a Thomas-Willey mill model 4, and sorted to a particle size between 40 and 60 mesh on a metal screen (250-420 μm). The extractive-free sweet gum particles were prepared according to the ASTM standard D1 105 [70]; and southern yellow pine particles were prepared according to the NREL standard Procedures [71]. Deionized water (DI water: 18.2 $\text{m}\Omega$) was used in all the steps of this research. The biomass samples were pretreated and then air dried. The enzymatic hydrolysis was carried out in the Renewable Resources Lab in the Centro of Biotecnología of Universidad de Concepción (Concepción, Chile). The enzyme cocktail Cellic Ctech3 was used for cellulose digestibility, containing 188 mg protein per mL. All feedstocks were further lyophilized overnight after the enzymatic hydrolysis to eliminate the moisture content, lyophilized and kept at 4°C in a cold room.

4.4.2 Glyceline deep eutectic solvent and chelator-mediated Fenton pretreatments

Extractive-free biomass (~6% MC) was subjected to single and double stage pretreatments with GLY deep eutectic solvent (1:10 dry mass basis) and heated in an oil bath at 150°C for 2 h; and also with a chelator-mediated Fenton system as detailed previously (Chapter 3). After the pretreatments, the pretreated biomass samples were air dry to eliminate the variable of moisture content.

4.4.3 Biomass Structural Carbohydrate Analysis

Lignin and carbohydrate contents of native, GLY, CMF, CMF followed by GLY (CMF+ GLY), and DES followed by CMF (GLY +CMF) pretreated SG and YP biomasses were analyzed according to the NREL laboratory analytical procedures (LAP) to determine and quantify the structural carbohydrates and lignin in the biomass [71-73]. Acid insoluble lignin (AIL - Klason lignin) was analyzed gravimetrically through the mass difference before and after heating the acid-hydrolyzed residue at 575°C. The carbohydrates in the filtrate were analyzed in triplicate using a Metrohm Ion Chromatography (IC) installed with a pulsed amperometric detector (PAD), Metrohm Inc., USA. Monosaccharides in the filtrate were separated by a Hamilton RCX-30 (250 × 4.6 mm) column with DI water as the eluent. The eluent flow rate was 1 mL/min, and the column temperature was 32°C. NaOH (350 mmol/L) and a flow rate of 0.43 mL/min was introduced after column separation to aid the PAD signal generation at 32 °C. Five sugars, L-(+)-arabinose, D-(+)-galactose, D-(+)-glucose, D-(+)-xylose, and D-(+)-mannose, were quantified using Mag IC Net software. Linear calibration curves ($R^2 > 0.9999$ and relative standard error < 5%) were run prior to every batch test. The monosaccharide concentrations were converted to the relative percentage of their anhydro-form in the biomass according to the NREL standard.

4.4.4 Enzymatic hydrolysis

Non-pretreated and pretreated SG and YP were enzymatic hydrolyzed in triplicate with a total volume of 25 mL composed of 2% solids (w/v). Hydrolysis using an enzymatic load of 0.022 g/g of solid (enzyme weight per g dry solid weight) and 0.05 M sodium citrate buffer of pH 4.8 was performed in a shaker at 50°C and 150 rpm for 72 h. The enzyme used was Cellic Ctec3.

(Novozymes, Denmark). The reactions were sampled (0.5 mL) at multiple time points (12, 24,

48 and 72 h). Samples were centrifuged at 10.000 rpm for 10 minutes, filtered and frozen for further analysis. The soluble glucose in the enzymatic hydrolysate was measured by HPLC.

4.4.5 Determination of released glucose

Glucose released during the enzymatic hydrolysis was determined on a Shimadzu high performance liquid chromatograph (HPLC) without dilution of enzymatic hydrolyzed samples. Enzymatic digestibility was measured using the enzymatic hydrolysis yield:

$$\% \text{ Digestibility} = \frac{G_h}{\left(\frac{180}{162}\right) \times G_i} \times 100\%$$

where G_h is the amount of soluble glucose after the enzymatic hydrolysis and G_i is the initial amount of glucan in the biomass before enzymatic hydrolysis. The concentration of monomeric sugars in the soluble fraction was determined by high-performance liquid chromatography using a HPLC LaChrom-Merck-Hitachi (Tokyo, Japan) equipped with a refractive index detector and Aminex HPX-87H column (Bio-Rad, Hercules, CA) at 45°C, a mobile phase of $5 \times 10^{-3} \text{ mol L}^{-1} \text{ H}_2\text{SO}_4$ and a flow rate of 0.6 mL min^{-1} [74]. Glucose and xylose were used as external calibration standards.

The glucan content was calculated by multiplying the glucose content by 0.9; the xylan content obtained from the xylose content multiplied by 0.88; and the acetyl groups content was calculated by multiplying the acetic acid content by 0.7 [75].

4.4.6 X-ray diffraction (XRD) of untreated and pretreated SG and YP biomass

The crystallinity index of the pretreated and the hydrolyzed biomass after pretreatment of SG and YP samples was measured in a Bruker D* Discover X-ray diffractometer with Cu K α radiation source ($\lambda = 0.154$ nm) generated at 40 KV and 40 mA. A 1 mm slit was used and a locked couple 2-theta and theta scan was performed from 10 $^\circ$ to 50 $^\circ$ at a scan speed of 4 $^\circ$ /min. All biomass samples were flattened on a quartz slide with a thickness of 1-2 mm to collect the diffraction profile. Untreated SG and YP were used as control samples. For SG and YP biomass samples after the enzymatic hydrolysis, the pretreated SG and YP biomass samples were used as references.

The crystallinity index (*CrI*) of the different SG and YP biomass samples tested was calculated according to the methods developed by Segal and coworkers [76]:

$$CrI = \frac{I_{200} - I_{AM}}{I_{200}} \times 100\%$$

Where I_{200} is the maximum intensity of the 200 lattice diffraction and I_{AM} is the minimum intensity between the 200 peak and the 101 peak. Other methods such as Ruland-Vonk method [77] and deconvolution method [41] were used for comparison.

4.5 Results and discussion

This study focuses on glucan digestibility of single and double stage GLY/CMF pretreated SG and YP biomasses. Overall mass balances and characterization of the hydrolyzed biomass and hydrolysate were also conducted. All untreated and pretreated SG and YP biomass samples were analyzed in triplicate according to NREL standard procedure [73]. The carbohydrates and lignin content of the treated biomass differ from the corresponded pretreated samples as can be seen in Table 4-1 and reveal a substantial removal of all biopolymers from lignocellulose during the

pretreatments. Pretreatments with GLY removed glucan marginally. However, lignin was extensively removed in all treatments as well as hemicelluloses, and consequently the pretreated biomass remained with a more enriched glucan fraction more suitable for enzymatic saccharification.

Table 4-1 Chemical composition (relative) of untreated and pretreated ground SG and YP biomass samples.

	AIL (%)	ASL (%)	Arabinan (%)	Galactan (%)	Glucan (%)	Xylan (%)	Mannan (%)	Total (%)
Untreated SG	22.2	3.5	0.6	0.6	38.7	19.8	1.9	87.2
GLY SG	20.1	3	0.1	0.4	50.8	20.4	2.1	96.8
CMF SG	18.3	4.4	0.2	0.4	38.6	18.5	1.5	81.8
CMF+GLY SG	10.7	2.5	0	0	68.2	12.6	1.6	95.5
GLY+CMF SG	18.4	1.7	0.1	0.1	54.1	15.2	1.6	91.0
Untreated YP	28.5	0.5	1	1.6	42.3	6.4	11.6	91.8
GLY YP	21.6	0.5	0.1	1.3	58.4	5.9	10.7	98.4
CMF YP	24.9	2.9	0.6	0.7	42.1	4.2	7.6	83.0
CMF+GLY SG	23.3	0.7	0	0.2	64.1	2.1	4.0	94.3
GLY+CMF SG	17.2	2.8	0.1	0.4	52.9	2.5	2.9	78.8

4.5.1 Enhanced enzymatic hydrolysis of biomass through lignin and hemicellulose removal during the single and double stage pretreatments with a deep eutectic solvent DES and a CMF system

A critical step in the biofuel production from lignocellulosic biomass is the saccharification of the cellulose and heteropolysaccharides to fermentable sugars in a cost-effective manner.

Untreated SG and YP samples were enzymatically hydrolyzed by commercial cellulase enzymes showing slow hydrolysis rates and low glucan digestibility yields of 6.1% and 6.3% for SG and YP samples, respectively. All pretreated biomass samples were air dried after the pretreatment, this may negatively impact the subsequent enzymatic hydrolysis due to the fact that changes

caused by the treatment such as bigger surface area or higher degree of porosity may disappear with drying. Both SG and YP pretreated biomasses exhibited similar trends in glucan digestibility but the efficiency was different (Figures 4-2 and 6-4). After GLY treatment, a moderate enhancement of enzymatic glucan digestibility was observed for SG (32%) and a slight enhancement for YP (9%). In the case of CMF treatment, glucan digestibility was enhanced up to 53% and 16.1% for SG and YP, respectively. This result confirmed the observations made by Goodell et al. [69] that CMF system did not increase the porous volume of CMF treated softwood, limiting enzyme accessibility to cellulose. A subsequent CMF pretreatment (double stage GLY followed by CMF pretreatment) enhanced the enzymatic hydrolysis with 50% of substrates hydrolyzed after 16 h, and reaching an ultimate glucan digestibility of 78.1%. This result was in agreement with the already reported by Zhang et al. [78] for pretreated GTP SG (SG treated by glycerol thermal processing pretreatment) which was 78% of glucan digestibility. Additionally, these data are comparable to the data reported by Procentese et al. [67] who treated corncob with GLY at 150°C for 15 h, the saccharification reaching a glucose yield of 70%. Also, Zhang et al. [68] studied corncob treatment with ChCl-gly DES at 90°C for 24 h and the subsequent saccharification resulted in a glucose yield of 94%. For YP biomass, the double stage DES followed by CMF treatment showed a slight enhancement of glucan digestibility up to 16.01%. The results for the other sequence CMF followed by GLY were different, for SG biomass, the increment of glucan digestibility was marginal when the second GLY treatment was applied (from 54% to 56%).

Whereas for YP, the enhancement of the saccharification was from 6% to 24.2% of glucan digestibility. This value is comparable to the 27.3% glucan digestibility reported by Kim and Hong [13] in supercritical CO₂ pretreated YP biomass. Yet, these data are considerably lower

than the glucose release reported recently for enzymatic hydrolysis of YP biomass pretreated with [Emim][Ac] IL at 130°C for 90 min, in which the glucose released reached 95% [79]. Mou et al. [80] treated ground YP species with sodium xylene sulphonate (SXS) solvent for 120 min to partially removed lignin, the pretreated YP biomass was then enzymatically hydrolyzed reaching a glucose yield of 15.5%, comparable to the data obtained in this research for the double stage pretreated DES followed by CMF YP biomass (16.1% glucose yield, Figure 4-3). In the same study, YP biomass was treated also with 1-ethyl-3-methyl imidazolium acetate [EmimAC] at 130°C (IL and then enzymatically hydrolyzed, the authors reported a low glucose yield due to the formation of pseudolignins consisting of carbohydrate degradation products (dehydration of C₆ and C₅ sugars) which covered the surface area of YP biomass decreasing the enzyme accessibility to cellulose [80-83].

More recently, Goodell et al. [69] have demonstrated the similarity of the CMF mechanism with the brown-rot fungal decay for all components of lignocellulose by analyzing sum frequency generation spectra of CMF and brown-rot fungi treated YP samples. These researchers found that using TEM analysis for softwoods after CMF treatment the biomass porosity did not increase even though cellulose and lignin were depolymerized by CMF reactions. These reactions generated glucose and oligosaccharides residues, although the cellulolytic enzymes (around 4 nm size) could not penetrate to contribute to the cell wall deconstruction. Further, they found that YP decayed by *G. Trabeum* showed an erosion in elementary microfibrils during the degradation by partial loss of glucose and cellulose crystallinity. However, SANS data revealed that the surface morphology of cell walls did not change during the degradation. It is known that iron redox cycling occurs via hydroquinone chelators produced by brown-rot fungi, so these SANS results support the hypothesis that CMF treatments were able to deconstruct lignocellulose cell wall.

The authors conducted the enzymatic hydrolysis of the treated CMF YP biomass and no further hemicellulose removal or lignin changes were observed. Goodell et al. [69] concluded that CMF treatment mimicking the brown-rot decay mechanism is a non-enzymatic degradation of polysaccharides accompanied by an aggregation and/or redistribution of lignin. CMF system does not open the softwood cell wall structure to enzymes in softwoods, so that enzymatic hydrolysis is less effective. [84-87].

On the other hand, CMF treatment applied to hardwood partially opens up the cell wall structure permitting the enzyme access to cellulose and enhancing glucan digestibility. In this work the glucan digestibility reached up to 54%. A subsequent GLY treatment of CMF SG did not contribute significantly to enhance the digestibility as it reached only 56% showing no synergy in the combination of these two pretreatments. Therefore, all pretreatments impacted the composition of the biomass, however, they did not all provide similar amounts of glucan digestibility.

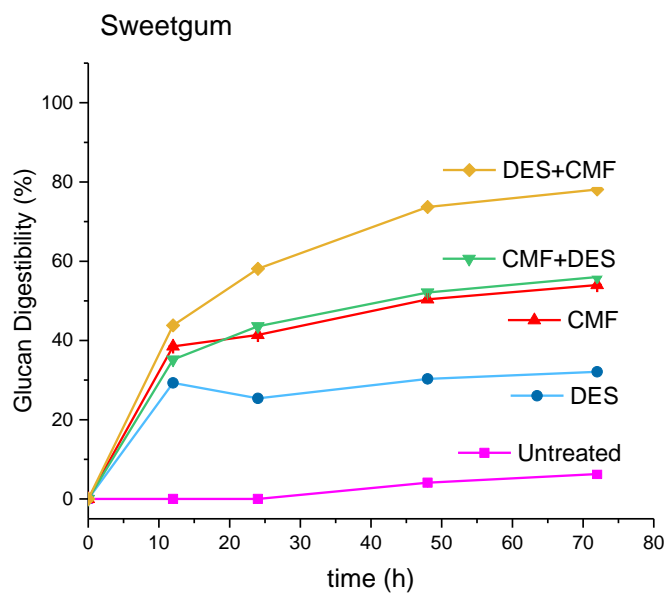


Figure 4-2 Enzymatic glucan digestibility profiles of untreated and pretreated SG with a DES and a CMF system.

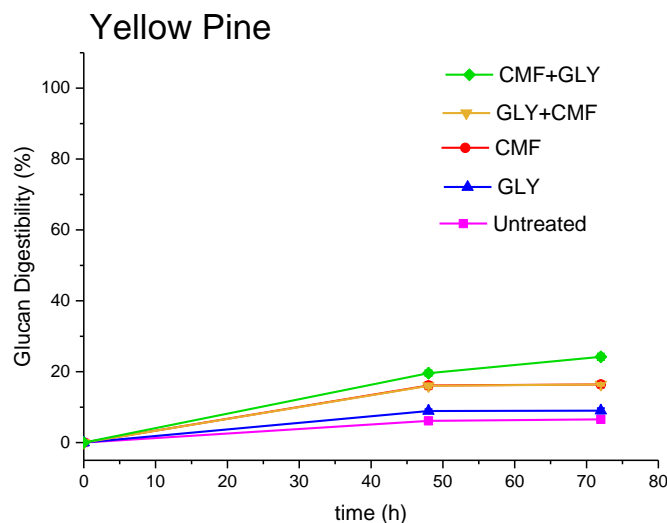


Figure 4-3 Enzymatic glucan digestibility profiles of untreated and pretreated YP with GLY and a CMF system.

4.5.2 XRD crystallinity of untreated and single and double stage DES and CMF pretreated biomass and cellulose

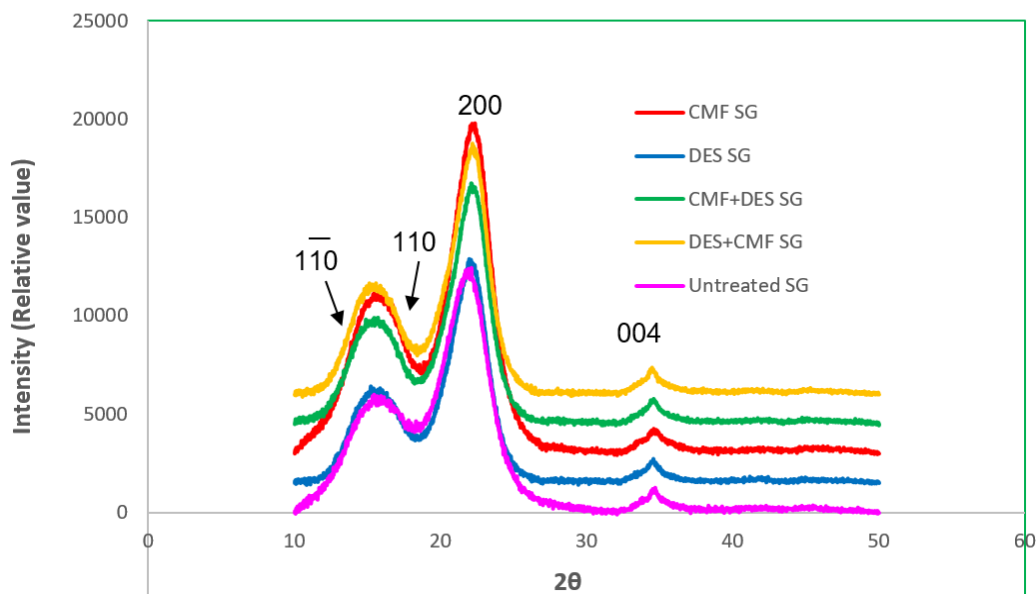
XRD technique is used to investigate the structural changes in the cellulose substrates due to pretreatments and enzymatic hydrolysis [88]. It is difficult to estimate the absolute crystalline and amorphous cellulose content in lignocellulosic biomass samples; the XRD peaks as an index are used to compare the relative differences among lignocellulose samples [32, 89]. All pretreatments studied in this research caused a disruption of the cell wall matrix and this was reflected with the degree of digestibility of the cellulose. The untreated SG and YP samples were used as controls and DES and CMF (single and double stage) pretreated samples were analyzed by changes in crystallinity index CrI using Seagal method [76] and depicted in the XRD

diffractograms shown in Figure 4-4. The intensities of the amorphous region at $2\theta = 18^\circ$ and the crystalline region at $2\theta = 22^\circ$ were used to calculate the *CrI* (Table 6-2.). It has been reported the relationship between *CrI* and enzyme digestibility in lignocellulosic biomass [69, 90-92], cellulose is considered to contain both crystalline and amorphous regions and heteropolysaccharides and lignin may provide background signal to the amorphous regions.

The XRD diffractogram analysis (Table 4-2) shows that the *CrI* of untreated SG and YP are 67.1% and 77.8%, respectively. This percentage is lower than Avicell cellulose reported as having a *CrI* of 91.7 ± 1.5 [41], as Avicell is highly crystalline after acid hydrolysis. It has been suggested that crystallinity decreases during the CMF treatment [93, 94]. However, more recently Goodell et al. [69] have reported a slight increase in *CrI* of CMF softwood treated biomass, in agreement with the results obtained in this study for softwood YP biomass which was 77.9%, similar to the initial *CrI* in the untreated YP biomass. The single stage pretreated CMF SG exhibited a slightly higher *CrI* of 80.8% indicating a slight change of the crystallinity compared to the untreated SG biomass. This can be explained by the amount of amorphous components of the lignocellulose cell wall (lignin and hemicellulose) that have been removed during the single stage CMF treatment (higher in SG than in YP, Table 4-2) as it has been already suggested for other research groups [88]. Additionally, the increase in the I_{200} peak showed an increase in the cellulose crystallinity of the single stage pretreated CMF SG samples as shown by [88].

Previous reports have mentioned that DES pretreatment caused an increment of crystallinity [67, 95], this is consistent with the findings in this study. The single stage pretreated DES YP presented a *CrI* of 79.0% indicating a slight increase compared to the untreated sample. In the

case of single stage pretreated DES SG, the *CrI* was 75.9% showing an increase in crystallinity. The double stage CMF followed by DES or the DES followed by CMF also had a considerable impact in the crystallinity of cellulose. For softwood pretreated CMF followed by DES YP, the second treatment increased the *CrI* up to 85.5% whereas with the other pretreatment DES followed by CMF, softwood crystallinity increased up to 82.3%. In the case of hardwood, CMF followed by DES pretreated SG exhibited a slightly increment in *CrI* (83.2%), meanwhile the DES followed by CMF pretreated SG showed a *CrI* of 83.9%.



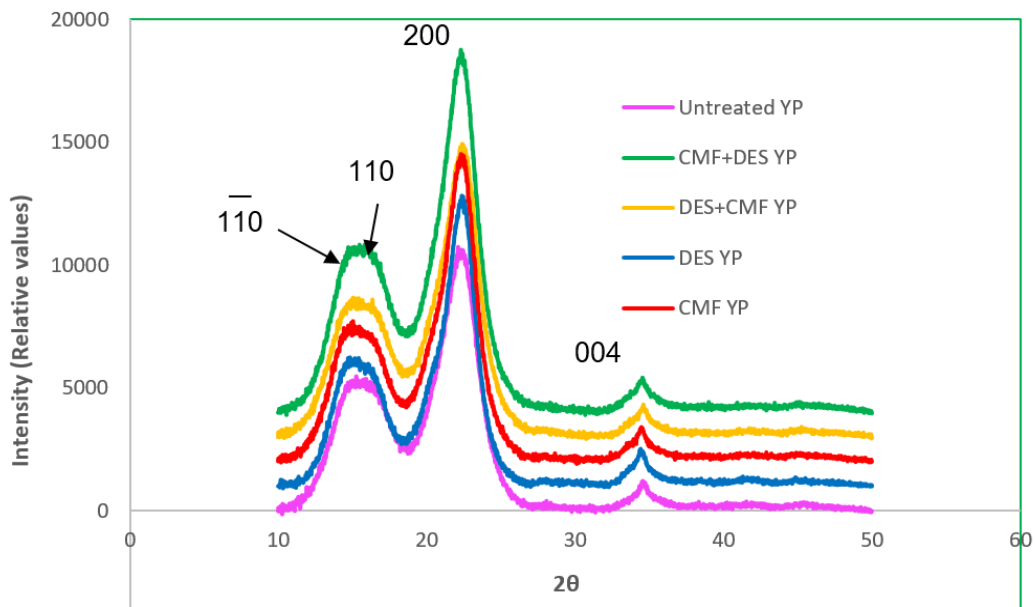


Figure 4-4 Figure XRD diffractograms of untreated and pretreated SG and YP biomass

Table 4-2 Effects of biomass composition in crystallinity and glucan digestibility

Pretreatment	Glucan (%)	Xylan (%)	Galactan (%)	Mannan (%)	Arabinan (%)	AIL (%)	ASL (%)	Crystallinity (%)	Glucan Digestibility (%)
Untreated SG								67.05	6.1
GLY SG	1	22	40	11	89	30	37	80.98	32
CMF SG	16	21	46	32	75	30	100	75.91	54
CMF+GLY SG	16	76	99	63	99	61	62	83.16	56
GLY+CMF SG	1	52	100	45	97	44	47	83.98	78
Untreated YP								77.77	6.3
GLY YP	0	33	43	33	95	45	34	78.96	8.9
CMF YP	11	40	62	41	49	22	-410	78.92	16.1
CMF+GLY YP	12	69	81	66	95	39	85	85.46	24.2
GLY+CMF YP	36	65	75	78	22	34	-416	82.27	16

4.5.3 Effect of delignification on single and double stage pretreated SG and YP with a Glyceline DES and a CMF system, on the crystallinity and on the enzyme digestibility

One of the major restrictions for lignocellulose digestibility is the presence of lignin [96] so that the removal of lignin during a pretreatment is desired, even though this may have little effect on the order of the structure of crystalline cellulose [97], yet may impact the crystallinity of lignocellulose samples. In this study, for SG biomass, the residual lignin in the pretreated lignocellulose biomass corresponding to the highest lignin removals were 61% of AIL and 62% of ASL and were reached during the CMF followed by GLY pretreatment which did not presented the highest hydrolysis rate (56%), neither the highest crystallinity (83%). The best results for glucan digestibility were found for double stage GLY followed by CMF SG samples which showed a lignin removal of 44% of AIL and 47% of ASL and it correlated with the highest crystallinity of the pretreated SG sample (84%). It should be noted that for this sample, glucan removal was trivial (1%) in both stages GLY and CMF sequential treatments, thus the integrity of glucan chains was preserved increasing the crystallinity and cellulase activity that led

to an enhancement of hydrolysis rate of up to 78.1%. This data confirm Chundawat et al. studies about cellulose crystallinity [36] discussed in the introduction section. It is worthy to point out that all the single and double stage pretreatments increased the crystallinity index while removed certain amounts of lignin and hemicelluloses.

The behavior for YP biomass was different than SG biomass, the lowest percentage of residual lignin for YP corresponding to the highest lignin removal was also obtained during the double stage CMF followed by DES pretreatment (39% AIL and 85% ASL) but in this case, these YP samples showed the best hydrolysis rate (24.2%). It should be noted that a removal of 16% of glucan in both pretreatment sequences was observed for both double stage sequences in YP biomass the integrity of glucan chain was altered, it should be noted that despite this the *CrI* was intensified. Thus, the composition of the pretreated biomass and the crystallinity of the samples are correlated with the rate of enzymatic hydrolysis and the extent of the glucan digestibility.

4.5.4 Effect of hemicellulose removal on single and double stage pretreated SG and YP with glycine and a CMF system, on the crystallinity and on the enzyme digestibility

Among the hemicelluloses, residual xylan is of great interest because has significant influence in the cellulose digestibility of pretreated biomass [98-100], commercial enzyme cocktails that include “accessory” xylanase enzymes are used to improve the yields of biomass saccharification especially for hardwoods [96, 101, 102]. DES pretreatment in SG showed a xylan removal of 22%, whereas the double stage DES followed by CMF pretreatment presented a xylan removal of 52% increasing the glucan digestibility up to 78.1% despite the increased of the *CrI*%. For the other pretreatment sequence in SG biomass, CMF treatment removed xylan reaching up to 21% and the second treatment in the sequence removed substantial cumulative amount of xylan 76%

for CMF followed by GLY SG, even though the *CrI*% increased the glucan digestibility was only 56%. For single stage pretreated GLY YP biomass, xylan was removed in a percentage of 33% and double stage DES followed by CMF pretreated YP samples resulted in a cumulative xylan removal of 65% resulting in a glucan digestibility of 24.2%. For single stage CMF YP pretreated biomass xylan was removed by 40% and in the sequential GLY YP pretreatment, xylan was removed in a cumulative percentage of 69%. Thus, results found for SG showed that for a hardwood species in the conditions of the pretreatments applied in this study, removal of around 50% of xylan from the original native sample, as presented in the GLY+CMF treatment, allowed an enhancement of glucan digestibility of 78.1%. Removal of greater amounts of xylan from lignocellulose as showed in the double stage CMF+GLY pretreatment did not increase hydrolysis rate or glucan digestibility, probably because a concomitant glucan removal of 16% during the CMF treatment impacted the rate of the enzymatic hydrolysis. Therefore, removing around 50% of initial xylan polysaccharide from SG biomass by GLY+CMF pretreatment along with around 50% removal of lignin enhanced the glucan enzymatic hydrolysis. The more lignin was removed by the pretreatments the more xylan also was removed (table 2) for both SG and YP pretreated biomass. For YP, these observations correlated also with an increase in crystallinity, however it was not the case for SG in which a greater lignin and xylan removal corresponded to a decreased in *CrI*. Therefore removal of xylan impacted directly the cellulose accessibility to enzymes and the rate of the glucan digestibility as already demonstrated by Zhang et al. [78].

4.6 Conclusions

Novel pretreatment methods combining the technology of DES and the CMF treatment applied alone (single stage) or in sequence (double stage) were used to study the impact of structure and composition of hardwood and softwood lignocellulose biomass on the enzymatic glucan digestibility. DES selectively extracts hemicellulose and lignin, with little impact in glucan. CMF system was nonspecific and effectively depolymerized polysaccharides and modified lignin. All pretreatments disrupted the cell wall and changing the composition and crystallinity and considerably impacted the enzymatic saccharification of cellulose. Best results were obtained by DES followed by CMF pretreated SG which presented glucan digestibility of 78.1%, whereas for YP biomass was the other sequence CMF followed by DES pretreatment that presented best glucan digestibility (24.2%). Higher crystallinity due to pretreatment has no negative impact on enzymatic hydrolysis.

4.7 Acknowledgements

The authors acknowledge the financial support from Secretaría Nacional de Ciencia y Tecnología SENECYT, the Instituto de Fomento al Talento Humano IFTH, and Universidad San Francisco de Quito for the scholarship awarded to Lourdes Orejuela to pursue a doctoral degree at Virginia Tech, along with support from the Institute for Critical Technology and Applied Science, the Macromolecules Innovation Institute and the Sustainable Biomaterials Department of Virginia Tech. Also, authors acknowledge the Department of Wood Sciences at the University of British Columbia and the Department of Microbiology at University of Massachusetts. Special acknowledgements are given to the Centro de Biotecnología of the University of Concepción for the award to conduct the experimental part of this research.

4.8 References

1. Balat, M., *Production of bioethanol from lignocellulosic materials via the biochemical pathway: a review*. Energy conversion and management, 2011. **52**(2): p. 858-875.
2. Demirbas, A., *Biofuels sources, biofuel policy, biofuel economy and global biofuel projections*. Energy conversion and management, 2008. **49**(8): p. 2106-2116.
3. Duff, S.J. and W.D. Murray, *Bioconversion of forest products industry waste cellulose to fuel ethanol: a review*. Bioresource technology, 1996. **55**(1): p. 1-33.
4. Pandey, A., et al., *Biotechnological potential of agro-industrial residues. I: sugarcane bagasse*. Bioresource technology, 2000. **74**(1): p. 69-80.
5. Prasad, S., A. Singh, and H. Joshi, *Ethanol as an alternative fuel from agricultural, industrial and urban residues*. Resources, Conservation and Recycling, 2007. **50**(1): p. 1-39.
6. Ragauskas, A.J., et al., *The path forward for biofuels and biomaterials*. science, 2006. **311**(5760): p. 484-489.
7. Cherubini, F., *The biorefinery concept: using biomass instead of oil for producing energy and chemicals*. Energy Conversion and Management, 2010. **51**(7): p. 1412-1421.
8. Fischer, G. and L. Schrattenholzer, *Global bioenergy potentials through 2050*. Biomass and bioenergy, 2001. **20**(3): p. 151-159.
9. Limayem, A. and S.C. Ricke, *Lignocellulosic biomass for bioethanol production: current perspectives, potential issues and future prospects*. Progress in Energy and Combustion Science, 2012. **38**(4): p. 449-467.
10. Merkle, S. and M. Cunningham, *Southern hardwood varietal forestry: a new approach to short-rotation woody crops for biomass energy*. Journal of Forestry, 2011. **109**(1): p. 7-14.
11. Kline, L.M., et al., *Simplified determination of lignin content in hard and soft woods via uv-spectrophotometric analysis of biomass dissolved in ionic liquids*. Bioresources, 2010. **5**(3): p. 1366-1383.
12. Adams, J.P., et al., *Sweetgum: a new look*. Iforest-Biogeosciences and Forestry, 2015. **8**.
13. Kim, K.H. and J. Hong, *Supercritical CO₂ pretreatment of lignocellulose enhances enzymatic cellulose hydrolysis*. Bioresource technology, 2001. **77**(2): p. 139-144.
14. Miller, S. and R. Hester, *Concentrated acid conversion of pine softwood to sugars. Part I: Use of a twin-screw reactor for hydrolysis pretreatment*. Chemical Engineering Communications, 2007. **194**(1): p. 85-102.
15. Cox, B.J. and J.G. Ekerdt, *Pretreatment of yellow pine in an acidic ionic liquid: Extraction of hemicellulose and lignin to facilitate enzymatic digestion*. Bioresource Technology, 2013. **134**: p. 59-65.
16. Gomez, L.D., C.G. Steele-King, and S.J. McQueen-Mason, *Sustainable liquid biofuels from biomass: the writing's on the walls*. New Phytologist, 2008. **178**(3): p. 473-485.
17. Quesada-Pineda, H.J., J. Withers, and R. Smith, *Perceptions on Internal and External Factors Impacting the US Nonfood Advanced Biofuel Industry*, in *Frontiers in Bioenergy and Biofuels*. 2017, InTech.
18. Blanch, H.W., B.A. Simmons, and D. Klein-Marcuschamer, *Biomass deconstruction to sugars*. Biotechnology Journal, 2011. **6**(9): p. 1086-1102.

19. de Souza, R., L.S.M. Miranda, and R. Luque, *Bio(chemo)technological strategies for biomass conversion into bioethanol and key carboxylic acids*. Green Chemistry, 2014. **16**(5): p. 2386-2405.
20. Lange, J.P., *Lignocellulose conversion: an introduction to chemistry, process and economics*. Biofuels, bioproducts and biorefining, 2007. **1**(1): p. 39-48.
21. Lee, R.A. and J.-M. Lavoie, *From first- to third-generation biofuels: Challenges of producing a commodity from a biomass of increasing complexity*. Animal Frontiers, 2013. **3**(2): p. 6-11.
22. Sun, Y. and J. Cheng, *Hydrolysis of lignocellulosic materials for ethanol production: a review*. Bioresource technology, 2002. **83**(1): p. 1-11.
23. Tao, F.R., H.L. Song, and L.J. Chou, *Catalytic conversion of cellulose to chemicals in ionic liquid*. Carbohydrate Research, 2011. **346**(1): p. 58-63.
24. Lee, J., *Biological conversion of lignocellulosic biomass to ethanol*. Journal of Biotechnology, 1997. **56**(1): p. 1-24.
25. Chen, H.N. and X. Fu, *Industrial technologies for bioethanol production from lignocellulosic biomass*. Renewable and Sustainable Energy Reviews, 2016. **57**: p. 468-478.
26. Mansfield, S.D., C. Mooney, and J.N. Saddler, *Substrate and enzyme characteristics that limit cellulose hydrolysis*. Biotechnology progress, 1999. **15**(5): p. 804-816.
27. Sathitsuksanoh, N., A. George, and Y.H.P. Zhang, *New lignocellulose pretreatments using cellulose solvents: a review*. Journal of Chemical Technology and Biotechnology, 2013. **88**(2): p. 169-180.
28. Meng, X.Z. and A.J. Ragauskas, *Recent advances in understanding the role of cellulose accessibility in enzymatic hydrolysis of lignocellulosic substrates*. Current Opinion in Biotechnology, 2014. **27**: p. 150-158.
29. Arantes, V. and J.N. Saddler, *Access to cellulose limits the efficiency of enzymatic hydrolysis: the role of amorphogenesis*. Biotechnol Biofuels, 2010. **3**(4): p. 1-11.
30. Grethlein, H.E., *The effect of pore size distribution on the rate of enzymatic hydrolysis of cellulosic substrates*. Nature Biotechnology, 1985. **3**(2): p. 155-160.
31. Chang, V.S. and M.T. Holtzapfel. *Fundamental factors affecting biomass enzymatic reactivity*. in *Twenty-First Symposium on Biotechnology for Fuels and Chemicals*. 2000. Springer.
32. Zhu, L.F., et al., *Structural features affecting biomass enzymatic digestibility*. Bioresource Technology, 2008. **99**(9): p. 3817-3828.
33. Dadi, A.P., C.A. Schall, and S. Varanasi, *Mitigation of cellulose recalcitrance to enzymatic hydrolysis by ionic liquid pretreatment*, in *Applied Biochemistry and Biotechnology*. 2007, Springer. p. 407-421.
34. Fan, L., Y.H. Lee, and D. Beardmore, *The influence of major structural features of cellulose on rate of enzymatic hydrolysis*. Biotechnology and Bioengineering, 1981. **23**(2): p. 419-424.
35. Gharpuray, M., Y.H. Lee, and L. Fan, *Structural modification of lignocellulosics by pretreatments to enhance enzymatic hydrolysis*. Biotechnology and bioengineering, 1983. **25**(1): p. 157-172.
36. Chundawat, S.P.S., et al., *Restructuring the Crystalline Cellulose Hydrogen Bond Network Enhances Its Depolymerization Rate*. Journal of the American Chemical Society, 2011. **133**(29): p. 11163-11174.

37. Gao, S., et al., *New insights into enzymatic hydrolysis of heterogeneous cellulose by using carbohydrate-binding module 3 containing GFP and carbohydrate-binding module 17 containing CFP*. *Biotechnology for biofuels*, 2014. **7**(1): p. 24.
38. Cheng, G., et al., *Transition of cellulose crystalline structure and surface morphology of biomass as a function of ionic liquid pretreatment and its relation to enzymatic hydrolysis*. *Biomacromolecules*, 2011. **12**(4): p. 933-941.
39. Agarwal, U.P., R.S. Reiner, and S.A. Ralph, *Cellulose I crystallinity determination using FT-Raman spectroscopy: univariate and multivariate methods*. *Cellulose*, 2010. **17**(4): p. 721-733.
40. Atalla, R.H. and D.L. VanderHart, *The role of solid state ¹³C NMR spectroscopy in studies of the nature of native celluloses*. *Solid State Nuclear Magnetic Resonance*, 1999. **15**(1): p. 1-19.
41. Park, S., et al., *Cellulose crystallinity index: measurement techniques and their impact on interpreting cellulase performance*. *Biotechnology for biofuels*, 2010. **3**(1): p. 10.
42. Ahvenainen, P., I. Kontro, and K. Svedström, *Comparison of sample crystallinity determination methods by X-ray diffraction for challenging cellulose I materials*. *Cellulose*, 2016. **23**(2): p. 1073-1086.
43. Bhuiyan, M.T., N. Hirai, and N. Sobue, *Changes of crystallinity in wood cellulose by heat treatment under dried and moist conditions*. *Journal of Wood Science*, 2000. **46**(6): p. 431-436.
44. Agger, J.W., et al., *Discovery of LPMO activity on hemicelluloses shows the importance of oxidative processes in plant cell wall degradation*. *Proceedings of the National Academy of Sciences*, 2014. **111**(17): p. 6287-6292.
45. Müller, G., et al., *Harnessing the potential of LPMO-containing cellulase cocktails poses new demands on processing conditions*. *Biotechnology for biofuels*, 2015. **8**(1): p. 187.
46. Hu, J., et al., *Substrate factors that influence the synergistic interaction of AA9 and cellulases during the enzymatic hydrolysis of biomass*. *Energy & Environmental Science*, 2014. **7**(7): p. 2308-2315.
47. Grethlein, H.E., *Process for pretreating cellulosic substrates and for producing sugar therefrom*. 1980, Google Patents.
48. Chang, V.S., B. Burr, and M.T. Holtzapple, *Lime pretreatment of switchgrass*. *Applied biochemistry and biotechnology*, 1997. **63**(1): p. 3-19.
49. Grous, W.R., A.O. Converse, and H.E. Grethlein, *Effect of steam explosion pretreatment on pore size and enzymatic hydrolysis of poplar*. *Enzyme and Microbial Technology*, 1986. **8**(5): p. 274-280.
50. Holtzapple, M.T. and A.E. Humphrey, *The effect of organosolv pretreatment on the enzymatic hydrolysis of poplar*. *Biotechnology and Bioengineering*, 1984. **26**(7): p. 670-676.
51. Zhao, X.C., K; and Liu, D., *Organosolv pretreatment of lignocellulosic biomass for enzymatic hydrolysis*. *Applied Microbiology and Biotechnology*, 2009. **82**: p. 815-827.
52. Mosier, N., et al., *Features of promising technologies for pretreatment of lignocellulosic biomass*. *Bioresource technology*, 2005. **96**(6): p. 673-686.
53. Liu, H.B., et al., *Understanding the Interactions of Cellulose with Ionic Liquids: A Molecular Dynamics Study*. *Journal of Physical Chemistry B*, 2010. **114**(12): p. 4293-4301.

54. Li, Q., et al., *Improving enzymatic hydrolysis of wheat straw using ionic liquid 1-ethyl-3-methyl imidazolium diethyl phosphate pretreatment*. *Bioresource Technology*, 2009. **100**(14): p. 3570-3575.
55. Schrems, M., et al., *Ionic liquids as media for biomass processing: opportunities and restrictions*. *Holzforschung*, 2011. **65**(4): p. 527-533.
56. Brandt, A., et al., *The effect of the ionic liquid anion in the pretreatment of pine wood chips*. *Green Chemistry*, 2010. **12**(4): p. 672-679.
57. Brandt, A., et al., *Deconstruction of lignocellulosic biomass with ionic liquids*. *Green Chemistry*, 2013. **15**(3): p. 550-583.
58. Verdia, P., et al., *Fractionation of lignocellulosic biomass with the ionic liquid 1-butylimidazolium hydrogen sulfate*. *Green Chemistry*, 2014. **16**(3): p. 1617-1627.
59. Abbott, A.P., et al., *Deep eutectic solvents formed between choline chloride and carboxylic acids: Versatile alternatives to ionic liquids*. *Journal of the American Chemical Society*, 2004. **126**(29): p. 9142-9147.
60. Durand, E., J. Lecomte, and P. Villeneuve, *From green chemistry to nature: The versatile role of low transition temperature mixtures*. *Biochimie*, 2015.
61. Francisco, M., A. van den Bruinhorst, and M.C. Kroon, *Low-transition-temperature mixtures (LTTMs): A new generation of designer solvents*. *Angewandte Chemie international edition*, 2013. **52**(11): p. 3074-3085.
62. De Oliveira Vigier, K., G. Chatel, and F. Jerome, *Contribution of Deep Eutectic Solvents for Biomass Processing: Opportunities, Challenges, and Limitations*. *ChemInform*, 2015. **46**(26).
63. Abougor, H., *Utilization of deep eutectic solvent as a pretreatment option for lignocellulosic biomass*. 2014, Tennessee Technological University.
64. Alvarez-Vasco, C., et al., *Unique low-molecular-weight lignin with high purity extracted from wood by deep eutectic solvents (DES): a source of lignin for valorization*. *Green Chemistry*, 2016. **18**(19): p. 5133-5141.
65. Jablonský, M., et al., *Deep Eutectic Solvents: Fractionation of Wheat Straw*. *BioResources*, 2015. **10**(4): p. 8039-8047.
66. Kumar, A.K., B.S. Parikh, and M. Pravakar, *Natural deep eutectic solvent mediated pretreatment of rice straw: bioanalytical characterization of lignin extract and enzymatic hydrolysis of pretreated biomass residue*. *Environmental Science and Pollution Research*, 2015: p. 1-11.
67. Procentese, A., et al., *Deep eutectic solvent pretreatment and subsequent saccharification of corncob*. *Bioresource Technology*, 2015. **192**: p. 31-36.
68. Zhang, C.-W., S.-Q. Xia, and P.-S. Ma, *Facile pretreatment of lignocellulosic biomass using deep eutectic solvents*. *Bioresource Technology*, 2016. **219**: p. 1-5.
69. Goodell, B., et al., *Modification of the nanostructure of lignocellulose cell walls via a non-enzymatic lignocellulose deconstruction system in brown rot wood-decay fungi*. *Biotechnology for biofuels*, 2017. **10**(1): p. 179.
70. ASTM, *Preparation of Extractive-Free Wood*. 1996 (Reapproved 2013).
71. Sluiter, A., et al., *Determination of extractives in biomass*. *Laboratory Analytical Procedure (LAP)*, 2005. **1617**.
72. Hames, B., et al., *Preparation of samples for compositional analysis*. *Laboratory Analytical Procedure (LAP)*. National Renewable Energy Laboratory, 2008.

73. Sluiter, A., et al., *Determination of structural carbohydrates and lignin in biomass*. Laboratory analytical procedure, 2008. **1617**: p. 1-16.
74. Araque, E., et al., *Evaluation of organosolv pretreatment for the conversion of Pinus radiata D. Don to ethanol*. Enzyme and Microbial Technology, 2008. **43**(2): p. 214-219.
75. Elissetche, J.-P., et al., *Thiobarbituric acid reactive substances, Fe³⁺ reduction and enzymatic activities in cultures of Ganoderma australe growing on Drimys winteri wood*. FEMS microbiology letters, 2006. **260**(1): p. 112-118.
76. Segal, L., et al., *An empirical method for estimating the degree of crystallinity of native cellulose using the X-ray diffractometer*. Textile Research Journal, 1959. **29**(10): p. 786-794.
77. Vonk, C., *Computerization of Ruland's X-ray method for determination of the crystallinity in polymers*. Journal of Applied Crystallography, 1973. **6**(2): p. 148-152.
78. Zhang, W., et al., *Enhanced enzymatic saccharification of pretreated biomass using glycerol thermal processing (GTP)*. Bioresource technology, 2016. **199**: p. 148-154.
79. Shill, K., et al., *Ionic liquid pretreatment of cellulosic biomass: enzymatic hydrolysis and ionic liquid recycle*. Biotechnology and bioengineering, 2011. **108**(3): p. 511-520.
80. Mou, H.-Y., et al., *Topochemical pretreatment of wood biomass to enhance enzymatic hydrolysis of polysaccharides to sugars*. Bioresource technology, 2013. **142**: p. 540-545.
81. Pu, Y., et al., *Assessing the molecular structure basis for biomass recalcitrance during dilute acid and hydrothermal pretreatments*. Biotechnology for biofuels, 2013. **6**(1): p. 15.
82. Sannigrahi, P., et al., *Pseudo-lignin and pretreatment chemistry*. Energy & Environmental Science, 2011. **4**(4): p. 1306-1310.
83. Hu, F., S. Jung, and A. Ragauskas, *Pseudo-lignin formation and its impact on enzymatic hydrolysis*. Bioresource Technology, 2012. **117**: p. 7-12.
84. Stewart, D., *Lignin as a base material for materials applications: Chemistry, application and economics*. Industrial crops and products, 2008. **27**(2): p. 202-207.
85. Xu, C., F. Ferdosian, and SpringerLink, *Conversion of Lignin into Bio-Based Chemicals and Materials*. 1st 2017 ed. 2017, Berlin, Heidelberg: Springer Berlin Heidelberg.
86. Hemingway, R.W., et al., *Adhesives from renewable resources*. Vol. 385. 1989, Washington, DC: American Chemical Society.
87. Abe, A., et al., *Biopolymers: lignin, proteins, bioactive nanocomposites*. Vol. 232;232.: 2 010, Berlin: Springer.
88. Guo, H., et al., *Changes in the supramolecular structures of cellulose after hydrolysis studied by terahertz spectroscopy and other methods*. RSC Advances, 2014. **4**(101): p. 57945-57952.
89. Kim, S. and M.T. Holtzapple, *Effect of structural features on enzyme digestibility of corn stover*. Bioresource Technology, 2006. **97**(4): p. 583-591.
90. Kim, S.B., et al., *Pretreatment of Rice Straw by Proton Beam Irradiation for Efficient Enzyme Digestibility*. Applied Biochemistry and Biotechnology, 2011. **164**(7): p. 1183-1191.
91. Kim, S.H., C.M. Lee, and K. Kafle, *Characterization of crystalline cellulose in biomass: basic principles, applications, and limitations of XRD, NMR, IR, Raman, and SFG*. Korean Journal of Chemical Engineering, 2013. **30**(12): p. 2127-2141.

92. Yang, S.J., et al., *Enhancement of enzymatic digestibility of Miscanthus by electron beam irradiation and chemical combined treatments for bioethanol production*. Chemical Engineering Journal, 2015. **275**: p. 227-234.
93. Goodell, B., et al., *Low molecular weight chelators and phenolic compounds isolated from wood decay fungi and their role in the fungal biodegradation of wood*. Journal of Biotechnology, 1997. **53**(2): p. 133-162.
94. Paszczynski, A., et al., *De Novo Synthesis of 4, 5-Dimethoxycatechol and 2, 5-Dimethoxyhydroquinone by the Brown Rot Fungus Gloeophyllum trabeum*. Applied and Environmental Microbiology, 1999. **65**(2): p. 674-679.
95. Xu, G.-C., et al., *Enhancing cellulose accessibility of corn stover by deep eutectic solvent pretreatment for butanol fermentation*. Bioresource Technology, 2015.
96. Várnai, A., M. Siika-aho, and L. Viikari, *Restriction of the enzymatic hydrolysis of steam-pretreated spruce by lignin and hemicellulose*. Enzyme and Microbial Technology, 2010. **46**(3): p. 185-193.
97. Zhao, H., et al., *Studying cellulose fiber structure by SEM, XRD, NMR and acid hydrolysis*. Carbohydrate polymers, 2007. **68**(2): p. 235-241.
98. Kumar, R. and C.E. Wyman, *Effect of xylanase supplementation of cellulase on digestion of corn stover solids prepared by leading pretreatment technologies*. Bioresource Technology, 2009. **100**(18): p. 4203-4213.
99. Chandra, R.P., et al., *Substrate pretreatment: The key to effective enzymatic hydrolysis of lignocellulosics?*, in *Biofuels*. 2007, Springer. p. 67-93.
100. Alvira, P., et al., *Pretreatment technologies for an efficient bioethanol production process based on enzymatic hydrolysis: a review*. Bioresource technology, 2010. **101**(13): p. 4851-4861.
101. Bura, R., R. Chandra, and J. Saddler, *Influence of xylan on the enzymatic hydrolysis of steam-pretreated corn stover and hybrid poplar*. Biotechnology progress, 2009. **25**(2): p. 315-322.
102. Hu, J., V. Arantes, and J.N. Saddler, *The enhancement of enzymatic hydrolysis of lignocellulosic substrates by the addition of accessory enzymes such as xylanase: is it an additive or synergistic effect?* Biotechnology for biofuels, 2011. **4**(1): p. 36.

Chapter 5 Structural analysis of recovered lignin fractions isolated from biomass after glyceline and chelator-mediated Fenton pretreatments

5.1 Abstract

Lignocellulose sweetgum (SG) and yellow pine (YP) biomass samples were treated individually (single stage) and in sequence (double stage) with a glyceline at 150°C for 2 h and a chelator-mediated Fenton system (CMF) at ambient temperature to achieve cell wall deconstruction. After the pretreatments, resulting products were washed with hot DI water and ethanol 90%. As a result three different streams were generated in each case: an aqueous-DES phase, an ethanol phase and the solid pretreated biomass. Aqueous-DES phases contained water insoluble precipitates (high molecular weight compounds - HMWC) and water soluble compounds (low molecular weight compounds LMWC) were centrifuged. The HMWC (lignin) fractions were isolated, lyophilized and labeled as single stage GLY SG and GLY YP, and double stage CMF followed by GLY SG and CMF followed by GLY YP lignin fractions, respectively. These fractions represented the 9%, %, 11%, 13% and 15% of klason lignin present in the starting biomass samples, respectively. Each isolated lignin fraction was quantified and analyzed by ³¹P NMR, 2D ¹³C-¹H heteronuclear single quantum coherence (HSQC) NMR and elemental analysis to determine pretreatment effects and evaluate changes in biopolymer structure. Gel permeation chromatography GPC showed that the MW of these lignin fractions had a relative high molecular weight. ¹H NMR indicated that these fractions were composed mainly of lignin, xylan (from 8 to 12%) and low concentrations of carbohydrates (from 1.7 to 2.9%). These pretreatments caused a significant β-O-4 bond disruption for both SG and YP samples compared to EMAL samples used as controls, especially during the double stage CMF followed by DES treatment. Both SG and

YP lignin fractions exhibited further condensation (β -5) phenylcoumaran. Moreover, β - β resinol bonds were significantly reduced especially in the double stage CMF+GLY SG and YP lignin fractions. Free aliphatic OH decreased in GLY SG lignin fraction showing depolymerization; however, the aliphatic OH significantly increased in CMF followed by GLY SG lignin fraction indicating that condensation has occurred. Free phenolic groups followed the same trend for SG lignin fractions. On the other hand, the free aliphatic OH for YP lignin fractions did not undergo significant changes, only a slight increment in GLY YP lignin fraction was observed whereas for CMF followed by GLY YP lignin fraction a slight decrease was observed indicating that GLY treatment caused a marginal condensation and the double stage treatment caused a slight depolymerization. For the free phenolic OH, results showed that single GLY SG and double stage CMF followed by GLY SG lignin fractions depolymerized, as a result free phenolic OH groups increased. For GLY YP lignin fractions, the phenolic OH increased showing depolymerization while for CMF followed by GLY YP lignin fractions, the phenolic OH significantly decreased indicating that repolymerization has occurred. These results indicate that the recovered lignin undergo structural changes common to GLY and CMF treatments.

5.2 Keywords

Lignin recovery, xylan, biomass valorization, depolymerization, repolymerization, biopolymers, biorefinery, single and double stage GLY/CMF pretreatments, structural analysis, NMR, MW.

5.3 Introduction

Lignocellulosic biomass is a renewable non edible resource with a relative low cost [1, 2]. From this biomass, lignin is the second most abundant aromatic biopolymer on our planet, and it has been considered as a sustainable source of aromatic carbon [3, 4]. An efficient utilization of

lignocellulose biomass requires an integrated process in which the majority of the wood components can be converted into useful products such as fuels and valuable chemicals with near neutral carbon emission [5, 6]. Currently, liquid fuels for transportation rely in non-renewable fossil resources, however studies in genetics, chemistry, biochemistry, and engineering are developing new manufacturing technologies (biorefinery) to obtain biofuels and bioproducts from lignocellulosic biomass for a bio-economy [7-9]. The plant cell wall is constituted mainly by two major polysaccharides: cellulose and hemicellulose, and lignin – a polyphenolic polymer [10]; all three components are tightly associated and contribute to biomass recalcitrance [11]. To get access to cellulose, lignocellulosic biomass needs a pretreatment that unlocks this recalcitrant structure so the polysaccharides will be susceptible for saccharification [12]. Along with the cell wall requirements for deconstruction, so that cellulose can be hydrolyzed chemically [13, 14] or enzymatically [15, 16] into sugars and fermented to bioalcohol [17], lignin needs to be isolated and converted into value-added chemicals [4, 18, 19]. Several pretreatments have been developed to achieve efficient separation of carbohydrates and lignin and these have been extensively reviewed [16, 20-22]. These methods include physical and mechanical treatments [23-25] as well as biological methods [26, 27]. Chemical treatments such as dilute acid soaking and alkali exposure and thermophysical treatments, steam explosion or hydrothermal have been also widely reviewed [28, 29], and these acid based treatments cause lignin degradation and can also cause equipment corrosion. Organosolv pulping has not been successfully adopted for biomass pretreatment, although it provides a high-quality lignin stream [30, 31]. New solvents such as ionic liquids and other solvents like phosphoric acid have been used to reach cell dissolution and cell wall deconstruction [32-35]. More recently, lignin fractionation by using deep eutectic solvents (DES) has also been introduced to achieve amenable biomass for

saccharification via enzymatic hydrolysis and subsequent fermentation to bioalcohol. These novel DESs have the advantage of being considered eco-friendly solvents [36-38]. Further novel pretreatments include biomimetic methods, such as the methods by Goodell et al. [39] who furthered a new non-enzymatic method of cell wall deconstruction called chelator-mediated Fenton system (CMF) to improve polysaccharide access for enzymatic digestibility and lignin fractionation to increase biorefinery cost-effectiveness.

Lignin is a complex crosslinked polymer constituted by phenylpropanoid subunits, and depending upon the species, consist of p-coumaryl, coniferyl and sinapyl alcohols. It is regarded as the most complex polymer of lignocellulose cell wall that provides strength and rigidity to the plant, at the same time binds the adjacent cells together and has the ability to form lignin-carbohydrate complexes (LCC) in the cell wall; lignin also plays a key role in water regulation and pathogen resistance [40]. Overall, lignin integration within the cell wall, can greatly inhibit lignocellulose enzymatic hydrolysis arising from limited accessibility and non-specific binding interactions [41]. During the pretreatment, the distribution, content, structure and molecular weight of lignin in the plant cell wall are typically modified [42]. The role of lignin in biorefining [19, 43] and the significance of NMR techniques such as ^{31}P and 2D-HSQC NMR for cell wall and biofuels precursors characterization have been highlighted by several researchers [44-50]. Moreover, special attention has been directed to lignin-carbohydrate linkages [51]. The relevance of the molecular weight of lignin and its relationship to recalcitrance has been studied by Ziebell et al. and other research groups [42, 52], according to these authors the lower recalcitrance in a transgenic alfalfa was due to the fact that the molecular weight of its lignin was low. Reducing the molecular weight of lignin would potentially enhance its removal, limiting biomass recalcitrance. Thus, a better understanding of lignin structure and its molecular weight

as well as its separation processes will lead to potential applications of lignin that will optimize the use of lignocellulosic biomass for the biorefinery and the valorization of lignin for novel and valuable chemicals.

5.4 Materials and Methods

5.4.1 Materials

Chemicals and reagents used in this study were purchased from Sigma-Aldrich and MP Biomedicals as used as received. A mature hardwood sweetgum (*Liquidambar styraciflua*) from Blacksburg, VA and southern yellow pine wood were selected as biomass resources in this research. Hardwood and softwood were machined to cubes and store in a freezer before use. Prior to pretreatment, the biomass was milled using a Wiley mill, and sorted to a particle size between 40-60 mesh on a metal screen (250 – 420 μm). Sequentially, sweetgum ground biomass was Soxhlet extracted with a mixture of toluene/ethanol (427 mL/1000 mL), followed by ethanol and then followed by hot water according to ASTM standard procedures [53]. Yellow pine ground biomass was Soxhlet extracted with DI water followed by ethanol as described in the standard protocol to produce extractive-free lignocellulose [54]. The resulting materials were air dried at ambient temperature for 48 h. Extractive-free SG and YP biomass were air dried and store in a cold room at 4°C.

5.4.2 Single and double stage DES and chelator-mediated Fenton pretreatments

Extractive-free biomass (~6% MC) was subjected to pretreatments with choline chloride:glycerol (1:2) deep eutectic solvent (1:10 dry mass basis) and heated in an oil bath at 150°C for 2 h; and

also with a chelator-mediated Fenton system, alone and in sequence (single and double stages) as detailed previously in Chapter 3.

5.4.3 Liquid-liquid extraction lignin recovery

After single stage DES and double stage CMF+DES pretreatments, each sample was vacuum filtered and washed with hot DI water until a clear filtrate was observed, a fair amount of dark brown precipitates were observed in the aqueous-DES liquor (aqueous phase). The pretreated biomass pellet was then washed with ethanol 90%, darker and finer particles soluble in ethanol were observed. Ethanol phases were evaporated in a rotary evaporator, freeze dried, labeled as ethanolic extracts and kept in at 4°C in the cold room. Aqueous-DES liquors were acidulated (pH=2) and subjected to a liquid-liquid extraction with ethyl acetate to separate the low molecular weight compounds. The ethyl acetate phases were isolated and the solvent was evaporated in a rotary evaporator under vacuum. Isolated ethyl acetate phases (low molecular weight compounds) were freeze dried, labelled as ethyl acetate extracts and kept in a cold room at 4°C. Subsequently, the aqueous phases containing high molecular weight (insoluble) lignin fractions were centrifuged, and lignin fractions were isolated, freeze-dried and labeled as GLY SG, GLY YP, CMF+GLY SG and CMF+GLY YP lignin fractions. Pretreated SG and YP biomasses (biomass residues) were air-dried at ambient temperature for 48 h and kept in the cold room at 4°C for further analysis. The lignin fractions recovery yield relative to the total initial biomass was calculated using the equation (1).

$$\text{Recovered lignin yield}\% = \frac{m_{rec\ lignin}}{m_0 \times Klignin_0} \times 100\% \quad (1)$$

$m_{rec\ lignin}$: dry mass of recovered GLY SG, GLY YP, CMF followed by GLY SG and CMF followed by GLY YP lignins for specific biomass input to pretreatment;

m_0 : total dry mass of biomass input to DES and CMF followed by DES pretreatments;

$Klignin_0$: Klason lignin content in biomass input.

Enzymatic mild acidolysis lignin (EMAL) from extractive free sweetgum from Zhang et al. work [49] was used as a reference for the GLY SG and CMF followed by GLY SG lignin fractions.

EMAL from southern yellow pine from the study of Guerra et al. [55] was used as reference for YP GLY and CMF followed by GLY YP lignin fractions.

5.4.4 Elemental analysis of GLY SG, GLY YP, CMF followed by GLY SG and CMF followed by DES YP lignin fractions

Elemental analysis (carbon, hydrogen and nitrogen) of recovered DES SG, DES YP, CMF followed by DES SG and CMF followed by DES YP lignin fractions was determined on automatic analyzer Fisons EA 1108. Results were reported as weight percentage of biomass dry weight (C%, H% and N%). Oxygen content was determined by subtracting the composition fraction of the carbon, hydrogen, and nitrogen from unity.

5.4.5 DES SG, DES YP, CMF followed by DES SG and CMF followed by DES YP lignin fractions acetylation

Lignin acetylation was performed according to the procedure of Glasser et al. [56]. 300 mg dried lignin fractions (DES SG, DES YP, CMF+DES SG and CMF+DES YP lignin samples) were dissolved in 9 mL of anhydrous pyridine followed by the addition of an equal volume of anhydrous acetic acid anhydride. Mixtures were sealed with rubber septum and reactions were performed at room temperature for 24 h under a nitrogen atmosphere with continuous stirring.

To recover the product, the solution was added dropwise into 600 mL of 0.01 N HCl. Precipitated acetylated lignin fractions were collected by filtration using 0.45 μ m nylon membrane and washed by another 200 mL 0.01 N HCl three times and 200 mL distilled water three times. Acetylated lignin fractions were dried in a vacuum oven at 50°C.

³¹P Phosphorous NMR of lignin spectra were acquired in Dr. Scott Rennecker's Advanced Renewable Materials Laboratory, in the University of British Columbia, Vancouver – Canada.

5.4.6 Quantitative ¹H NMR analysis

An amount of 20 mg acetylated lignin powders were dissolved in 800 μ L CDCl₃, following by the addition of 5 mg 4-nitrobenzaldehyde as internal standard. After dissolution, mixtures were transferred into 5mm NMR tubes and measured by Bruker Avance 300MHz spectrometer (Bruker Corp., MA Billerica, USA) with a relaxation delay 10 s, 30° pulse width, acquisition time 1.3 s, and scan number 256. This analysis was conducted in University of British Columbia, Vancouver.

5.4.7 Quantitative ³¹P-NMR analysis of recovered DES SG, DES YP, CMF+DES SG and CMF+DES YP lignin fractions

Quantitative ³¹P nuclear magnetic resonance spectroscopy analysis was adapted from Argyropoulos and his research group [57-61] as described by Zhang et al. [49] and was used to analyze the recovered single stage DES SG and DES YP lignin fractions and double stage CMF followed by DES SG and CMF followed by DES YP lignin fractions. The analysis was performed on a Varian INOVA 400 MHz multinuclear spectrometer at a frequency of 162.07 MHz for ³¹P spins. Prior to analysis, all lignin samples were stored in a vacuum oven for 48 h.

A solvent mixture of pyridine/chloroform-d₆ (CDCl₃) with a ratio of 1.6/1 (v/v) was prepared for ³¹P NMR, the pyridine was protected from the moisture with molecular sieves. The internal

standard *Endo* N-Hydroxy-5-norbornene-2,3-didicarboximide (e-HNDI) [62] and the relaxation reagent chromium (III) acetylacetonate ($\text{Cr}(\text{acac})_3$) [63] were prepared by dissolving in CDCl_3 , with a concentration of 5.6 mg/mL and 0.0 mg/mL, respectively. An exact amount of 20 mg of dried lignin powders were then dissolved in 400 μL of the solvent mixture followed by the addition of 100 μL internal standard solution, 40 μL relaxation reagent solution, and 50 μL 2-Chloro-4,4,5,5-tetramethyl-1,3,2-dioxaphospholane (TMDP) used as phosphitylation agent were added under continuous mixing until complete lignin fractions dissolution. The final solution was immediately transferred to a 5 mm NMR tube and quantitative ^{31}P -NMR spectra were acquired in a Bruker Avance 300 MHz spectrometer (Bruker Corp., MA Billerica, USA). An inverse gated decoupling pulse was employed to obtain quantitative ^{31}P NMR with the following parameters: number scans 800, relaxation delay 5 s, acquisition time 1.4 s, pulse length 6 μs , and 90° pulse width. The chemical shift of phosphitylation products were calibrated with a product of TMDP with water (residual moisture), which gave a sharp and stable signal at 132.2 ppm, and different functional groups were assigned as showed in (Figure 6-3), based on previous reports [60, 62]. It should be noted that syringyl phenolic groups were integrated separately from the C_5 condensed units based on literature [60].

5.4.8 Two dimensional ^{13}C - ^1H heteronuclear single quantum coherence (HSQC) NMR spectroscopy of recovered DES SG, DES YP, CMF+DES SG and CMF+DES YP lignin fractions

All dry lignin samples (approximately 40 mg) were prepared using 600 μL of DMSO-d_6 and mixed in vortex until homogenous (about 30 min) at around 25°C . The dissolved lignin fractions were transferred to 5 mm NMR tubes according to the method previously developed [49, 64-66]. HSQC spectra were acquired at 25°C using a Bruker spectrophotometer, Ascend TM 400MHz

model, equipped with a multinuclear inverse liquid probe with inverse geometry, with an acquisition: F2: 0.0800768 sec y F1: 0.0053004 sec, d1: 1 sec., TD (fid size): F2: 1024 F1: 256, and a SN (scan number): 64 (Bruker's standard pulse). Chemical shifts were referenced to the central DMSO peak at 39.5/2.5 ppm. (δ_C/δ_H). Assignments of the HSQC spectra were described elsewhere [67, 68]. A semi-quantitative analysis of the volume integrals of the HSQC correlation peaks was performed using Bruker's Topspin 3.2 processing software.

Zhang and Gellerstedt [69] developed an analytical method based on 2D-HSQC-NMR sequence and quantitative ^{13}C -NMR, which can be applied for quantitative structural determination of complicated polymers, such as lignin. A semi-quantitative (relative) method based on 2D-HSQC spectra without internal standard [70, 71] has been established to calculate the relative abundance of different structures and are estimated via the analysis of the volume integral of the HSQC cross-signal following the formula:

$$I_x\% = I_x / (I_A + I_B + I_C + I_D) \times 100\% \quad (2)$$

where I_A , I_B , I_C and I_D are the integral values of α position of β -O-4 (A), β -5 (B), β - β (C), and β -1 (D), respectively. All the integrals should be performed at the same contour level. Changes in lignin structure were determined based on volume integration of HSQC spectral contour correlations. The C_2 - H_2 positions of the guaiacyl unit and the $\text{C}_{2,6}$ - $\text{H}_{2,6}$ positions in the syringyl unit were considered to be stable. Therefore they were used as internal standard and represented the aromatic C_9 units in the lignin fraction. Spectra integration was performed on the same contour level. Since the integral of the correlation peak corresponding to these resonances represents for the double of the syringyl C_9 units present, the amount of the C_9 units present in hardwood can be quantified by the following equation [46]:

$$C_9 \text{ units} = 0.5 (S_{2,6}) + G_2 \quad (3)$$

And for softwoods is:

$$C_9 \text{ units} = 0.5G_2$$

where $S_{2,6}$ is the integral value of $S_{2/6}$ and includes S and S', G_2 is the integration of G_2 . Since syringyl units are absent in softwood, the amount of guaiacyl C_2 -H₂ signal reflects the total number of aromatic C_9 units in lignin. Therefore, the C_9 represents the integral value of the aromatic ring and according with the internal standard, the amount of $I_x\%$ is obtained according to the following formula:

$$I_x\% = I_x / C_9 \times 100\%$$

All integrals displayed less than 10% error (based on the use of organosolv lignin in triplicate – data not shown), confirming the precision of the quantification from 2D HSQC spectra.

5.4.9 Gel permeation chromatography of recovered GLY SG, GLY YP, CMF followed by GLY SG and CMF followed by GLY YP lignin fractions

The molecular weight distribution of acetylated lignin was performed via gel permeation chromatography (GPC), according to the method already described by Zhang et al. [49]. The lignin samples were previously acetylated to increase their solubility in organic solvents [72, 73]. Dried lignin powder was mixed with 6ml glacial acetic acid/pyridine (1:1 v/v) for 48 hours under nitrogen atmosphere with stirring. Lignin was precipitated through acidification by adding solvent into 200mL 0.01N aqueous HCl. The solvent was then carefully removed through filtering through 0.45 μ m paper, and the residue was vacuum oven dried. The dried acetylated lignin was dissolved into THF at 5mg/ml. the solvent was then stabilized for 48 hours at room temperature prior to filtering over 0.45 μ m filter. 100 μ L lignin solution was injected and analyzed

at a time. The system temperature was maintained at 35°C and THF (HPLC grade, Fisher Scientific) was used as elutes. GPC analyses were performed using Agilent 1100 GPC equipment (USA). The GPC system equipped with Agilent 1260 ISO pump, Styragel columns HR 4, HR 3, and HR 1 (Waters, Milford, MA), 1260 VWDVL UV (Agilent), WYATT 323-V2 viscostar, WYATT 477-TREX optilab T-rex, WYATT 800-H2HC MALLS. Light scattering and RI detector was performed at 785nm. Polystyrene (Mw 1300, 2000, 2500, 5780, 17500, 30000, 200000) received from Pressure Chemical Company was used for calibration. The sample analysis was performed using RI intensity, and (light scattering). EMAL SG molecular weights [49] and [55] already published were used as controls.

5.5 Results and Discussion

5.5.1 Single stage GLY and CMF and double stage GLY+CMF and CMF+GLY lignin yields through liquid-liquid extraction

Lignocellulose delignification through GLY extraction and CMF system treatment was reflected in percentages of lignin recovery of 13.72%, 19.11%, 20.42% and 20.15% for GLY SG, GLY YP, CMF GLY SG and CMF GLY YP as detailed in chapter 3. These results represent the 97%, 87%, 99% and 98% of the dried solids (cellulose, hemicellulose and/or lignin fractions) present in the filtrates after washing the pretreatment resulting products (mass balance chapter 3).

5.5.2 Quantitative ³¹P-NMR of recovered single stage GLY and CMF and double stage GLY followed by CMF and CMF followed by GLY lignin fractions

The chemical composition of the recovered lignin fractions was assessed by elemental analysis and ¹H-NMR. Table 5-1 reports the elemental composition, methoxyl content, calculated C₉ formulae and carbohydrates content of single stage GLY and CMF and double stage GLY+CMF

and CMF+GLY lignin fractions. These lignin fractions also contain xylan and small amounts of other carbohydrates. DES treatment extracted less amount of xylan from SG biomass (8.86%) than from YP biomass (12.19%). Regarding the other carbohydrates content, SG lignin fractions had a slightly higher content (2.89%) than YP lignin fraction (1.69%). Interestingly, when the double stage pretreatments were applied, GLY treatment after CMF treatment extracted larger amounts of xylan from SG biomass (12.19) whereas from YP biomass the percentage of extracted xylan was 7.9%. This result most likely related to the starting higher amount of xylan in the sweetgum biomass.

Table 5-1 Chemical composition of isolated GLY SG, GLY YP, CMF+GLY SG and CMF+GLY YP lignin fractions

Lignin sample	Elemental Analysis (%)				OCH ₃	C ₉ formulae	Xylan (%)	Carbohydrates (%)
	C	H	N	O				
GLY SG	53	5.44	1.3	31.4	8.86	C ₉ H _{0.92} O _{5.33} (OCH ₃) _{1.50}	8.86	2.89
CMF+GLY SG	56.93	6.18	1.1	23.6	12.19	C ₉ H _{0.98} O _{3.7} (OCH ₃) _{1.93}	10.49	2.17
GLY YP	59.1	6.36	1.07	22.98	10.49	C ₉ H _{0.97} O _{3.5} (OCH ₃) _{1.60}	12.19	1.69
CMF+GLY YP	55.9	6.33	1.33	28.47	7.97	C ₉ H _{1.22} O _{4.5} (OCH ₃) _{1.28}	7.97	1.5

Contents of aliphatic, free phenolic hydroxyl and carboxylic acid groups in the recovered single stage GLY SG and GLY YP and double stage GLY+CMF SG and CMF+GLY YP lignin fractions were calculated via quantitative ³¹P NMR [57, 74] and are shown in Figure 6-1. Total free phenolic OH increased from 0.93 mmolg⁻¹ in the EMAL SG [49] to 1.69 mmolg⁻¹ in the single stage GLY SG, and to 2.28 mmolg⁻¹ in the double stage CMF+GLY SG; the latest is comparable to the GTP sweetgum lignin recovered by Zhang [49] after the highest severity

glycerol thermal processing pretreatment (free phenolic OH of 2.33 in GTP lignin). The amount of free phenolic hydroxyl groups in CMF+GLY SG lignin increased to 2.28 mmolg⁻¹, greater than the free hydroxyl group content in EMAL SG (0.98 mmol/g) showing that an increased degree of depolymerization had occurred during the double stage CMF+DES pretreatments.

For softwood YP lignin fraction, the total free phenolic hydroxyl groups in EMAL YP is 2.22 mmolg⁻¹ [50] while the GLY YP lignin fraction presented a phenolic hydroxyl content of 2.30 mmolg⁻¹ indicating minimal fragmentation or depolymerization. Whereas the CMF+GLY YP lignin fraction presented 0.97 mmol/g showing that condensation may have occurred during the first applied CMF treatment of YP samples, and or severe lignin modification.

Previous studies have demonstrated that alkyl aryl ether bonds are the most exposed linkage to be cleaved due to thermolysis [75], acid catalyzed steam explosion [76] and organosolv pretreatment [30, 77, 78] and form a large amount of free phenolic hydroxyl groups. Moreover, the amount of phenolic OH groups in CMF+GLY SG lignin fractions was much greater than in Alcell and kraft lignins prepared at similar delignification level (50-60% delignification) [79]. Similarly, the single stage GLY and double stage CMF+GLY pretreatments produced aromatic hydroxyls in the isolated SG lignin. For the YP sample, potential for condensation on the aromatic ring may have limited the solubility of lignin fragments.

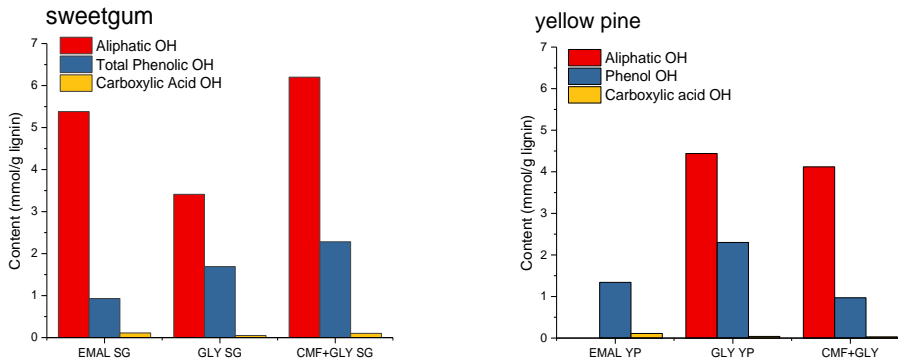


Figure 5-1 ^{31}P NMR functional group analysis: aliphatic OH, phenolic OH and carboxylic OH groups of recovered lignin fractions from sweetgum (A) and yellow pine (B).

The amount of total aliphatic hydroxyl groups decreased from 5.38 mmol g^{-1} lignin in EMAL SG (control) to 3.41 mmol g^{-1} in GLY pretreated SG (Figure 5-1), comparable to 3.39 mmol g^{-1} of GTP lignin (glycerol thermal processing) [49]. As already stated by Zhang et al. [49] this decrease of aliphatic OH groups may be assigned to thermally induced formaldehyde release through the cleavage of aliphatic OH groups [75, 80, 81]. It has been reported that formaldehyde release occurred due to the thermal scission of $\gamma\text{-CH}_2\text{OH}$ at temperatures around 200°C [80]. Kawamoto and Saka [82] have hypothesized that the hydrogen bonds are formed between $\alpha\text{-O}$ and $\gamma\text{-OH}$, and facilitate the C- γ elimination with release of formaldehyde. These results show the sensitivity of the native structure of SG to GLY pretreatment, most likely, due to the temperature of the pretreatment. For CMF+GLY SG lignin fraction, the amount of aliphatic OH increased to 6.20 mmol g^{-1} showing that CMF treatment applied prior to GLY treatment increased the side chains in the lignin fractions, and or, changed because of the total addition of the carbohydrate contamination with the lignin (Table 5-1). For softwood YP biomass, the amount of aliphatic hydroxyl groups underwent a slight increase from 3.5 mmol g^{-1} in EMAL YP [55] to 4.44 mmol g^{-1} and to 4.12 mmol g^{-1} in GLY YP and CMF+GLY YP lignin fractions. Changes in the recovered GLY and CMF+GLY YP lignin fractions show interactions between the side

chains in lignin were not significant. These data indicate that for SG lignin, single stage GLY pretreatment was less effective for total OH than double stage CMF+GLY pretreatment, whereas for yellow pine lignin the single stage GLY was more effective to produce enhanced OH than double stage CMF+GLY treatment.

Minimal carboxylic acid amounts were detected in all the samples - EMAL SG, GLY SG, CMF+GLY SG, EMAL YP, GLY YP and CMF+GLY YP lignin fractions were observed such as 0.11; 0.05; 0.10; 0.11; 0.04 and 0.03, respectively (Fig. 2 A and B) demonstrating that limited lignin oxidation occurred during the high temperature of GLY pretreatments, which was reported for oxidation and radical attack in CMF treatments. Further, Argyropoulos et al. [55] that EMAL is an appropriate model for monooxidized lignin with low carboxylic content. In this study, the isolated GLY SG lignin had even less degree of oxidation and CMF+GLY SG presented the same COOH amount as EMAL SG. Both GLY YP and CMF+GLY YP lignin fractions showed less degree of oxidation than EMAL YP.

Quantitative ^{31}P NMR spectroscopy with phosphitylation has been reported to resolve various phenolic structures, particularly in isolating syringyl and C₅-condensed OH groups [60]. Figure 6-3 shows, quantitatively, the different hydroxyl groups in recovered single stage GLY and CMF and double stage GLY+CMF and CMF+GLY lignin fractions. The ratio syringyl/guaiacyl (S/G) phenolics increased from 0.98 in EMAL SG to 1.35 in GLY SG lignin fraction and to 1.95 for CMF+GLY SG lignin fraction. The free phenolic S/G ratio increased from 0.83 for EMAL SG to 3.39 and 3.66 for GLY SG and CMF+GLY SG lignin fractions, respectively; higher than the S/G reported for GTP SG (2.6). These results point out that the syringyl phenolic OH was the major product released from alkyl aryl ether bond rupture during the single stage and double stage

GLY and CMF+GLY pretreatments of SG showing that syringyl release is correlated to the capability to access and remove lignin from the cell wall. The free phenolic S/G ratio increased to 0.11 and 0.22 for GLY YP and CMF+GLY YP, respectively. Although softwoods samples do not have syringyl alcohol monomers, substituted phenolics at the 5 position produce a pseudo S-lignin like signal. Overall, the YP lignin fractions that were able to be isolated was less affected by these pretreatments.

C₅ condensed phenolic structures are the phenolic rings with C-C bonds at the C₅ position, such as biphenolic units and diaryl methanes [74, 75]. It has been hypothesized that these structures derive from the condensation of the benzylic carbon of guaiacyl and *p*-hydroxyphenyl units with the free C₅ position under acid or alkali conditions. Figure 5-3 A shows that the amount of C₅ condensed OH groups in GLY SG and CMF+GLY SG lignin fractions was 0.30 and 0.50 mmolg⁻¹, respectively. The latest amount is comparable to the GTP SG lignin reported by Zhang et al. [49] which was 0.55 mmolg⁻¹, therefore DES SG lignin fraction is almost twice and CMF+GLY SG lignin fraction is three times more than in EMAL, denoting that the C₅ condensation occurred during the single DES and double CMF+GLY pretreatments. These result confirm the less effective enzymatic hydrolysis of SG biomass during the CMF+GLY pretreatment (Chapter 4).

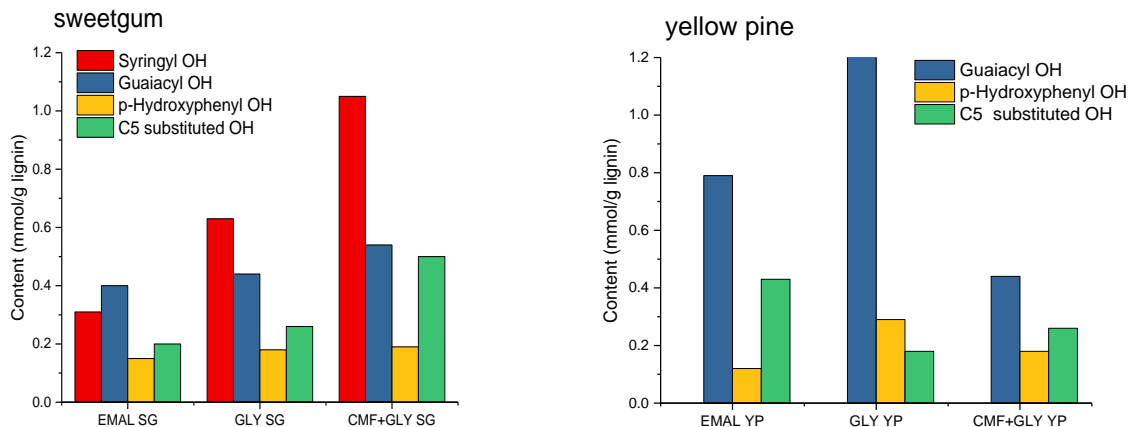


Figure 5-2 ^{31}P NMR functional group analysis: syringyl OH, guaiacyl OH, p-hydroxyphenyl OH and C5 condensed OH groups of recovered lignin fractions from SG (A) and YP (B).

For EMAL YP, the amount of C₅ condensed OH groups has been reported as being 0.43 mmol⁻¹, increasing to 0.55 mmol⁻¹ in GLY YP lignin fractions and decreasing to 0.26 in CMF+GLY YP lignin fractions. Hence, GLY pretreatment increased the C₅ condensation whereas CMF+GLY YP decreased the C₅ condensation to 0.26 mmol⁻¹ which also correlates to the more effective enzymatic hydrolysis of pretreated CMF+GLY YP biomass. Argyropoulos et al. [83] have reported that amount of C₅ condensed OH in Kraft and organosolv lignin was between 0.35 and 0.75 mmol⁻¹ at comparable delignification degrees, particularly for GLY SG. Isolated GLY SG lignin fractions correspond to a delignification degree of 41% compared to the Argyropoulos's report of 40% of extent of delignification for isolated Kraft and Alcell. Hence the GLY and CMF+GLY treatments in SG and YP biomasses resulted in similar C₅ phenolic condensation in the Isolated lignin fractions. Additionally, according to Landucci [85], DPM type condensation occurred in alkaline conditions as well. In this work, GLY could assist during the pretreatments and could cause this type of DPM condensation by improving lignin mobility at temperature of the pretreatment which is 150°C.

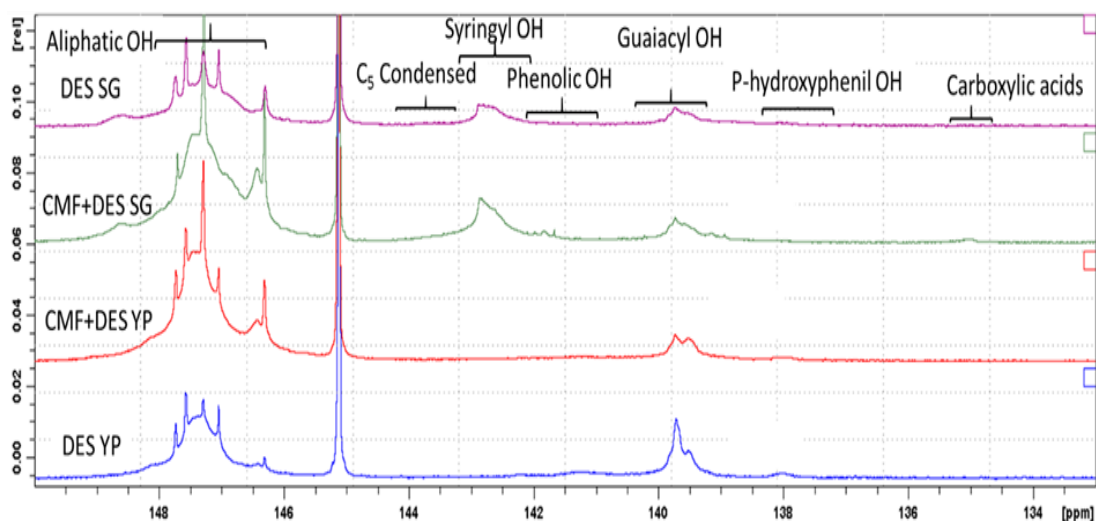


Figure 5-3 ^{31}P -NMR Spectra with assignments of single and double stage isolated GLY/CMF sweetgum and yellow pine lignin fractions.

5.5.3 Two Dimensional HSQC Nuclear Magnetic Resonance of single stage GLY and CMF and double stage GLY followed by CMF and CMF followed by GLY lignin fractions

2D HSQC NMR was utilized to examine changes in chemical structure in EMAL and GLY and CMF+GLY SG and YP lignin fractions. Main structures in the HSQC spectra were color-coded and assigned following previous published scientific reports [46, 48, 49, 67, 68, 86, 87]. Figure 5-4 and 5-5 show different lignin units and side-chain bonds present in the aromatic (Figure 5-4) and aliphatic regions (Figure 5-5).

5.5.3.1 Aromatic region ($\delta_{\text{C}}/\delta_{\text{H}}$ 90-130/5.5-8.0 ppm)

The main cross signals in the aromatic (unsaturated) region correspond to the aromatic rings of the S and G units of lignin. Figure 5-4 reveals that no H units were detected in sweet gum and yellow pine lignin fractions which is consistent with the minimum presence of p-hydroxyphenyl

units from ^{31}P -NMR. The ratio S/G was calculated from the contour volume for the C_2 and C_6 carbons on S and oxidized S' rings, as well as the C_2 carbon on G rings (Figure 5-4). As shown, the ratio of S and G units changed after single and double stage DES and CMF pretreatment, from 3.2 in EMAL SG [49] to 4.6 for GLY SG lignin fraction. This S/G value of GLY treated lignin is larger than usual values for hardwood lignin, which regularly is in the range of 1.5 to 3.3 [88, 89]. The S/G ratio for CMF+GLY SG was 1.5 which is in the range of common S/G ratios for hardwood lignin fractions. This may be a factor to explain the reason why the pretreated CMF+GLY SG samples presented a less efficient enzymatic hydrolysis (56%, chapter 5) than the double stage GLY+CMF SG (opposite sequence), which reached 78% as additional lignin was extracted. It has been reported [46, 67, 68, 90] that the $\text{S}_{2/6}$ cross peak placed between 6.4 and 7.1 ppm with center at 6.7 ppm on ^1H dimension corresponds to unmodified native lignin present in nonderivatized cell walls. It should be noted the low degree of oxidized S-type units in the GLY lignin (Figure 7-4) depicted in the peak S' oxidized syringyl units and assigned to chemical shifts $\delta_{\text{C}}/\delta_{\text{H}} = 107.44 \text{ ppm}/7.2 \text{ ppm}$ (Table 7-3), this shows the correlation between $\text{C}_{2,6}\text{-H}_{2,6}$ in S' units. This peak is bigger in the spectrum of CMF+GLY SG lignin, showing more oxidation of S units in this isolated lignin. On the other hand, the aromatic region for recovered GLY and CMF+GLY YP lignin fractions (Fig. 6-4) show that yellow pine lignin fractions are only G type lignins.

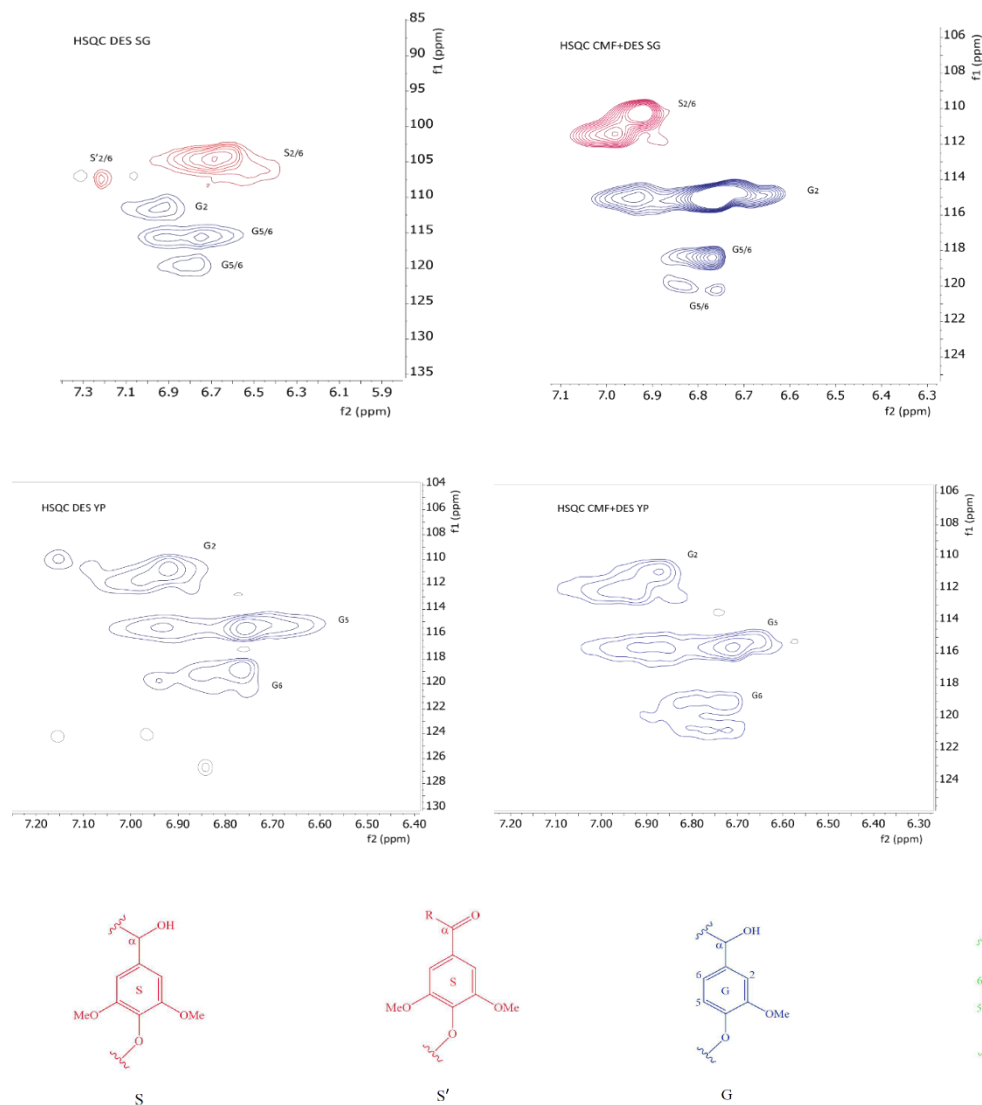


Figure 5-4. HSQC NMR spectra of recovered single stage and double stage SG and YP lignin fractions - Main structures: (S) Syringyl units, (S') Oxidized syringyl units (G) Guiacyl units and p-hydroxyphenyl units.

Table 5-2 Aromatic region - Assignments of the ^{13}C - ^1H correlation signals for the lignin structures observed in the 2D HSQC NMR spectra of recovered lignin fractions

Contour	Assignment	Reference	$\delta_{\text{C}}/\delta_{\text{H}}$			
			Lignin fraction			
			GLY SG	CMF+GLY SG	GLY YP	GLY+CMF YP
S _{2/6}	C _{2,6} -H _{2,6} in etherified Syringyl unit (S)	[Wen et al. 2013], [Rencoret et al. 2015], [Zhang et al. 2016]	104.64/6.68	110.26/6.9 & 11.42/6.98		

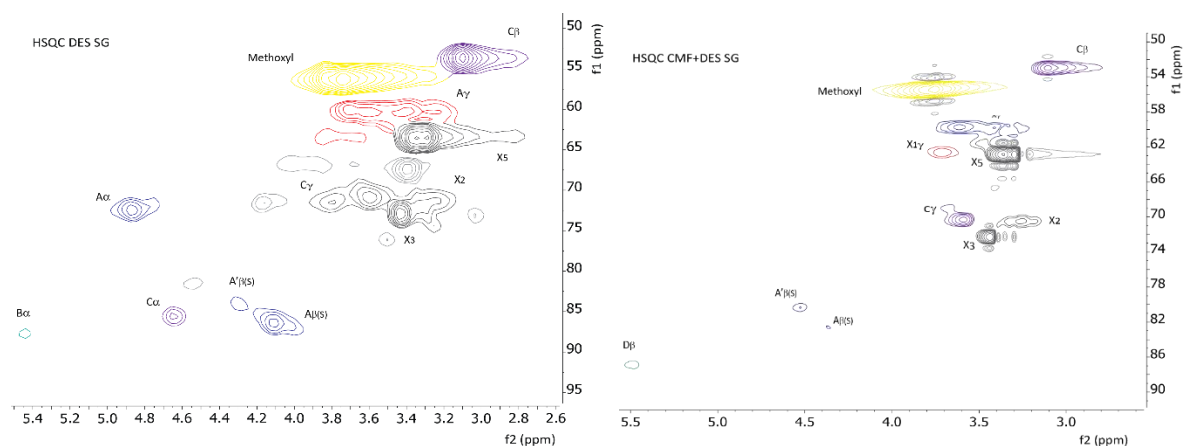
S' _{2/6}	C _{2,6} -H _{2,6} in oxydized Syringyl unit (S')	[Wen et al. 2013], [Zhang et al. 2016]	107.44/7.21			
G ₂	C _{5,6} -H _{5,6} in Guaiacyl unit (G)	[Wen et al. 2013], [Rencoret et al. 2015], [Zhang et al. 2016], [Sathitsuksanoh et al. 2014]	111.45/6.92 & 111.8/6.98	115.06/6.74 & 114.87/6.63	110.95/6.87 & 110.73/6.91	109.94/7.15 & 110.74/6.91
G _{5/6}	C _{5,6} -H _{5,6} in Guaiacyl unit (G)	[Rencoret et al. 2015], [Zhang et al. 2016]	115.72/6.75 & 115.67/6.91	118.4/6.77		
G _{5/6}	C _{5,6} -H _{5,6} in Guaiacyl unit (G)	[Rencoret et al. 2015], [Zhang et al. 2016]	119.27/6.76 & 119.59/6.83	119.99/6.83 & 120.21/6.75		
G ₅	C ₅ -H ₅ in Guaiacyl unit (G)	[Rencoret et al. 2015], [Sathitsuksanoh et al. 2014]			115.64/6.91 & 115.64/6.86	115.44/6.93 & 115.57/6.75
G ₆	C ₆ -H ₆ in Guaiacyl unit (G)	[Rencoret et al. 2015], [Sathitsuksanoh et al. 2014]			119.86/6.88 & 119.74/6.94	118.85/6.76 & 119.75/6.93

5.5.3.2 Aliphatic side chain region (δ_C/δ_H 50-90/2.5-5.7 ppm)

The aliphatic region of the 2D HSQC NMR spectra of GLY SG, CMF+GLY SG, GLY YP, and CMF+GLY YP lignin fractions is shown in Figure 5-5 and correspond to the side chains of the different S and G units. The cross-peaks of the NMR spectra revealed resolved correlations of the common linkages in the lignin structure. It is known that β -O-4 (substructure A) are the major linkages coupled with small amounts of phenylcoumaran β -5 (substructure B), resinol β - β (substructure C), with the cinnamyl alcohol end-groups (substructure X1) as shown via HSQC NMR spectra [83]. Semi quantitative characterization of the lignin linkages reveal the modifications in softwood and hardwood lignin fractions after single and double stage GLY and CMF pretreatments (Figure 5-5).

The number of β -O-4 bonded S and G units decreased during the single and double stage GLY and CMF pretreatments compared to EMAL SG, as an indication of depolymerization (Table 5-5). CMF+GLY SG samples have a higher extent of depolymerization than single stage GLY lignin fractions. YP lignin samples had the opposite trend, both GLY and CMF+GLY depolymerized during the treatments, but single stage GLY YP lignin fractions showed a greater extent of depolymerization than double stage CMF+GLY YP lignin fractions.

The β -aryl ether interunit linkages are also the main structures in yellow pine lignins. Other structures observed in lignin 2D HSQC NMR spectra for yellow pine were phenylcoumaran and resinol linkages (Figure 5-5 and Table 5-4). The C_α - H_α in β -O-4' substructure (A) linked to an S or G lignin unit was observed at 72.46/4.87. Similarly, C_β - H_β in β -O-4' substructure (A) linked to S or G unit was detected at 85.66/4.65. And, C_γ - H_γ in β -O-4' substructure (A) at 70.31/3.78, 70.94/3.54 & 72.9/3.39, and 70.94/3.54 & 72.9/3.39. Additionally, cross peaks for phenylcoumaran substructures (B) were found for all the recovered GLY and CMF+GLY SG and YP lignin fractions at 53.65/3.11, 52.98/3.11, 53.4/3.09, and 53.4/3.09, respectively.



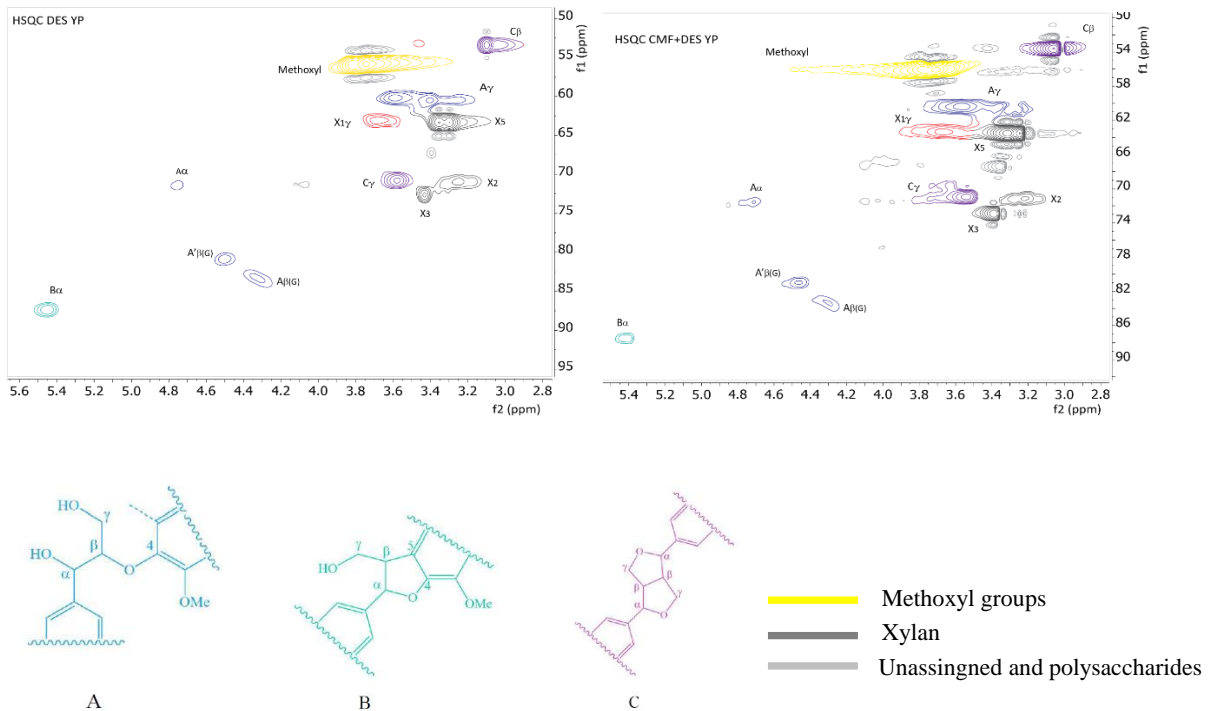


Figure 5-5. Side chain ($\delta C/\delta H$ 50-90/2.5-5.8) regions in the 2D (HSQC) NMR spectra of isolated single stage GLY SG and GLY YP and double stage CMF followed by GLY SG and CMF followed by GLY YP.

Table 5-3 Assignments of the ^{13}C - ^1H correlation signals for the lignin structures observed in the 2D HSQC NMR spectra

Contour	Assignment	Reference	$\delta_{\text{C}}/\delta_{\text{H}}$			
			Lignin fraction			
			GLYSG	CMF+GLY SG	GLY YP	GLY+CMF YP
C $_{\beta}$	C $_{\beta}$ - H $_{\beta}$ in β - β' phenylcoumaran (C)	[Rencoret et al. 2015], Zhang et al. [2016]	53.66/3.11	52.98/3.10	53.4/3.09	53.61/3.05
OCH $_3$	C -H in the methoxyls	[Wen et al. 2013], [Rencoret et al. 2015], [Zhang et al. 2016]	56.22/3.74	55.44/3.75	55.83/3.74	56.06/3.70 & 56.03/4.09
A $_{\gamma}$	C $_{\gamma}$ - H $_{\gamma}$ in β -O-4' substructure (A)	[Wen et al. 2013], [Rencoret et al. 2015], [Zhang et al. 2016]	60.34/3.60	60.45/3.39	60.51/3.40	60.38/3.56
XI $_{\gamma}$	C $_{\gamma}$ - H $_{\gamma}$ in cinnamyl alcohol end-groups (I) linked to ylan units	[Wen et al 2013], [Zhang et al 2016]	63.48/3.83	62.62/3.71	62.64/3.71	63.38/3.68
C $_{\gamma}$	C $_{\gamma}$ - H $_{\gamma}$ β - β' resinol substructures (C)	[Wen et al. 2013], [Rencoret et al. 2015], [Zhang et al. 2016]	70.91/3.59	70.31/3.78	70.31/3.58	70.94/3.52
A $_{\alpha}$	C $_{\alpha}$ - H $_{\alpha}$ in β -O-4 substructure (A)	[Wen et al. 2013], [Rencoret et al. 2015], [Zhang et al. 2016], [Sathitsuksanoh et al. 2014]	72.46/4.87		71.45/4.74	71.59/4.70
A' $_{\beta(S)}$	C $_{\beta}$ - H $_{\beta}$ in β -O-4' substructure (A) linked to S unit	[Rencoret et al. 2015]	83.98/4.29	80.97/4.46		
A $_{\beta(S)}$	C $_{\alpha}$ - H $_{\alpha}$ in β -O-4 phenylcoumaran substructures (B)	[Rencoret et al. 2015]	86.38/4.11	83.28/4.29		
C $_{\alpha}$	C $_{\alpha}$ - H $_{\alpha}$ in β - β' resinol substructures (C)	[Wen et al. 2013], [Rencoret et al. 2015], [Zhang et al. 2016]	85.64/4.46			
A' $_{\beta(G)}$	C $_{\beta}$ - H $_{\beta}$ in β -O-4' substructure (A) linked to Gunit	[Wen et al. 2013], [Rencoret et al. 2015]			80.83/4.5	80.99/4.45
A $_{\beta(G)}$	C $_{\beta}$ - H $_{\beta}$ in β -O-4 substructure (A) linked to Gunit	[Wen et al. 2013], [Rencoret et al. 2015], [Sathitsuksanoh et al. 2014]			83.37/4.32	83.21/4.28
B $_{\alpha}$	C $_{\beta}$ - H $_{\beta}$ in β - β resinol substructures (B)	[Rencoret et al. 2015], [Zhang et al. 2016]	86.88/5.48	87.49/5.4	87.38/5.44	87.48/5.40
X $_5$	Acetylated mannan and xylan units	[Mansfield et al. 2012]	63.53/3.34	62.85/3.26	62.85/3.36	63.51/3.31 & 63.53/3.39
X $_2$	Acetylated mannan and xylan units	[Mansfield et al. 2012]	71.34/3.24	70.48/3.25	70.46/3.25	71.17/3.22
X $_3$	Acetylated mannan and xylan units	[Mansfield et al. 2012]	72.89/3.43	72.28/3.43	72.28/3.43	72.91/3.38

The molar abundance (per 100C₉) of β-O-4 substructures is shown in Table 5-5. For EMAL SG was 58.6% and decreased to 48.5% and 32.6% for GLY SG and CMF+GLY SG, respectively. These data indicate rupture of the linkages and depolymerization of these lignin fractions. The effect of the pretreatment in GLY and CMF+GLY SG YP lignin fractions were the opposite, the molar abundance for β-O-4 substructure increased from 13.5% for GLY YP to 49.6% for CMF+GLY YP. This is in agreement with the lower enzymatic glucan digestibility of pretreated yellow pine (chapter 4).

Table 5-4 Molar abundance (per 100C₉) of side chain linkages in lignin

Sample	β-O-4	β-5	β-β	β-1
EMAL SG	58.6	2.4	17.6	
GLY SG	48.5	6.3	0.0	0.0
CMF+GLY SG	32.6	3.4	18.9	3.6
DES YP	13.5	0	20	0
CMF+DES YP	49.8	0	39.7	0

5.5.4 Molecular weight of single stage GLY and CMF and double stage GLY followed by CMF and CMF followed by GLY lignin fractions

The molecular weight of lignin is a fundamental property that impacts the recalcitrance of biomass and the valorization of lignin [42]. The relative molecular weight of isolated GLY SG, CMF+GLY SG, GLY YP, and CMF+GLY YP lignin fractions were determined by size exclusion chromatography (SEC) using a calibration method. Figure 5-6 shows the molecular weight distribution curves and Table 5-5 indicates the number average molecular weight (M_n), weight average molecular weight (M_w), and polydispersity index (PDI, M_w/M_n) of this isolated lignin fractions. EMAL SG [49] and EMAL YP [42, 55] have served as references to lignin fractions isolated from GLY and CMF+GLY SG and YP pretreatments to assess the changes in molecular weight and hence the changes in structure of lignin arising from the pretreatments.

Since the lignin structure has been fragmented, a decrease in molecular weight of recovered lignin fractions from single and double stage GLY and CMF pretreatments compared to EMAL samples for both SG and YP biomasses was expected. A small decrease of 1.5 KDa in M_n for GLY SG lignin compared to EMAL SG was observed, same observation was made by Zhang et al. for GTP lignin at the highest pretreatment severity [49]. This result follows the change in β -O-4 bonds of native lignin occurred during the pretreatment as demonstrated in 2D HSQC – NMR analysis. Moreover, the M_w decreased substantially from 21.9 Da in EMAL to 10.9 KDa for GLY SG lignin. For CMF+GLY SG lignin, the results show the opposite behavior for M_w , M_n and D, M_n decreased from 7.7 KDa in EMAL SG to 4.9 KDa in isolated GLY+CMF SG lignin showing a decrease compared to GLY SG lignin, M_w decreased from 21.9 KDa to 13.1 KDa. Remarkably, the SEC results demonstrated a small polydispersity index for all the isolated lignin fractions of this study ranging from 1.8 to 2.7, with a smaller variation than that of EMAL SG (PDI = 2.8). This is atypical for processes involving depolymerization and repolymerization and was already observed by Zhang et al. [49]. This results are opposed to the data published in the literature for lignin isolated from steam explosion or other pretreatments that involved high temperatures.

Results from elution profiles of single and double stage GLY/CMF YP lignin fractions suggest that both isolated GLY and CMF+GLY YP lignin fractions have undergone extensive depolymerization compared to EMAL YP. M_w has significantly decreased from 57.6 of EMAL YP to 9.2 and 15.9 Da for recovered DES and CMF+GLY YP lignin fractions, respectively. This results show that in the case of the double stage CMF+GLY treatment, the first CMF treatment condensed lignin in such a way that the second GLY treatment depolymerized it in a lesser extent so that this extractable fraction contained larger molecular weight lignin products. For M_n ,

there was a decrease from 9.7 KDa of EMAL YP to 4.5 KDa and 5.8 KDa of GLY YP and CMF+GLY YP lignin fractions, respectively. These data are in agreement with the result obtained in ^{31}P -NMR analysis that revealed higher aromatic OH for GLY YP lignin (2.30 mmol/g) than for CMF+GLY YP (0.97 mmol/g). Interestingly, the results show a small PDI for both GLY and CMF+GLY YP lignin (2.0 and 2.7, respectively) compared to EMAL YP that presents a PDI = 5.9, indicating that EMAL YP contains larger molecular mass lignin products.

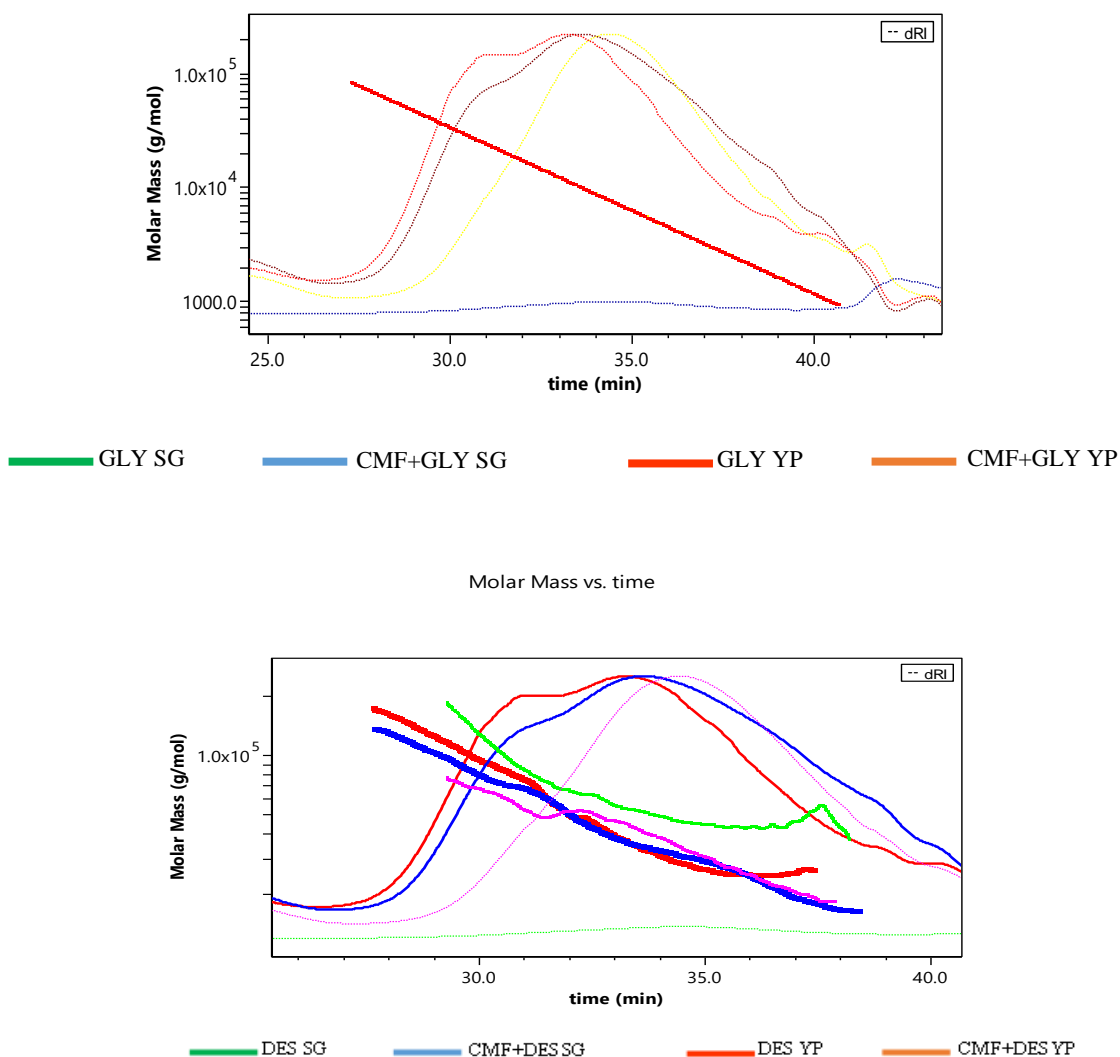


Figure 5-6 Molar mass distribution curves of recovered GLY and CMF+GLY SG and YP lignin samples – Light Scattering Data

For M_n , there was a decrease from 9.7 KDa of EMAL YP to 4.5 KDa and 5.8 KDa of GLY YP and CMF+GLY YP lignin fractions, respectively. These data are in agreement with the result obtained in ^{31}P -NMR analysis that revealed higher aromatic OH for GLY YP lignin (2.30 mmol/g) than for CMF+GLY YP (0.97 mmol/g). Interestingly, the results show a small PDI for both GLY and CMF+GLY YP lignin (2.0 and 2.7, respectively) compared to EMAL YP that presents a PDI = 5.9, indicating that EMAL YP contains larger molecular mass lignin products.

Table 5-5 Molar Masses of recovered GLY SG, CMF+GLY SG, GLY YP and CMF+GLY YP lignin fractions.

Sample	M_w (g/mol)	M_n (g/mol ⁻¹)	M_w/M_n
EMAL SG*	21.9	7.7	2.8
GLYSG	10.9	6.2	1.8
CMF+GLY SG	13.1	4.9	2.7
EMAL YP**	57.6	9.7	5.9
GLY YP	9.2	4.5	2.0
CMF+GLY YP	15.9	5.8	2.7

*From reference [49]

**From reference [55] and [42]

5.6 Conclusions

Due to limited enzymatic digestibility of native biomass, two novel pretreatment methods were developed to isolate biomass polymers. Lignin isolated in ethanol streams were analyzed with elemental analysis, ^{31}P -NMR and 2D-HSQC NMR for structure determination and GPC for molecular weight determination. After the GLY and/or CMF pretreatments, resulting reaction products generate three different streams: 1) pretreated fiber, 2) aqueous phase fraction containing high molecular weight compounds (water insoluble) and low molecular weight compounds (water soluble); and 3) ethanol phase fraction. Aqueous phases were centrifuged and decanted to isolate the high molecular weight fraction (HMWC). The supernatants then went

liquid-liquid extraction with ethyl acetate to isolate low molecular weight compounds (LMWC). In this study, high molecular weight fractions were recovered and analyzed. These fractions represent the 19%, 24%, 32% y 26% of the Klason lignin present in the starting material in GLY SG, GLY YP, CMF+GLY SG and double stage CMF+GLY YP, respectively. GPC results show that these isolated lignin fractions were relative high molecular weight compared to native like samples. ¹H NMR indicates that these fractions contain also xylan in percentage ranging from 7.97% to 12.19%, as well as small amounts of other carbohydrates. Single and double stage GLY/CMF pretreatments facilitated a significant β -O-4 bond disruption resulting in phenolic hydroxyl liberation as well as cleavage of C-C bonds of the aliphatic chain. In addition to degradation reactions, repolymerization (condensation) reactions also take place appearing new C_{arom}-O-C and C_{arom}-C bonds. The structural characterization of these lignin fractions is important and conceive further studies for lignin valorization to enhance the use of lignocellulosic biomass and biorefineries efficiency.

5.7 Acknowledgements

The authors acknowledge the financial support from Secretaría Nacional de Ciencia y Tecnología SENECYT, Instituto de Fomento al Talento Humano IFTH, and Universidad San Francisco de Quito for to Lourdes Orejuela to pursue a doctoral degree at Virginia Tech, along with support from the Institute for Critical Technology and Applied Science, the Macromolecules Innovation Institute and the Sustainable Biomaterials Department of Virginia Tech. Also, authors acknowledge the Department of Wood Sciences at the University of British Columbia and the Department of Microbiology at University of Massachusetts. Special acknowledgements are given to the Centro de Biotecnología of the University of Concepción for the award to conduct the experimental part of this research.

5.8 References

1. Gnansounou, E., et al., *Life cycle assessment of biofuels: Energy and greenhouse gas balances*. Bioresource Technology, 2009. **100**(21): p. 4919-4930.
2. Bauen, A.B., G.; Junginger, M.; Londo, M.; Vuille, F.; Ball, R.; Bole, T.; Chudziak, C.; Faaij, A.; Mozaffarian, H., *Bioenergy: a sustainable and reliable energy source. A review of status and prospects*. 2009.
3. Isikgor, F.H. and C.R. Becer, *Lignocellulosic biomass: a sustainable platform for the production of bio-based chemicals and polymers*. Polym. Chem, 2015. **6**(25): p. 4497-4559.
4. Kai, D., et al., *Towards lignin-based functional materials in a sustainable world*. Green Chem, 2016. **18**(5): p. 1175-12.
5. Zhou, C.H., et al., *Catalytic conversion of lignocellulosic biomass to fine chemicals and fuels*. Chemical Society Reviews, 2011. **40**(11): p. 5588-5617.
6. Chen, X., et al., *Valorization of Renewable Carbon Resources for Chemicals*. Chimia, 2015. **69**(3): p. 120-124.
7. Huber, G.W., S. Iborra, and A. Corma, *Synthesis of transportation fuels from biomass: chemistry, catalysts, and engineering*. Chemical reviews, 2006. **106**(9): p. 4044-4098.
8. Ragauskas A.J., W.C.K., Davison B.H., Britovsek G., Cairney J., Eckert C.H., Frederick Jr. W.J., Hallett J.P., Leak D.J., Iotta C.L., Mielenz J.R., Murphy R., Templer R., Tschaplinski T., *The Path Forward for Biofuels and Biomaterials*. Science, 2006. **311**(5760): p. 484-489.
9. Sannigrahi, P., Y. Pu, and A. Ragauskas, *Cellulosic biorefineries—unleashing lignin opportunities*. Current Opinion in Environmental Sustainability, 2010. **2**(5–6): p. 383-393.
10. Harris, P.J. and B.A. Stone, *Chemistry and molecular organization of plant cell walls*. Biomass recalcitrance: deconstructing the plant cell wall for bioenergy, 2008: p. 61-93.
11. Himmel, M.E., *Biomass recalcitrance: deconstructing the plant cell wall for bioenergy*. 2009: Wiley-Blackwell.
12. Kumar, P., et al., *Methods for pretreatment of lignocellulosic biomass for efficient hydrolysis and biofuel production*. Industrial & Engineering Chemistry Research, 2009. **48**(8): p. 3713-3729.
13. Binder, J.B. and R.T. Raines, *Simple chemical transformation of lignocellulosic biomass into furans for fuels and chemicals*. Journal of the American Chemical Society, 2009. **131**(5): p. 1979-1985.
14. Camacho, F., et al., *Microcrystalline-cellulose hydrolysis with concentrated sulphuric acid*. Journal of chemical technology and biotechnology, 1996. **67**(4): p. 350-356.
15. Chandra, R.P., et al., *Substrate pretreatment: The key to effective enzymatic hydrolysis of lignocellulosics?*, in *Biofuels*. 2007, Springer. p. 67-93.
16. Alvira, P., et al., *Pretreatment technologies for an efficient bioethanol production process based on enzymatic hydrolysis: a review*. Bioresource technology, 2010. **101**(13): p. 4851-4861.
17. Blanch, H.W., B.A. Simmons, and D. Klein-Marcuschamer, *Biomass deconstruction to sugars*. Biotechnology Journal, 2011. **6**(9): p. 1086-1102.

18. Guo, H.W., et al., *Valorization of Lignin to Simple Phenolic Compounds over Tungsten Carbide: Impact of Lignin Structure*. Chemsuschem, 2017. **10**(3): p. 523-532.
19. Ragauskas, A.J., et al., *Lignin Valorization: Improving Lignin Processing in the Biorefinery*. Science, 2014. **344**(6185): p. 709-+.
20. Oh, Y.H., et al., *Recent advances in development of biomass pretreatment technologies used in biorefinery for the production of bio-based fuels, chemicals and polymers*. Korean Journal of Chemical Engineering, 2015. **32**(10): p. 1945-1959.
21. Agbor, V.B., et al., *Biomass pretreatment: Fundamentals toward application*. Biotechnology Advances, 2011. **29**(6): p. 675-685.
22. Brodeur, G., et al., *Chemical and physicochemical pretreatment of lignocellulosic biomass: a review*. Enzyme research, 2011. **2011**.
23. Tabasso, S., et al., *Microwave, ultrasound and ball mill procedures for bio-waste valorisation*. Green Chemistry, 2015. **17**(2): p. 684-693.
24. Chatel, G., K.D. Vigier, and F. Jerome, *Sonochemistry: What Potential for Conversion of Lignocellulosic Biomass into Platform Chemicals?* Chemsuschem, 2014. **7**(10): p. 2774-2787.
25. Bussemaker, M.J. and D.K. Zhang, *Effect of Ultrasound on Lignocellulosic Biomass as a Pretreatment for Biorefinery and Biofuel Applications*. Industrial & Engineering Chemistry Research, 2013. **52**(10): p. 3563-3580.
26. Tian, X.F., Z. Fang, and F. Guo, *Impact and prospective of fungal pre-treatment of lignocellulosic biomass for enzymatic hydrolysis*. Biofuels Bioproducts & Biorefining-Biofpr, 2012. **6**(3): p. 335-350.
27. Duff, S.J. and W.D. Murray, *Bioconversion of forest products industry waste cellulose to fuel ethanol: a review*. Bioresource technology, 1996. **55**(1): p. 1-33.
28. Chundawat, S.P.S., et al., *Thermochemical pretreatment of lignocellulosic biomass*. Bioalcohol Production: Biochemical Conversion of Lignocellulosic Biomass, 2010(3): p. 24-72.
29. Singh, J., M. Suhag, and A. Dhaka, *Augmented digestion of lignocellulose by steam explosion, acid and alkaline pretreatment methods: A review*. Carbohydrate Polymers, 2015. **117**: p. 624-631.
30. Zhao, X.C., K; and Liu, D., *Organosolv pretreatment of lignocellulosic biomass for enzymatic hydrolysis*. Applied Microbiology and Biotechnology, 2009. **82**: p. 815-827.
31. Zhang, K., Z.J. Pei, and D.H. Wang, *Organic solvent pretreatment of lignocellulosic biomass for biofuels and biochemicals: A review*. Bioresource Technology, 2016. **199**: p. 21-33.
32. Brandt, A., et al., *Deconstruction of lignocellulosic biomass with ionic liquids*. Green Chemistry, 2013. **15**(3): p. 550-583.
33. Gunny, N., A. Anas, and D. Arbain. *Ionic liquids: green solvent for pretreatment of lignocellulosic biomass*. in *Advanced Materials Research*. 2013. Trans Tech Publ.
34. Hossain, M.M. and L. Aldous, *Ionic Liquids for Lignin Processing: Dissolution, Isolation, and Conversion*. Australian Journal of Chemistry, 2012. **65**(11): p. 1465-1477.
35. Sathitsuksanoh, N., et al., *Solvent fractionation of lignocellulosic biomass*. Bioalcohol Production: Biochemical Conversion of Lignocellulosic Biomass, 2010(3): p. 122-140.
36. Pandey, M.P. and C.S. Kim, *Lignin Depolymerization and Conversion: A Review of Thermochemical Methods*. Chemical Engineering & Technology, 2011. **34**(1): p. 29-41.

37. Vigier, K.D., G. Chatel, and F. Jerome, *Contribution of Deep Eutectic Solvents for Biomass Processing: Opportunities, Challenges, and Limitations*. Chemcatchem, 2015. **7**(8): p. 1250-1260.
38. Alvarez-Vasco, C., et al., *Unique low-molecular-weight lignin with high purity extracted from wood by deep eutectic solvents (DES): a source of lignin for valorization*. Green Chemistry, 2016. **18**(19): p. 5133-5141.
39. Goodell, B., et al., *Modification of the nanostructure of lignocellulose cell walls via a non-enzymatic lignocellulose deconstruction system in brown rot wood-decay fungi*. Biotechnology for biofuels, 2017. **10**(1): p. 179.
40. Pu, Y., et al., *Assessing the molecular structure basis for biomass recalcitrance during dilute acid and hydrothermal pretreatments*. Biotechnology for biofuels, 2013. **6**(1): p. 15.
41. Zhu, L.F., et al., *Structural features affecting biomass enzymatic digestibility*. Bioresource Technology, 2008. **99**(9): p. 3817-3828.
42. Tolbert, A., et al., *Characterization and analysis of the molecular weight of lignin for biorefining studies*. Biofuels, Bioproducts and Biorefining, 2014. **8**(6): p. 836-856.
43. Yuan, T.Q., F. Xu, and R.C. Sun, *Role of lignin in a biorefinery: separation characterization and valorization*. Journal of Chemical Technology & Biotechnology, 2013. **88**(3): p. 346-352.
44. Lupoi, J.S., et al., *Recent innovations in analytical methods for the qualitative and quantitative assessment of lignin*. Renewable & Sustainable Energy Reviews, 2015. **49**: p. 871-906.
45. Yang, D., et al., *Studies on the structural characterization of lignin, hemicelluloses and cellulose fractionated by ionic liquid followed by alkaline extraction from bamboo*. Industrial Crops and Products, 2013. **43**: p. 141-149.
46. Sette, M., R. Wechselberger, and C. Crestini, *Elucidation of lignin structure by quantitative 2D NMR*. Chemistry—A European Journal, 2011. **17**(34): p. 9529-9535.
47. Mansfield, S.D., et al., *Whole plant cell wall characterization using solution-state 2D NMR*. Nature protocols, 2012. **7**(9): p. 1579-1589.
48. Wen, J.-L., et al., *Recent advances in characterization of lignin polymer by solution-state nuclear magnetic resonance (NMR) methodology*. Materials, 2013. **6**(1): p. 359-391.
49. Zhang, W., et al., *Revealing the thermal sensitivity of lignin during glycerol thermal processing through structural analysis*. RSC Advances, 2016. **6**(36): p. 30234-30246.
50. Pu, Y., S. Cao, and A.J. Ragauskas, *Application of quantitative 31P NMR in biomass lignin and biofuel precursors characterization*. Energy & Environmental Science, 2011. **4**(9): p. 3154-3166.
51. Balakshin, M., et al., *Quantification of lignin—carbohydrate linkages with high-resolution NMR spectroscopy*. Planta, 2011. **233**(6): p. 1097-1110.
52. Ziebell, A. and K. Gracom, Katahira, R., Chen, F., Pu, Y., Ragauskas A., Dixon, R., Davis, D., *Increase in 4-Coumaryl Alcohol Units during Lignification in Alfalfa (Medicago sativa) Alters the Extractability and Molecular Weight of Lignin*. 2010, USDOE Office of Science (SC), Biological and Environmental Research (BER): United States.
53. International, A., *Standard Test Method for Preparation of Extractive-Free Wood, in D1105 96 (Reapproved 2013)*. 96 (Reapproved 2013), ASTM International: United States. p. 2.

54. Sluiter, A., et al., *Determination of extractives in biomass*. Laboratory Analytical Procedure (LAP), 2005. **1617**.
55. Guerra, A., et al., *Comparative evaluation of three lignin isolation protocols for various wood species*. Journal of Agricultural and Food Chemistry, 2006. **54**(26): p. 9696-9705.
56. Glasser, W.G., V. Davé, and C.E. Frazier, *Molecular Weight Distribution of (Semi-) Commercial Lignin Derivatives*. Journal of Wood Chemistry and Technology, 1993. **13**(4): p. 545-559.
57. Argyropoulos, D.S., *Quantitative P-31 NMR Analysis of lignins, a new tool for the lignin chemist*. Journal of Wood Chemistry and Technology, 1994. **14**(1): p. 45-63.
58. Argyropoulos, D.S., et al., *P-31 NMR-Spectroscopy in wood chemistry .4. lignin models - spin-lattice relaxation-times and solvent effects in P-31 NMR*. Holzforschung, 1993. **47**(1): p. 50-56.
59. Argyropoulos, D.S., F.G. Morin, and L. Lapcik, *Magnetic-field and temperature effects on the solid-state proton spin-lattice relaxation-time measurements of wood and pulps*. Holzforschung, 1995. **49**(2): p. 115-118.
60. Granata, A. and D.S. Argyropoulos, *2-Chloro-4, 4, 5, 5-tetramethyl-1, 3, 2-dioxaphospholane, a reagent for the accurate determination of the uncondensed and condensed phenolic moieties in lignins*. Journal of Agricultural and Food Chemistry, 1995. **43**(6): p. 1538-1544.
61. Li, B., et al., *Factors Affecting Wood Dissolution and Regeneration of Ionic Liquids*. Industrial & Engineering Chemistry Research, 2010. **49**(5): p. 2477-2484.
62. Zawadzki, M. and A. Ragauskas, *N-Hydroxy Compounds as New Internal Standards for the 31P-NMR Determination of Lignin Hydroxy Functional Groups*. Holzforschung, 2001. **55**(3).
63. Kasler, F. and M. Tierney, *Determination of phosphorus in organic compounds by NMR*. Mikrochimica Acta, 1978. **70**(5-6): p. 411-422.
64. Heikkinen, S., et al., *Quantitative 2D HSQC (Q-HSQC) via suppression of J-dependence of polarization transfer in NMR spectroscopy: application to wood lignin*. Journal of the American Chemical Society, 2003. **125**(14): p. 4362-4367.
65. Dolan, J.A., et al., *Biocomposite adhesion without added resin: understanding the chemistry of the direct conversion of wood into adhesives*. RSC Advances, 2015. **5**(82): p. 67267-67276.
66. Araya, F., et al., *Condensed lignin structures and re-localization achieved at high severities in autohydrolysis of Eucalyptus globulus wood and their relationship with cellulose accessibility*. Biotechnology and bioengineering, 2015. **112**(9): p. 1783-1791.
67. Kim, H. and J. Ralph, *Solution-state 2D NMR of ball-milled plant cell wall gels in DMSO-d6/pyridine-d5*. Organic & biomolecular chemistry, 2010. **8**(3): p. 576-591.
68. Yelle, D.J., J. Ralph, and C.R. Frihart, *Characterization of nonderivatized plant cell walls using high-resolution solution-state NMR spectroscopy*. magnetic Resonance in Chemistry, 2008. **46**(6): p. 508-517.
69. Zhang, L. and G. Gellerstedt, *Quantitative 2D HSQC NMR determination of polymer structures by selecting suitable internal standard references*. Magnetic Resonance in Chemistry, 2007. **45**(1): p. 37-45.
70. Rencoret, J., et al., *Structural characterization of milled wood lignins from different eucalypt species*. Holzforschung, 2008. **62**(5): p. 514.

71. Wen, J.-L., et al., *Structural Characterization of Alkali-Extractable Lignin Fractions from Bamboo*. Journal of Biobased Materials and Bioenergy, 2010. **4**(4): p. 408-425.
72. Brunow, G., *Methods to reveal the structure of lignin*. Biopolymers Online, 2005.
73. Brunow, G., K. Lundquist, and G. Gellerstedt, *Lignin*, in *Analytical methods in wood chemistry, pulping, and papermaking*. 1999, Springer. p. 77-124.
74. Archipov, Y., et al., *³¹P NMR spectroscopy in wood chemistry. I. Model compounds*. Journal of Wood Chemistry and Technology, 1991. **11**(2): p. 137-157.
75. Brežný, R., V. Mihalov, and V. Kováčik, *Low Temperature Thermolysis of Lignins-I. Reactions of β -O-4 Model Compounds*. Holzforschung-International Journal of the Biology, Chemistry, Physics and Technology of Wood, 1983. **37**(4): p. 199-204.
76. Li, J., G. Henriksson, and G. Gellerstedt, *Lignin depolymerization/repolymerization and its critical role for delignification of aspen wood by steam explosion*. Bioresource technology, 2007. **98**(16): p. 3061-3068.
77. Sundquist, J., *Organosolv pulping*. Chemical pulping. Helsinki: Fapet Oy, 1999. **404**: p. 405.
78. Muñoz, C., et al., *Bioethanol production from bio-organosolv pulps of Pinus radiata and Acacia dealbata*. Journal of Chemical Technology and Biotechnology, 2007. **82**(8): p. 767-774.
79. Liu, Y., et al., *A comparison of the structural changes occurring in lignin during Alcell and kraft pulping of hardwoods and softwoods*. 2000, ACS Publications.
80. Jakab, E., O. Faix, and F. Till, *Thermal decomposition of milled wood lignins studied by thermogravimetry/mass spectrometry*. Journal of Analytical and Applied Pyrolysis, 1997. **40**: p. 171-186.
81. Sturgeon, M.R., et al., *A mechanistic investigation of acid-catalyzed cleavage of aryl-ether linkages: Implications for lignin depolymerization in acidic environments*. ACS Sustainable Chemistry & Engineering, 2013. **2**(3): p. 472-485.
82. Kawamoto, H., S. Horigoshi, and S. Saka, *Pyrolysis reactions of various lignin model dimers*. Journal of wood science, 2007. **53**(2): p. 168-174.
83. Y. Liu, S.C., K. Pye and D.S. Argyropoulos, *A Comparison of the Structural Changes Occurring in Lignin during Alcell and Kraft Pulping of Hardwoods and Softwoods*, in *Lignin: Historical, Biological, and Materials Perspectives*, R.A.N. W. G. Glasser, and T.P. Schultz, Editor. 1999, ACS Symposium Series: Washington, DC. p. 447 - 464.
84. Funaoka, M., T. Kako, and I. Abe, *Condensation of lignin during heating of wood*. Wood Science and Technology, 1990. **24**(3): p. 277-288.
85. Landucci, L.L., *Search for lignin condensation-reactions with modern nmr techniques*. ACS symposium series, 1989. **385**: p. 27-42.
86. Rencoret, J., et al., *Isolation and structural characterization of the milled-wood lignin from Paulownia fortunei wood*. Industrial Crops and Products, 2009. **30**(1): p. 137-143.
87. Rencoret, J., et al., *Isolation and structural characterization of the milled wood lignin, dioxane lignin, and cellulolytic lignin preparations from brewer's spent grain*. Journal of agricultural and food chemistry, 2015. **63**(2): p. 603-613.
88. Rencoret, J., et al., *Lignin Composition and Structure in Young versus Adult Eucalyptus globulus Plants*. Plant Physiology, 2011. **155**(2): p. 667-682.
89. Kim, H. and J. Ralph, *Solution-state 2D NMR of ball-milled plant cell wall gels in DMSO-d₆/pyridine-d₅*. Org. Biomol. Chem, 2010. **8**(3): p. 576-591.

90. Rencoret, J., et al., *HSQC-NMR analysis of lignin in woody (Eucalyptus globulus and Picea abies) and non-woody (Agave sisalana) ball-milled plant materials at the gel state 10th EWLP, Stockholm, Sweden, August 25–28, 2008*. *Holzforschung*, 2009. **63**(6).
91. Sathitsuksanoh, N., et al., *Lignin fate and characterization during ionic liquid biomass pretreatment for renewable chemicals and fuels production*. *Green Chemistry*, 2014. **16**(3): p. 1236-1247.

Chapter 6 Summary and Conclusions

A deep eutectic solvent and a chelator-mediated Fenton system, applied individually or in sequence, were studied as novel pretreatment methods for plant cell wall deconstruction. This approach was used to facilitate biopolymer fractionation by treating ground sweetgum and ground southern yellow pine with GLY at 150°C for 2h and a CMF system applied at 30°C, in single and double stage modes to determine synergism of both chemistries. With DES first applied, CMF reactants should have better diffusion into the cell wall for deconstruction, while CMF applied first will cause degradation of linkages within the cell wall allowing for higher extraction of the biopolymer components. The GLY complex mixture and the interactions between its components with lignocellulose matrix was analyzed in this research to understand the impact of the pretreatments on the enzyme accessibility to cellulose and biomass saccharification and how the main lignocellulose biopolymers cellulose, hemicellulose and lignin were affected by these pretreatments.

Qualitative information observed from the isolated biopolymers and softwood and hardwood biomass as well as the role of lignocellulose swelling were provided to gain insights of the interactions between GLY and biopolymers within the plant cell wall during the pretreatments. The degree of solubility of cellulose, xylan and kraft lignin of commercially available biopolymers was conducted in GLY, at various temperatures. Solubility in GLY components at room temperature served as control. Solubility was evaluated visually, none of the isolated biopolymers were dissolved in ChCl alone at ambient temperature nor at 150°C. Only kraft lignin partially dissolved in glycerol and to a greater extent in GLY at 150°C. Solubility in GLY was as follows kraft lignin > xylan >> cellulose. Swelling of hardwood and softwood biomass

samples soaked in DI water, glycerol, ChCl, and GLY as solvent systems was conducted at ambient temperature and at 150°C for 2 h to evaluate the interactions between solvent-substrate and their impact on lignocellulose biopolymers. Biomass samples were partially dissolved in glycerol and GLY at 150°C. To understand the mechanism by which GLY and lignocellulose biomass interact, a comparison between ILs and DESs swelling based on literature was presented. Fragments of cell wall biopolymers remain in the GLY liquor and can be recovered whereas cellulose undergoes little or no change. In this way, GLY pretreatment has unlocked cellulose within the lignocellulose network and has less lignin and hemicellulose content. This would facilitate accessibility of the enzymes to cellulose and improve hydrolysis and saccharification yields for further fermentation and bioalcohol production.

As a result of the impact of the pretreatments on biomass main components cellulose, hemicellulose and lignin, a biopolymer fractionation occurs so that mass loss was monitored as a means of pretreatments performance. Mass loss during the pretreatments showed the following values, for single stage DES pretreatment percentages of 24% and 28% for SG and YP biomass were observed, whereas for single stage CMF pretreatment percentages of 16% and 10% for SG and YP biomass samples were measured. Double stage CMF followed by GLY treatment exhibits a mass loss of 34% and 35% for SG and YP biomasses, respectively while double stage GLY followed by CMF treatment, mass loss percentages were only 6% and 17% for SG and YP biomass, respectively. Pretreatments in sequence CMF followed by ChCl-gly DES show a cumulative mass loss of 49% and 45% for SG and YP biomasses, respectively. While the other sequence, CMF followed by GLY treatment present cumulative mass losses of 31% and 45% for SG and YP biomass samples, respectively. Total mass balances were determined for each pretreatment to estimate the total amount of biopolymer removal from treated biomass samples

that remained in supernatants during the cell wall deconstruction. Mass balances were used to assess the distribution of these biopolymers.

After the pretreatments, pretreated fibers are washed and air dried. The liquors of the reactions were centrifuged and successive L/L extractions result in three different streams: 1) high molecular weight fractions (water insoluble), 2) ethanol fractions and 3) ethyl acetate fraction (low molecular weight compounds). These fractions were isolated from the supernatants, and then dried and weighed. Yields of recovered HMWC (water soluble), ethanol and ethyl acetate fractions were determined for GLY SG, CMF followed by GLY, GLY YP, and CMF followed by GLY pretreatments. Water Insoluble fractions exhibited percentages of 2.19%, 2.8%, 3.63% and 4.25%, respectively. For ethanol fractions yields are 8.97%, 11.04%, 10.8% and 11.66%, respectively. Additionally, ethyl acetate fractions present yields of 2.57%, 5.27%, 5.9% and 4.24%, respectively. Total recovery of biomass materials reflected in the percentages of mass loss of each treatment and recovered from the supernatants indicate percentages of 97.68%, 86.98%, 98.75% and 98.05% for these pretreatments.

Partial removal of cellulose, lignin and hemicellulose were quantified via compositional analysis and mass balance after each treatment. Single stage GLY treatment had no impact on cellulose as glucan biopolymer was not soluble. Delignification was higher from SG biomass than from YP biomass (30% vs 22%), whereas removal of xylan was 22% from SG samples compared to 33% from YP biomass. Overall, the removal of other heteropolysaccharides was higher for YP samples.

Single stage CMF treatment was non selective, CMF reagents effectively removed cellulose, hemicellulose and lignin from both SG and YP biomass samples. Delignification and cellulose removal was higher from SG biomass (30%) than from YP biomass (22%). Cellulose was removed in a percentage of 11% from YP samples and 16% from SG biomass.

Heteropolysaccharides removals were higher for YP samples than for SG biomass, except for arabinose side groups.

In double stage treatment GLY followed by CMF, the second treatment extracted additional 10% and 19% of lignin fractions from SG and YP biomass, respectively. Cellulose was not depolymerized into soluble fragments by CMF reagents applied after GLY treatment, as glucan biopolymer was not removed from both SG and YP biomass samples based on compositional analysis and mass balance calculations. Whereas YP biomass, after the initial CMF treatment, had a cellulose removal of 25%, combined with a 44% removal of xylan from YP biomass, compared to 23% of xylan for SG biomass. Overall, higher removals of lignin, galactan and mannan from YP biomass than from SG biomass were observed if the DES was applied prior to CMF treatment.

In the other sequence, double stage CFM followed by GLY, SG had higher delignification (43%) than YP biomass (31%). Similar amounts of xylan removal occurred for both SG and YP samples (43% and 41% respectively), a higher amount of galactan from SG biomass, and a higher amount of mannan/arabinan from YP biomass were detected. It was noteworthy that in this sequence of treatments, cellulose was not removed from SG nor YP biomass. These results indicated that the sequence in which treatments were applied and wood species were crucial for biopolymer fractionation.

Results of the cumulative biopolymer removal for the sequence CMF followed by GLY showed that SG had a total delignification of 73% of acid insoluble lignin components (AIL) compared to 56% of AIL for YP biomass, a higher removal of glucan from SG biomass (16%) compared to glucan removal from YP biomass (12%), and a less removal of xylan from SG biomass (74%) compared to xylan removal from YP biomass (81%). Results of the cumulative biopolymer removal for the sequence GLY followed by CMF treatment showed that SG presented a total delignification of 41% of AIL compared to 64% of AIL for YP biomass, no removal of glucan from SG biomass, but a moderate 25% of glucan removal from YP biomass, and less removal of xylan from SG biomass (45%) compared to xylan removal from YP biomass (77%), detected during these pretreatments. These findings indicated that a successful cell wall deconstruction was achieved applying these pretreatments.

In addition to the successful biopolymer fractionation, enzymatic saccharification for the pretreated biomass was studied to reveal the efficacy of the pretreatments. Compared to the untreated sweet gum biomass, the pretreatments significantly increased the rate of cellulose digestibility, best results were found for the double stage GLY followed by CMF pretreatment, reaching up to 78% glucose yield, even though the residual pretreated SG biomass presented higher crystallinity. The data revealed that the disrupted structure with the bulk of the cellulose present in the residual fiber had enhanced enzyme hydrolysis after the combined pretreatment. In contrast, an extensive removal of biopolymers such as 73% of delignification, a 74% of xylan and 16% of glucan removals presented by CMF+GLY SG sample results in a 56% of glucan digestibility. This might have arisen because of the additional removal of the more accessible cellulose in the pretreatment (56% enzyme degraded and 16% hydrolyzed cellulose) lowered the

overall saccharification level due to enzyme treatments. Further, the enzymatic hydrolysis for single stage GLY or CMF treatments exhibited lower percentages of glucan digestibility showing that pretreatments in sequence enhanced glucose release from pretreated biomass samples. In the case of YP biomass, the enhancement of the enzyme digestibility was low for all pretreatments and the trend was opposite to SG pretreated biomass. Best results were achieved for the biomass pretreated with double stage CMF followed by GLY which exhibited a maximum glucan digestibility of 24%. These results indicated that even though, the degree of delignification in pretreated YP biomass was high and most of hemicelluloses were removed, the pretreatments in the conditions applied in this study were not appropriate. Therefore, these findings demonstrate that a controlled cell wall deconstruction facilitates biopolymer fractionation and enhance saccharification yields but still in limited amounts that require further investigation. The results found for pretreated SG biomass with double stage GLY followed by CMF treatment were promising.

Structural analysis of lignin fractions (HMWC fractions) isolated from SG and YP biomasses was performed to gain understanding of how the pretreatments impacted lignin structure of softwood and hardwood, as well as to identify the structure-properties and envisage potential applications of the isolated lignin. These polymeric lignin fractions represented 19%, 32%, 24% and 26% of the Klason lignin present in their corresponding native SG and YP biomass samples after the different pretreatment stages. Quantitative ^{31}P -NMR was used as a tool to reveal the different hydroxyl groups in the isolated lignin. Double stage CMF followed by GLY SG lignin fraction had a percentage of 6.20 mmol g^{-1} of free aliphatic OH groups, higher than the 5.38 mmol g^{-1} in EMAL SG. On the other hand, DES YP lignin and double stage CMF followed by GLY YP lignin fractions has a percentage of 4.44 and 4.12 mmol g^{-1} of free OH

groups indicating that not significant changes occur applying GLY after CMF treatment. Free Phenolic OH increases from 0.93 mmolg⁻¹ in EMAL SG to 1.69 mmolg⁻¹ and 2.28 mmolg⁻¹ in GLY SG and CMF followed GLY lignin fractions, demonstrating that lignin depolymerization during the pretreatments.

Gel permeation chromatography results show that these isolated lignin fractions had relatively high molecular weight. Further, ¹H-NMR analysis indicated the presence of xylan in all samples ranging from 7.97 to 12.19 mmolg⁻¹ as well as small amounts of hydrocarbon contaminants. From this data, single and double stage pretreatments facilitate a significant β-O-4 bond disruption resulting in phenolic hydroxyl liberation as well as cleavage of C-C bond of the aliphatic chain. In addition to degradation products, condensation reactions also have taken place appearing new C_{arom}-O-C and C_{arom}-C bonds confirmed by the aliphatic OH group increment in both GLY and CMS followed by GLY SG and YP lignin fractions and with the relative high molecular weight of the lignin fractions.

Overall, the approach of combining the DES technology with the chemistry of Fenton system was used as a novel approach for biopolymer fractionation into different lignocellulose species. For lignocellulose to be used as substrate for enzyme saccharification removal of biopolymers to increase enzyme accessibility should not be more than 40-45%. On the other hand, a highly delignified biomass (73%) with low content of polysaccharides and only 16% of glucan removal limited enzyme hydrolysis as only 56% digestibility occurred in the case of CMF followed by GLY SG biomass. At the same time, lignin fractions of relatively high molecular weight were isolated and have potential roles in polymeric applications as carbon fibers, polymer modifiers, resins, adhesives and binders.

Appendix A Physical and chemical effects of choline chloride-glycerol deep eutectic solvent in lignocellulose biomass

A1.1 Abstract

This appendix intends to provide qualitative evidence on the solubility behavior of isolated biopolymers at 60, 100 and 150°C in glyceline (GLY). Additionally, quantitative information of lignocellulose swelling in contact with gly at ambient temperature as well as at 150°C are provided. The purpose of this study is to gain insights into the interactions between this solvent system and lignocellulose during biomass processing as GLY has been described as a green solvent with good lignin solubility properties and has emerged as a novel solvent for lignocellulose biomass pretreatment. Solubility tests were performed using isolated CF11 cellulose, beech xylan and softwood kraft lignin biopolymers as well as with hardwood and softwood samples. Cellulose did not display much solubility in glycerol, ChCl or GLY at any of the temperatures chosen for this study. Xylan presented partial solubilization in glyceline at 150°C and kraft lignin presented good solubility in glycerol and GLY at temperatures above 100°C. Regarding lignocellulose biomass, it was better solubilized by GLY at 150°C (observing change of the recovered and dried sample). Further, when lignocellulose samples were conditioned for 6 days and then submerged in either DI water, glycerol or GLY at ambient temperature and at 150°C for 2 hrs, volumetric swelling in DI water occurred in both SG and YP samples, but not in GLY. At 150°C, glycerol swelled both SG and YP samples, up to 28% and 81% respectively. GLY swelled biomass samples to a lesser extent than glycerol, SG samples reached up to 25% and YP samples up to 39%. These results show that a DES solvent swelling behavior occurred only at elevated temperatures. At 150°C, glycerol presented a higher degree of

swelling for both SG and YP biomass samples than GLY. Lignocellulose swelling behavior typically affects cell wall deconstruction by increasing the free volume of the amorphous sections of the cell wall, “weakening” native interactions. The low degree of swelling with DES may be related to the reduced hydrogen bonding capacity of the glycerol in the DES as glycerol is reported to form more of a cage with interacting with Cl⁻ ions. Deeper studies in the interaction of Ch⁺ cation and lignin would be crucial for a better understanding of the mechanism involved in the interaction between lignin and glyceline to develop industrial applications in the biorefining field towards a biobased-economy.

A1.2 Key words

Choline chloride-glycerol (glyceline), deep eutectic solvent (DESs), lignocellulose, solubility, swelling.

A1.3 Introduction

Lignocellulose is a renewable abundant resource that has a complex structure, its conversion to biofuels precursors requires the access to sugars, and this implies the plant cell wall disruption through methods called pretreatments. Most pretreatments, except the mechanical grading, require high temperatures and exposure to reactive agents that break linkages, increase porosity, extract/remove lignocellulose components that impact cellulose accessibility. Most recent advances in pretreatment technologies highlight the use of deep eutectic solvents (DESs) as pretreatment agents for lignin dissolution to decrease cellulose crystallinity and/or decrease biomass recalcitrance and increase biopolymers depolymerization in order to enhance enzyme hydrolysis [1-3]. Choline chloride-based DESs, considered green solvents for lignocellulose processing, have been extensively reported. Deeper studies on physical and chemical interactions

between DESs, particularly glyceline and lignocellulose would benefit their applications and as they are considered promising solvent systems.

Glycerol is a colorless and odorless viscous liquid with properties such as hygroscopicity and water miscibility. It is generated as waste by the biodiesel industry and has been studied as an alternative to volatile organic solvents [8]. Glycerol possesses properties similar to water such as availability, renewability, low toxicity and low price, and low vapor pressure. Glycerol is a sustainable solvent in green chemistry [9] and has been used in biopolymers processing to protect them from high temperature dehydration reactions to limit the acid formation that occurs in autohydrolysis conditions [10]. Lately, glycerol has also been used as an organosolv pretreatment to improve cellulose accessibility and ensure an enhanced enzymatic hydrolysis and saccharification for biofuels production [13-20]. Since the mechanism of reaction of ILs with lignocellulose is through swelling it could be helpful to explore isolated biopolymers and biomass swelling in glyceline. Chowdhury and Frazier have already reported glycerol as a weak lignocellulose swelling agent [11] compared to other organic media. However, information of swelling with glyceline is not available in the literature. Therefore, this study reports the results of lignocellulose isolated biopolymers solubility and biomass swelling with glycerol and glyceline and hypothesizes a possible mechanism of interaction between lignocellulose and glyceline and lignocellulose.

A1.4 Materials and Methods

A1.4.1 Materials

Glycerol and choline chloride reagents for this work were purchased from Sigma-Aldrich and used as received. A mature sweet gum (SG) (*Liquidambar styraciflua*) hardwood tree from

Blacksburg, VA was debarked, machined to cubes, and stored in a freezer before use. Southern yellow pine samples were donated by Brooks Center, Blacksburg VA.

A1.4.2 Methods

A1.4.2.1 Glyceline solvent system preparation

Choline chloride, a hydrogen bond acceptor (HBA), and glycerol, a hydrogen bond donor (HBD) were purchased from Sigma-Aldrich (>98%), and were used as received. Raw materials were mixed at different molar ratios from 1:0.5 of HBA and HBD to 1:3 to explore their stability as liquid solvents at room temperature. The system was heated with stirring in an oil bath at 80°C until the mixture became a transparent homogeneous liquid (~ 30 min). (Adapted from [21]. Molar ratio HBA:HBD was confirmed by ¹H-NMR.

A1.4.2.2 Qualitative solubility tests of isolated biopolymers and lignocellulose biomass

Solubility of isolated biopolymers and was tested by soaking and heating samples in DI water, glyceline molar ratio (1:2) at ambient temperature and at 60°C, 100°C and 150°C for CMC CF11 cellulose, beech xylan, and kraft lignin. Solubility of ground sweetgum and yellow pine biomass samples (40-60 mesh) was performed by soaking ground wood samples in a S/L ratio of 1:10 in the solvents. Experiments were performed at ambient temperature and also heating at 150°C for 2 h under continuous stirring.

A1.4.2.3 Biomass samples conditioning and swelling

Samples of sweetgum and southern yellow pine were prepared following the ASTM 1037-06a international standard procedure for accelerating aging test. Wood samples were cut into pieces

of 60x60x10 mm and placed in a conditioning chamber Brooks Center VA, at 65% relative humidity during 6 days until the moisture content of the samples did not change. Swelling tests were performed in Sustainable Biomaterials Laboratory in Virginia Tech VA by soaking wood pieces into DI water and glyceline at ambient temperature and measuring volume and weight changes after 2 h and 24h. A second experiment was conducted soaking wood samples in glycerol and glyceline at 150°C with modifications. Changes in weight were recorded when samples cooled down after 2h, 4h and 6h of soaking.

A1.5 Results and Discussion

A1.5.1 Glyceline DES preparation

Glyceline was prepared using four different molar ratios 1:0.5, 1:1, 1:2, and 1:3, heated in an oil bath for approximately 30-45 min at 80°C, until clear and transparent solutions were reached.

The only mixture that was in liquid state after cooling and stabilized (24 and 48 h) was glyceline at 1:2 molar ratio and was confirmed by ¹H-NMR.

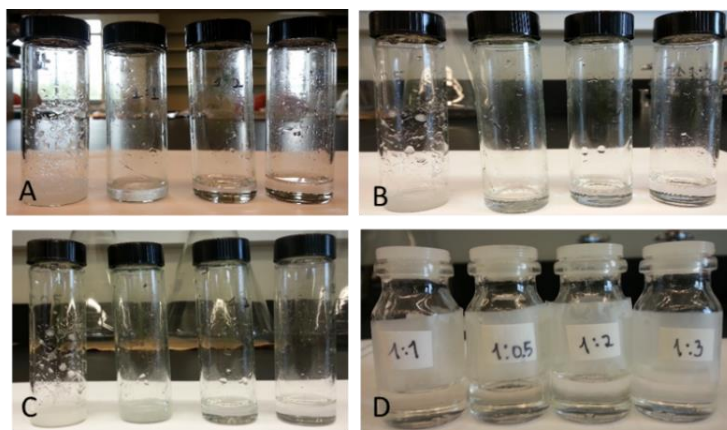


Figure A1-1 GLY after heating at 80°C for 30 min (A), after 2h of cooling (B), after 24 h of stabilization (C) and after 2 h of heating (simulating the pretreatment) (D).

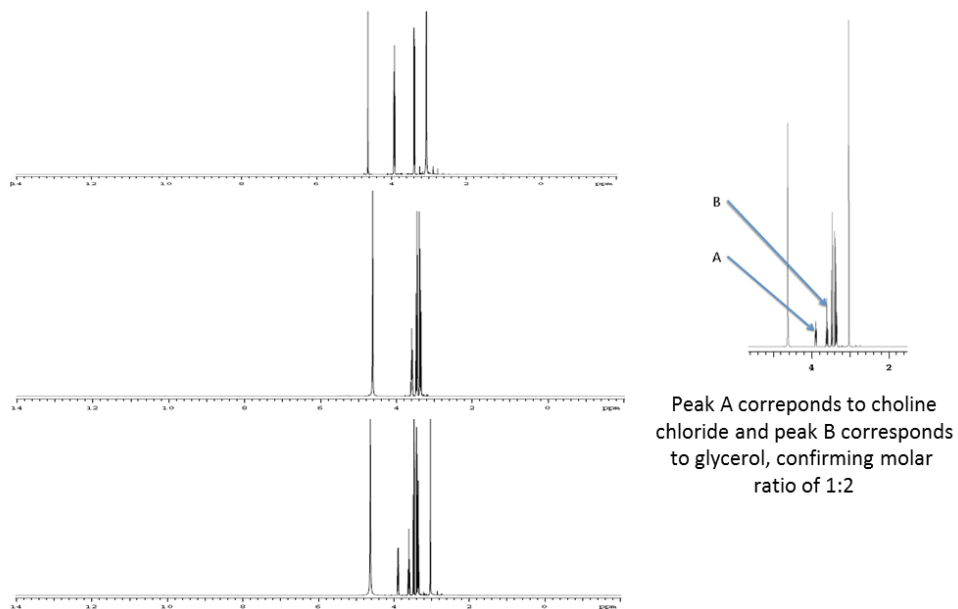


Figure A1-2 $^1\text{H-NMR}$ of GLY mixture at molar ratio (1:2)

A1.5.2 Qualitative solubility of isolated biopolymers with ChCl, glycerol and GLY

Solubility of cellulose, xylan and kraft lignin in glyceline was measured at 60°C, 100°C, and 150°C to explore their solubility and the temperature at which this phenomenon could occur. Kraft lignin presented a good solubility in glyceline in all three temperatures. Table A1-1 shows solubilization of beech xylan and CMC cellulose at 150°C, xylan presented a slight solubilization at 100°C while a suspension of cellulose was seen at this temperature. At 150°C, kraft lignin was solubilized almost completely, a thick viscous solution was observed in the case of xylan indicating a good solubility whereas only a cloudy suspension of cellulose was observed at this temperature.

Table A1-1 Dissolution of Isolated biopolymers in glyceline at 150°C

Biopolymer sample	Observations after 2 h 150°C	Analysis
Kraft lignin	Dark brown, viscous. Separation by centrifuging the sample	Suspension. Separation by centrifuging the sample
Beech Xylan	light yellow, turbid, sticky, very viscous, as a gel	sticky, very viscous, as a gel
CF1 Cellulose	lightly cloudy solvent, cellulose as precipitate	turbid solvent, most of cellulose as precipitate

Table A1-2 Kraft lignin treated in ChCl, glycerol and glyceline at 150°C for 2h

Biomass	Sample mass (g)	Solvent	Solvent (g)	Observations
Kraft lignin	0.0507	Glycerol	2.0213	It dissolved quickly
Kraft lignin	0.0500	Glycerol	2.0275	It dissolved quickly
Kraft lignin	0.0507	ChCl	1.0425	It dissolved quickly
Kraft lignin	0.0523	ChCl	1.0256	It dissolved quickly

A1.5.3 Qualitative Observations of SG and YP biomass pretreatments with glycerol and glyceline

Test of solubility in GLY of ground SG and YP biomass samples in different concentrations (25, 50, 75, 100 and 125 µg in 2 g of GLY) at 150°C for 2 h were also conducted. In general, GLY liquor color changed, the more concentration in lignin a darker brown color was observed, which showed greater lignin extractions. ChCl and glycerol were used as controls for solubilization.

Extraction or removal of lignin from SG or YP biomass with glycerol was poor at room temperature, however at temperature of 150°C a better solubility was observed.

A1.5.4 Swelling of sweetgum and yellow pine biomass

It is well known that swelling and shrinking of wood is a very important aspect in lignocellulose processing that dictates its physical properties and therefore its applications. Swelling of SG and YP biomasses with DI water at ambient temperature showed a 9.8% and 7.3%, respectively in 24h, in agreement with the trend of density being a controlling factor for swelling [22] (Figure A1-3). Glycerol swelled SG biomass marginally, only a percentage of 0.27% in 24 h was observed. Whereas YP biomass presented a slight shrinkage (-0.657%), more likely due to slight variation in measurement area. It should be noted in this sample there was a color change of the DES after 24h of submersion.

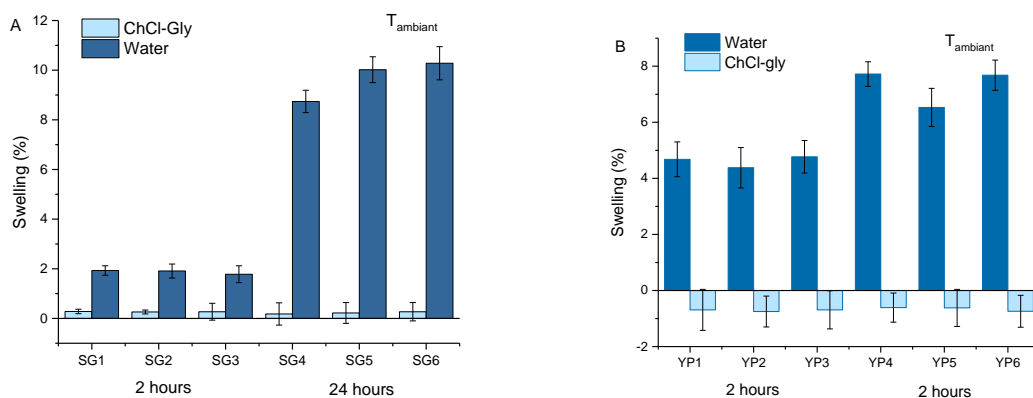


Figure A1-3 Swelling of SG and YP in water and GLY at ambient temperature

The protocol was modified for glycerol and glyceline heated up to 150°C. It was difficult to measure the volume of hot samples, thus the weight of all samples subjected to submersion in glycerol and glyceline were measured. The measurements were taken when the samples reached

ambient temperature. Glycerol swelled SG hardwood up to 28.7% and YP softwood up to 81.9% at 150°C. This temperature has been reported as above the glass transition temperature of lignin (T_g) [11] and presents irreversible change.

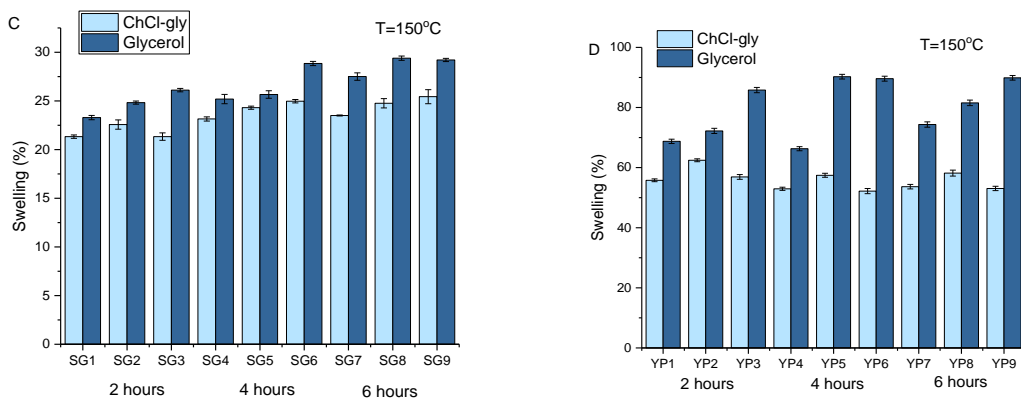


Figure A1-4 Swelling of SG and YP in glycerol and GLY at 150°C

On the other hand, SG samples soaked in GLY and heated at 150°C swelled up to 24.6%, whereas YP softwood samples swelled a percentage of 39.23%. In both SG and YP biomass samples, the swelling with glycerol was higher than the volumetric swelling with GLY. The experimental data showed that glycerol swelled lignocellulose biomass more than GLY at the same temperature. However, this temperature was in the range of lignin T_g of wood. It has been suggested that GLY may have the ability to soften lignin, similar to ILs behavior with lignocellulose biomass. This may lead to disruption of cell wall matrix initiating a partial removal of lignin as well as a partial removal of hemicellulose, without significant degradation of cellulose. It is already well established the presence of covalent bonds between cellulose and lignin forming a lignin carbohydrate complex (LCC) [23, 24], hence lignocellulose delignification requires breakage of C-O bonds between polysaccharides and lignin. The extent of the delignification depends upon the temperature at which a pretreatment is conducted, the

quality of the solvent and the extent of the reactions during the pretreatment, several studies already published have stated that the higher the temperature and the longer the time the more amount of lignin and hemicellulose removals will be observed. These experimental observations in biomass swelling with GLY show coloration of the solvent suggesting a partial disruption of covalent bonds. Thus, the question would be if GLY is effective as a lignocellulose pretreatment agent to achieve the degree of lignification required to improve cellulose accessibility and therefore enhance the enzyme saccharification to produce bioethanol?

Studies on the performance of GLY show the following observation and evidences: **1)** GLY is constituted by ChCl crystals and glycerol. ChCl has in two different structures depending upon the temperature, at ambient temperature has α form and at temperatures above 78°C has β form [25], hence can pack in an orthorhombic structure that allows six Cl⁻ anions for each Ch⁺ cation [26] thus each Cl⁻ anion is surrounded by three nitrogen atoms and one oxygen atom and no oxygen-oxygen hydrogen bond is observed. **2)** It has been reported a fastest diffusing activity of glycerol in glyceline (chapter 2) as well as significant interactions of hydrogen bonds due to the additional OH functional group in glycerol molecule. Perkins et al. [27] have conducted structural analysis and computational studies about the contact of different functional groups and the relative proportions of hydrogen bonds in GLY and have found that there are three major types of interactions that contribute to the H-bond network at different distances: HBD-anion, preferentially between Cl⁻ anion of the ChCl (HBA) and the two terminal OH of the glycerol molecule (HBD) relative to the OH group in the middle ; HBD-HBD; and HBD-cation. At larger distances, anion-anion and cation-cation interactions have also been detected and can influence the structure of the H-bond network. **3)** Abbott [28] has stated that GLY is a viscous solvent because it has large ions Ch⁺ and small void volume (chapter 2). **4)** The viscosity of GLY

decreases at elevated temperatures, Mjalli and Ahmed [29] have determined that the viscosity of glyceline at 25°C is 376 cP, presenting a rigid hydrogen bond network and less mobility than water. The increase of the temperature to 60°C causes a viscosity decrease to 50 cP and the viscosity decreases linearly with temperature. Hence, the mobility of GLY within the cell wall is enhanced, a thermal expansion takes place and heat and mass transfer are improved in the ChCl-based DESs [29, 30]. **5)** At higher temperatures GLY becomes slightly acidic, its pH at a temperature of 20°C is 7.54 (slightly basic) [29], and decreases to pH=6.828 at 80°C. The increase in temperature results in a distortion of hydrogen bond network and more H⁺ dissociates, reducing the [OH⁻] ions with the consequent reduction of pH of GLY. This may favors the fractionation on lignocellulose components, hence the resulting products may contribute to reduce pH to a greater extent. **6)** GLY interactions with cellulose are very low so cellulose integrity is preserved and therefore it can be used in lignocellulose pretreatments. **7)** Lignin molecule has the property of π -stacking and can facilitate hydrogen bonding with cations [31], Ch⁺ cations may tune the relative solubility of lignin. **8)** Cations are involved in interactions with polymers [32], FT-IR studies have revealed hydrophobic behavior of Ch⁺ cations and properties for self-aggregation and self-assembly, therefore Ch⁺ cations formed micelles in aqueous solutions. It has not been reported this kind of behavior for lignin biopolymer, studies to gain some insights on this would help to a better understanding of the interactions between Ch⁺ cation and lignin molecules. **9)** Aromatic interactions between cations and π systems, studies in biopolymers such as proteins have found strong electrostatic interactions between a cation and π systems, when the cation interact with the quadrupole moment of benzene rings (Figure A1-3) which arises from the “tail to tail” alignment of two dipoles [33]. These interactions also have been reported for lignin cation interactions for thin film assembly [34]. These cation- π

interactions are as important as H-bonding, ion-pairing and hydrophobic effects in determining protein structure and are located in the surface [35] (Figure A1-5). The flat π -electrons surfaces of aromatic molecules are non-polar so the solvophobic forces favor stacking [36]. The interactions between cations with aromatic rings in biomolecules such as proteins has been extensively studied because of their importance in biochemical reactions. Hence, these cation- π interactions may be the reason why Alvarez et al. [37] have found DESL in the liquor of pretreatment reactions, Ch^+ cation could undergo similar cation- π interactions with aromatic rings of lignin. However, the complexity of studying these interactions between GLY and lignin relies in the fact that larger functional groups are involved, additional analysis of these Ch^+ cation interactions with lignin will provide information on the mechanism of action of Ch-based DESs and lignocellulose biomass processing.

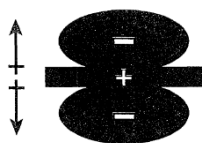


Figure A1-5 Schematic of the quadrupole moment of benzene, viewed edge-on, showing regions of positive and negative partial charges, taken from reference [38]. Use under fair use.

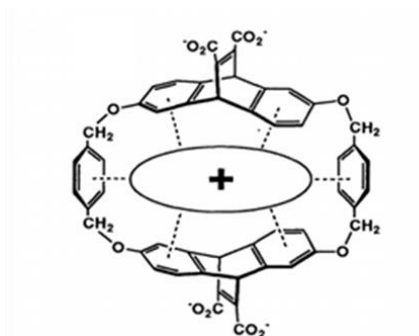


Figure A1-6 Schematic of the quadrupole moment of benzene, viewed edge-on, showing regions of positive and negative partial charges, taken from reference [38]. Use under fair use.

A1.6 Conclusions

The present study investigated qualitatively the solubility of cellulose, xylan and kraft lignin isolated biopolymers commercially available, as well as swelling of hardwood and softwood biomass samples soaked in DI water, glycerol, ChCl, and GLY as solvent systems. To evaluate their impact, solubility of isolated biopolymers and swelling of wood samples were conducted at ambient temperature and at 150°C for 2 h. Solubility was evaluated visually, none of them dissolved in ChCl alone at ambient temperature nor at 150°C. Only kraft lignin dissolved in glycerol and glyceline to a greater extent at 150°C. Solubility in GLY was as follows kraft lignin > xylan > cellulose. Lignocellulose biomass samples partially dissolved in glycerol and GLY at 150°C. To understand the mechanism by which GLY and lignocellulose biomass interact comparison between ILs and DESs swelling based on literature has been presented. ILs undergo swelling and dissolve lignocellulose components. At this temperature and in the presence of GLY, lignin softens and undergoes thermal expansion (lignin T_g = 100-170°C). Cl⁻ anions of the DES interact with the two OH groups of the ends of glycerol molecule, the other OH group of glycerol is involved in hydrogen bonding intermolecularly. Ch⁺ cations may have cation- π interactions with aromatic rings of lignin and along with the interactions between glycerol and Cl⁻ anion of ChCl disrupt the cell wall and therefore partially remove lignin and hemicellulose. Fragments of these biopolymers remain in the DES liquor and can be recovered. On the other hand, cellulose undergoes little change. In this way, lignocellulose biomass pretreated with GLY can be used as pretreatment to facilitate accessibility of the enzymes to cellulose and improve hydrolysis and sachariffication yields for further fermentation and bioalcohol production.

A1.7 References

1. Zhang, Q.H., et al., *Green and Inexpensive Choline-Derived Solvents for Cellulose Decrystallization*. Chemistry-a European Journal, 2012. **18**(4): p. 1043-1046.
2. De Oliveira Vigier, K., G. Chatel, and F. Jerome, *Contribution of Deep Eutectic Solvents for Biomass Processing: Opportunities, Challenges, and Limitations*. ChemInform, 2015. **46**(26).
3. Brandt, A., et al., *Deconstruction of lignocellulosic biomass with ionic liquids*. Green Chemistry, 2013. **15**(3): p. 550-583.
4. Dai, Y., et al., *Tailoring properties of natural deep eutectic solvents with water to facilitate their applications*. Food chemistry, 2015. **187**: p. 14-19.
5. Bahcegul, E., et al., *Different ionic liquids favor different lignocellulosic biomass particle sizes during pretreatment to function efficiently*. Green Chemistry, 2012. **14**(7): p. 1896-1903.
6. Nor, N.A.M., W.A.W. Mustapha, and O. Hassan, *Deep Eutectic Solvent (DES) as a Pretreatment for Oil Palm Empty Fruit Bunch (OPEFB) in Sugar Production*, in *Molecular and Cellular Life Sciences: Infectious Diseases, Biochemistry and Structural Biology 2015 Conference*, T. Hase, et al., Editors. 2016. p. 147-154.
7. Procentese, A., et al., *Deep eutectic solvent pretreatment and subsequent saccharification of corncob*. Bioresource Technology, 2015. **192**: p. 31-36.
8. Yu, B., *Glycerol*. Synlett, 2014. **25**(4): p. 601-602.
9. Gu, Y. and F. Jérôme, *Glycerol as a sustainable solvent for green chemistry*. Green Chemistry, 2010. **12**(7): p. 1127-1138.
10. Morikawa, H., et al., *Characterization of aspen exploded wood lignin*. Canadian Journal of Chemistry, 1982. **60**(18): p. 2372-2382.
11. Chowdhury, S. and C.E. Frazier, *Thermorheological complexity and fragility in plasticized lignocellulose*. Biomacromolecules, 2013. **14**(4): p. 1166-1173.
12. Havimo, M., *A literature-based study on the loss tangent of wood in connection with mechanical pulping*. Wood Science and Technology, 2009. **43**(7-8): p. 627-642.
13. Demirba, A., *Aqueous glycerol delignification of wood chips and ground wood*. Bioresource Technology, 1998. **63**(2): p. 179-185.
14. Sun, F. and H. Chen, *Evaluation of enzymatic hydrolysis of wheat straw pretreated by atmospheric glycerol autocatalysis*. Journal of chemical technology and biotechnology, 2007. **82**(11): p. 1039-1044.
15. Sun, F. and H. Chen, *Enhanced enzymatic hydrolysis of wheat straw by aqueous glycerol pretreatment*. Bioresource technology, 2008. **99**(14): p. 6156-6161.
16. Zhao, X.C., K.; and Liu, D., *Organosolv pretreatment of lignocellulosic biomass for enzymatic hydrolysis*. Applied Microbiology and Biotechnology, 2009. **82**: p. 815-827.
17. Martín, C., et al., *Effect of glycerol pretreatment on component recovery and enzymatic hydrolysis of sugarcane bagasse*. Cellulose Chemistry and Technology, 2011. **45**(7): p. 487.
18. Romaní, A., et al., *Fractionation of Eucalyptus globulus wood by glycerol–water pretreatment: optimization and modeling*. Industrial & Engineering Chemistry Research, 2013. **52**(40): p. 14342-14352.

19. Zhang, Z., et al., *Laboratory and pilot scale pretreatment of sugarcane bagasse by acidified aqueous glycerol solutions*. *Bioresource technology*, 2013. **138**: p. 14-21.
20. Zhang, W., J.R. Barone, and S. Renneckar, *Biomass Fractionation after Denaturing Cell Walls by Glycerol Thermal Processing*. *ACS Sustainable Chemistry & Engineering*, 2015. **3**(3): p. 413-420.
21. Francisco, M., A. van den Bruinhorst, and M.C. Kroon, *New natural and renewable low transition temperature mixtures (LTTMs): screening as solvents for lignocellulosic biomass processing*. *Green Chemistry*, 2012. **14**(8): p. 2153-2157.
22. Hernández, R.E., *Influence of accessory substances, wood density and interlocked grain on the compressive properties of hardwoods*. *Wood Science and Technology*, 2007. **41**(3): p. 249-265.
23. Jin, Z., et al., *Covalent linkages between cellulose and lignin in cell walls of coniferous and nonconiferous woods*. *Biopolymers*, 2006. **83**(2): p. 103-110.
24. Yuan, T.-Q., et al., *Characterization of lignin structures and lignin-carbohydrate complex (LCC) linkages by quantitative ¹³C and 2D HSQC NMR spectroscopy*. *Journal of agricultural and food chemistry*, 2011. **59**(19): p. 10604-10614.
25. Petrouleas, V., R.M. Lemmon, and A. Christensen, *X-ray diffraction study of choline chloride's β form*. *The Journal of Chemical Physics*, 1978. **68**(5): p. 2243-2246.
26. Senko, M.E. and D.H. Templeton, *Unit cells of choline halides and structure of choline chloride*. *Acta Crystallographica*, 1960. **13**(4): p. 281-285.
27. Perkins, S.L., P. Painter, and C.M. Colina, *Experimental and computational studies of choline chloride-based deep eutectic solvents*. *Journal of Chemical & Engineering Data*, 2014. **59**(11): p. 3652-3662.
28. Abbott, A.P., *Deep Eutectic Solvents*. University of Leicester, 2014.
29. Mjalli, F.S. and O.U. Ahmed, *Characteristics and intermolecular interaction of eutectic binary mixtures: Reline and Glyceline*. *Korean Journal of Chemical Engineering*, 2016. **33**(1): p. 337-343.
30. D'Agostino, C., et al., *Molecular motion and ion diffusion in choline chloride based deep eutectic solvents studied by H-1 pulsed field gradient NMR spectroscopy*. *Physical Chemistry Chemical Physics*, 2011. **13**(48): p. 21383-21391.
31. Janesko, B.G., *Modeling interactions between lignocellulose and ionic liquids using DFT-D*. *Physical Chemistry Chemical Physics*, 2011. **13**(23): p. 11393-11401.
32. Khan, I., et al., *Structural insights into the effect of cholinium-based ionic liquids on the critical micellization temperature of aqueous triblock copolymers*. *Physical chemistry chemical physics : PCCP*, 2016. **18**(12): p. 8342-8351.
33. Sunner, J., K. Nishizawa, and P. Kebarle, *Ion-solvent molecule interactions in the gas phase. The potassium ion and benzene*. *The Journal of Physical Chemistry*, 1981. **85**(13): p. 1814-1820.
34. Pillai, K.V. and S. Renneckar, *Cation- π Interactions as a Mechanism in Technical Lignin Adsorption to Cationic Surfaces*. *Biomacromolecules*, 2009. **10**(4): p. 798-804.
35. Gallivan, J.P. and D.A. Dougherty, *Cation- π Interactions in Structural Biology*. *Proceedings of the National Academy of Sciences of the United States of America*, 1999. **96**(17): p. 9459-9464.
36. Hunter, C.A., et al., *Aromatic interactions*. *Journal of the Chemical Society, Perkin Transactions 2*, 2001(5): p. 651-669.

37. Alvarez-Vasco, C., et al., *Unique low-molecular-weight lignin with high purity extracted from wood by deep eutectic solvents (DES): a source of lignin for valorization*. *Green Chemistry*, 2016. **18**(19): p. 5133-5141.
38. Dougherty, D.A., *Cation-pi interactions in chemistry and biology: A new view of benzene, Phe, Tyr, and Trp*. *Science*, 1996. **271**(5246): p. 163-168.